UNIVERSITÀ DEGLI STUDI DI PALERMO
Dottorato in Energia e Tecnologie dell'Informazione
Dipartimento di Energia, Ingegneria dell'Informazione e Modelli Matematici
Settore Scientifico Disciplinare - Fisica Tecnica Ambientale (ING-IND/11)

Reuse of electric vehicle batteries in a residential stationary application: an integrated load match analysis and life cycle assessment approach

IL DOTTORE
Maria Anna Cusenza

IL COORDINATORE
Prof. Maurizio Cellura

IL TUTOR
Prof. Maurizio Cellura

IL CO TUTOR
Dott.ssa Sonia Longo

CICLO XXXI
ANNO CONSEGUIMENTO TITOLO 2019

Abstract

The increasing use of renewable energy technologies for the electricity generation in buildings will require a growing number of battery energy storage systems (BESS) in the next years, in order to reduce the mismatch between the highly variable on-site electricity generation and the building load. The increasing number of retired electric vehicle (EV) batteries, expected in the near future from the automotive sector, can be used for this purpose, before the final treatments at the end-of-life. In fact, according to recent literature and technical analysis, retired EV batteries still retain 70–80% of their original capacity and they have enough capacity to be used in secondary applications, which have a much lower capacity limit and hence are less demanding applications.

In this context, this dissertation aims to identify the optimal BESS size, expressed as energy capacity, and to analyse the environmental implication of a second life stationary application of a BESS made of the retired Li-ion EV batteries to a residential nearly net Zero Energy Building (nZEB), equipped with a photovoltaic power plant (PV), by an integrated approach based on load match considerations and life-cycle environmental impacts. In line with this goal, the detailed analysis of the operational phase in terms of load – match and grid interaction is combined with the Life Cycle Assessment (LCA) (ISO 14040) of the energy system.

The system examined is made of a PV plant, a BESS and the electrical grid (PV plant + BESS + electrical grid). The functional unit of the analysis is the electricity required by the building in a time scale of 12 years.

The assessment of the environmental sustainability of using retired EV batteries in stationary second life applications is based on comparing the associated energy and environmental impacts with those of two scenarios, providing the same function. In a first scenario, named “Reference scenario”, it is not employed a BESS, and the system “PV plant – electricity grid” provides the electricity to the examined residential nZEB. In the second one, named “Fresh battery scenario”, the BESS is realized with fresh EV batteries. In addition, in order to highlight the effective environmental benefits resulting from the application of circular economy and industrial symbiosis principles of reusing retired EV batteries in stationary storage applications, avoiding the need to produce a new BESS, the system boundaries are expanded in order to include also the first application of the batteries in the EV.

The integration of the results obtained in the load match analysis and the LCA allows to identify the configuration that could represent the best BESS size in terms of load matching and environmental sustainability. In detail, for the examined nZEB, characterized by a PV peak power of 20 kWp and an average yearly electricity demand of about 25 MWh, the installation of a BESS capacity of 46.5 kWh (corresponding to the employment of five retired EV batteries) results the best solution. In fact, both the environmental and load match improvement achievable increasing the BESS size are negligible.

The comparison between the reuse and the reference battery scenarios highlights that the installation of a BESS causes an improvement of the environmental performance of the energy system in almost all the examined impact categories, the exceptions are the abiotic depletion potential, human toxicity – cancer and non-cancer effect and freshwater ecotoxicity impact categories, which increase, respectively, of about 100%, 30%, 11% and 12%.

The comparison between the reuse and the fresh battery scenario shows that, under the assumption made in this dissertation, they are equivalent in terms of energy and environmental impacts. Since, in order to compare the scenarios based on an equivalent function, four fresh EV batteries are needed to perform the same function of five retired EV batteries. However, considering the volume of EV batteries expected in the near future, potential benefits could arise by reusing retired EV batteries as stationary storage system in second life applications as this can delay the recycling process up to 10 years permitting the development of new recycling technologies and practices allowing a high rate of recovery.

Finally, the expansion of the system boundaries in order to include also the first life in the EV shows that reusing EV batteries as stationary storage system in residential building can enhance the overall environmental sustainability of the investigated systems. In detail, the impacts decrease of a percentage ranging from around -2% (in cumulative energy demand) to -13% (in abiotic depletion potential).

The study represents an original environmental sustainability assessment, combining the load match analysis and the life cycle approach. It highlights the potential synergy inspired to the principles of the circular economy and industrial symbiosis, between the household and the automotive sector.

Table of contents

Nomenclature

ADP	abiotic depletion potential
ANL	Argonne National Laboratory
AP	Acidification potential
B_c	Battery energy capacity
BESS	Battery Energy Storage System
BEV	battery electric vehicle
BL	building load
BMS	battery management system
BoM	bill of materials
C	configuration
CCS	carbon capture and storage
CED	cumulative energy demand
CMC	carboxymethyl cellulose
COP	Conference of the Parties
E_{BDmax}	Maximum energy discharge from the BESS
EEA	European Energy Agency
E_{FW}	freshwater ecotoxicity
EoL	end of life
EPBD	Energy Performance of Buildings Directive
ESS	energy storage system
EU	European Union
EU_F	freshwater eutrophication
EU_M	marine eutrophication
EU_T	terrestrial eutrophication
EV	electric vehicle
FU	functional unit
GHG	Greenhouse house
GWP	global warming potential
HEV	Hybrid electric vehicle
HT-ce	human toxicity – cancer effect
HT-nce	human toxicity – non cancer effect
ICE	internal combustion engine
IEA	International Energy Agency
IR-hh	ionizing radiation – human health
JRC	Joint Research Centre
LCA	life cycle assessment
LCI	life cycle inventory
LCIA	life cycle impact assessment
LFP	$LiFePO_4$
LH	Leaf House
Li-ion	lithium-ion
LMO	$LiMn_2O_4$
LMO - NMC	Lithium manganese oxide - nickel manganese cobalt
LULUCF	Land Use, Land Use Change and Forestry
ne	Net exported electricity
NiMH	nickel metal hydride
NMC	$Li(Ni_xCo_yMn_{1-x-y})O_2$
NMP	N-methyl-2-pyrrolidone
nZEB	nearly zero-energy building
ODP	ozone depletion potential
PAA	polyacrylic acid

PbA	lead-acid
PE	polyethylene
PEF	product environmental footprint
PHEV	plug-in hybrid electric vehicle
PM	particulate matter
POFP	photochemical ozone formation potential
PP	polypropylene
PV	photovoltaic
PVDF	polyvinylidene fluoride
PWB	printed wiring board
RES	renewable energy source
SDG	Sustainable Development Goal
SoC	state of charge
SoC_{max}	maximum battery state of charge
SoC_{min}	minimum battery state of charge
UNFCCC	United Nations Framework Convention on Climate Change
α_{fII}	allocation factor for the second life application
γ_{load}	Load cover factor
η_B	Battery charge/discharge efficiency
EoL	end of life
CRM	Critical Raw Material
BNEF	Bloomberg New Energy Finance
GHP	geothermal heat pump
EER	energy efficiency ratio
DHW	domestic hot water
AHU	air handling unit

List of Figures

List of Tables

Summary

Coupling the electrification of end-use services in the transportation and buildings sectors with low - carbon electricity generation, through the exploitation of renewable energy sources (RESs), has recognised as a key strategy in the transition towards a more competitive, secure, sustainable and decarbonized European Union (EU) economy.

EU policy makers recognised the importance of the employment of the distributed RESs in buildings in the effort to mitigate the climate change by introducing the concept of “nearly zero-energy building” (nZEB). A nZEB is a building that has a very high-energy performance, in which the nearly zero or very low amount of energy required should be covered to a very significant extent by energy from renewable sources, including energy from renewable sources produced on-site or nearby (distributed self – generation).

In this kind of building, the distributed self-generation from RESs is an issue in terms of power quality, voltage regulation, stability and reliability, since the local generation is highly variable and intermittent, it has a different profile from the demand, and the local demand has limited flexibility.

In order to balance supply and demand of electricity and to reduce the stress on the grid, one of the main strategies for residential buildings is the use of battery energy storage systems (BESS).

Considering the need of distributed RESs generation in the building sector in the near future, an increasing demand of grid connected BESSs is expected. However, their market penetration is currently restricted by the high cost of batteries

In the transportation sector, the electrification of the mobility emerges as one of the major low – carbon pathways. Replacing conventional vehicles with electric vehicles (EVs) can help reduce emissions and energy consumption. According to the International Energy Agency forecast, the number of EVs will increase from 2 million units in 2016 to 56 million by 2030.

According to several studies available in literature, the preferred option for traction batteries is the lithium-ion technologies, owing to their high energy and power density and long life cycle.

The increasing demand for lithium-ion batteries goes along with an increasing demand in materials, especially metals, required for their production, and with an increasing flow of waste batteries

reaching their end-of-life that need to be collected and properly treated in order to avoid the disposal of potentially hazardous materials and to recover the valuable materials. However, considering the volume of EV batteries expected in the near future due the forecast growth of electric mobility, key uncertainties surround the ability of the currently domestic recycling to manage an increasing number of EV batteries in the waste stream and to recover scarce and valuable materials from a highly variable mix of discarded batteries.

According to recent literature and technical analyses, due to the need of periodically replacement in order to do not affect the vehicle performance, the lithium – ion EV batteries still retain 70–80% of their original capacity at the point of retirement and they have enough capacity to be used in stationary applications, which are less demanding.

In this context, in this dissertation the life cycle environmental sustainability of the circular economy and industrial symbiosis inspired pathway to reuse the retired EV battery as a storage stationary system in a residential nZEB equipped with a photovoltaic (PV) power plant is explored by using an integrated sizing approach based on load match considerations and life-cycle environmental impacts. In detail, the analysis is focused to the system that provides the electricity to the examined building; it consists of the photovoltaic power plant, the BESS and the electrical grid (PV – BESS – electrical grid).

The aim of the research is to identify the best trade-off between the BESS size and the associated environmental impacts in a life cycle perspective and to assess the potential benefits related to the employment of BESS made of retired EV batteries in substitution of new batteries.

In line with this goal, the detailed analysis of the operational phase in terms of load – match and grid interaction is combined with the Life Cycle Assessment (LCA) of the energy system.

The load match refers to how the local energy generation matches the building load and is closely related with grid interaction (i.e. energy exchange between the building and the power grid).

The LCA is a standardized methodology (ISO 14040) widely adopted by the scientific community to assess the environmental impacts of products and services from a life cycle perspective (i.e. including extraction of raw materials, transports, manufacturing processes, use and end-of-life).

Starting from the one year monitored data on the on-site electricity generation from the PV plant and the building electricity requirement, the “PV plant + BESS + electrical grid” system proving the electricity required by the nZEB is modelled.

The BESS is made of retired EV lithium-ion batteries. Different configurations characterized by a BESS made of an increasing number of batteries ranging from one (Configuration 1 – C1) to ten (Configuration 10 – C10) are simulated.

The operational phase modelling is based on the analysis of available high-resolution real data of PV electricity generation and building load. The PV – BESS – electrical grid system is modelled assuming that: (1) the PV system always feeds first the load and then, if a surplus is available, in order of priority, the BESS and the electrical grid; and 2) the batteries cannot be used to feed the grid and vice versa. In addition, a battery capacity fade model and a linear decrease of the initial battery round trip efficiency are introduced by combining results obtained from laboratory test on the examined EV Li-ion battery and literature studies.

The energy flows obtained from the energy model are the input of the integrated load match and the life cycle environmental impacts analysis.

Moreover, the assessment of the environmental sustainability of using retired EV batteries in stationary second life applications is based on comparing the associated energy and environmental impacts with those of two scenarios, providing the same function. In a first scenario, named “Reference scenario” it is not employed a BESS, and the system “PV plant – electricity grid” provides the electricity to the examined residential nZEB. In the second one, named “Fresh battery scenario”, the BESS is realized with fresh EV batteries. In addition, in order to highlight the effective environmental benefits resulting from the application of circular economy and industrial symbiosis principles of reusing retired EV batteries in stationary storage applications, avoiding the need to produce a new BESS, the system boundaries are expanded in order to include also the first application of the batteries in the EV.

Finally, considering that the lithium ion technologies have emerged as a promising energy storage solution for both the EV and renewable energy technology a detailed LCA of the Lithium-ion EV battery pack reused in the stationary application is carried out.

Concerning the production phase of the lithium-ion battery pack, it is modelled based on a bill of material compiled by using both primary and secondary data.

Concerning the battery EoL, it is assumed that the components are dismantled and treated for recycling. In particular, detailed data on the EoL processes tailored to the specific case study are presented and the potential environmental impacts and benefits from the production of secondary raw materials are identified. With particular reference to the battery cells, the recycling is modelled in accordance with recent studies, such as on the product environmental footprint category rules (PEFCRs) on rechargeable batteries, research on the recyclability of different materials, and values from specialized industries sectors. More specifically, a pyrometallurgical recycling treatment followed by a hydrometallurgical one is considered, and the potential environmental credits resulting from the recycling of recoverable products, depending on the composition of the battery cell examined, are assessed. This is an important contribution of the research as most previous LCAs of Li-ion batteries have not provided a detailed analysis of recycling in terms of environmental impacts and credits.

Concerning the LCA of the EV lithium-ion battery pack reused in the stationary application, the analysis is carried out with reference to one battery pack by using both primary and literature data.

The study confirms that the electricity required for cell assembly is responsible for the greatest contribution to life cycle impacts of the battery production. The results obtained allow some recommendations for decreasing the impact of EVs. In particular, reducing the electricity consumed during the battery production and using a low carbon electricity mix could provide a significant contribution in improving the environmental sustainability of the EVs, especially considering the target of reducing overall global warming potential.

The energy analysis of the PV – BESS – electrical grid system highlights that the installation of an increasing BESS size allows to reduce the electricity imported from the electrical grid and then to increase the building self-consumption of the electricity locally produced by PV. However, the improvement becomes negligible to justify the installation of a larger BESS exceeded a certain size based on the specific application. This outcome demonstrates that it is important to perform an ex-ante and detailed modelling of the operational phase in order to identify the maximum size of the storage

beyond which the obtained benefits could become marginal and then avoid an unusual additional investment in terms of cost and resource employment.

The energy and environmental impact assessment demonstrates that the installation of an increasing energy storage capacity causes an improvement of the energy system environmental performance in almost all the examined impact categories with the exception of the abiotic depletion potential, human toxicity – cancer and non cancer effect and freshwater ecotoxicity. In general, the reduction of the electricity imported from the grid, due to the increasing size of the BESS, is mainly responsible for the impacts reduction. However, in general the environmental benefits are partially offset by the increasing impacts associated to the production of larger BESS and to the increasing consumption of the PV electricity generated on-site.

The integration of the results obtained in the load match analysis and the life cycle assessment allows to identify the configuration that could represent the best BESS size in terms of load matching and environmental sustainability. In detail, for the examined nZEB, characterized by a PV peak power of 20 kWp and an average yearly electricity demand of about 25 MWh, the installation of a BESS capacity of 46.5 kWh (corresponding to the employment of five retired EV batteries) results the best solution. In fact, both the environmental and load match improvement achievable increasing the BESS are negligible. This consideration could be supported also by economic consideration, if a market for retired EV battery will develop in the future, since in this case configuration with a lower number of batteries, less expensive, will be more appreciate.

The comparison between the reuse battery scenario and the reference battery scenario highlights that the second life use of the retired EV batteries as stationary storage system in a residential application improve the environmental sustainability of providing the electricity required by the building. In detail, the reuse battery scenario allows significant decrease in almost all the examined impact categories compared with the reference scenario. The exceptions are of the abiotic depletion potential, human toxicity cancer and non cancer effect and freshwater ecotoxicity, due to the increased electricity consumption from PV and to the BESS production process.

The obtained results suggest that although the integration of storage systems allows the improvement of the environmental sustainability of the electricity supply in a residential building equipped with

RESs in almost all the impact categories examined, it is necessary to improve the technologies currently available in order to obtain better performance in a wide range of environmental impact categories. In particular, it is relevant to improve the design of the PV system (in terms of resources efficiency and the chemical toxicity control) and the battery production process in order to increase the environmental performance both in the automotive (first life application) and in the building sector (second life application).

Concerning the comparison between the reuse and the fresh battery scenario, from the analysis results that, under the assumption made in this dissertation, they are equivalent in terms of energy and environmental impacts. Since, in order to compare the scenarios based on an equivalent function, four fresh EV batteries are needed to perform the same function of five retired EV batteries. However, considering the volume of EV batteries expected in the near future, key uncertainties surround the emergence and management of this increasing number of EV batteries in the waste stream and the ability of domestic recycling infrastructure to recover scarce and valuable materials from a highly variable mix of discarded batteries. In this context, potential benefits could arise by reusing retired EV batteries as stationary storage system in second life applications as this can delay the recycling process up to 10 years permitting the development of new recycling technologies and practices allowing a high rate of recovery.

The potential benefits related to the extension of the EV batteries lifetime and the partitioning of the environmental impacts between the EV and the stationary applications are offset by the lower number of fresh EV battery employed, by the higher lifetime and charge/discharge efficiency of fresh batteries compared to the retired ones. This is an important outcome of the dissertation, demonstrating the relevance of comparing the product system based on an equivalent function in order to avoid misleading results.

The comparison highlights that the extended reuse battery scenario presents better environmental performance in all the examined impacts categories. Then, extending the EV batteries lifetime by reusing them in stationary storage application allows to reduce the overall impacts of the system including both the EV and the building, demonstrating the potential environmental benefits of the proposed circular economy application

The approach proposed integrates the life cycle perspective in the design choices of a BESS. This allows an environmental sustainability oriented design, that takes into account the repercussions of the design choices not only to the operational phase performances but also to the whole life cycle of the system, in order to avoid the shifting of environmental and energy burdens from the operation phase to others life cycle phases.

The battery second life proposed is a synergy between the building and the automotive sector that enhances their environmental sustainability. The proposed strategy is in line with circular economy and industrial symbiosis principles and the waste management hierarchy in which reuse is preferable to recycling.

1 Introduction

1.1 European Union strategy for a more competitive, secure and sustainable economy

The transition towards a more competitive, secure and sustainable and decarbonized economy are some of the most relevant goals of the European Union (EU).

In line with these goals, in recent years the concept of circular economy has gained a growing interest in the scientific community, policy makers and industry.

The circular economy is an alternative to the traditional linear take-make -consume-dispose economic model that currently predominates. In a linear economy, the value chains are based on extracting resources, using them to make products, which are discarded at their end-of-life (EoL). Based on such logic, the current production system implies two problematic aspects in terms of resource availability and production of large amounts of waste [1].

Europe's economy depends on an uninterrupted flow of natural resources and materials, including water, crops, timber, metals, minerals and energy carriers, with imports providing a substantial proportion of these materials in many cases. Increasingly, this dependence could be a source of vulnerability, as growing global competition for natural resources has contributed to marked increases in price levels and volatility [2]. At the same time, rapid increases in extraction and exploitation of natural resources are having a wide range of negative environmental impacts (air, water and soil pollution, acidification of ecosystems, biodiversity loss, climate change and waste generation) in Europe and beyond [3].

The circular or closed-loop economy proposes an alternative flow model that aims to eliminate waste by cycling materials and products within the system. The circular economy can help to address the challenges of the EU economy, improving the efficiency of resource use results in obvious economic benefits, reducing costs and risks while enhancing competitiveness.

In a circular economy, the value of products and materials is maintained for as long as possible [4], and when a product reaches the end of its life, it is used again to create further value through reuse, recycling, remanufacturing, refurbishment, cascading use, etc. (Figure 1), reducing the need of primary materials use and the waste production.

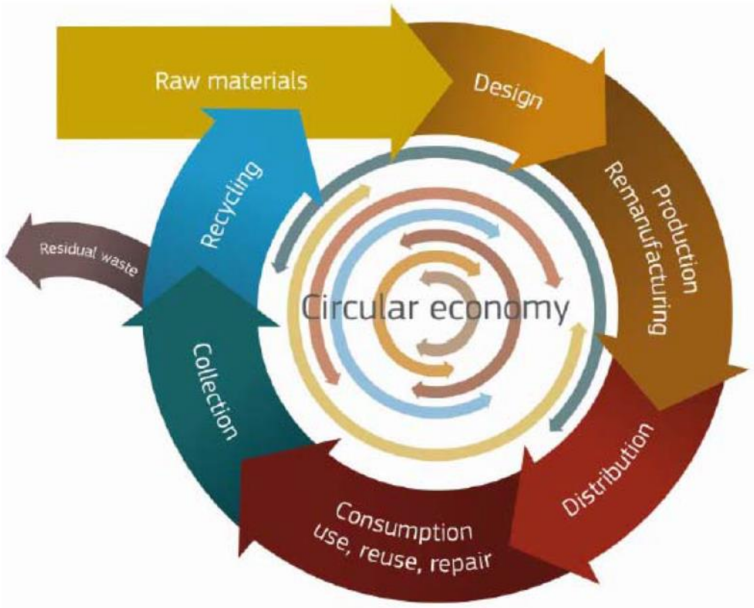

Figure 1. Circular Economy [5].

The transition towards a more circular economy is essential for the EU to develop a sustainable, low carbon, resource efficient and competitive economy [6]. As outlined in the monitoring framework for a circular economy of the European Commission "*The transition to a circular economy is a tremendous opportunity to transform our economy and make it more sustainable, contribute to climate goals and the preservation of the world's resources, create local jobs and generate competitive advantages for Europe in a world that is undergoing profound changes*" [7].

The wider benefits of the circular economy also include lowering energy consumption and carbon dioxide emissions levels. First, reducing, reusing and recycling avoid GHG emissions by reducing emissions from traditional waste management strategies (energy recovery, landfill). Second, circular economy strategies help cut GHG emissions by reducing the amount of energy needed by industrial production processes to transform primary raw materials into usable products [8].

Hence, the circular economy has strong synergies with the EU's objectives on climate and energy set in the 2030 Framework for climate and energy [9,10] and with the longer-term perspective set out in the Roadmap for moving to a competitive low carbon economy in 2050 to cut GHG emissions to 80% below 1990 levels, by 2050 [2].

Circular economy also is instrumental in supporting the EU's commitments on sustainability, as outlined in the Communication 'Next steps for a sustainable European future' [7] and in particular to reach Sustainable Development Goal 12 on sustainable consumption and production patterns [11].

Delivering on the EU Action Plan for the circular economy is therefore a clear priority for the Commission.

In 2015, the European Commission adopted an ambitious Circular Economy Package that establishes a concrete and ambitious programme of action, with measures covering the whole cycle: from production and consumption to waste management and the market for secondary raw materials and a revised legislative proposal on waste [12]. The revised legislative proposals on waste, amending Directive 2008/98/EC on waste [13], set clear targets for reduction of waste and establish an ambitious and credible long-term path for waste management and recycling and include concrete measures to promote re-use and stimulate industrial symbiosis - turning one industry's by-product into another industry's raw material [8]. The proposal includes the full implementation of the waste hierarchy established in the Directive 2008/98/EC on waste [13]. According to the Directive 2008/98/EC [13], the following waste hierarchy shall apply as a priority order in waste prevention and management legislation and policy: 1) prevention; 2) preparing for re-use; 3) recycling; 4) other recovery, e.g. energy recovery; and 5) disposal (Figure 2).

Figure 2. Waste management hierarchy [13].

The pathway towards a circular and decarbonized economy requires fundamental changes throughout the value chain, from product design and technology to new business models, new ways of preserving natural resources and turning waste into a resource. In this framework, it is important to identify the main environmental issues of the economic sectors, the potential environmental strategies and the potential synergies among the different economic sectors based on circular economy and industrial symbiosis principles, focusing mainly on those sectors responsible for the highest energy and environmental impacts.

1.2 European Union greenhouse gas emissions by sector

To meet the ambitious goals set to reduce the EU GHG emissions, Member States have to implement environmental strategies that aim to reach the long-term GHG goal and that decarbonise the economic sectors responsible for the highest GHG emissions.

In 2016, total GHG emissions — excluding Land Use, Land Use Change and Forestry (LULUCF) — in the EU-28 amounted to 4300 million tonnes CO_{2eq} (including indirect CO_2 emissions). In 2016, total GHG emissions were 24.0% (1356 million tonnes CO_{2eq}) below 1990 levels [14]. The reduction in GHG emissions over the 26-year period was due to a variety of factors, including the growing share in the use of renewables, the use of less carbon intensive fuels and improvements in energy efficiency, as well as to structural changes in the economy and the economic recession. GHG emissions decreased in the majority of sectors between 1990 and 2016, with the exception of transport and refrigeration and air conditioning (Table 1) [14].

Table 2 shows the source categories making the largest contribution to the change in GHG emissions, in the EU-28 between 2015 and 2016.

Total GHG emissions (excluding LULUCF) decreased in 2016 by 26.8 million tonnes, or – 0.6% compared to 2015. This small decrease in emissions came along with an increase in Gross Domestic Product (GDP) of 2%. The overall net decrease in total GHG emissions was partly offset by increased fuel-use for road transportation as well as by higher heat consumption in the building sectors (Table 2).

The building sector, which comprises commercial, public and residential buildings is responsible for approximately 40% of energy consumption and 36% of CO_2 emissions in the EU [15].

Table 1. Overview of EU-28 plus Iceland source categories whose emissions increased or decreased by more than 20 million tonnes CO_{2eq} in the period 1990–2016 [14].

Source category	**Million tonnes (CO_{2eq})**
Road Transportation	163
Refrigeration and Air conditioning	97
Aluminium Production	-21
Agricultural Soils: Direct N_2O Emissions From Managed Soils	-26
Fugitive emissions from Natural Gas	-26
Cement Production	-28
Fluoro-chemical Production	-29
Commercial/Institutional	-40
Enteric Fermentation: Cattle	-44
Nitric Acid Production	-46
Adipic Acid Production	-57
Manufacture of Solid Fuels and Other Energy Industries	-61
Coal Mining and Handling	-69
Managed Waste Disposal Sites	-73
Residential: Fuels	-109
Iron and steel production	-120
Manufacturing industries	-278
Public Electricity and Heat Production	-420
Total	**-1356**

Table 2. Overview of EU-28 plus Iceland source categories whose emissions increased or decreased by more than 3 million tonnes CO_{2eq} in the period 2015–2016 [14].

Source category	**Million tonnes (CO_{2eq})**
Road transportation	19
Residential: Fuels	15
Commercial/Institutional	4
Iron and steel production	-8
Public electricity and heat consumption	-49
Total	-27

Concerning the residential or households sector, in 2016, it represented 25.4% of final energy consumption in the EU [16]. Households use energy for various purposes: space and water heating, space cooling, cooking, lighting and electrical appliances and other end-uses, which mainly cover uses of energy by households outside the dwellings themselves. Most of the EU final energy consumption in the residential sector is covered by natural gas (37.1%) and electricity (24.5%). Renewables account for 16.0%, followed by petroleum products and derived heat. A small proportion is still covered by coal products (solid fuels) (Figure 3)

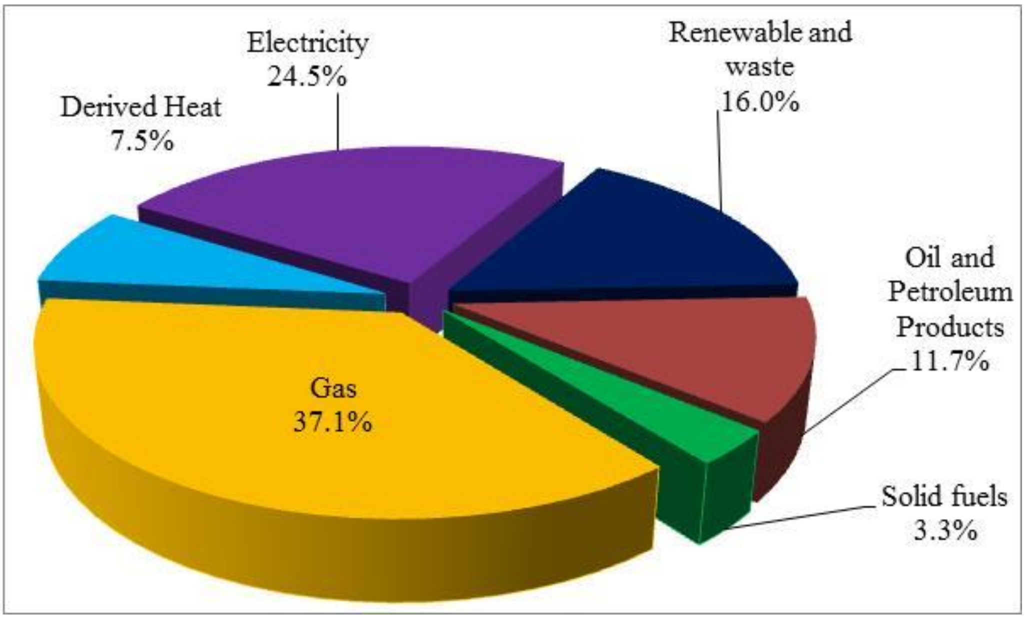

Figure 3. Final energy consumption in the residential sector by fuel, EU-28, 2016 [16].

Reductions in household energy consumption and the shift towards cleaner energy sources are necessary if Europe is to achieve the low-carbon growth envisaged in the 2050 Energy Roadmap.

The energy and emissions savings potential remains largely untapped because of continued use of less efficient technologies, lack of effective policies and weak investments in sustainable buildings [17]. Moreover, currently, about 35% of the EU's buildings are over 50 years old and almost 75% of the building stock is energy inefficient [16]. Therefore, more renovation of existing buildings and the employment of more efficient technologies has the potential to lead to significant energy savings – potentially reducing the EU's total energy consumption and lowering CO_2 emissions [17].

Concerning the transport sector, it represents almost a quarter of Europe's GHG emissions and is the main cause of air pollution in cities. The transport sector has not seen the same gradual decline in emissions as other sectors: emissions remain higher than in 1990 (Figure 4).

In 2015, the transport sector contributed 25.8% of total EU-28 greenhouse gas emissions [18].

Within this sector, road transport is by far the biggest emitter accounting for more than 70% of all GHG emissions from transport (Figure 5).

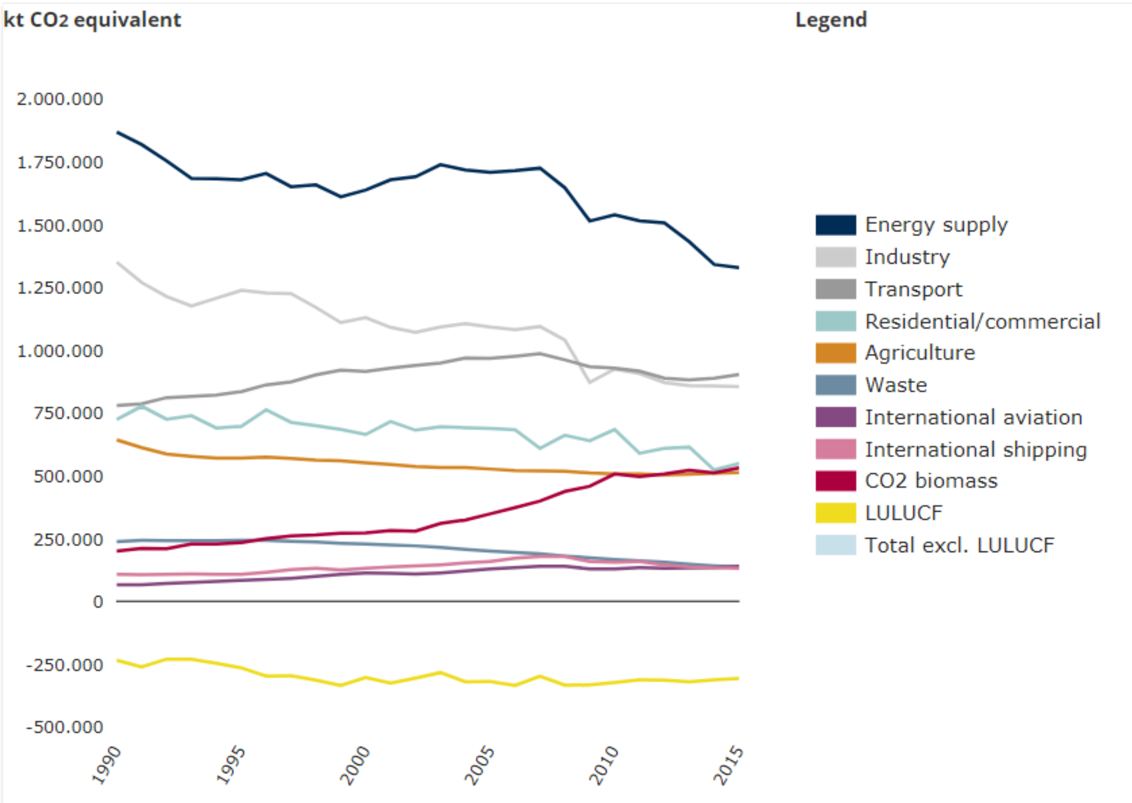

Figure 4. GHG emissions trends by aggregated sector [19]

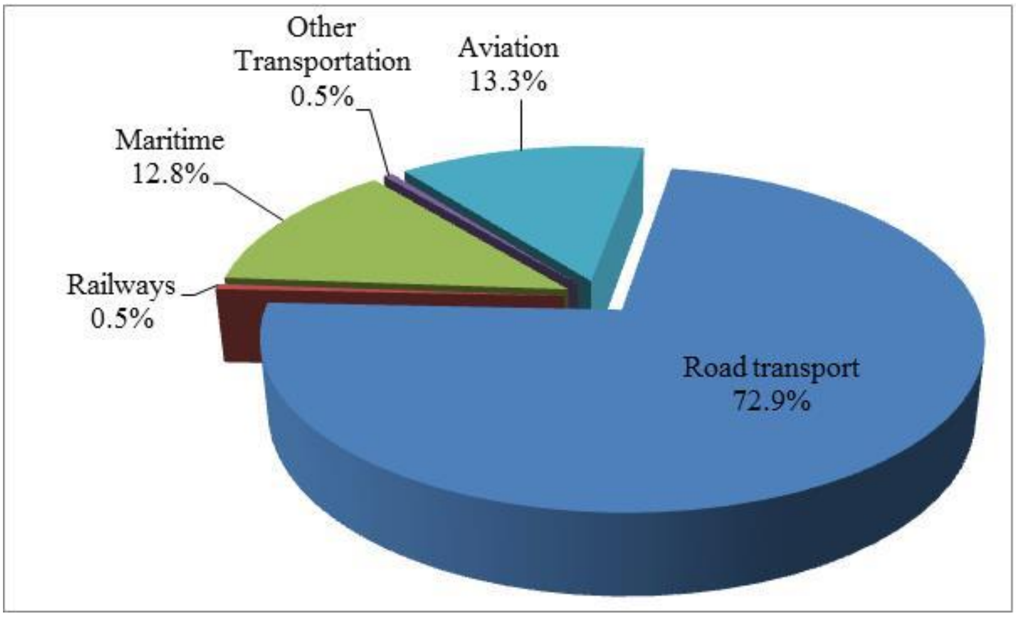

Figure 5. Share of transport GHG emissions [18].

The above figures highlight that transport and building sector represents two important areas of intervention for reducing GHG emissions and achieve the EU climate goals.

1.3 Towards a decarbonized building and transportation sectors

Electricity is currently emerging as one of the most relevant energy carriers to be deployed in decarbonisation pathways for the energy sector applied to either building [20,21] and transportation sector [22]. In all scenarios towards decarbonisation of the energy system, examined in the context of the "Energy roadmap 2050", electricity is forecasted to play a much greater role than now (almost doubling its share in final energy demand to 36–39% in 2050 (Figure 6)) [23].

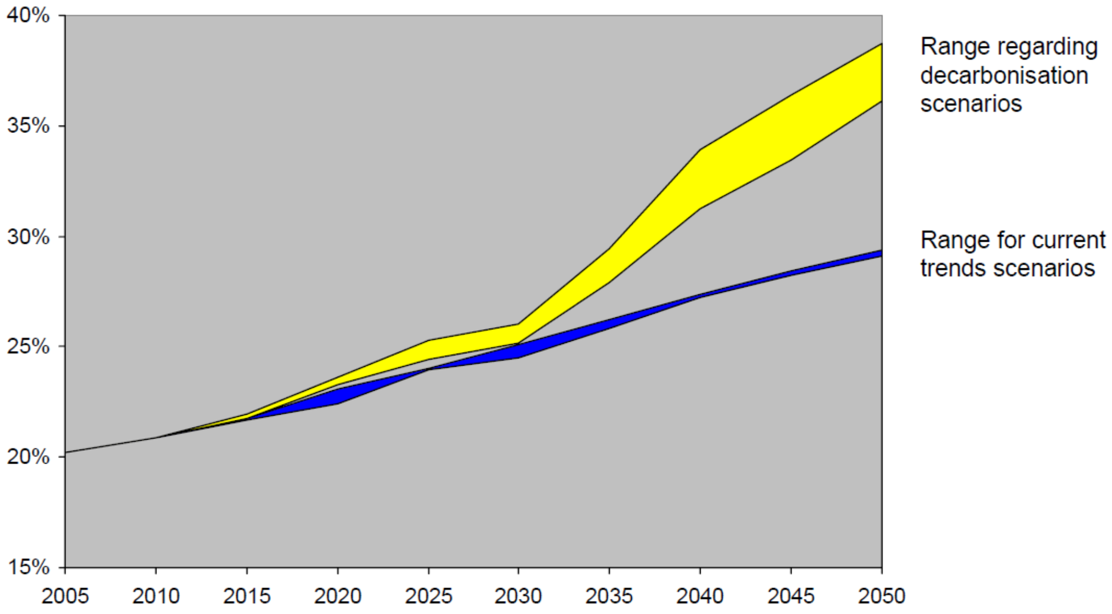

Figure 6. Share of electricity in current trend and decarbonisation scenarios (in % of final energy demand) [24].

Increasing the share of electricity in final energy use, will be essential for creating a carbon-neutral and energy efficient economy in the EU as it eliminates the need to burn fossil fuels to provide energy for buildings and transport [25]. Coupling the electrification of end-use services in the transportation and buildings sectors with decarbonisation of electricity generation, through the exploitation of renewable energy sources (RESs), are important measures needed to reduce the EU's energy dependency and GHG emissions. The electricity, in fact, can play an important role in deep GHG emissions cut, as the decarbonisation of electricity generation can be achieved at a much higher pace than in the rest of the energy system [26]. A variety of mitigation options exists in this sector, including renewable, nuclear power plants or fossil fuel power stations equipped with carbon capture and storage (CCS) technologies [27].

The primary production of renewable energy within the EU-28 in 2016 was 211 million tonnes of oil equivalent (toe). The quantity of renewable energy produced within the EU-28 increased overall by 66.6 % between 2006 and 2016, equivalent to an average increase of 5.3 % per year [28]. Among renewable energies, the most important source in the EU-28 was wood and other solid biofuels as well as renewable wastes, accounting for 49.4 % of primary renewables production in 2016 (Figure 7). Hydro power was the second most important contributor to the renewable energy mix (14.3 % of the total), followed by wind power (12.4 %).

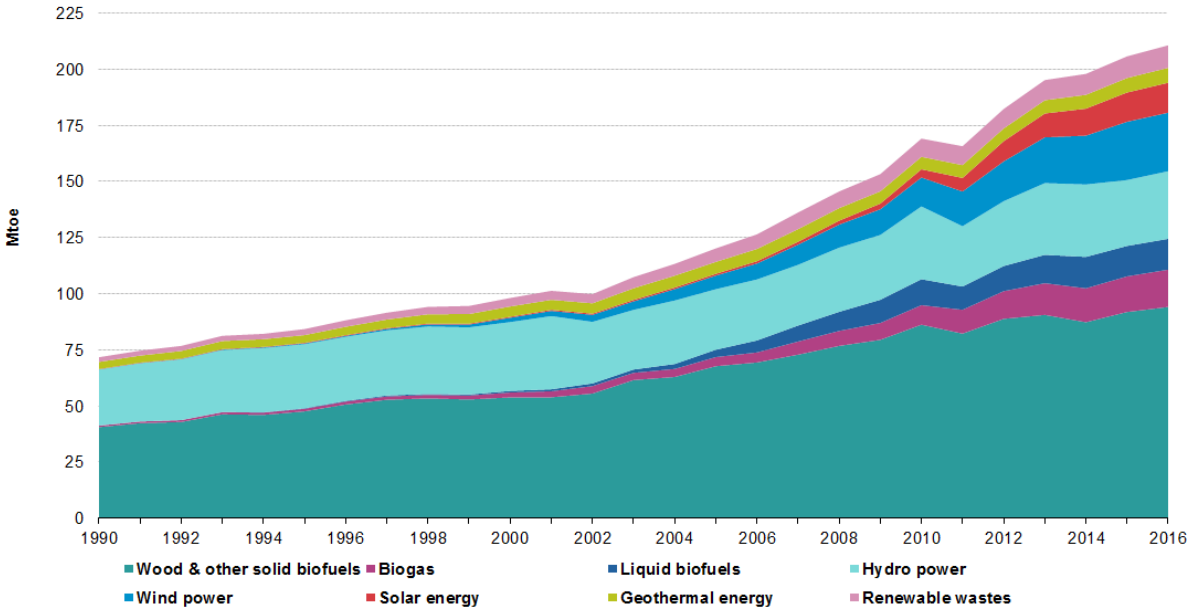

Figure 7. Primary production of energy from renewable sources EU-28 1990-2016 [28].

Concerning the electricity, in 2016, the generation from renewable sources contributed more than one quarter (29.6 %) to total EU-28 gross electricity consumption. Hydro power is the most important source, followed closely by wind power (Figure 8).

In the building sector, the employment of distributed and low-carbon energy generation from RESs, like solar photovoltaic and wind, is an important measure towards its decarbonisation [29,30].

According to the report *"Renewable Energy Prospects for the European Union (REmap EU)"* [31] developed by the International Renewable Energy Agency (IRENA) in close collaboration with the European Commission, in a forecasted scenario in line with the EU's 40% GHG emission reduction objective by 2030, in the building sectors the share of renewables in the final energy use would increase from 17% registered in 2010 up to 42% in 2030.

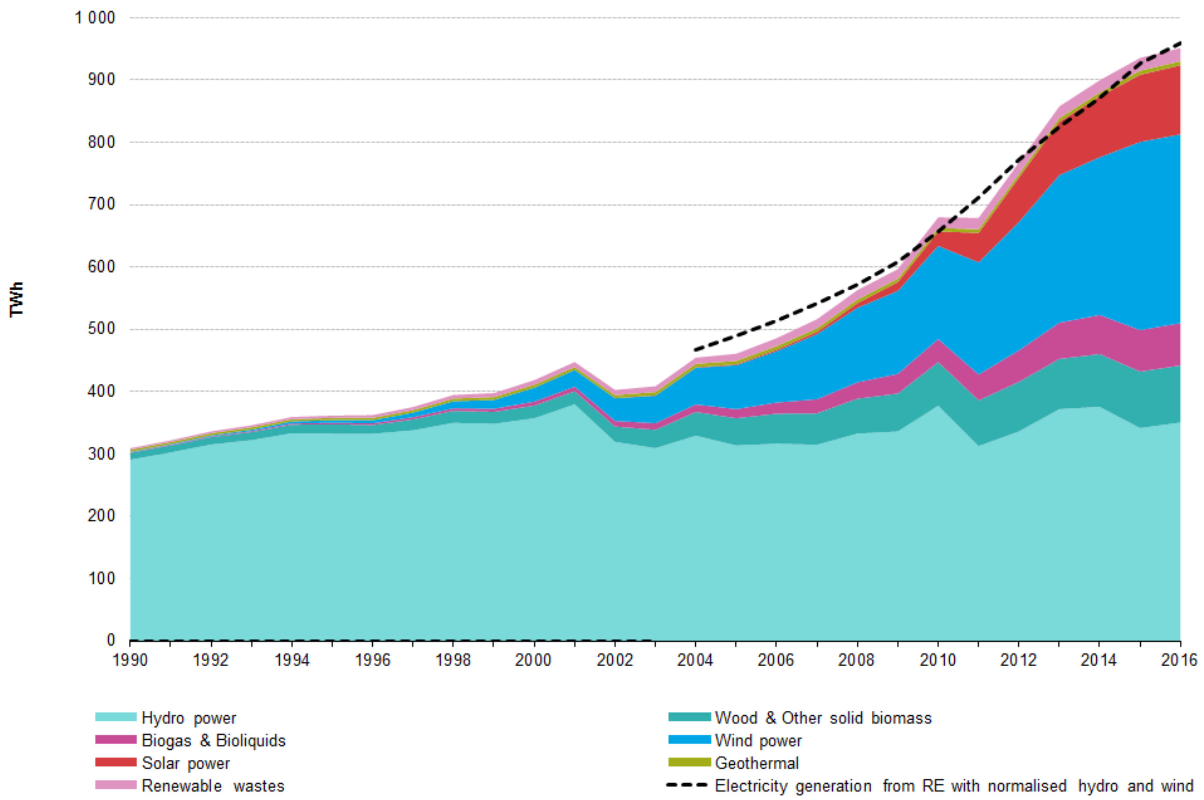

Figure 8. Gross electricity generation from renewable sources, EU-28, 1990-2016 (TWh) [28].

EU policy makers have for a long time recognised the importance of the employment of the distributed RESs in buildings in the effort to mitigate climate. The 2010 Energy Performance of Buildings Directive (EPBD) (Directive 2010/31 /EU [32], and the 2012 Energy Efficiency Directive (Directive 2012/27/EU [33]) are the EU's main legislative instruments promoting the improvement of the energy performance of buildings within the EU. In particular, the Directive 2010/31 /EU (EPBD recast) on the energy performance of buildings introduced the term "nearly zero-energy building" (nZEB). A nZEB is a building that has a very high-energy performance, in which the nearly zero or very low amount of energy required should be covered to a very significant extent by energy from renewable sources, including energy from renewable sources produced on-site or nearby [32].

The EPBD (recast) states that Member States shall ensure that new buildings occupied and owned by public authorities are nZEBs after December 31, 2018. Moreover, all new buildings have to be nZEBs by December 31, 2020.

The Directive 2012/27/EU, in the Article 4 "Building renovation", affirms that Member States shall establish a long-term strategy for mobilising investment in the renovation of the national stock of residential and commercial buildings, both public and private.

On 19 June 2018 Directive 2018/844/EU [34], amending the EPBD (recast) Directive, was published. The revised EPBD introduces targeted amendments to the current Directive aimed at accelerating the cost-effective renovation of existing buildings. The Directive states that to meet the goal of the EU to develop a sustainable, competitive, secure and decarbonised energy system, Member States shall establish a long-term renovation strategy to support the renovation of the national stock of residential and non-residential buildings, both public and private, into a highly energy efficient and decarbonised building stock by 2050, facilitating the cost-effective transformation of existing buildings into nZEB [34].

The distributed self-generation from RESs will certainly become an issue in terms of power quality, voltage regulation, stability and reliability [35] since the local generation is highly variable and intermittent, with a different profile from the demand, and the local demand has limited flexibility [36–38]. Moreover, the high penetration of RESs on electric grids can cause coal or natural gas–fired plants to turn on and off more often or to modify their output levels more frequently to accommodate changes in variable generation. This type of cycling of fossil-fueled generators can result in a decrease in efficiency and consequently in an increase of the associated environmental impacts.

In this framework, energy storage is a key component in providing flexibility and supporting the integration of higher shares of variable renewable energy in transport, buildings or industry [39].

The employment of distribuited local energy storage systems (ESS) will certainly be an important resource to balance supply and demand and to address the grid integration challenges related to the high penetration of RESs. ESSs allow energy to be stored chemically which can be converted when needed to electricity and used as a source of power. Storage technologies can reduce the RESs output variability, bring additional flexibility to energy systems, an essential prerequisite for high penetration of stochastically variable RESs [40]. Moreover, without storage, the house uses only the grid to compensate the generation – comsumption mistmatch [41] and on an hourly basis, only 25% of electricity generated on-site might be used exactly at the time step of generation, while 75% is sent to the grid at a certain time step and taken from the grid at a different one [42].

Among the available ESS technologies, batteries, flywheels, pumped storage, heat storage, compressed air, etc., the most promising for increase the self-consumption in household equipped with RESs is the electrochemical storage system, i.e. battery ESS (BESS) [40].

Considering the need of distributed RESs generation in the building sector in the near future, an increasing demand of grid connected BESSs is expected, however, their market penetration is currently restricted by the high cost of batteries. Currently for building applications lead acid batteries are the most common technology because of the low investment costs compared to Lithium ion (Li-ion) battery technologies that are generally better in efficiency and in the number of cycles, but they have much higher investment costs [43].

In the transportation sector, the electrification of the mobility emerges as one of the major low – carbon pathways. Replacing conventional vehicles with electric vehicles (EVs) can help reduce emissions and energy consumption. In particular, as an energy carrier for vehicle propulsion, electricity offers the possibility to substitute fossil fuels with a wide diversity of primary energy sources, e.g. RESs, allowing to reduce CO_2 emissions and other pollutants such as nitrogen oxides, non-methane hydrocarbons and particulate matter at the point of use and then to improve air quality, to reduce of crude oil dependence and to increase energy security [50].

In 2016, European Commission published the European Strategy for low-emission mobility [44]. The longer-term objective of the new strategy is to decrease oil import dependency [45]. Furthermore, it highlights the importance of removing obstacles to the electrification of transport, and improving the efficiency of Europe’s transport system by moving towards low and zero-emission vehicles as well as scaling up the use of low-emission alternative energy sources such as renewable electricity. The bulk of renewable energy use in the EU transport sector comes from biofuels [46], in fact renewable electricity currently plays only a small role in this sector. In 2015, the EVs still make up only a small fraction of all new vehicles sold in the EU, just 1.2 % [47], but an increase of this fraction is expected in the future.

The EVs can be classified in hybrid EVs (HEV), plug-in hybrid EVs (PHEV) and battery EVs (BEV). An HEV has both an electric motor and an internal combustion engine (ICE). The battery is recharged by the ICE. A PHEV has both an electric motor and an ICE, as HEV, but it can charge its battery by plugging in to a grid-provided electricity system, as well as it can use gasoline to power the battery. Finally, a BEV is entirely powered by batteries that are recharged by plugging in to a grid-provided electricity system [48].

The global stock of electric cars reached 3.1 million in 2017 (Figure 9) an increase of 57% from the previous year [45].

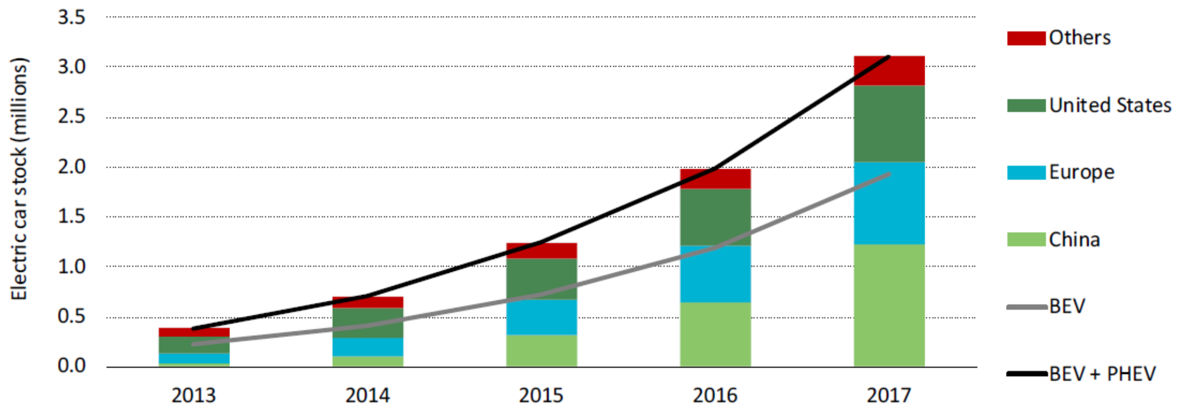

Figure 9. Evolution of the global electric car stock, 2013-17 [45].

According to the International Energy Agency (IEA), the number of EVs will increase from 2 million units in 2016 to 56 million by 2030 in the IEA reference technology scenario (RTS) [49]. The RTS incorporates technology improvements in energy efficiency and modal choices that support the achievement of policies that have been announced or are under consideration.

Figure 10 shows the deployment scenarios for the stock of electric cars to 2030 developed by IEA. The 2DS is consistent with a 50% probability of limiting the expected global average temperature increase to 2°C. The B2DS falls within the Paris Agreement range of ambition, corresponding to an average increase in the global temperature by 1.75°C.

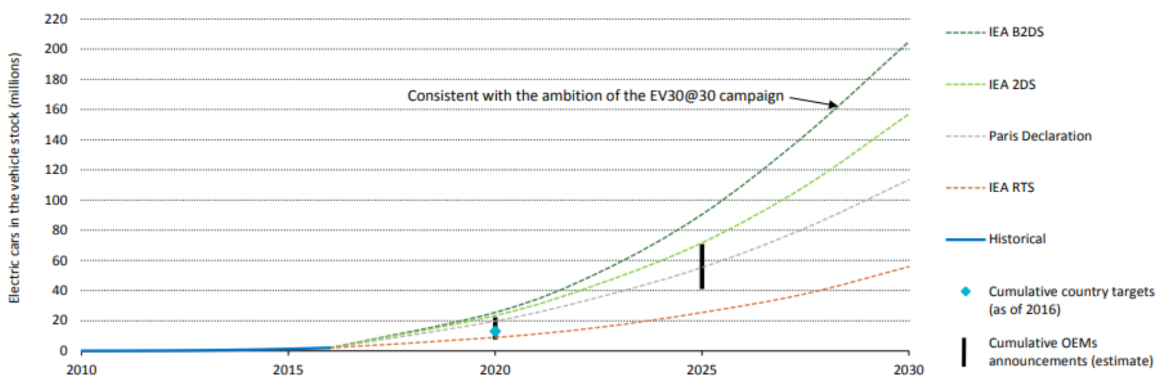

Figure 10. Deployment scenarios for the stock of electric cars to 2030 [50].

In 2013, in EU-28 the total sales of EVs reached just over 49,000 units, of which half were BEVs, and half PHEVs. The number of electric vehicles sold has increased steeply in each year since [46]. The latest preliminary data for 2015 indicate that almost 150,000 new PHEVs and BEVs were sold in the EU-28 [46].

According to several studies available in literature, the preferred option for traction batteries is the Li-ion technology [47,51–54]. These have certain advantages over most other battery types (like lead-acid (PbA), nickel metal hydride (NiMH)), including higher specific energy, high energy efficiency and longer lifespans [55].

Considering the projected scale of Li-ion deployment the automotive sector, it is paramount to consider the environmental footprint of batteries themselves across a range of impacts, including energy consumption, GHG emissions, resource depletion, etc. and over the product's life cycle, from raw material acquisition or generation from natural resources to final disposal at the EoL.

The increasing demand for Lithium-ion batteries goes along with an increasing demand in materials, especially metals, required for their production [56], and with an increase of flows of waste batteries reaching their EoL that need to be collected and properly treated in order to avoid the disposal of potentially hazardous materials.

Concerning the production phase, although the EVs allow for avoiding or reducing the tailpipe emissions, several studies shown that the environmental contributions of the batteries production in the EVs life cycle impacts can be significant [57–59] due to the initial material and energy investment and associated environmental aspects of producing large battery packs that represent a significant investment in resources and materials [60–63] E.g., in Zackrisson et al. [64], the manufacturing of the batteries resulted responsible for about 50-60% of the life cycle impact on GWP, in Majeau-Bettez et al. [65] the production phase of the examined battery technologies represented more than 50% in GWP and fossil depletion impact categories. According to several literature studies, the cathode and the anode are the most important components of a Li-ion battery with respect to resource depletion and environmental impacts [66]. A wide range of raw materials is used in Li-ion battery cells including lithium, nickel, cobalt, manganese, aluminium, copper, silicon, tin, titanium and carbon in a variety of forms, e.g. natural graphite [67], which can present issues in relation to resource availability, toxicity, safety, production and recycling or disposal impacts [68]. Primary extraction and beneficiation of these metals are responsible for 10-40% of most impacts related to battery manufacturing [48,69].

Although all raw materials are important, some of them are of more concern than others in terms of secure and sustainable supply [70]. On 13 September 2017, the European Commission published the 2017 list of Critical Raw Materials [71], which features 27 raw materials and updates the 2014 list. CRMs are both of high economic importance for the EU and vulnerable to supply disruption. Vulnerable to supply disruption means that the supply is associated to a high risk of not being adequate to meet EU industry demand. High economic importance means that the raw material is of fundamental importance to industry sectors that create added value and jobs, which could be lost in case of inadequate supply and if adequate substitutes cannot be found [72].

The European Commission had puts forward the regular identification of CRMs and the improvement of resource efficiency [73] and of conditions for recycling as crucial components of its raw materials policy. The importance of these two components and their close interrelation was recently reinforced in the Communication on the ‘Closing the loop – An EU action plan for the Circular Economy’ [6].

Concerning the EoL management, currently, the Directives on the end-of-life of vehicles [74] and on batteries and accumulators [75] support the recycling as EoL management for batteries with the aim to recover valuable metals, like cobalt, nickel, lithium, etc. and to minimize the negative impact of hazardous waste disposal on the environment. In particular, cobalt is a cathode material in lithium-ion batteries that needs addressing urgently. It has a risky supply chain, partly due to geopolitical issues.

Figure 11 shows the CRMs identified by the European Commission.

The majority (64%) of the world’s cobalt is mined in the Democratic Republic of Congo, a politically instable country, as a by- or co-product of copper or nickel, and so its supply also depends on demand for these parent materials. Cobalt is important in giving lithium-ion batteries their high energy density and is, therefore, difficult to substitute. Cobalt is twice as expensive as nickel and 15 times more expensive than copper [76]. Thus, recycling of materials containing cobalt is particularly important.

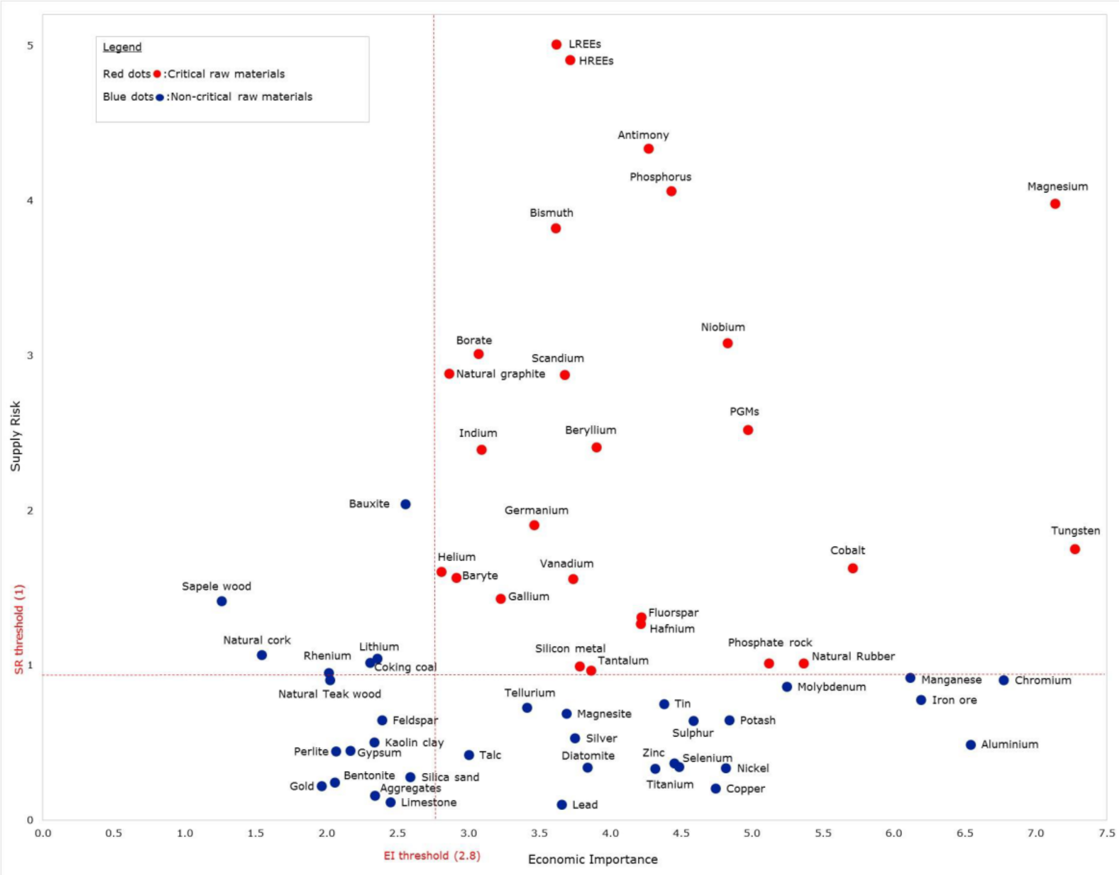

Figure 11. Economic importance and supply risk results of 2017 criticality assessment [77].

The most common recycling processes used to recover materials from the batteries are based on hydrometallurgical process and high-temperature or pyrometallurgical process. A typical pyrometallurgical process for recycling valuable metals from spent Lithium-ion batteries consists in a high-temperature smelting reduction; after this process, valuable metals are reduced and then recovered in the form of alloys. The hydrometallurgical method involves leaching, which dissolves the metallic fraction and recycled metal solutions or subsequent separation and recovery. With the reuse of recovered raw materials in new (battery) manufacturing processes the material cycle closes. Then, recycling allows for reducing the impacts associated with mining and resource extraction, since the demand for new virgin materials is decreased. Nevertheless, the recycling of batteries can also be associated with high efforts (temperature treatment, chemical treatment), which might even outweigh the positive environmental effects for some environmental indicators. Most of the recycling processes for spent lithium-ion batteries are currently based on pyrometallurgical processes [76]. While life cycle assessment studies confirm the environmental benefit from recovery of Lithium-ion battery materials [48,78–80] recycling will never be 100% efficient. Moreover, potential transitions away from cobalt-rich battery chemistries (where cobalt drives the economic revenue of recycling) to lower-cost chemistries (containing manganese or iron) by EV manufacturers [68,81] and use of energy-intensive pyrometallurgical recovery processes [82] can reduce the economic and environmental benefits related to metal recovery.

Moreover, key uncertainties surround the emergence and management of an increasing number of EV batteries in the waste stream and the ability of domestic recycling infrastructure to recover scarce and valuable materials from a highly variable mix of discarded batteries considering also the volume of EV batteries expected in the near future due the forecast growth of electric mobility. Finally, currently recycling lithium-ion batteries is technologically challenging, for many reasons. They contain a large number of blended materials, which makes recycling more complex than for simpler technologies like lead-acid, and a battery pack for an electric vehicle or energy storage is likely to contain 100 or more individual cells [68]. It is difficult for recycling companies to adapt to the continually evolving composition of electrodes, which may never standardise [83,84]. Moreover, the two main methods of recycling for lithium-ion batteries (pyrometallurgical and hydrometallurgical process) are energy intensive.

Finally, it is worth mentioning that due to the need of periodically replacement of the EV batteries in order to do not affect the vehicle performance, according to recent literature and technical analysis they still retain 70–80% [60,81,85–89] of their original capacity and they have enough capacity to be used in secondary applications, which have a much lower capacity limit and hence are less demanding applications [90]. Then, recycling them without any consideration for reuse can forgo the potential benefit associated to the exploitation of this remaining capacity [4].

1.4 A circular economy inspired strategy for a more sustainable building and transportation sector

The analysis of the decarbonisation pathways for building and transportation sectors carried out in the previous sections highlights that in the building sector the increasing penetration of RESs will result in an increasing demand of BESS in the near future. At the same time, in the transportation sector, due to the diffusion of the electric mobility, an increased demand is expected for high-energy density traction

Li-ion batteries. This trend will inevitably lead to an increase of flows of waste batteries that need to be collected and treated but that retain enough capacity to be used in secondary applications.

In this framework, a circular economy and industrial symbiosis inspired pathway is emerging between the building and the transportation sector, retired EV batteries can be repurposed[1] and reused in less strenuous applications such as stationary applications, where they are generally charged and discharged at small rates and operate in a controlled environment and secured working space. Besides capacity fade, these batteries also present reductions in terms of other parameters such as power, voltage and discharge current. However, in the second use in stationary applications, like energy storage in residential building, the requirements of such parameters are much lower than in an EV application.

According with the Bloomberg New Energy Finance (BNEF) forecasts, about 95 GWh of lithium-ion batteries are expected to come out of cars by 2025, and about 26 GWh of them will be converted to stationary storage systems (Figure 12).

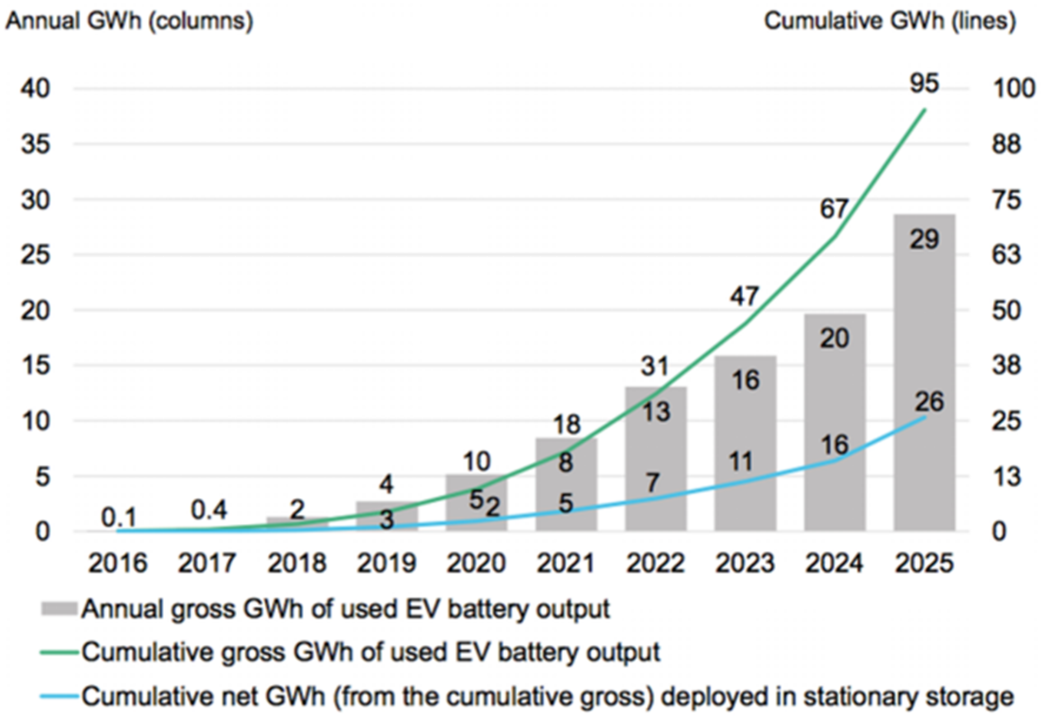

Figure 12. BNEF forecast of gross second-life battery availability and estimate of net GWh being used for stationary storage, 2016 – 2015 (nominal GWh).

[1] According to Ardente et al. [18], “repurposing” refers to utilizing products in other, different applications (often referred to as “second-use” applications) respect the purpose for which it was conceived.

Repurposed Li-ion batteries could be used in several applications (e.g. utility operations, commercial and residential buildings) depending on their characteristics [91]. From a financial standpoint, the creation of smaller applications in a larger market is a less risky investment, and would harmonize better with EV market penetration rates [92]. A key issue when handling Li-ion batteries is the risk of fire and explosion [93]. Given these factors, it is less risky to invest in a large number of small applications than a small number of large applications. Smaller applications can include numerous residential customers and a wide variety of commercial customers, including telecommunications companies (which may require 5 to 10 EV battery packs each), light commercial buildings (which may require 10 to 15 packs each) [94].

An analysis of recent European and international industrial activities, research and innovation projects and research studies, using repurposed EV batteries, revealed that the most frequently reviewed applications are those for integrating renewable energy into the grid [89]. Examples are smoothing for renewable energy systems [95–97]; energy storage of a single wind turbine/photovoltaic (PV)/battery system [36]; off-grid PV vehicle charging system [98]; and diurnal energy shifting, allowing intermittent renewable energy sources to be used more widely (e.g. wind and solar) [99]. Other applications relate, for example, to transmission and distribution upgrade [100–102], regulation services [100,101,103] and supplemental reserves [85,99,104,105].

Even though the term “second use” is not currently defined in the Batteries Directive [75], nor in any of the various Waste Directives [13,74,106], the second-use of EV batteries is aligned with both the waste management hierarchy (i.e. prevent, preparation for reuse, recycle, other recovery, disposal) as established by the Waste Framework Directive 2008/98/EC [13] and the 2015 Circular Economy action plan of the European Commission [6], especially concerning actions on lifetime and improved raw materials flows [107]. In fact, this EoL option can keep the added value in products for as long as possible and minimizes waste. Resources are kept within the economy when a product has reached the end of its life, so that they can be productively used again and hence create further value.

Stationary second use applications can delay the recycling process and extend the useful lifetime up to 10 years thereby obtaining new revenues in the meantime. In fact, second-life batteries can provided the same services as new batteries, but at a fraction of the cost, and avoid the need to produce and use less efficient lead acid battery that has been the most used technology in stationary energy storage application.

As discussed in Section 1.3, in the near future the number of residential and commercial buildings that will adopt technologies to reduce their dependence from the electrical grid, by becoming self-sustainable (nZEB) through the usage of PV systems with a connected storage system, is likely to significantly increase [108]. The local production of energy from RES (PV or wind) generation and electricity consumption do not have the same variation profile. Such mismatch brings the need to export to the electrical grid a significant part of the locally generated energy, even though the same amount of energy is later imported back for local consumption. These aspects are a source of inefficiency and may create problems to the electrical grid management [109]. The opportunity for using energy storage systems to store excess production for later use is becoming increasingly attractive. Nevertheless, despite the continuous fall in battery prices and a forthcoming decrease in the price of energy storage technologies, they still are an expensive asset for the average consumer. Re-purposed batteries coming from a first use in EV can represent an economic and environmental sustainable answer of the increasing demand of BESS in the building sector [110].

Extracting a second use from repurposed EV batteries may also assist EV owners in recovering some of the initial costs of vehicle purchase. By increasing the lifetime, value of the battery second life battery usage will lower the cost for both primary and secondary users. In fact, accelerated market penetration of EVs is currently restricted by the high cost of batteries, then the second use of the EV batteries would enable original equipment manufacturers to distribute the high initial cost of the EV battery over two life cycles [104].

Cascaded use also has the potential to mitigate waste disposal risks, for example in the context of emerging regulations and concerns of handling and transporting spent Li-ion batteries [81].

After the second life stationary applications, the EV batteries have to be recycled. A converse consideration arising from re-purposing in that there is that delay in the recycling availability of metals and other materials, although this delay in processing recycled Li-ion batteries may permit the development of new technologies and practices [111] allowing a high rate of recovery.

1.5 Statement of research problem and dissertation aim

The circular economy inspired strategy of employing retired EV as stationary energy storage system requires proven methodologies to test its effective environmental sustainability in a life cycle perspective [112–114].

Sizing a BESS made of retired EV batteries together with RESs requires an assessment of the energy flows of the system through the daily production and demand curves of the renewable system [115]. In the literature the modelling the energy flows of the second use of a battery in a specific application often uses average data or is based on previous studies [89]. However, in order to assess properly the energy flows in specific repurposed scenarios it is relevant to model the system energy using real data, combining the characteristics of both the battery and its application. The operation phase of the energy storage is generally recognized as extremely important, and consequently it is relevant to perform a detailed analysis taking into account the relative amount of remaining performance of the battery after the EV application and its degradation pattern during the second use phase.

Moreover, considering the key role of the battery, it is relevant to create a detailed model to assess the environmental impacts related to both battery production and EoL recycling processes.

According to Peters et al. [116] and Ellingsen et al. [117], few studies have so far provided an original and detailed life cycle inventory on battery production and these data were systematically used in various environmental analysis. Therefore, to increase the assessment's reliability, it was important to use primary industry data as far as possible. Regarding the modelling of the EoL phase, it was observed that few studies provide a detailed description of the recycling process and that several LCAs did not include this phase in the analysis because of the greater uncertainty, mainly due to lack of data [118]. However, considering that the recycling of batteries that reached their end of their life is mandatory, it is relevant to quantify the potential impacts and environmental credits associated with this process, based on the most widespread current technologies.

In this context, this dissertation aims to analyse the environmental implication of a second life stationary application of a BESS made of the retired PHEV Li-ion battery to a residential nZEB, equipped with a photovoltaic power plant by an integrated approach based on load match considerations and life-cycle environmental impacts.

The main goal of the research is to identify the best trade-off between the BESS size and the associated environmental impacts in a life cycle perspective and to assess the potential benefits related to the employment of BESS made of retired EV batteries in substitution of new batteries.

In line with this goal the research proposed addresses:

- the detailed analysis of the potential life cycle environmental impacts related to the Lithium-ion battery production;
- the detailed modelling of the operational phase based on the analysis of available real high-resolution data of PV electricity generation and building load. The modelling is carried out considering the remaining performance of the battery after the first life in the EV and its degradation during the use phase;
- the detailed analysis of the potential environmental impacts and benefits (due to the production of secondary raw materials) at the battery's EoL.

2 State-of-the-art

In this chapter, it is illustrated a literature review on the LCAs on traction Lithium-ion batteries suitable for applications in PHEV and BEV and on the reuse of the retired EV Lithium-ion batteries as stationary storage system.

2.1 Life cycle assessment of Lithium – ion traction batteries

Several LCA studies on traction Li-ion battery suitable for applications in PHEV and BEV are available in the literature. In this section, some of these are analysed in order to identify the source of inventory data, the methodological assumptions and key issues and, their environmental hot spots.

The comparison of studies is complex because they are very heterogeneous [116] differing on the assumptions, in terms of both method (e.g. system boundaries) and battery characteristics (e.g. cathode and anode composition). Then, in this section the comparison of results focuses on the production phase, since this is generally the phase more precisely assessed and less affected by the variability of assumptions regarding the operation and EoL stages [59]. Moreover, only the impacts on global warming potential are considered, since this is the only impact category reported in all of the reviewed studies and, additionally, it is estimated using the same impact assessment method [119].

Kim et al. [120] carried out an LCA of a 24 kWh LMO-NMC traction battery for BEV. The assessment was based on the BoM and primary data from the battery industry, i.e. energy and materials input data from the battery cell and pack supplier.

Ellingsen et al. [54] performed an LCA of a Li-ion battery pack for use in BEVs. The components of the battery pack have been grouped into four main components: battery cells, packaging, cooling system and BMS. The battery cells were made with a cathode based on $LiMn_{1/3}Ni_{1/3}Co_{1/3}O_2$ and an anode based on graphite. The FU was chosen as one traction battery. The BoM of the cells, the cooling system, the battery management system, the battery packaging and the energy required for battery and cell assembly were provided by battery producer [121]. The inventory to model the cathode material was inferred from Majeau-Bettez et al. [65]. The LCI data for the materials and processes in the background system are taken from the Ecoinvent database [122] and Hischier et al. [123].

Li et al. [124] carried out an LCA of high capacity Li-ion battery for EVs. The battery cells were made with a cathode based on $LiMn_{1/3}Ni_{1/3}Co_{1/3}O_2$ (NMC) and an anode based on silicon nanowires (SiNW). The FU was selected as one average kilometre driven by an EV powered by the LIB pack under average U.S. operating conditions. The LCI analysis of the anode and cell manufacturing are conducted using process-based LCA method, with the SiNW synthesis data collected from author's lab experimentation and the Li-ion battery cell manufacturing data collected from the industrial LIB cell prototyping facilities (Johnson Controls' advanced battery lab). The LCI data for other stages are retrieved from GaBi professional database.

U.S. EPA [125] presented a LCA study of Li-ion batteries used in BEVs and in PHEVs. The analysed battery chemistries were: LMO ($LiMnO_2$) and NMC ($LiNi_{0.4}Co_{0.2}Mn_{0.4}O_2$) for which primary data were provided by manufactures; and LFP modelled using secondary data [65]. The anodes are composed of graphite. In order to protect the confidential data provided by manufactures and researcher, the authors provided the bill of material (BoM) for an average Li-Ion battery indicating for each component a range in weight. Through the manufacturers, suppliers, and recyclers in the partnership, primary data were obtained for the component manufacture, product manufacture, and EoL stages. Secondary data, needed to supplement data gaps and protect confidential data, were primarily obtained from Notter et al. [69] and Majeau – Bettez et al. [65]. LCI data available within GaBi database[2] were also used for upstream materials and fuel inputs, as the scope of the project and resources were limited to collecting primary data from the product manufacture and recycling stages. The analysed battery packs included the battery cells, battery management system (BMS), battery pack and passive cooling system.

Hawkins et al. [58] carried out a LCA with the aim to compare the environmental impacts of an EV and an ICEV over their entire life cycle. The FU is 1 kilometre (km)[2] driven under European average conditions. The EV powertrain configurations were modelled roughly after that of the Nissan Leaf EV. Two 24 kWh Li-ion EV were analysed. The analysed battery chemistries were: NMC and LFP. Battery inventories were adapted from Majeau-Bettez et al. [65], while Ecoinvent v2.2 [126] was used as a background dataset.

[2] http://www.gabi-software.com/international/databases/

Majeau-Bettez et al. [65] presented the LCA of two lithium ion batteries for plug-in hybrid and full performance electric vehicle. The positive active materials for the Li-ion battery are $LiFePO_4$ (LFP) and $LiNi_{0.4}Co_{0.2}Mn_{0.4}O_2$ (NMC), while the negative active material is composed of graphite. 50 MJ of energy accumulated by the battery and delivered to the powertrain is selected as FU (moreover authors provided the results with reference to the battery mass and nominal energy capacity). The authors compiled the iLCIs for NCM and LFP battery packs by combining electrochemical studies, dismantling reports, and industry figures, and the inventories reported in Gains and Cuenca [127], Schexnayder et al. [51]. The LCI data for the materials and processes in the background system are taken from the Ecoinvent 2 database [122] assuming average European conditions. A process – specific manufacturing energy requirement is compiled taking as starting point the energy inventory compiled by Rydh and Sandén [128], while direct water, transport and infrastructure input are taken from Hischier et al. [123].

Zackrisson et al. [64] performed a LCA study of two 10 kWh LFP batteries for PHEVs using two different solvents, water and N-methyl-2-pyrrolidone (NMP), in the cathode. The functional unit is defined as a battery with an energy capacity of 10 kWh able to sustain 3000 charge cycles at 80% maximum depth of discharge (DoD). The assessment was carried out using both primary and literature data. In detail, the mass of the cell materials was modelled based on literature references [127] and laboratory tests, and the energy needed for cell manufacturing and module and battery assembly was approximated from battery industry report (Saft annual report [129]). The LCI data for the materials and processes in the background system are taken from the Ecoinvent database [122]. The authors provide the weights of cell materials used in both analysed configurations.

Notter et al. [69] provided a detailed inventory for a traction lithium-ion battery for BEVs using $LiMn_2O_4$ as positive active material. The mass used for the calculation are based on a battery produced by Kokam Company[3]. The functional unit of the study is one average kilometre driven by a vehicle with electric drivetrain and Li-ion batteries on the European road network. LCI data for the battery production and for the production and use of an EV are compiled specifically for the study, while LCI

[3] http://kokam.com/

data for the materials and processes in the background system are taken from the Ecoinvent database [122].

Samaras and Meisterling [57] performed an LCA analysis of an HEV with a Li-ion battery weighing 16 kg, and of a PHEVs with a Li-ion battery weighing 75–250 kg, depending on electric range considered, ranging from 30 km to 90 km. The FU of analysis is 1 km of travelled range. The employed battery is characterized by a metal oxide-based cathode (Co, Mn, Al) and carbon anode (graphite). Data on primary energy use for battery production, resource extraction and processing, and recycling are inferred from Rydh and Sandén's [128,130].

Matheys and Autenboer [131], **Van den Bossche et al.** [52], **and Matheys and Timmermans** [132] performed an LCA of five traction battery technologies for BEVs and PHEVs: lead – acid (PbA), nickel cadmium, nickel-metal hydride, lithium-ion, sodium-nickel chloride (NaNiCl). The functional unit correspond to a battery enabling the car to cover a specific range, with one charge. The use phase is modelled including the energy to move the car, the additional energy do to the battery efficiency and the additional energy due to the battery mass of the battery. The recycling of the discharged battery and the final disposal or incineration. The studies does not provide information on the battery chemistries and on the inventory data used for battery production and EoL modelling.

Ishihara and Kihira [133] perfomed an LCA of four types of 2-4 kWh lithium-ion battery modules, for stationary and EV applications. Two different cathode materials are considered: Nickel – cobalt and manganese. The functional unit of the assessment is 1 kWh of energy capacity and the system boundaries include the production, collection, recycling and waste disposal. The recycling is based on metallurgical process.

The main battery characteristics, system boundaries, inventory data source and the global warming potential of the battery production process per kWh reported in the studies examined are listed in Table 3**.**

Table 3 LCA studies on traction Lithium-ion batteries.

References and year of the study	Battery characteristics	System boundaries	Battery data sources	GWP associated with the production phase per kWh of battery energy capacity
Kim et al., 2016 [120]	BEV Lithium-ion traction battery; cathode: LMO–NMC; anode: graphite; energy capacity: 24 kWh	Materials production, cell and component manufacturing, and battery pack assembly, including transportation	Primary data from battery industry	140 $kgCO_{2eq}$
Li et al., 2014 [124]	BEV Lithium-ion traction battery; cathode: NMC; anode: SiNW; Weight: 120 kg; energy capacity: 43.2 kWh	Resource extraction, material processing, component manufacturing, battery manufacturing, battery use, and recycling (current recycling technologies including direct physical recycling, hydrometallurgical and pyrometallurgical recovery)	Own primary data, US-EPA [125]	N.A.
Ellingsen et al., 2014 [54]	BEV Lithium-ion traction battery; cathode: NMC; anode: synthetic graphite; energy capacity: 26.6 kWh	Materials production, cell and battery manufacturing	Own primary data from battery manufacturer + literature data [65]	172 $kgCO_{2eq}$ (cell assembly 586 MJ/kWh); 240 $kgCO_{2eq}$ (cell assembly 960 MJ/kWh); 487 $kgCO_{2eq}$ (cell assembly 2318 MJ/kWh)
Hawkins et al., 2013 [58]	BEV Lithium-ion traction battery; cathode: NMC; anode: graphite; energy capacity: 24 kWh BEV Lithium-ion traction battery; cathode: LFP; anode: graphite; energy capacity: 24 kWh	Battery production, battery EoL (dismantling and a cryogenic shattering process) together with all relevant supply chains	Literature data [65] [123]	N.A.
US EPA, 2013 [125]	BEB BEV Lithium-ion traction battery; cathode: LMO, LFP, NMC; anode: graphite; energy capacity: 40 kWh PHEV Lithium-ion traction battery; cathode: LMO, LFP, NMC; anode: graphite; energy capacity: 11.6 kWh	Battery production, use in the EV, recycling (hydrometallurgical, pyrometallurgical, direct recycling processes)	Own primary data + literature data [69] [65]	112 $kgCO_{2eq}$

Majeau-Bettez et al., 2011 [65]	BEV and PHEV Lithium-ion traction battery, cathode: LFP, NMC; anode: graphite	Production of all battery components including BMS, the battery assembly and the battery use	Own primary data + literature data [128] [51] [127]	NMC 200 $kgCO_{2eq}$ LFP: 250 $kgCO_{2eq}$
Zackrisson et al., 2010 [64]	PHEV Lithium-ion traction battery, cathode: LFP (NMP as a solvent) PHEV Lithium-ion traction battery, cathode: LFP (water as a solvent); anode: graphite; energy capacity: 10 kWh	Materials production, the battery manufacturing, the use in the car (electricity related to internal battery efficiency and the extra electricity needed to carry the weight of the battery) and the collection for recycling	Literature data [127] [123] + manufacturer data report [129]	266 $kgCO_{2eq}$ (NMP as a solvent); 166 $kgCO_{2eq}$ (water as a solvent)
Notter et al., 2010 [69]	BEV Lithium-ion traction battery, cathode: LMO; anode: graphite; energy capacity: 34.2 kWh	Production, maintenance, EoL and operation of the Li-ion battery	Own primary data (battery produced by Kokam Company [134])	52.6 $kgCO_{2eq}$
Samaras and Meisterling, 2008 [57]	PHEV Lithium-ion traction battery; cathode: NiCoAl; anode: graphite PHEV Lithium-ion traction battery; cathode: NiCoAl; anode: graphite PHEV Lithium-ion traction battery; cathode: NiCoAl; anode: graphite	Resource extraction, material processing, assembly	Cell, materials and assembly based on literature data [128]	120 $kgCO_{2eq}$
Matheys and Autenboer, 2006 [131]	BEV Lithium-ion traction battery; energy capacity: 11.5 kWh	Raw material extraction, processing of materials and components, use of the battery in the vehicle, the recycling of discarded batteries, the final disposal or incineration	N.A.	N.A:
Ishihara et al., 2002 [133]	BEV Lithium-ion traction battery module; cathode: Ni/Co, Mn; anode: N.A; energy capacity: 2-4 kWh-class	Material production, battery production, transport (collection after use), recycling, waste disposal, credits from recycling	N.A.	75 $kgCO_{2eq}$

The literature examined highlights the difficulty of carrying out an LCA of Li-ion battery production relying on only primary inventory data for foreground processes, i.e. those processes that the decision maker or the product's owner can influence directly [135]. The amounts of original LCI are limited and numerous studies use or re-compile LCI from other works. Therefore, a deeper analysis of the battery components is needed, paying particular attention to the battery cells. As the review shows, these are the components mainly responsible for the battery's environmental impacts.

Concerning the lithium-ion technology, among the studies summarized in this section, three considered LMO technology, five considered NMC technology, four LFP technologies, one NiCoAl technology, and one study referred to LMO–NMC technology. Moreover, only five LCAs provide the contribution analysis of the cell materials based on primary data, i.e. Ellingsen et al. [54] for NMC technology, US EPA [131] for LMO and NMC technologies, Majeau-Bettez et al. [65] for NMC and LFP technologies, Zackrisson et al. [64] for the LFP technology and Notter et al. [69] for LMO technology.

Regarding the modelling of the EoL phase, pyrometallurgical or hydrometallurgical processes are assumed in the studies reviewed. However, among the LCAs examined [69,87,95,125], only Richa et al. [104] provide a detailed description of the recycling process, modelled on the basis of a pyrometallurgical process for 50% of the EoL Li-ion cells and a hydrometallurgical one for the remaining 50%, and of the related impacts and benefits. Furthermore, several LCAs do not include the EoL phase in the analysis because of the greater uncertainty (mainly due to lack of data) [54,60,65,120,136].

2.2 Life Cycle assessment on second life stationary applications of retired EV batteries

Several LCAs on the second use of EV batteries as energy storage system in stationary applications are available in the literature. Some of these are analysed in this section in order to identify the methodological issues and the key drivers of uncertainty.

Many factors determine the environmental sustainability of the second use of EV batteries in stationary energy storage applications. Then, multiple aspects should be considered in the LCA model in order to provide a complete and reliable assessment. The main methodological aspects and assumptions of the some examined LCAs are listed in Table 4.

The LCAs applied to second use of EV batteries are characterized by different methodological assumptions concerning the functional unit (Table 4), the system boundaries, allocation procedure[4], etc. Further, they rely on different inventory data (i.e. primary data versus secondary data).

Concerning the system boundaries three different options are identified in the examined studies. Some of them considered all life-cycle stages of the EV battery (car manufacturing, using the battery both in a car and in second use, and recycling) [95,104]. Differently, Faria et al. [87] and Sathre et al. [99] included only the stages directly related to the second use of the EV battery; therefore, only the energy impacts of battery charging were considered in the environmental assessment of the second use, whereas the impacts of the manufacturing and EoL stages were fully considered for the first use.

The repurposing stage entails collecting the battery after it has been used in an EV, and may involve disassembling the battery to the module/cell level and testing the health of the battery/modules/cells [9,33]. Faria et al. [87] did not assess any impacts related to repurposing. Canals Casals et al. [95] considered the impacts of materials for repurposing negligible, whereas Sathre et al. [99] did not take into account the energy for testing, since tests are already carried out at local car dealerships. Other studies assumed both the substitution of some components and the energy needed for tests [104] or specific cell failure rates and pack recovery rates [60]. Concerning the methodological aspect of the allocation, five different options are identified. In Faria et al. [87] and Casals et al. [95] no environmental impacts are allocated to the second life application as, according to the authors, the

[4] Rule for partitioning the impact of the battery production and EoL phases between the first and the second battery application

primary function of the battery pack is to be used in the EV; in Richa et al. [104] the allocation is based on three different rules: market price, energy storage and equally divided. In Ahmadi et al. [88] and Casals et al. [95] the system investigated included both the first and the second life of the EV battery, then allocation was not necessary; in Bobba et al. [89] two different options are investigated: 0% and 25% of the environmental impacts related to battery production and EoL treatment allocated to the second life application.

Concerning the operational phase, according to Bobba et al. [89], in the literature the modelling is often based on average data or previous studies [87,88,95,104]. Moreover, based on author knowledge, only Bobba et al. [89] proposes a detailed energy model of the system investigated including both the battery capacity and efficiency degradation in a time-step modelling of 15 minutes. Primary data on the PV generation are used, while data on the building load were generated through the ResLoadSIM tool[5].

Battery degradation is a significant factor for EV batteries. All batteries experience calendar aging, a gradual decomposition of the electrolyte for a given temperature over the life of the battery simply to basic material degradation. However, the cycling of batteries accelerates their degradation especially if the thermal cycling is not closely controlled [60]. The battery degradation results in capacity fade, but also in charge/discharge efficiency fade. The battery lifetime should be estimated according to the battery degradation, which depends on both the battery’s initial characteristics (e.g. first lifetime, residual capacity, battery efficiency, etc.) and the second-use specific conditions (e.g. load profile, temperature, etc.). The lack of data in this field is reflected by the fact that the lifetime of the battery during its second-use is based on manufacturer warranties [60,87].

This literature review pointed out the complexity of the topic and its novelty. To assess the environmental performances of second-use of repurposed EV batteries, multiple aspects should be considered in order to provide a complete assessment and to ease the comparison between EV batteries to be used in different applications. Moreover, lack of data availability strengthens the need of improving the data collection concerning all the life-cycle stages, focusing especially of the use stage.

[5] https://ses.jrc.ec.europa.eu/power-system-modelling.

Table 4 LCA studies on second use of the EV batteries.

References	Battery chemistry, second use application and sizing	Methodological assumption	Energy modelling parameters
Bobba et al. [89]	• Chemistry: Lithium-ion (LMO-NMC) [118]; • Application: Increase of self-consumption in a residential building equipped with a PV system; • Sizing: it was assumed the installation of one battery pack.	• FU: average yearly energy balance of the building examined; • System boundary: battery production, re-purposing, second use in stationary ESS, EoL; • Allocation*: 0% (base case); 25% (for sensitivity analysis).	• PV generation: primary data (15 min resolution for 1 year); • Building load: ResLoadSIM software (time resolution 1 min); • Retained battery capacity after the first life in the EV: primary data based on laboratory test. • Energy flows: detailed energy simulation of the system (time resolution 15 min); • Battery capacity degradation: linear degradation during the use phase based on laboratory data and literature data; • Battery efficiency: linear degradation during the use phase based on literature data; • Battery lifetime in second life application: based on residual capacity after fist life, battery capacity degradation and battery capacity end of life.
Ahmadi et al. [88]	• Chemistry: Li-ion; • Application: daily peaking power delivery (no further detail are available); • Sizing: it was assumed the installation of one battery pack.	• FU: total electricity delivered by the battery during the first and second life; • System boundary: battery production, use in the EV, re-purposing, second use in stationary ESS, EoL; • Allocation: not applicable**.	• Building load: (no detail are available); • Retained battery capacity after the first life in the EV: based on literature; • Energy flows: simplified energy model based on the daily energy required; • Battery capacity degradation: not considered in the energy model; • Energy efficiency: considered constant in the energy model; • Battery lifetime: average lifetime based on the literature.
Casals et al. [95]	• Chemistry: Li-ion; • Application: Energy arbitrage; no grid connected stationary application (RES + ESS); grid connected system with RES (no further detail are available). • Sizing: It was assumed the installation of one	• FU: energy (kWh) received by the consumer directly from the battery; • System boundary: battery production, use in the EV, re-purposing, second use in stationary ESS, EoL. • Allocation: not applicable**.	• Retained battery capacity after the first life in the EV: calculated based on assumption on temperature, C-rate, average state of charge (SoC), number of cycle and DoD; • Energy flows: no detail available • Battery capacity degradation: not considered in the

	battery pack.		energy model; • Energy efficiency: constant value; • Battery lifetime: calculated based on assumption on temperature, C-rate, average SoC, number of cycle and DoD.
Richa et al. [104]	• Chemistry: Lithium-ion [137]; • Application: stationary application (no further detail are available). • Sizing: stationary ESS able to deliver 150 kWh of energy on a daily basis.	• FU: delivering 150 kWh of energy on a daily basis for 20 years; • System boundary: battery re-purposing, second use in stationary ESS, EoL; • Allocation*: 1) energy storage – based; 2) market price – based; 3) 50%.	• Retained battery capacity after the first life in the EV: based on literature. • Energy flows: simplified energy model based on the daily energy required. • Battery capacity degradation: linear degradation during the use phase based on own assumption; • Battery efficiency: linear degradation during the use phase based on own assumption; • Battery lifetime: own assumption.
Faria et al. [87]	• Chemistry: Lithium-ion (LMO) [69]; • Application: Peak shaving and load shifting in a residential building. • Sizing: It was assumed the installation of one battery pack.	• FU: electricity required by the building during the battery lifetime; • System boundary: battery re-purposing, second use in stationary ESS, EoL; • Allocation*: 0%.	• Building load: literature data; • Battery capacity degradation after the first life based: on literature data; • Energy flows: simplified energy model based on building load. • Battery capacity degradation: linear degradation during the use phase based on own assumptions. • Battery efficiency: constant value; • Battery lifetime in second life application: based on residual capacity after fist life, battery capacity degradation and battery capacity end of life.

*Percentage of the battery production and EoL impacts allocated to the second application; **The system investigated includes both the first application in the EV and the second application as stationary storage system, then allocation is not necessary.

3 Case study: description of the examined system

In this chapter, the examined system is described. It consists of a PV plant, a BESS and the electrical grid (PV plant + BESS + electrical grid). Its function is to provide electricity in a nearly zero energy building. The BESS is made by using retired Li-ion EV battery pack.

In the first part of this chapter, the EV battery pack used as stationary energy storage system is described. In detail, both the characteristics of the fresh and retired battery pack are illustrated. In the second part, the PV plant characteristics and the monitored data of the electricity generated are presented. Finally, in the third part, the building, in which the operational phase of the examined system is modelled, is described.

3.1 The battery energy storage system (BESS)

The BESS examined is made of a retired Lithium-ion (Li-ion) battery pack used in a Mitsubishi Outlander LEV40 LMO–NMC PHEV (Figure 13) [89,118].

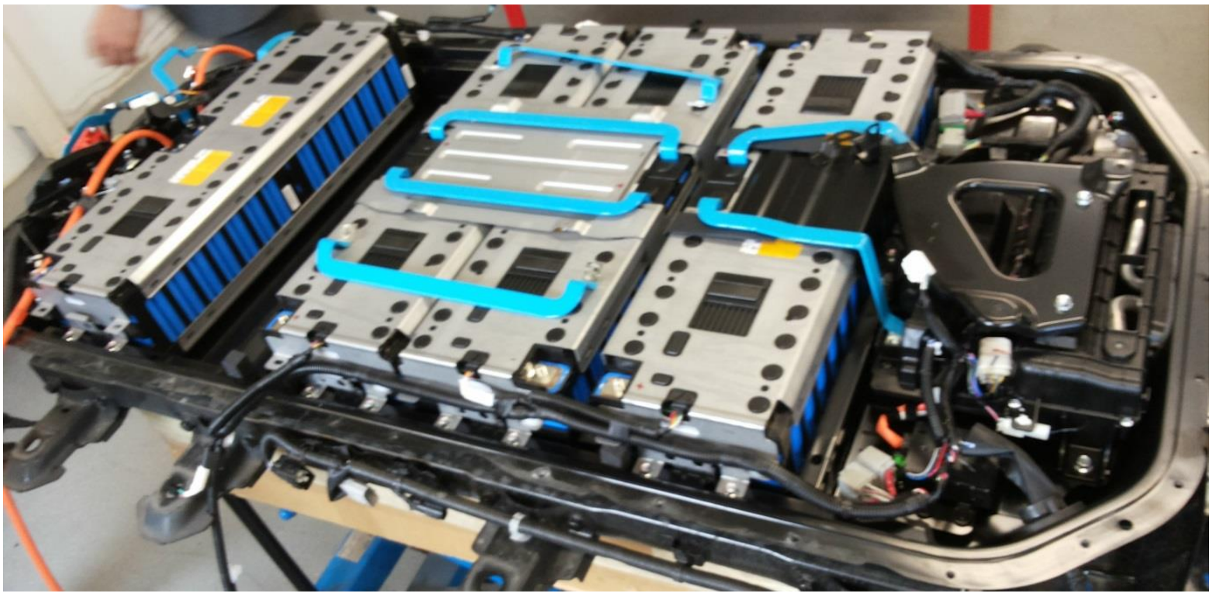

Figure 13. Mitsubishi Outlander PHEV battery pack.

According to Ellingsen et al. [54], the battery components are classified as battery cells, BMS, cooling system and battery packaging (Figure 14).

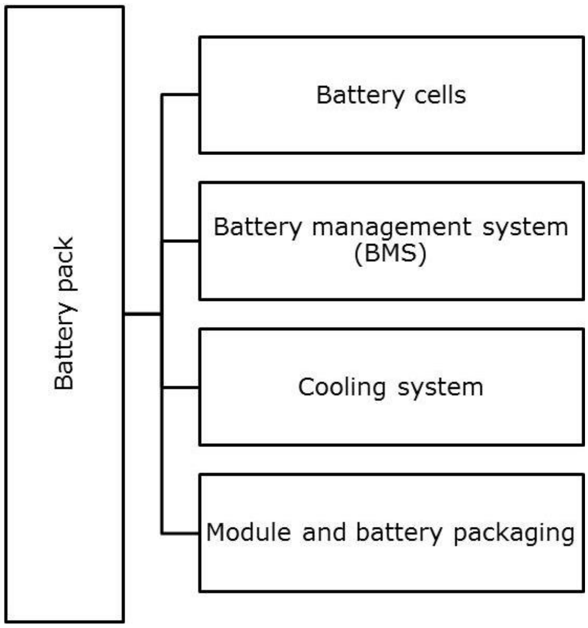

Figure 14. Battery pack components.

The battery cells are the electrochemical units of the battery. They contain the electrodes (cathode and anode), the separator and the electrolyte packet enclosed in the cell case. The cathode is composed of a positive current collector with a coat of positive electrode paste. The positive electrode paste is composed of a positive active material, a binder and carbon black, which improves conductivity. The cathode releases lithium ions to the anode during charging and receives lithium ions during discharging. The anode is composed of the negative current collector with a coat of negative electrode paste that consists of a negative active material and a small amount of binder. The anode receives lithium ions from the cathode during charging and releases lithium ions during discharging. The electrolyte is the medium through which the charge is transferred in the cell. The separator separates the cathode from the anode to prevent short circuits between them. It has a microporous polymer membrane allowing Li ions to pass through the pores.

The BMS manages the battery cells to ensure that they operate within safe parameters, and it includes electronics boards, fasteners and high- and low-voltage systems.

The cooling system ensures that the battery cells work in a safe-operating temperature range. Finally, the battery packaging serves as a structural support.

The battery pack examined is made of 80 battery cells connected in series and grouped into 10 modules. Each battery cell is made with a composite cathode based on lithium manganese oxide – nickel manganese cobalt cathode (LMO-NMC) and a graphite carbon anode.

The concept of composite electrodes promises to combine the merits of several active materials into a hybrid electrode for optimized performance [138–140]. In fact, LMO (spinel), with a three-dimensional structure and Li-ion diffusion, offers high rate capability and good structural stability [141], as well as relatively low production costs [140]. However, it has a relatively small capacity (around 100–150 Wh/kg) and a cycle life of about 300–700 [142], and it can degrade if manganese (Mn^{2+}) dissolves in the electrolyte and is subsequently deposited on the anode in the charge regime. NMC has a greater capacity (150–220 Wh/kg) and a cycle life of about 1000–2000 [142,143] but can suffer from structural and/or chemical instabilities during cycling [141]. Moreover, although Lithium-ion–cobalt chemistries perform better than other Lithium-ion technology, cobalt is on the list of critical raw materials for the European economy [72,144] because of its economic importance and the risks associated with its supply. The LMO–NMC composite cathode is a compromise to provide an electrode that exhibits good performance in terms of capacity and structure stability: the LMO part of the battery provides a high boost of current on acceleration and the NMC part gives a long driving range [142]. Moreover, this chemistry can guarantee a lower price and less vulnerability to supply disruption because of its lower levels of cobalt, which is the most costly item [76]. Various EVs, such as the Nissan Leaf, Chevy Volt and BMW i3, have adopted the LMO–NMC chemistry [142].

The main characteristics of the fresh LMO-NMC Lithium-ion PHEV battery pack are illustrated in Table 5. The detailed description of each component of the examined LMO-NMC cell is reported in Section 5.3.2.1.

Figure 15 shows the battery pack examined with an indication of the placement of the 10 modules, with a closer view of one module with its eight cells. The approximate location of the air cooling heat exchanger is also shown, while the BMS is embedded and distributed in the pack.

The battery pack under investigation was disassembled from a Mitsubishi Outlander PHEV, after it had driven 136,877 km [89,107].

Table 5. Technical characteristics of the fresh battery pack [89,118,145].

Characteristics	**Battery pack**
Battery cell technology	Li-ion (LMO-NMC)
Nominal voltage (V)	300
Nominal capacity (Wh)	11,400
Battery round trip efficiency (%)	98
Number of cells	80 (grouped in 10 modules)
Type of cell	Prismatic
Weight of the cells (W_c) (kg)	105.6
Weight of the battery pack (kg)	175

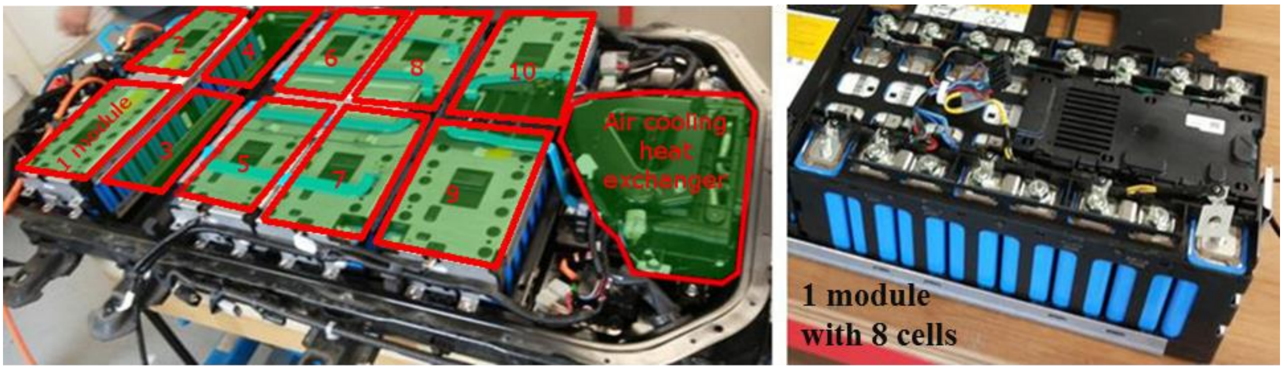

Figure 15. Left, battery pack; right, battery cells grouped into one module.

Aged and fresh LMO – NMC cells were purchased and tested by the Joint Research Centre (JRC) in order to evaluate the performance of the cells after the first use in the EV compared to the fresh cells. The rated capacity of the fresh battery cell is 38 Ah. Concerning the aged battery cell, the capacity recorded by the BMS after the first use in the EV, and then available for the stationary second life applications, is 30.91 Ah. Thus, the residual capacity of the aged cells results equal to 81.31% of the nominal capacity of the fresh battery cells.

The capacity of the aged and fresh battery cells under investigation are illustrated in Table 6. During the use phase, in both stationary or mobile applications, battery cells undergo in a degradation mechanism that can contribute to either capacity fading or power fading, or both of them [146]. The aging of a battery cell occurs due to the electrochemical degradation processes that take place during the operation phase, called cycling aging, and also to processes that lead to a degradation of a battery cell independent of charge-discharge cycling, called calendar aging [87,147]. The aging process leads to an increase of the internal resistance and to a reduction of the battery cell performance.

Table 6. Capacity of the fresh and aged Li-ion battery cells investigated.

Characteristics	**Aged battery cell**	**Fresh battery cell**
Battery cell capacity [Ah]	30.91	38

The performance of the battery cells were assessed through an experimental campaign designed for the both fresh and aged cells in order to evaluate the calendar and cycling aging under different conditions and duty cycles, for first EV life and the potential stationary second use in utility grid applications.

The experimental campaign was performed within the SASLAB (Sustainability Assessment of Second Life Application of Automotive Batteries) project[6].

Table 7 illustrates the planned experimental and their status of achievement at the end of SASLAB project [107].

Table 7. Planned experimental test in the context of SASLAB project [107].

Type of test	**Scope of the test**	**Chemistry and number of samples**	**Conditions**	**Expected duration**	**Situation (July 2018)**
Calendar ageing	Assess the degradation of cells without charging or discharging	6 aged and 6 fresh LMO-NMC/graphite cells	Temperature: 25°C and 45°C; SoC: 100% and 50%	As long as possible	Completed as planned. Still running for long term assessment
Cycle ageing (charge/discharge at CC-CV/CC)	Assess the degradation of cells with 100% DoD at C/5 and 1C rate	2 aged and 2 fresh LMO-NMC/graphite cells	Temperature: 25°C and 45°C	6 months	The C/5 series is not completed as planned, 3 month performed. The 1C series not running
Automotive use cycle ageing (WLTC driving duty cycle)	Assess the degradation of cells for automotive applications	2 aged and 2 fresh LMO-NMC/graphite cells	Temperature: 25°C	3 months	Not running. Possibly to be cancelled
Second use cycle ageing (duty cycles: PV firming; PV smoothing; primary frequency regulation; peak shaving)	Assess the degradation of cells for second use applications	28 aged LMO-NMC/graphite cells	Temperature: 25°C, 45°C and 5°	6-9 months	Almost 2 months performed and still running (since November 2017) for 25°C and 45°C (23 samples). Not running the 5°C (5 samples)

[6] SASLAB is an exploratory project led by JRC under its own initiative in 2016-2017, aims at assessing the sustainability of repurposing EV batteries to be used in energy storage applications from technical, environmental and social perspectives

With reference to the calendar aging, LMO-NMC aged and fresh Mitsubishi cells were kept under different conditions to assess the calendar ageing process: at a temperature of 25°C or 45°C and at 100% or 50% SOC following the standard of the International Electro-technical Commission (IEC) 62660-1:2010, 2011 [148].

For designing the experimental procedures to assess the ageing process associated to cycling, several standards and protocols were consulted [148–152].

Results that are relevant inputs to the environmental assessment model are the average energy capacity degradation for the cells calendar aged at temperature of 45°C and 100% SOC resulted of - 0.11 Wh/day [107] and the Round Trip Efficiency (RTE) at the beginning of the second life: around 95%. These data are used in the energy simulation of the PV plant + BESS + electrical grid system.

3.2 The photovoltaic system

The PV system consists of 115 grid-connected polycrystalline silicon panels and it is located in S. Angeli di Rosora (Marche, Italy). The peak power of the PV system is approximately 20 kW_p; the system covers, overall, approximately 150 m^2. Each module has a declared efficiency of 12%. The panels are arranged in nine strings and are connected to three inverters.

The geographical and climate data are summarized in Table 8 [153].

Table 8. Geographical and climate data.

Parameters	**Value**
Latitude	43°28′ N
Longitude	13°04′ E
Altitude (m)	130
Minimum and maximum annual temperature (°C)	-5; 37
Mean annual humidity (%)	67
Mean annual horizontal solar radiation (W/m^2)	302

The solar radiation maximum and average values for horizontal radiation are shown in Figure 16.

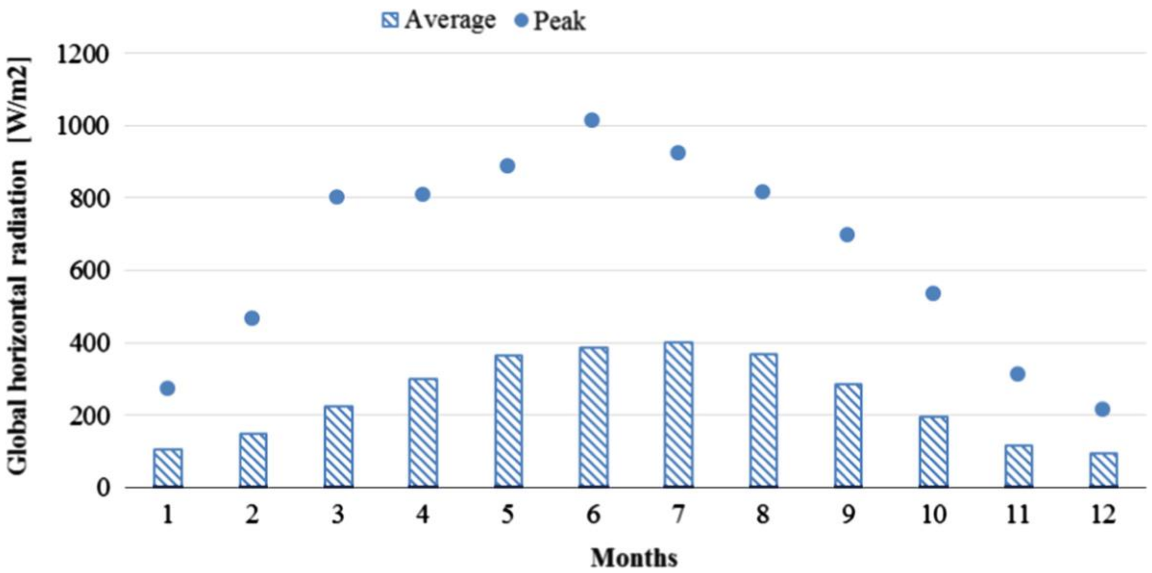

Figure 16. Horizontal solar radiation trends for the site of the case study [154].

The yearly PV electricity generation is about 25 MWh. The on-site electricity generation is estimated through a one-year monitoring activity carried out in 2010. The data collected are illustrated in Figure 17.

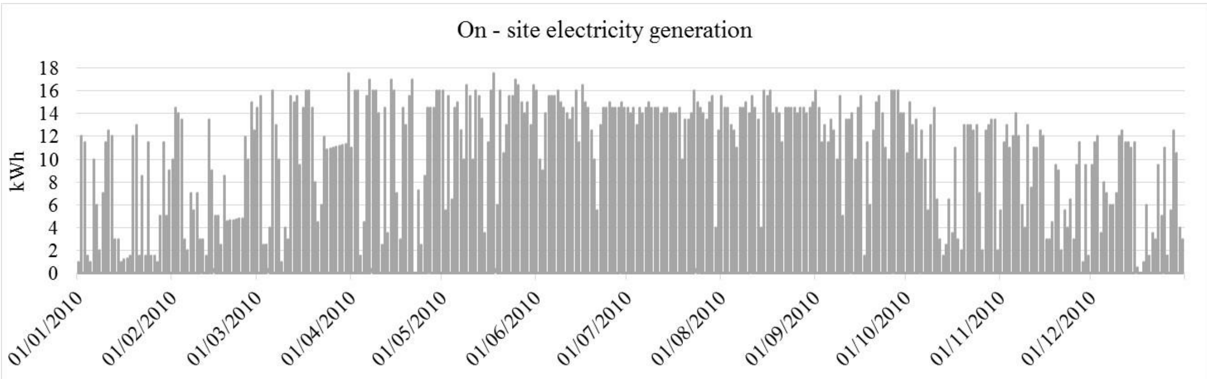

Figure 17. On – site electricity generation from PV power plant in 2010.

3.3 The Leaf House

The PV – BESS – electrical system is simulated as installed in an Italian nearly zero energy building called “Leaf House” (LH) [154]: a single house located in S. Angeli di Rosora (Marche, Italy) (Figure 18). The LH is built according to the Italian requirements of the energy regulation in force, integrating different sources of renewable energy.

The building is south oriented (latitude 43°28'43.16 N, longitude 13°04'03.65 E), the altitude is 130 m. The site is characterized by a moderate climate, in detail:

- minimum annual temperature is -5°C;
- maximum annual temperature is 37°C;
- mean annual humidity is 67%;
- mean annual horizontal solar radiation is 302 W/m^2.

The building is composed by three levels; every one contains a couple of twin flats. Its net conditioned floor area is 477 m^2. Four apartments are occupied by two people each, while two apartments are only occasionally occupied. Each flat at the ground and the first floors measures 85.39 m^2, while the second floor flats measure 70.1 m^2 each.

Figure 18. The LH south façade.

The ground and first floors (Figure 19-a) comprise two symmetrical flats, and the second one is made of two offices (Figure 19-b).

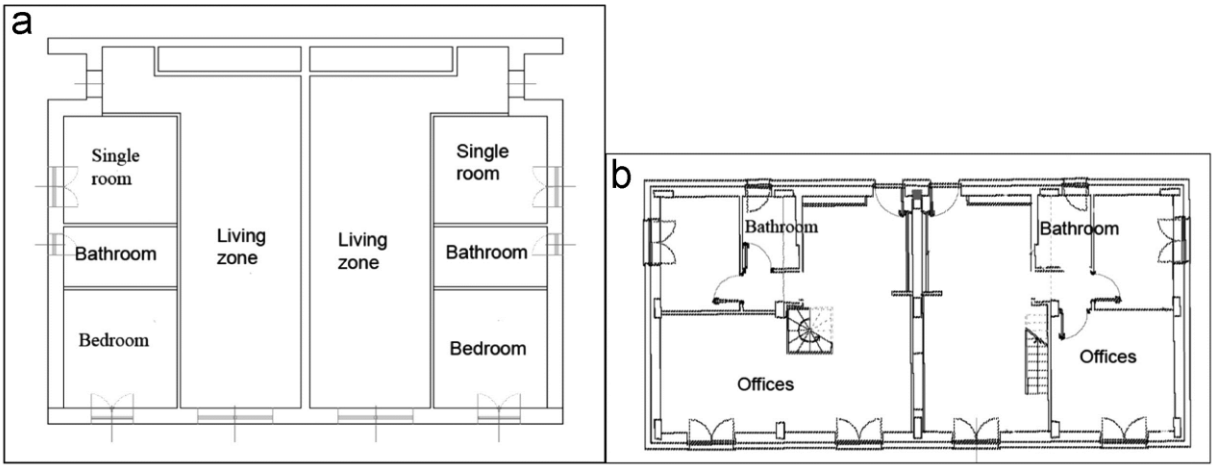

Figure 19. (a) Ground and first floor of the Leaf House. (b) Second floor of the Leaf House (scale 1:200) [155].

The LH energy system includes seven sub-systems:

- the solar collector system;
- the geothermal probes;
- the heat pump;
- the air handling unit (AHU);
- the auxiliary boiler;
- the photovoltaic system;

In detail, the heat generation is carried out by a geothermal heat pump (GHP), which has an energy efficiency ratio (EER) of 4.6 and is connected to 100 m long vertical probes, the solar thermal collectors and the auxiliary boiler. Each flat is heated by means of a radiant floor supplied by the GHP. The indoor air temperature is controlled by a regulation system that is able to check the hot water flow through each tubing loop. Zoning valves and thermostats optimize the performances of the heat delivery system. In winter, the water that circulates in the tubing has a temperature of 25–28 C. In the heating season, the solar system is integrated by the GHP in heating mode in order to reach around 40 C in the upper part of the storage tank, thus allowing the production of domestic hot water (DHW) and of water for feeding the radiant floors from the middle area of the tank. Therefore, DHW is heated and then collected in a smaller secondary tank, connected to the auxiliary gas boiler. The geothermal circuit is connected to a free-cooling heat exchanger during summer. Thus cooling is provided by the GHP and, to a small extent, rooms can be free-cooled with the water provided by a ground-coupled heat exchanger, during the start-end of the cooling season. In summer, the solar system fulfils the

DHW requirement, and the GHP is used in cooling mode to produce cold water at 15–18 C with mixing valves, for feeding the radiant floors. The ventilation rate is automatically provided according to a fixed level of CO_2: suitable sensors activate the system when the CO_2 concentration is higher than the set point value, while others stop the mechanical ventilation when the windows are open. The efficiency of the heat recovery system is about 80%.The air handling unit (AHU) supplies the air in rooms and a heat recovery system receives air before the expulsion outdoor. The outer air is naturally pre-conditioned (heated in winter and cooled in summer) through a 10 meter long underground duct placed before entering the air into the AHU. The solar thermal system (seven collectors of 1.44 m^2 each) is installed to integrate the GHP in the DHW generation. The heat is transferred from the solar collectors to the internal heat exchanger of the storage tank by means of a glycol-water mixture, a pump drives the fluid back to the collectors. The difference between the outlet water temperature of the solar panels and the water inside the storage tank is less than 10 degrees; otherwise, the pump is turned off.

The electricity requirement of the LH is supplied by the grid-connected PV system described in Section 3.2.

A proper monitoring system records the energy and environmental data of all rooms of the six apartments. LH monitoring is performed by sensors and actuators that are integrated with drivers and allow communication between devices and systems. The sensors are classified into the following three primary groups: room sensors (e.g., CO_2 concentration, air temperature and humidity), thermal plant sensors (e.g., thermal energy metres, water flow metres, etc.) and weather station sensors. All data are normalised and stored in a database.

The average yearly electricity consumption of the building was about 25 MWh, in 2010. The highest contribution to the electricity use is from the heat pump, approximately 35%, and lighting and plug loads, 35%, while the pumps, auxiliary loads, and the air handling unit account for the remaining 30% of the total consumption. Figure 20 shows the electricity required by the LH in 2010.

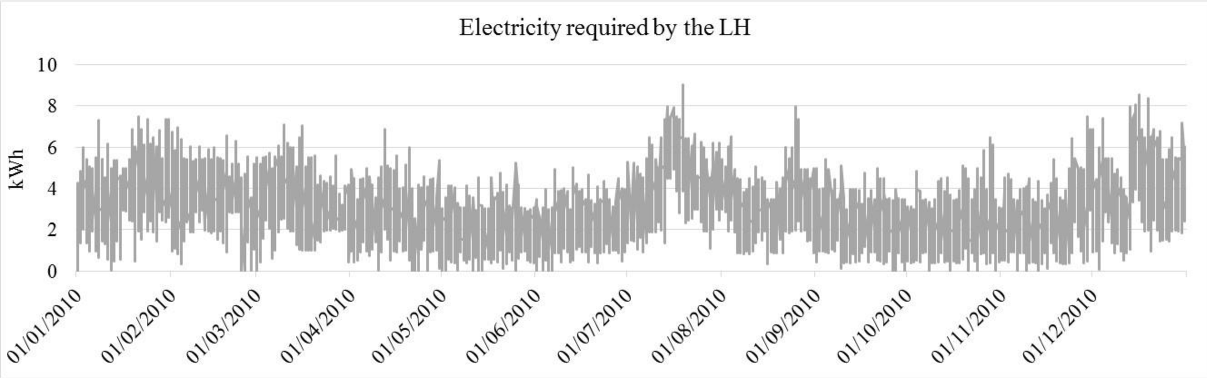

Figure 20. Electricity required by the LH in 2010.

In order to characterize the building load profile with respect to the PV generation, Table 9 reports the monthly peak-power and the monthly electricity consumption for each month.

Table 9. Parameters describing the building load.

Parameter	Jan	Feb	Mar	Apr	May	Jun	Jul	Aug	Sept	Oct	Nov	Dec
Monthly peak-power [kW]	7.47	6.97	7.09	6.89	5.24	5.01	9.02	7.97	5.42	6.47	7.47	8.57
Monthly electricity consumption [kWh]	2700	2286	2371	1736	1363	1521	3051	2271	1618	1496	1748	2897

Figure 21, Figure 22, Figure 23 and Figure 24 show, respectively, the mean daily electricity consumption and PV electricity generation over 4 months, January, April, July and October, which are chosen to represent different seasons.

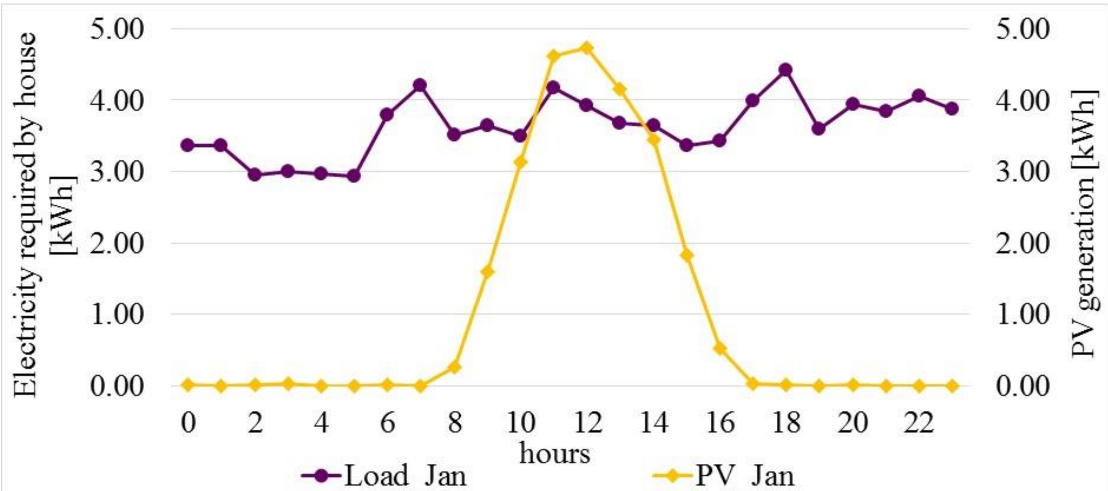

Figure 21. Mean daily electricity consumption and PV production of the examined case study in January.

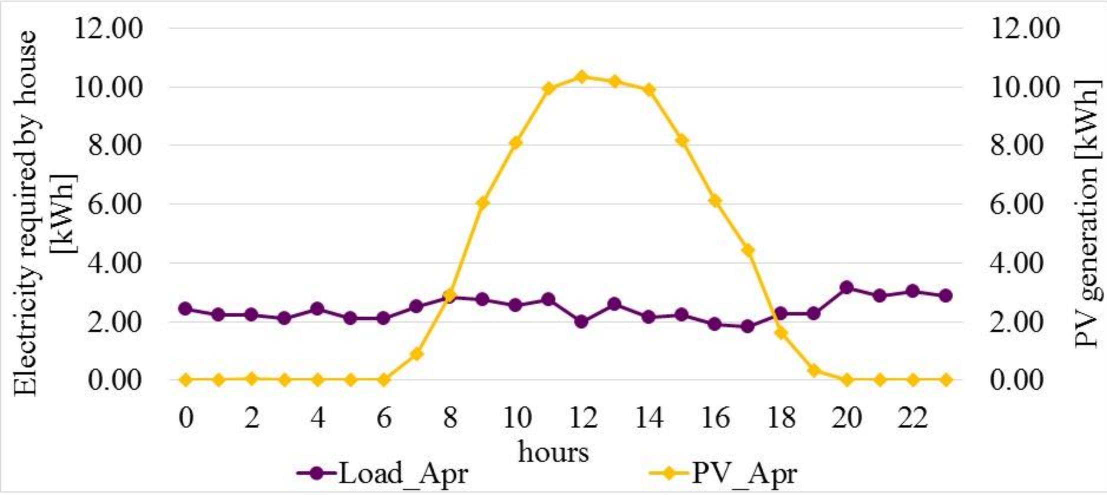

Figure 22. Mean daily electricity consumption and PV production of the examined case study in April.

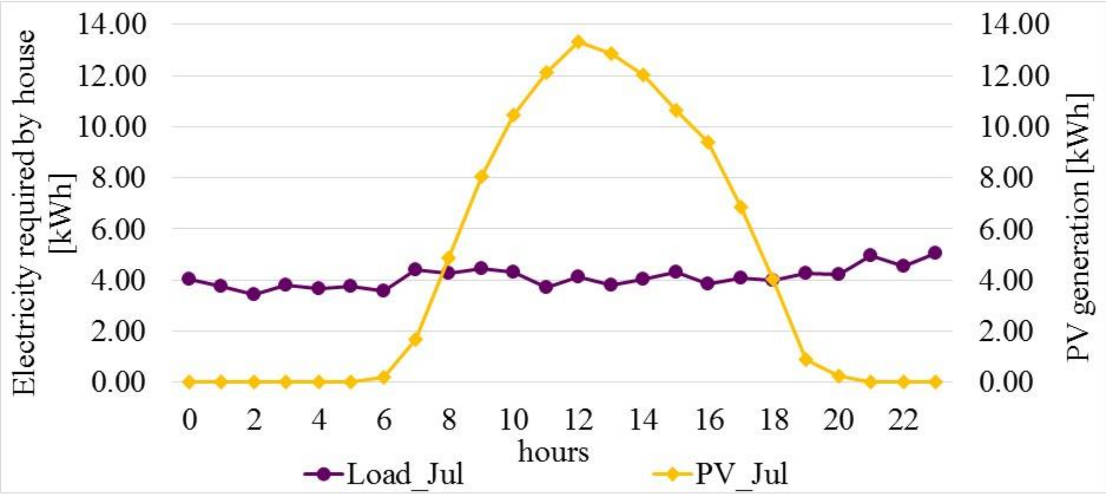

Figure 23. Mean daily electricity consumption and PV production of the examined case study in July.

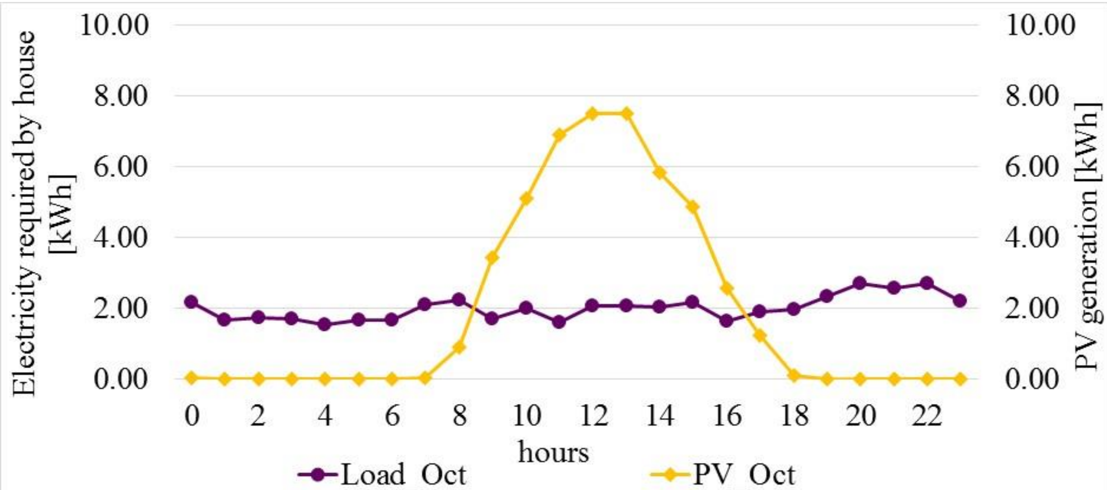

Figure 24. Mean daily electricity consumption and PV production of the examined case study in October.

4 Method

This section describes the method followed to model the PV plant + BESS + electricity grid system that provide the electricity required by the building examined. The proposed method integrated the load match analysis with the LCA methodology.

The load match analysis provides information on the degree of agreement or disagreement of the on-site generation with the building load profiles [156,157].

The LCA is a standardized methodology (ISO 14040) widely adopted by the scientific community to assess the environmental impacts of products and services from a life cycle perspective (i.e. including extraction of raw materials, transports, manufacturing processes, use and end-of-life) [113,114].

In the following the energy model used for the PV plant + BESS + electricity grid simulation, the load match and grid interaction indicators adopted and the LCA methodology are briefly described. More specifically, in this section a general overview of the methodology applied is provided, while the specific assumptions related to the application of the methodology to the case study are discussed in chapter 5

4.1 Modelling of the PV – BESS – electrical grid

The PV – BESS – electrical grid system is modelled following the procedure described in Ciocia et al. [55]. The model assumes that: (1) the PV system always feeds first the load and then, if a surplus is available, the BESS and at the end the grid; and 2) the batteries cannot be used to feed the grid and vice versa. In addition, a battery capacity fade model and a linear decrease of the initial battery efficiency (η_B) (5 percentage points in 5 years) are introduced according to Bobba et al. [89]. In detail, the battery's ageing at specific intervals is estimated taking into consideration both the calendar ageing and the cycling ageing according to the literature [87] and laboratory tests. Cycling ageing is considered proportional to the cycles performed. The battery capacity at each time step is calculated with the following Equation 4.1:

$$B_c(t) = B_c(t-1) - \left(B_{cf-cal} + B_{cf-cyc(DoDmax)} \cdot \frac{DoD(t-1)}{DoD_{max}}\right) \tag{4.1}$$

where:

$B_c(t)$ is the energy capacity of the storage at the time step t [kWh];

B_{cf-cal} is the battery capacity fade due to the calendar aging [kWh/day] (Table 11);

$B_{cf-cyc(DoDmax)}$ is the battery capacity fade due to the cycling aging referred to a complete cycle of charge/discharge [kWh/cycle] (Table 11);

$DoD(t-1)$ is the depth of discharge at the time step (t-1) [%] (Table 11);

DoD_{max} is the maximum depth of discharge [%] (Table 11).

At each time step, the model, starting from the comparison among the on – site electricity production from PV (El_{PV}), the building load (BL) and the state of charge (SoC) of the BESS, allows for calculating the following energy flows:

- PV electricity generated on-site and directly consumed by the building ($El_{PV \rightarrow BL}$);
- PV electricity used to charge the BESS ($El_{PV \rightarrow BESS}$);
- PV electricity injected into the electrical grid ($EL_{PV \rightarrow grid}$);
- Electricity delivered from the BESS to feed the building load ($El_{BESS \rightarrow BL}$);
- Electricity adsorbed from the electrical grid to feed the building load ($El_{grid \rightarrow BL}$);
- Electricity losses due to the charge/discharge efficiency ($El_{\eta loss}$).

The diagram of the analysed system and the modelled energy flows are shown in Figure 25.

The first step of the model consists in the comparison of the electricity generated from the PV power plant with the building load, in order to establish if the BESS and/or the grid have to be used to match the building load. The BESS can be empty: $SoC(t) = SoC_{min}$; partially discharged: $SoC_{min} \leq SoC(t) < SoC_{max}$; or fully charged: $SoC(t) = SoC_{max}$. The control system checks if there is an energy deficit or surplus of electricity from PV respect to the load, after checks the status of the BESS, i.e. its $SoC(t)$, and it establishes if the BESS has to be used and it calculates the amount of electricity available for charging or the amount dischargeable. In case of charging, if the available electricity from PV is higher than the amount storable in the BESS at the considered time step, the surplus is fed into the grid. In case of discharging, if storage is not sufficient to handle the power in the local system, the grid is used.

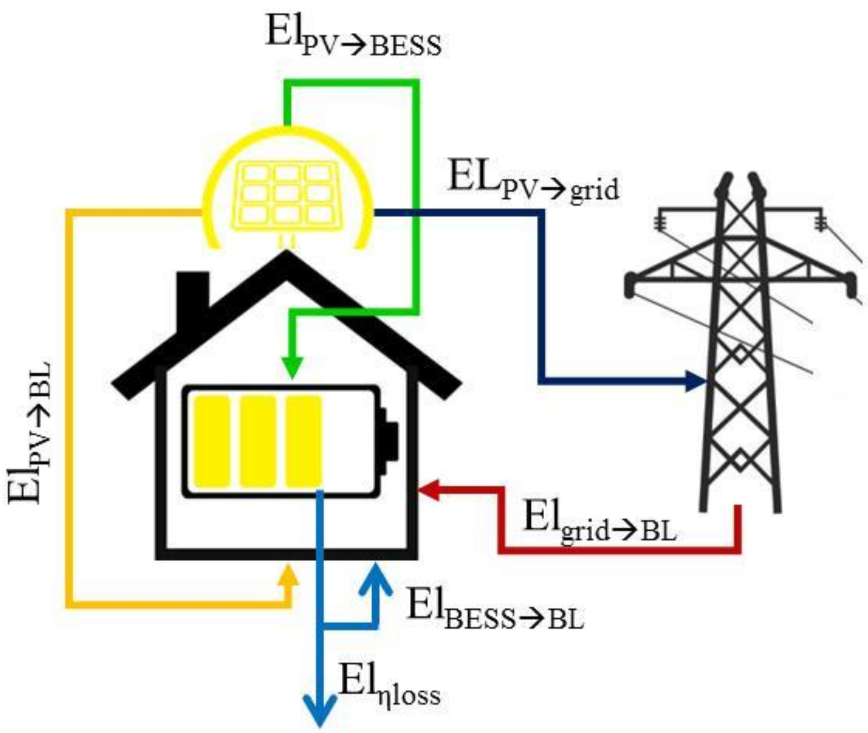

Figure 25. Diagram of the PV – BESS – Electrical grid system and of the energy flows.

In particular, at each time step, the maximum energy flow from the BESS ($E_{BD}(t)$) is calculated, according to its $SoC(t)$, considering the following Equation 4.2:

$$E_{BD}(t) = \ (SoC(t) - SoC_{min}) * \ B_C(t) * \eta_B(t) \quad (4.2)$$

where:

SoC_{min} is the minimum value that the BESS SoC can achieve. It is set in order to limit battery degradation and aging [55,60,89]. The model stops the electricity discharge from the BESS when the SoC reaches the minimum value set.

If $SoC(t) = SoC_{max}$, the $E_{BD}(t)$ correspond to the maximum energy dischargeable by the BESS in an hour ($E_{BDmax}(t)$), which it is calculated with the following Equation 4.3:

$$E_{BD}(t) = \ (SoC_{max} - SoC_{min}) * \ B_C(t) \quad (4.3)$$

Six different cases can be modelled:

- Case 1: generation from renewables is higher than load $El_{PV}(t) \geq BL(t)$ and storage is full $SoC(t) = SoC_{max}$;

- Case 2: generation from PV is lower than load $El_{PV}(t) < BL(t)$ and the BESS is full $SoC(t) = SoC_{max}$;
- Case 3: generation from PV is higher than building load $El_{PV}(t) > BL(t)$ and BESS is empty, $SoC(t) = SoC_{min}$;
- Case 4: generation from renewables is lower than load $El_{PV}(t) < BL(t)$ and the BESS is empty, $SoC(t) = SoC_{min}$;
- Case 5: generation from renewables is lower than load $El_{PV}(t) < BL(t)$ and storage is partially full $SoC_{min} < SoC(t) < SoC_{max}$;
- Case 6: generation from renewables is higher than load $El_{PV}(t) > BL(t)$ and storage is partially full $SoC_{min} < SoC(t) < SoC_{max}$.

The simulation starts from the first hour of the year with the BESS fully charged ($SoC(t) = 100\%$); at the end of the first time step (1 hour), the $SoC(t)$ is updated and this this value is an input for the following time step.

Case 1: generation from renewables is higher than load $El_{PV}(t) \geq BL(t)$ and storage is full $SoC(t) = SoC_{max}$. Thus, the load is fed by the PV plant and the energy surplus, corresponding to the difference $El_{PV}(t) - BL(t)$ (i.e. $EL_{\mathrm{PV \rightarrow grid}}$), is injected in the grid, because BESS is already full.

In this first case:

$$El_{\mathrm{PV \rightarrow BL}}(t) = BL(t)$$

$$El_{\mathrm{PV \rightarrow BESS}}(t) = 0$$

$$El_{\mathrm{PV \rightarrow grid}}(t) = El_{PV}(t) - BL(t)$$

$$El_{\mathrm{BESS \rightarrow BL}}(t) = 0$$

$$El_{\mathrm{grid \rightarrow BL}}(t) = 0$$

The $SoC(t)$ does not change:

$$SoC(t+1) = SoC(t) = SOC_{max}.$$

Case 2: generation from PV is lower than load $El_{PV}(t) < BL(t)$ and the BESS is full $SoC(t) = SoC_{max}$. Thus, the building load cannot be fed by only PV source and the energy deficit, corresponding to the difference $El_{PV}(t) - BL(t)$ has to be absorbed from BESS and grid. This case is more difficult, respect to the previous one, because the storage works and it has to be simulated considering its energy limit.

In fact, the maximum energy that can be discharged at the time t, El_{BDmax}, by the BESS is function of SoC_{max}, SoC_{min} and battery capacity, and it is calculated with the following Equation 4.4:

$$El_{BDmax}(t) = (SoC_{max} - SoC_{min}) \cdot B_C(t) \tag{4.4}$$

where $B_C(t)$ is the BESS energy capacity at time t.

After the definition of the maximum energy E_{BDmax} that can be discharged by the BESS, this value can be compared with the energy deficit of the PV generation respect the building load.

If the energy required to batteries is lower than the limit $BL(t) - El_{PV}(t) < E_{BDmax}(t)$ thus the BESS can completely feed the load and the use of the grid is not necessary:

$$El_{\mathrm{PV \to BL}}(t) = El_{PV}(t)$$

$$El_{\mathrm{PV \to BESS}}(t) = 0$$

$$El_{\mathrm{PV \to grid}}(t) = 0$$

$$El_{\mathrm{BESS \to BL}}(t) = BL(t) - El_{PV}(t)$$

The SoC decreases by the energy provided to the building, and it is calculated as in Equation 4.5:

$$SoC(t+1) = SoC_{max} - \left(\frac{E_{BESS \to BL}(t)}{B_C(t)}\right) \tag{4.5}$$

$$El_{\mathrm{grid \to BL}}(t) = 0$$

If the energy required to batteries is higher than the limit $BL(t) - El_{PV}(t) > E_{BDmax}(t)$ the BESS cannot completely fed the building load. The dischargeable energy corresponds to the limit, $E_{BDmax}(t)$) and the grid provides the remaining part:

$$El_{\mathrm{PV}\rightarrow\mathrm{BL}}(t) = El_{PV}(t)$$

$$El_{\mathrm{PV}\rightarrow\mathrm{BESS}}(t) = 0$$

$$El_{\mathrm{PV}\rightarrow\mathrm{grid}}(t) = 0$$

$$El_{\mathrm{BESS}\rightarrow\mathrm{BL}}(t) = E_{BDmax}(t)$$

$$SoC(t+1) = SoC_{max} - \left(\frac{El_{\mathrm{BDmax}}(t)}{B_C(t)}\right) = SoC_{min}$$

$$El_{\mathrm{grid}\rightarrow\mathrm{BL}}(t) = BL(t) - El_{\mathrm{PV}}(t) - E_{BDmax}(t)$$

In **Case 3**: generation from PV is higher than building load $El_{PV}(t) > BL(t)$ and BESS is empty $SoC(t) = SoC_{min}$. Thus, the building load is fed by the PV plant and the energy surplus, corresponding to the difference, $El_{PV}(t) - BL(t)$, can be used to recharge the empty BESS. As in previous case, also the recharge is limited by battery constraints in term of energy, i.e. the maximum energy that can be injected in an hour in the empty storage and it is calculated by the expression (4.1) (absolute value). After the definition of the maximum energy that can be injected to the BESS ($El_{BCmax}(t)$), this value is compared with the surplus of the electricity generated from PV compared to the building load ($El_{PV}(t) - BL(t)$).

If the energy available to charge the empty storage is lower than the limit ($El_{BCmax}(t)$), i.e. $El_{PV}(t) - BL(t) < El_{BCmax}(t)$, the amount of electricity corresponding to the difference $\frac{El_{PV}(t)-BL(t)}{\eta_B(t)}$ can be used to charge the BESS:

$$\mathrm{El}_{\mathrm{PV}\rightarrow\mathrm{BL}}(t) = BL(t)$$

$$E_{PV\rightarrow BESS}(t) = \frac{El_{PV}(t) - BL(t)}{\eta_B(t)}$$

$$EL_{\text{PV}\rightarrow\text{grid}}(t) = 0$$

$$El_{\text{BESS}\rightarrow\text{BL}}(t) = 0$$

The SoC increases by the energy provided by the PV plant, and it is calculated as in Equation 4.6:

$$SoC(t+1) = SoC(t) + \left(\frac{E_{PV\rightarrow BESS}(t)}{B_C(t)}\right) \tag{4.6}$$

$$El_{\text{grid}\rightarrow\text{BL}}(t) = 0$$

If the energy available to charge the empty storage is higher than the limit $El_{PV}(t) - BL(t) > El_{BCmax}(t)$, the amount of electricity corresponding to $\frac{(El_{PV}(t)-BL(t))}{\eta_B} = El_{BCmax}(t)$, is used to charge the BESS and the remaining amount is exported into the grid.

$$\text{El}_{\text{PV}\rightarrow\text{BL}}(t) = BL(t)$$

$$E_{PV\rightarrow BESS}(t) = El_{BCmax}(t)$$

$$EL_{\text{PV}\rightarrow\text{grid}}(t) = \text{El}_{\text{PV}\rightarrow\text{BL}}(t) - E_{PV\rightarrow BESS}(t)$$

$$El_{\text{BESS}\rightarrow\text{BL}}(t) = 0$$

$$SoC(t+1) = SoC(t) + \left(\frac{E_{PV\rightarrow BESS}(t)}{B_C(t)}\right)$$

$$El_{\text{grid}\rightarrow\text{BL}}(t) = 0$$

In **Case 4**, generation from renewables is lower than load $El_{PV}(t) < BL(t)$ and the BESS is empty, $SoC(t) = SoC_{min}$. In this case, the load is partially fed by the PV and the energy deficit corresponding to the difference $El_{PV}(t) - BL(t)$ is absorbed by the grid.

$$\text{El}_{\text{PV}\rightarrow\text{BL}}(t) = El_{PV}(t)$$

$E_{PV \to BESS}(t) = 0$

$EL_{\mathrm{PV \to grid}}(t) = 0$

$El_{\mathrm{BESS \to BL}}(t) = 0$

$EL_{\mathrm{grid \to BL}}(t) = BL(t) - El_{PV}(t)$

$SoC(t+1) = SoC_{min}$

In **Case 5**, generation from renewables is lower than load $El_{PV}(t) < BL(t)$ and storage is partially full $SoC_{min} < SoC(t) < SoC_{max}$. Thus, the building load cannot be fed by only PV source and the energy deficit, corresponding to the difference $El_{PV}(t) - BL(t)$ has to be absorbed from BESS and grid. As in Case 2, the energy limit of the BESS is considered. The maximum energy that can be provided in a hour by the BESS is function of the *SOC(t)* and $B_c(t)$.

$El_{\mathrm{PV \to BL}}(t) = El_{PV}(t)$

$El_{\mathrm{PV \to BESS}}(t) = 0$

$El_{\mathrm{PV \to grid}}(t) = 0$

$El_{\mathrm{BESS \to BL}}(t) = (SoC(t) - SoC_{min}(t)) \cdot B_c(t)$

$$SoC(t+1) = SoC(t) - \left(\frac{El_{\mathrm{BESS \to BL}}(t)}{B_C(t)}\right)$$

$El_{\mathrm{grid \to BL}}(t) = BL(t) - El_{\mathrm{PV}}(t) - El_{\mathrm{BESS \to BL}}(t)$

In **Case 6**, generation from renewables is higher than load $El_{PV}(t) > BL(t)$ and storage is partially full $SoC_{min} < SoC(t) < SoC_{max}$. Thus, the load can be fed by the PV plant and the energy surplus, corresponding to the difference, $El_{PV}(t) - BL(t)$, can be injected in the BESS and grid. Also in this case, as in Case 2, the limit of the energy dischargeable at the time t from the BESS, $El_{BD}(t)$ has to be considered.

$$El_{BD}(t) = \left(SoC_{max} - SoC(t)\right) \cdot B_C(t)$$

$$El_{\text{PV}\rightarrow\text{BL}}(t) = BL(t)$$

$$El_{\text{PV}\rightarrow\text{BESS}}(t) = \frac{\left(\left(SoC_{max} - SoC(t)\right) \cdot B_c(t)\right)}{\eta_B(t)}$$

$$SoC(t+1) = SoC(t) + \left(\frac{El_{\text{PV}\rightarrow\text{BESS}}(t)}{B_C(t)}\right)$$

If $El_{PV}(t) - BL(t) > El_{BD}(t) \rightarrow El_{\text{PV}\rightarrow\text{grid}}(t) = El_{PV}(t) - BL(t) - El_{\text{PV}\rightarrow\text{BESS}}(t)$

If $El_{PV}(t) - BL(t) < El_{BD}(t) \rightarrow El_{\text{PV}\rightarrow\text{grid}}(t) = 0$

$El_{\text{grid}\rightarrow\text{BL}}(t) = 0.$

4.2 Load matching and grid interaction analysis

To quantify the load-matching levels for the case study, the load cover factor (γ_{load}) index, defined in [157] is used. It represents the percentage of the electrical demand covered by on-site electricity generation and is calculated as in Equation 4.7:

$$\gamma_{load} = \frac{\int_{t1}^{t2} min[g(t) - S(t) - \xi(t), l(t)]dt}{\int_{t1}^{t2} l(t)dt} \tag{4.7}$$

where:

$g(t)$ is the on-site generation (kW);

$S(t)$ is the storage balance (kW), calculated as in Equation 4.8:

$$S(t) = S_{ct}(t) - S_{dc}(t) \tag{4.8}$$

$\xi(t)$ are losses (kW);

$l(t)$ is the building load (kW);

t is the time;

τ_1 and τ_2 are the start and the end of the evaluation period, respectively.

Moreover, to quantify the energy exchange between the building and the electrical grid to which it is connected, the net exported electricity (kWh), ne, is calculated as in Equation 4.9:

$$ne = \int_{t1}^{t2} e(t)dt - \int_{ti}^{t2} d(t)dt \tag{4.9}$$

where $e(t)$ and $d(t)$ are the mean exported power (kW) and mean imported power (kW).

Figure 26 provides an overview of relevant terminology addressing the energy use in buildings and the connection between buildings and the power grid.

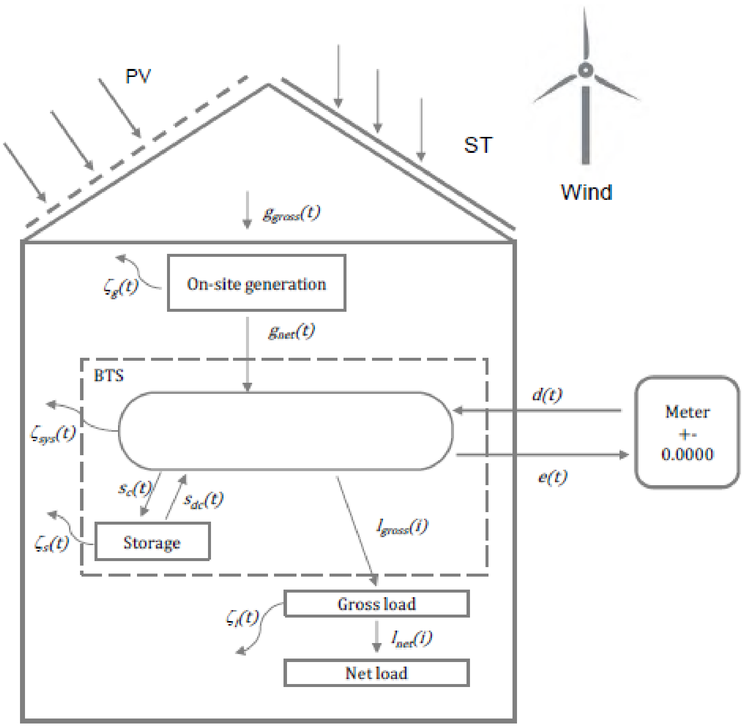

Figure 26. Schematic view of the energy flows in a building equipped with renewable energy technologies and energy storage system [157].

4.3 Life Cycle Assessment

Life Cycle Thinking (LCT) and Life Cycle Assessment (LCA) are the scientific approaches behind modern environmental policies and business decision support towards a circular economy [158,159].

LCA is a structured, comprehensive and internationally standardised method. It quantifies all relevant emissions and resources consumed and the related environmental and health impacts and resource depletion issues that are associated with any good or service (“products). LCA takes into account a product’s full life cycle: from the extraction of resources, through production, use, and recycling, up to the disposal of remaining waste. Critically, LCA studies thereby help to avoid resolving one environmental problem while creating others. This unwanted “shifting of burdens" is where you reduce the environmental impact at one point in the life cycle, only to increase it at another point.

LCA can assist in identifying opportunities to improve the environmental performance of products at various points in their life cycle; informing decision-makers in industry, government or non-government organizations for the purpose of strategic planning, priority setting, product or process design or redesign; the selection of relevant indicators of environmental performance, including measurement techniques; and marketing (e.g. implementing an eco-labelling scheme, making an environmental claim, or producing an environmental product declaration) [113].

The ISO 14040 [113] and 14044 [114] standards provide the indispensable framework for LCA.

The standards are organized into the different phases of an LCA study. These are:

- goal and scope definition;
- inventory analysis;
- life cycle impact assessment;
- life cycle interpretation.

Typically, LCA starts by defining goal and scope, then proceeds to the inventory analysis, then optionally continues to impact assessment, and it ends with the interpretation. However, as indicated in Figure 27, LCA study is a highly iterative process, so that the LCA practitioner may need to go back to goal and scope after the preliminary inventory work, to move back from impact assessment to inventory analysis, to have a look at the interpretation in an early stage, etc. [160].

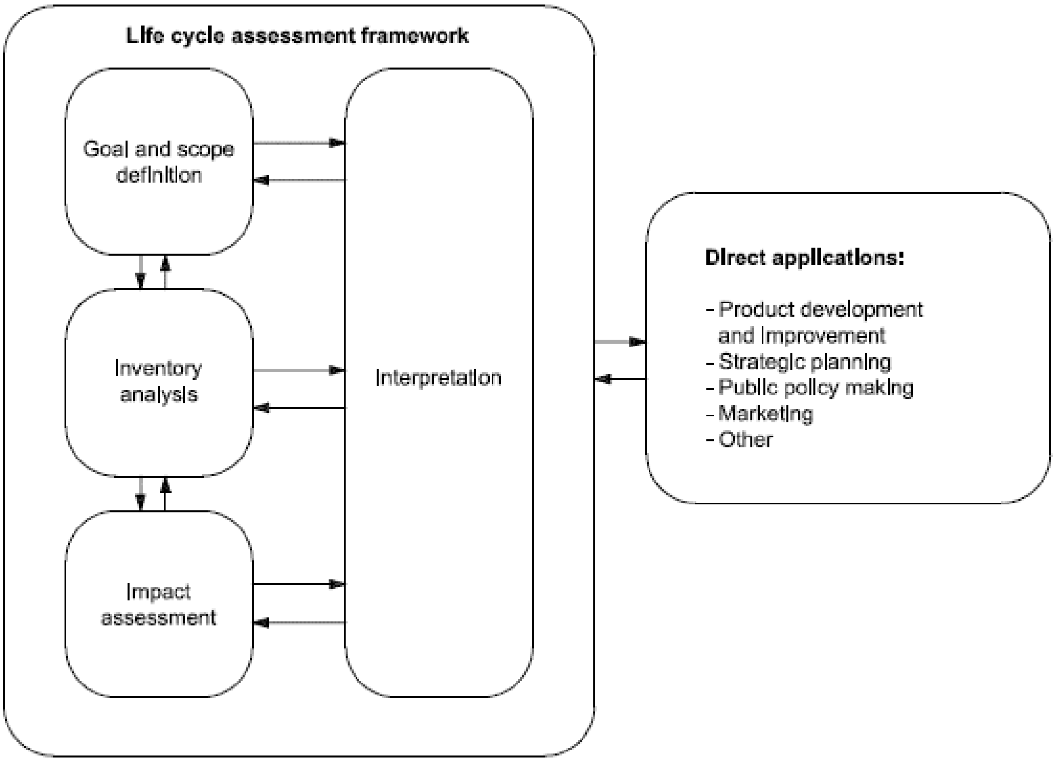

Figure 27. Framework for life cycle assessment (from [113]).

During the goal definition the intended application/s of the study and the targeted audience/s are identified. The scope definition involves the detailed description of the object of the LCA study (i.e. the exact product to be analysed) and of the main methodological aspects.

The life cycle inventory analysis phase (LCI phase) is the second phase of LCA. It is an inventory of input/output data with regard to the system being studied. It involves the collection and elaboration of the data necessary to meet the goals of the defined study.

The life cycle impact assessment phase (LCIA) is the third phase of the LCA. The purpose of LCIA is to assess the potential environmental impacts using the LCI results.

Life cycle interpretation is the final phase of the LCA procedure, in which the results of a LCI and/or an LCIA, or both, are summarized and discussed as a basis for conclusions, recommendations and decision-making in accordance with the goal and scope definition.

4.3.1 Methodological framework

4.3.1.1 Goal and scope definition

The goal definition is the first phase of any LCA. During the goal definition, intended application(s) and the targeted audience(s) of the study are identified. A clear, initial goal definition is essential for a correct later interpretation of the results. Six aspects shall be addressed and documented during the goal definition: 1) Intended application(s) of the deliverables/results; 2) Limitations due to the method, assumptions, and impact coverage; 3) Reasons for carrying out the study and decision-context; 4) Target audience of the deliverables/results; 5) Comparative studies to be disclosed to the public; 6) Commissioner of the study and other influential actors.

During the scope definition phase the object of the LCA study (i.e. the exact product or other system(s) to be analysed) is identified and defined in detail. This shall be done in line with the goal definition.

During the scope definition the following items shall be clearly described and/or defined:

- the product system that is studied and its function(s), functional unit, and reference flow(s);
- LCI modelling framework and handling of multifunctional processes and products (i.e. processes provide more than one function, i.e. delivering several goods and/or services, often also named simplified “co-products” (Figure 28);
- the system boundary and related cut-off criteria (i.e. specification of the amount of material or energy flow or the level of environmental significance associated with unit processes or product system to be excluded from a study);
- impact categories selected and methodology of impact assessment, and subsequent interpretation to be used;
- data requirements (regarding technological, geographical and time related representativeness and appropriateness); assumptions and limitations;
- type of critical review, if any;
- type and format of the report required for the study.

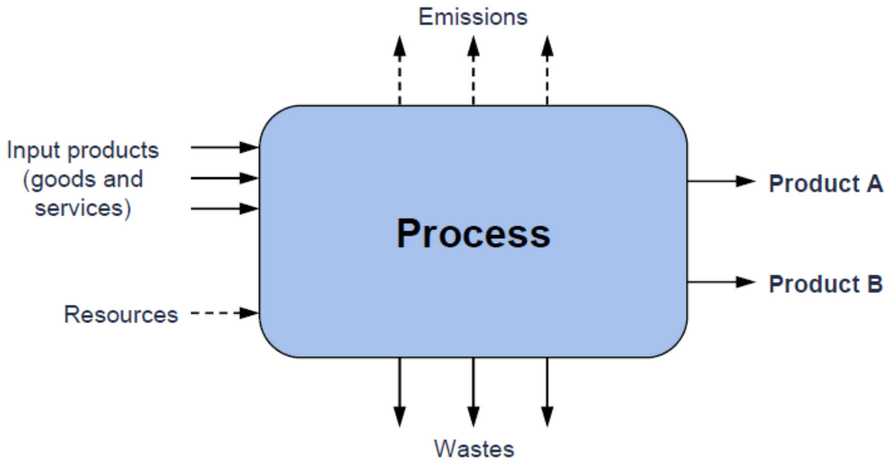

Figure 28. Example of multifunctional process (source [161]).

A system may have a number of possible functions and the one(s) selected for a study depend(s) on the goal and scope of the LCA. The functional unit defines the quantification of the identified functions (performance characteristics) of the product. The primary purpose of a functional unit is to provide a reference to which the inputs and outputs are related. This reference is necessary to ensure comparability of LCA results. Comparability of LCA results is particularly critical when different systems are being assessed, to ensure that such comparisons are made on a common basis. It is important to determine the reference flow in each product system, in order to fulfil the intended function, i.e. the amount of products needed to fulfil the function.

Two main LCI modelling principles are in use in LCA practice: attributional and consequential modelling. The attributional life cycle inventory modelling principle depicts the potential environmental impacts that can be attributed to a system (e.g. a product) over its life cycle, i.e. upstream along the supply-chain and downstream following the system's use and end-of-life value chain. Attributional modelling makes use of historical, fact-based, measureable data of known (or at least knowable) uncertainty, and includes all the processes that are identified to relevantly contribute to the system being studied. The consequential life cycle inventory aims at identifying the consequences that a decision in the foreground system has for other processes and systems of the economy, both in the analysed system's background system and on other systems. It models the analysed system around these consequences. The consequential life cycle model is hence not reflecting the actual (or forecasted) specific or average supply-chain, but a hypothetic generic supply-chain is modelled that is prognosticated along market mechanisms, and potentially including political interactions and consumer behaviour changes.

ISO 14044:2006 presents a hierarchy of different approaches to solve the multi-functionality problem.

According to the ISO hierarchy, the study shall identify the processes shared with other product systems and deal with them following the stepwise procedure presented below.

a) **Step 1:** Wherever possible, allocation should be avoided by dividing the unit process to be allocated into two or more sub-processes and collecting the input and output data related to these sub-processes, or expanding the product system to include the additional functions related to the co-products.

b) **Step 2**: Where allocation cannot be avoided, the inputs and outputs of the system should be partitioned between its different products or functions in a way that reflects the underlying physical relationships between them; i.e. they should reflect the way in which the inputs and outputs are changed by quantitative changes in the products or functions delivered by the system.

c) **Step 3**: Where physical relationship alone cannot be established or used as the basis for allocation, the inputs should be allocated between the products and functions in a way that reflects other relationships between them. For example, input and output data might be allocated between co-products in proportion to the economic value of the products.

In case of reuse and recycling additional elaboration is needed because both (as well as composting, energy recovery and other processes that can be assimilated to reuse/recycling) may imply that the inputs and outputs associated with unit processes for extraction and processing of raw materials and final disposal of products are to be shared by more than one product system and reuse and recycling may change the inherent properties of materials in subsequent use. Several allocation procedures are applicable for reuse and recycling: a) a closed-loop allocation procedure applies to closed-loop product systems. It also applies to open-loop product systems where no changes occur in the inherent properties of the recycled material. In such cases, the need for allocation is avoided since the use of secondary material displaces the use of virgin (primary) materials. An open-loop allocation procedure applies to open-loop product systems where the material is recycled into other product systems and the material undergoes a change to its inherent properties.

The system boundary defines the unit processes to be included in the system. When setting the system boundary, several life cycle stages, unit processes (smallest element considered in the life cycle inventory analysis for which input and output data are quantified) and flows should be taken into consideration depends on the goal and scope definition of the study, its intended application and audience, the assumptions made, data and cost constraints, and cut-off criteria, for example, the following:

- acquisition of raw materials;
- inputs and outputs in the main manufacturing/processing sequence;
- distribution/transportation;
- production and use of fuels, electricity and heat;
- use and maintenance of products;
- disposal of process wastes and products;
- recovery of used products (including reuse, recycling and energy recovery);
- manufacture of ancillary materials;
- manufacture, maintenance and decommissioning of capital equipment;
- additional operations, such as lighting and heating.

Several cut-off criteria are used in LCA practice to decide which inputs are to be included in the assessment, such as mass, energy and environmental significance. Making the initial identification of inputs based on mass contribution alone may result in important inputs being omitted from the study. Accordingly, energy and environmental significance should also be used as cut-off criteria. The description of the mass, energy and environmental significance cut-off criteria is provided in the following list:

- mass: an appropriate decision, when using mass as a criterion, would require the inclusion in the study of all inputs that cumulatively contribute more than a defined percentage to the mass input of the product system being modelled;

- energy: similarly, an appropriate decision, when using energy as a criterion, would require the inclusion in the study of those inputs that cumulatively contribute more than a defined percentage of the product system's energy inputs;
- environmental significance: decisions on cut-off criteria should be made to include inputs that contribute more than an additional defined amount of the estimated quantity of individual data of the product system that are specially selected because of environmental relevance.

The selection of impacts categories and LCIA methods shall be in accordance with the goal of the study. All impact categories that are environmentally relevant for the LCA study shall be included. All included LCIA methods shall meet the following requirements l be scientifically and technically valid, as far as possible.

The data quality requirements should address the time-related coverage (age of data and the minimum length of time over which data should be collected), geographical coverage (geographical area from which data for unit processes should be collected to satisfy the goal of the study), technology coverage (specific technology or technology mix), precision (measure of the variability of the data values for each data expressed), completeness (percentage of flow that is measured or estimated), representativeness (qualitative assessment of the degree to which the data set reflects the true population of interest (i.e. geographical coverage, time period and technology coverage)), consistency (qualitative assessment of whether the study methodology is applied uniformly to the various components of the analysis), reproducibility (qualitative assessment of the extent to which information about the methodology and data values would allow an independent practitioner to reproduce the results reported in the study), sources of the data, uncertainty of the information (e.g. data, models and assumptions). Descriptions of data quality are important to understand the reliability of the study results and properly interpret the outcome of the study.

The scope of the study shall define whether a critical review is necessary and, if so, how to conduct it, the type of critical review needed the level of expertise of the reviewer/s.

Finally, the type and format of the report shall be defined in the scope phase of the study. The results and conclusions of the LCA shall be completely and accurately reported without bias to the intended audience. The results, data, methods, assumptions and limitations shall be transparent and presented in sufficient detail to allow the reader to comprehend the complexities and trade-offs inherent in the LCA. The report shall also allow the results and interpretation to be used in a manner consistent with the goals of the study.

4.3.1.2 Life cycle inventory analysis

Inventory analysis involves data collection and calculation procedures to quantify relevant inputs and outputs of a product system. Data for each unit process within the systems boundary can be classified under major headings, including

- energy inputs, raw material inputs, ancillary inputs, other physical inputs;
- products, co-products and waste;
- emissions to air, discharges to water and soil; and
- other environmental aspects.

Typically, the LCI phase requires the highest efforts and resources of an LCA: for data collection, acquisition, and modelling. All calculation procedures shall be explicitly documented and the assumptions made shall be clearly stated and explained.

4.3.1.3 Life cycle impact assessment (LCIA)

LCIA is the phase in an LCA where the inputs and outputs of elementary flows that have been collected and reported in the inventory are translated into impact indicator results related to human health, natural environment, and resource depletion. LCIA is composed of mandatory and optional steps (Figure 29). The LCIA phase shall include the following mandatory elements:

- selection of impact categories, category indicators and characterization models;
- classification: in this phase all elementary flows of the inventory have to be assigned to those one or more impact categories to which they contribute and that were selected for the impact assessment in the scope definition of the study;
- characterization: in this phase, to each classified elementary flow one quantitative characterisation factor has to be assigned for each category to which the flow relevantly

contributes. That factor expresses how much that flow contributes to the impact category indicator.

In a subsequent, optional step, the LCIA results can be multiplied with normalisation factors that represent the overall inventory of a reference (e.g. a whole country or an average citizen), obtaining dimensionless, normalised LCIA results and in a further optional step these normalised LCIA results can be multiplied by a set of weighting factors, that indicate the different relevance that the different impact categories (midpoint level related weighting) or areas-of-protection (endpoint level related weighting) may have, obtaining normalised and weighted LCIA results that can be summed up to a single-value overall impact indicator.

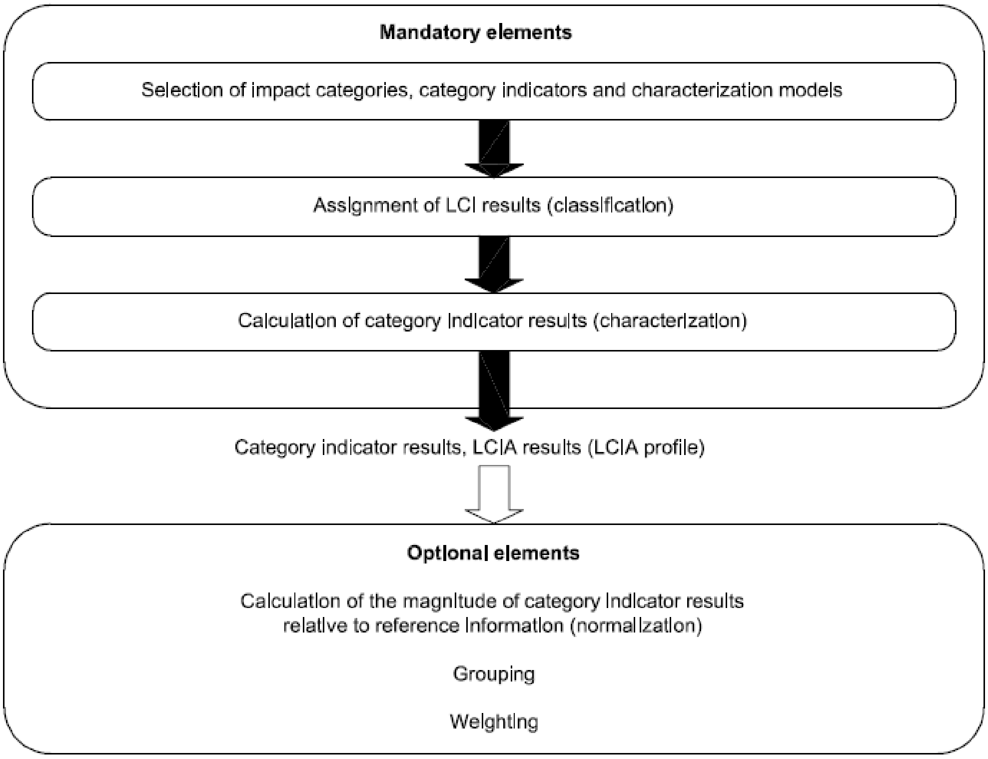

Figure 29. LCIA: mandatory and optional steps [114].

4.3.1.4 Life cycle interpretation

Interpretation is the phase of LCA in which the findings from the inventory analysis and the impact assessment are considered together. The interpretation phase should deliver results that are consistent with the defined goal and scope and which reach conclusions, explain limitations and provide recommendations.

The interpretation proceeds through three activities:

1. Identification of the significant issues (i.e. the key processes, parameters, assumptions and elementary flows);
2. Evaluation of the significant issue with regard to their sensitivity or influence on the overall results of the LCA;
3. Finally, the results of the evaluation are used in the formulation of conclusions and recommendations from the LCA study.

5 Methodology application to the examined case study

This chapter deal with the application of the methodology illustrated in Chapter 4 to the case study examined. The specific assumptions and choices related to each methodological aspect, previously discussed, are detailed in the following.

The methodology is based on the analysis of available high-resolution real data (mainly hourly) from monitored residential nZEB, described in Section 3.

Starting from the one year monitored data on the on-site electricity generation from the PV plant and the building electricity requirement, the "PV plant + BESS + electrical grid" system proving the electricity required by the nZEB is modelled.

The BESS is made of retired PHEV Lithium-ion batteries. Different configuration characterized by a BESS made of an increasing number of batteries ranging from one (Configuration 1 – C1) to ten (Configuration 10 – C10) are simulated.

The energy flows obtained from the energy model are the input of the integrated load match and the life cycle environmental impacts analysis.

The combined analysis is applied to identify the best design solution in terms of load match and environmental impacts.

The assessment of the environmental sustainability of using retired EV batteries in stationary second life applications is based on comparing the associated energy and environmental impacts with those of two scenarios, providing the same function. In a first scenario, named "Reference scenario" it is not employed a BESS, and the system "PV plant – electricity grid" provides the electricity to the examined residential nZEB. In the second one, named "Fresh battery scenario" the BESS is realized with fresh EV batteries.

In addition, in order to highlight the effective environmental benefits resulting from the application of circular economy and industrial symbiosis principles of reusing retired EV batteries in stationary storage applications, avoiding the need to produce a new BESS, the system boundaries are expanded in order to include also the first application of the batteries in the EV. The Reuse battery scenario including also the first life of the battery in the EV is compared with a scenario, named "Currently EV battery scenario”, in which it is assumed that after the first use in the EV the batteries are collected and recycled and a new BESS is produced to store the electricity in the examined building.

The methodology followed can be recapped in 5 steps:

1. step 1 – Simulation of the energy system, including the PV, the BESS and their mutual interactions with the energy grid (Reuse battery scenario) for different values of BESS energy capacity;
2. step 2 – Identification of the load match and grid integration level for the configurations simulated in step 1;
3. step 3 – Assessment of the life cycle energy and environmental impacts of the examined scenarios through the LCA methodology;
4. step 4 – Identification of the best design solution/s in terms of system efficiency and environmental and economic sustainability based on the results obtained in steps 2 and 3;
5. step 5 – Comparison of the life cycle environmental impacts associated to the best design solution/s with the “reference scenario” and with the “fresh battery scenario”.

In addition, in order to highlight the effective environmental benefits resulting from the application of circular economy and industrial symbiosis principles of reusing retired EV batteries in stationary storage application avoiding the need to produce a new BESS, the system is expanded in order to include also the first application of the batteries in the EV. The expanded Reuse battery scenario (Figure 30) is compared with the expanded Fresh battery scenario” (Figure 31), in which it is assumed that after the first use in the EV the batteries are collected and recycled. Then in this scenario a new BESS is produced to store electricity the in the examined building. The environmental benefits are assessed through difference between the expanded Currently EV and reuse battery scenarios.

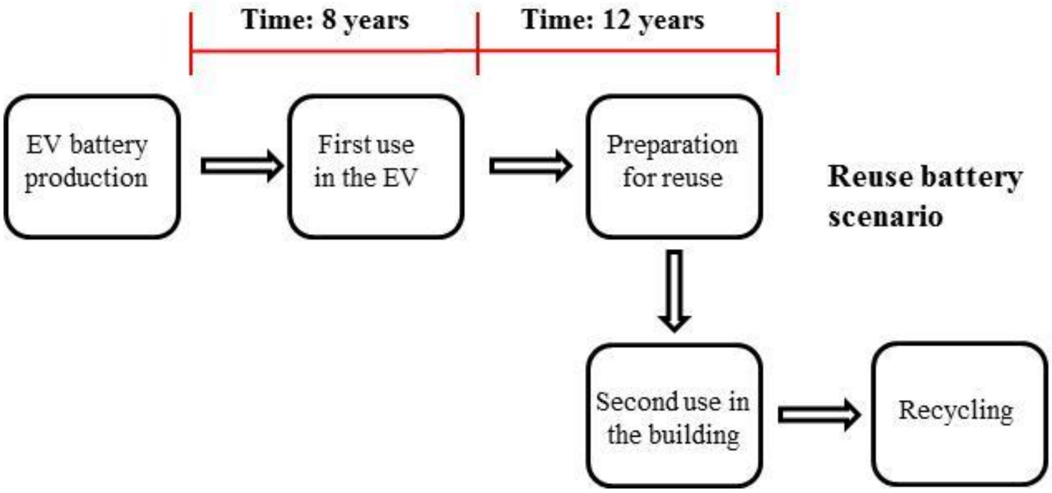

Figure 30. Reuse battery scenario – Expanded.

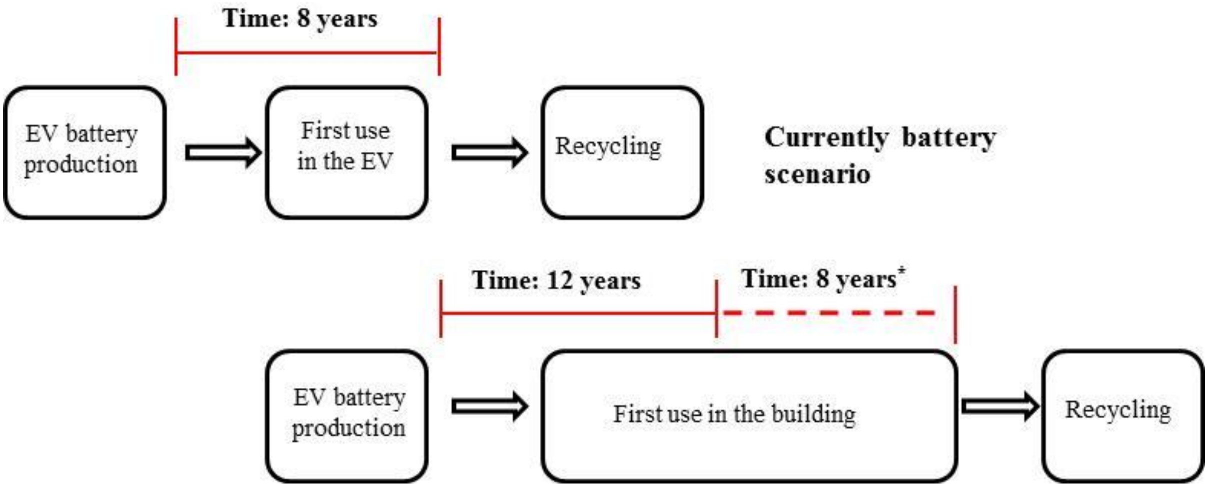

*The impacts associated to the operation phase in these eight years is not considered because the examined FU is represented by the electricity required in the building in twelve years (Section 5.1 and 5.4). The impacts associated to the battery production and recycling are allocated to the investigated system proportionally to the actual operation years in the investigated system.

Figure 31. Fresh battery scenario – Expanded.

5.1 PV – BESS – electrical grid system: energy modelling

The simulation of the PV – BESS – electrical grid was carried out for 10 configurations corresponding to the employment of a number of retired batteries ranging from 1 (C1) to 10 (C10).

The number of retired EV batteries employed and the corresponding installed energy capacity are illustrated in Table 10.

Table 10. Installed energy storage capacity of each examined configuration – reuse battery scenario.

Parameters	**C1**	**C2**	**C3**	**C4**	**C5**	**C6**	**C7**	**C8**	**C9**	**C10**
Installed energy capacity (B_c) – "reuse battery scenario" [kWh]	9.3	18.6	27.9	37.2	46.5	55.8	65.1	74.4	83.7	93.0
Number of batteries	1	2	3	4	5	6	7	8	9	10

The battery parameters used to model the "PV – BESS – electricity grid" are summarized in Table 11.

Table 11. Retired EV battery model parameters.

Parameters	**Value**	**Data source**
Residual capacity [kWh]	9.3	[89]
SoC_{max} [%]	100	
SoC_{min} [%]	20	
DoD_{max} [%]	80	
Charge/Discharge battery efficiency η_B [%]	95%	Laboratory test
B_{cf-cal} [Wh/day]	-0.11	Laboratory test
$B_{cf-cyc(DoDmax)}$ [Wh/cycle]	-3	Literature

The model is run until the battery energy capacity reached 60% of its nominal capacity. In fact, when the battery capacity falls below 60% of its initial capacity, the BESS is no longer able to satisfy the system requirements [86,95] and it is replaced. Moreover, based on previous study on battery second life application [95,111], it is assumed a maximum BESS lifetime of 20 years. Therefore, considering that in a EVs the BESS has a service life of about 8 years [88,104] a maximum lifetime of 12 years is available in a potential second life application, i.e. after 12 years of second use, the BESS reached the EoL even if its energy capacity is not below the 60% of its initial nominal capacity.

Regarding the electricity generation from the PV power plant, since only one year of monitored data are available, in order to consider the degradation of the modules reducing efficiency after the first operation year a linear degradation of 0.4% per year is assumed according to Jordan and Kurtz [162].

The results of the energy model for each configuration examined are illustrated in the following.

In Table 12 are summarized the annual monitored data on PV electricity generation and building load and the electricity produced by the PV plant and directly consumed by the building resulting from the "PV-BESS-electrical grid" energy modelling. These energy flows are independent of both the BESS installation and size and then they assume the same value in each examined configuration.

Table 12. Electricity generation from PV, building load and electricity from PV directly consumed by building.

Parameter	**Use phase modelling**					
Year	1	2	3	4	5	6
El_{PV} [kWh/year]	24,481.59	24,432.97	24,335.04	24,237.12	24,139.19	24,041.26
BL [kWh/year]	25,060.19	25,060.19	25,060.19	25,060.19	25,060.19	25,060.19
$El_{PV\rightarrow BL}$ [kWh/year]	8,298.50	8,295.25	8,288.13	8,280.86	8,273.50	8,266.02
Year	7	8	9	10	11	12
El_{PV} [kWh/year]	23,943.34	23,845.41	23,747.48	23,649.56	23,551.63	23,453.70
BL [kWh/year]	25,060.19	25,060.19	25,060.19	25,060.19	25,060.19	25,060.19
$El_{PV\rightarrow BL}$ [kWh/year]	8,258.39	8,250.64	8,242.82	8,234.93	8,226.96	8,218.97

Table 13, Table 14 and Table 15 illustrate the modelling results obtained in C1, C2 and C3. In these configurations, the BESS is not able to perform its function for the entire period analysed and a BESS replacement during the examined time – frame is required.

Table 13. Energy model results in C1 (one retired EV battery).

C1 - use phase	**BESS (9.3 kWh) – 3 replacement**					
	First BESS			**Second BESS**		
Year	**1**	**2**	**3**	**4**	**5**	**6**
$El_{BESS\rightarrow BL}$ [kWh]	2,122.44	1,921.69	1,742.40	2,117.75	1,917.35	1,739.04
$El_{\eta loss}$ [kWh]	240.27	239.38	236.54	239.74	238.84	236.09
$El_{grid\rightarrow BL}$ [kWh]	14,639.25	14,843.24	15,029.66	14,661.57	14,869.33	15,055.12
$EL_{PV\rightarrow grid}$ [kWh]	13,827.34	13,976.21	14,067.57	13,605.71	13,709.06	13,799.71
	Third BESS			**Fourth BESS**		
Year	**7**	**8**	**9**	**10**	**11**	**12**
$El_{BESS\rightarrow BL}$ [kWh]	2,112.13	1,913.03	1,735.87	2,106.77	1,908.57	1,732.78
$El_{\eta loss}$ [kWh]	239.10	238.31	235.66	238.50	237.76	235.25
$El_{grid\rightarrow BL}$ [kWh]	14,689.67	14,896.52	15,081.50	14,718.48	14,924.66	15,108.44
$EL_{PV\rightarrow grid}$ [kWh]	13,340.66	13,443.00	13,532.73	13,076.30	13,177.91	13,266.31

In C1 (Table 13), four BESS, each with an energy capacity of 9.3 kWh (corresponding to one retired EV battery), are used to cover the overall timeframe. Each battery works for three years before reaching the EoL. In the timeframe examined, overall, four retired EV batteries are employed. Table 13 shows the energy simulation results referred to the examined time – frame.

In C2 (Table 14), two BESS, each with an energy capacity of 18.6 kWh (corresponding to two retired EV batteries), are used to cover the overall timeframe. Each BESS works for six years before reaching the EoL. In this configuration, four retired EV batteries are used.

Table 14. Energy model results in C2 (two retired EV batteries).

C2 - use phase	**BESS (18.6 kWh) – 1 replacement**					
			First BESS			
Year	**1**	**2**	**3**	**4**	**5**	**6**
$El_{BESS \rightarrow BL}$ [kWh]	4,060.64	3,869.34	3,697.74	3,533.16	3,375.17	3,223.17
$El_{\eta loss}$ [kWh]	459.61	482.01	502.02	520.01	536.07	550.25
$El_{grid \rightarrow BL}$ [kWh]	12,701.05	12,895.60	13,074.32	13,246.16	13,411.51	13,571.00
$EL_{PV \rightarrow grid}$ [kWh]	11,677.28	11,785.98	11,846.79	11,902.72	11,954.10	12,001.50
			Second BESS			
Year	**7**	**8**	**9**	**10**	**11**	**12**
$El_{BESS \rightarrow BL}$ [kWh]	4,036.97	3,847.29	3,678.30	3,515.07	3,358.42	3,208.08
$El_{\eta loss}$ [kWh]	456.91	479.26	499.38	517.35	533.41	547.67
$El_{grid \rightarrow BL}$ [kWh]	12,764.83	12,962.26	13,139.07	13,310.19	13,474.81	13,633.14
$EL_{PV \rightarrow grid}$ [kWh]	11,205.50	11,267.84	11,326.63	11,381.85	11,432.51	11,478.66

In C3 (Table 15), two BESS, each with an energy capacity of 27.9 kWh (corresponding to three retired EV batteries), are used to cover the overall timeframe. In this case, the BESS is able to provide its function for ten years, then the new BESS works for only two years in the examined timeframe. For the second BESS the same degradation pattern as the first one is assumed and then the same service life (ten years). However, only the first two years are analysed in order to cover the examined time – frame of twelve years.

Starting from C4, in which one BESS with an energy capacity of 37.2 kWh corresponding to four retired EV batteries is employed, the BESS is able to work for the entire time – frame, then it is not replaced in twelve years. The installation of a higher energy storage capacity allows for a longer battery lifetime. In fact, in C1, C2 and C3 the lower energy capacity installed causes a fast degradation of the BESS. In configurations C2 and C3 the increased installed capacity allows a lower stress for the

BESS compared with C1 and a slightly energy capacity degradation resulted in an increased BESS lifetime.

The battery degradation in both the first and the second services life is an important parameter in evaluating the feasibility of the second use applications of retired EV batteries. The degradation pattern affects the battery residual energy capacity after the first use in the EV and other parameters such as power, charge and discharge efficiency. Although, in energy storage systems applied in residential building, the requirements of such parameters are much lower than in an EV application, it is paramount to take in account the degradation as it affects the EV battery performance after the first life and both the performance and the lifetime of the EV batteries in the second life application. Prediction of battery degradation is currently a working area of research in the battery community. The lack of data in this field is reflected by the fact that, in several studies, the estimated life of a battery during its second use is based on manufacturer warranties [60,87] or assumptions and average data [95,104,163]. Considering the high relevance of this parameter, it is important to simulate the degradation of the battery capacity throughout the years after its installation in order to provide reliable estimation on EV battery lifetime. In this dissertation, the battery capacity face is modelled combining primary data on battery degradation derived from laboratory tests performed by the JRC [89] with data from the literature [87].

Table 15. Energy model results in C3 (three retired EV batteries).

C3 - use phase	**BESS (27.9 kWh) – 1 replacement**					
	First BESS					
Year	**1**	**2**	**3**	**4**	**5**	**6**
$El_{BESS \rightarrow BL}$ [kWh]	5,769.37	5,599.70	5,451.80	5,305.55	5,159.30	5,015.05
$El_{\eta loss}$ [kWh]	652.94	697.60	740.16	780.85	819.41	856.09
$El_{grid \rightarrow BL}$ [kWh]	10,992.32	11,165.24	11,320.26	11,473.77	11,627.38	11,779.12
$EL_{PV \rightarrow grid}$ [kWh]	9,782.67	9,840.07	9,854.61	9,869.52	9,886.65	9,903.79
	First BESS			**Second BESS**		
Year	**7**	**8**	**9**	**10**	**11**	**12**
$El_{BESS \rightarrow BL}$ [kWh]	4,874.18	4,735.34	4,599.02	4,465.89	5,706.17	5,536.40
$El_{\eta loss}$ [kWh]	891.17	924.43	955.98	986.00	645.76	689.73
$El_{grid \rightarrow BL}$ [kWh]	11,927.62	12,074.21	12,218.35	12,359.37	11,127.06	11,304.82
$EL_{PV \rightarrow grid}$ [kWh]	9,919.29	9,934.70	9,949.37	9,962.45	8,994.63	9,008.27

The yearly energy capacity degradation trend, corresponding to the configurations involving one (C1), two (C2) and three (C3) EV batteries, is illustrated in Figure 32, where the line with higher slope represents the battery capacity degradation in C1.

Table 16. Energy model results in C4 (four retired EV batteries).

C4 - use phase	**BESS (37.2 kWh) – no replacement**					
Year	**1**	**2**	**3**	**4**	**5**	**6**
$El_{BESS \rightarrow BL}$ [kWh]	7,105.52	6,970.41	6,860.70	6,749.52	6,636.21	6,522.39
$El_{\eta loss}$ [kWh]	804.05	868.52	931.61	993.54	1,054.14	1,113.56
$El_{grid \rightarrow BL}$ [kWh]	9,656.17	9,794.53	9,911.35	10,029.81	10,150.48	10,271.77
$EL_{PV \rightarrow grid}$ [kWh]	8,302.86	8,298.46	8,254.28	8,212.88	8,175.03	8,138.98
Year	**7**	**8**	**9**	**10**	**11**	**12**
$El_{BESS \rightarrow BL}$ [kWh]	6,408.36	6,294.72	6,180.57	6,066.35	5,950.98	5,834.82
$El_{\eta loss}$ [kWh]	1,171.82	1,228.99	1,284.86	1,339.47	1,392.52	1,444.01
$El_{grid \rightarrow BL}$ [kWh]	10,393.44	10,514.83	10,636.80	10,758.90	10,882.25	11,006.40
$EL_{PV \rightarrow grid}$ [kWh]	8,104.47	8,070.77	8,038.95	8,008.52	7,980.90	7,955.64

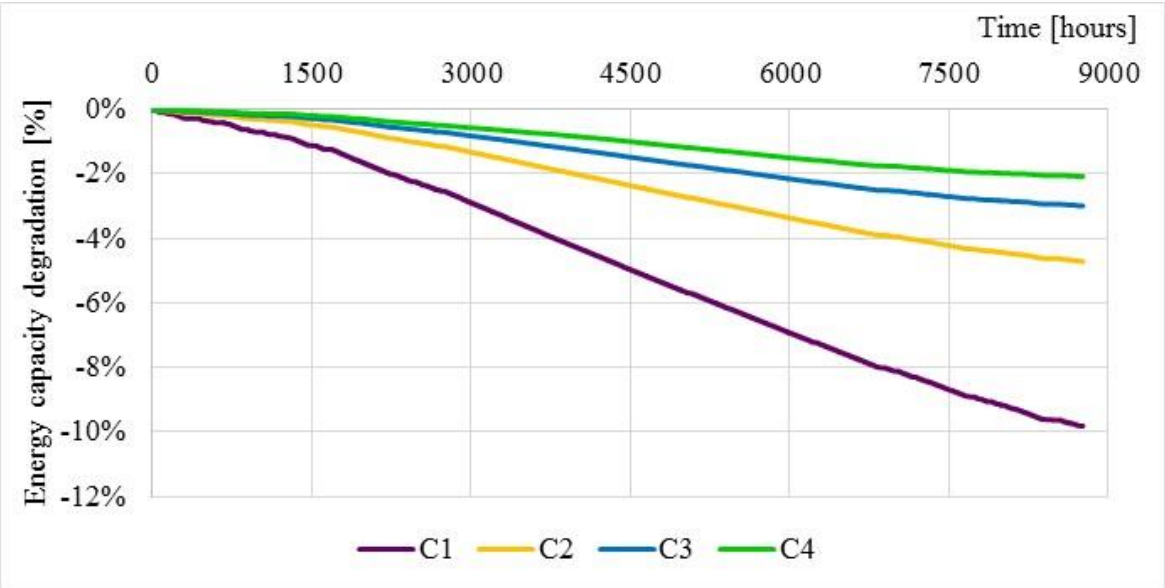

Figure 32. Yearly energy capacity degradation corresponding to different installed BESS capacities.

In the following, from Table 17 to Table 22, are illustrated the energy model results obtained in configurations from C5 to C10.

Table 17. Energy model results in C5 (five retired EV batteries).

C5 - use phase	BESS (46.5 kWh) – no replacement					
Year	**1**	**2**	**3**	**4**	**5**	**6**
$El_{BESS \rightarrow BL}$ [kWh]	7,951.88	7,849.67	7,777.02	7,703.49	7,628.02	7,549.62
$El_{\eta loss}$ [kWh]	899.29	978.00	1,055.98	1,133.94	1,211.68	1,288.96
$El_{grid \rightarrow BL}$ [kWh]	8,809.81	8,915.27	8,995.04	9,075.84	9,158.66	9,244.55
$EL_{PV \rightarrow grid}$ [kWh]	7,368.69	7,309.74	7,213.61	7,118.53	7,025.69	6,936.37
Year	**7**	**8**	**9**	**10**	**11**	**12**
$El_{BESS \rightarrow BL}$ [kWh]	7,470.11	7,388.33	7,305.99	7,222.66	7,137.02	7,049.52
$El_{\eta loss}$ [kWh]	1,366.02	1,442.58	1,518.90	1,594.88	1,670.15	1,744.73
$El_{grid \rightarrow BL}$ [kWh]	9,331.68	9,421.21	9,511.38	9,602.59	9,696.21	9,791.70
$EL_{PV \rightarrow grid}$ [kWh]	6,848.53	6,763.58	6,679.50	6,596.81	6,517.24	6,440.22

Table 18. Energy model results in C6 (six retired EV batteries).

C6 - use phase	BESS (55.8 kWh) – no replacement					
Year	**1**	**2**	**3**	**4**	**5**	**6**
$El_{BESS \rightarrow BL}$ [kWh]	8,450.27	8,357.72	8,303.31	8,248.38	8,192.54	8,135.50
$El_{\eta loss}$ [kWh]	954.98	1,041.20	1,127.33	1,214.02	1,301.21	1,388.83
$El_{grid \rightarrow BL}$ [kWh]	8,311.42	8,407.21	8,468.75	8,530.95	8,594.14	8,658.67
$EL_{PV \rightarrow grid}$ [kWh]	6,822.05	6,738.52	6,616.00	6,493.58	6,371.66	6,250.64
Year	**7**	**8**	**9**	**10**	**11**	**12**
$El_{BESS \rightarrow BL}$ [kWh]	8,077.81	8,019.43	7,960.27	7,900.13	7,838.06	7,773.99
$El_{\eta loss}$ [kWh]	1,476.97	1,565.61	1,654.74	1,744.28	1,834.01	1,923.84
$El_{grid \rightarrow BL}$ [kWh]	8,723.99	8,790.12	8,857.10	8,925.13	8,995.17	9,067.23
$EL_{PV \rightarrow grid}$ [kWh]	6,129.90	6,009.46	5,889.39	5,769.95	5,652.35	5,536.65

Table 19. Energy model results in C7 (seven retired EV batteries).

C7 - use phase	BESS (65.1 kWh) – no replacement					
Year	**1**	**2**	**3**	**4**	**5**	**6**
$El_{BESS \rightarrow BL}$ [kWh]	8,735.05	8,646.23	8,602.17	8,558.15	8,513.35	8,468.35
$El_{\eta loss}$ [kWh]	986.45	1,077.09	1,167.85	1,259.56	1,352.11	1,445.60
$El_{grid \rightarrow BL}$ [kWh]	8,026.64	8,118.71	8,169.89	8,221.18	8,273.33	8,325.81
$EL_{PV \rightarrow grid}$ [kWh]	6,513.24	6,414.14	6,276.63	6,138.29	5,999.97	5,861.04
Year	**7**	**8**	**9**	**10**	**11**	**12**
$El_{BESS \rightarrow BL}$ [kWh]	8,420.54	8,371.38	8,321.07	8,269.42	8,216.70	8,161.29
$El_{\eta loss}$ [kWh]	1,539.58	1,634.26	1,729.67	1,825.74	1,922.53	2,019.60
$El_{grid \rightarrow BL}$ [kWh]	8,381.26	8,438.17	8,496.30	8,555.84	8,616.53	8,679.93
$EL_{PV \rightarrow grid}$ [kWh]	5,724.58	5,588.89	5,453.69	5,319.22	5,185.21	5,053.61

Table 20. Energy model results in C8 (eight retired EV batteries).

C8 - use phase	**BESS (74.4 kWh) – no replacement**					
Year	**1**	**2**	**3**	**4**	**5**	**6**
$El_{BESS \rightarrow BL}$ [kWh]	8,916.68	8,823.08	8,781.45	8,739.03	8,695.80	8,652.70
$El_{\eta loss}$ [kWh]	1,006.15	1,099.03	1,192.10	1,286.09	1,380.99	1,476.98
$El_{grid \rightarrow BL}$ [kWh]	7,845.01	7,941.86	7,990.61	8,040.30	8,090.88	8,141.47
$EL_{PV \rightarrow grid}$ [kWh]	6,319.34	6,215.37	6,073.12	5,930.91	5,788.66	5,645.33
Year	**7**	**8**	**9**	**10**	**11**	**12**
$El_{BESS \rightarrow BL}$ [kWh]	8,607.55	8,560.75	8,513.22	8,465.48	8,416.41	8,365.57
$El_{\eta loss}$ [kWh]	1,573.69	1,671.16	1,769.54	1,868.97	1,969.20	2,070.10
$El_{grid \rightarrow BL}$ [kWh]	8,194.24	8,248.80	8,304.15	8,359.77	8,416.82	8,475.65
$EL_{PV \rightarrow grid}$ [kWh]	5,503.47	5,362.64	5,221.68	5,079.95	4,938.84	4,798.85

Table 21. Energy model results in C9 (nine retired EV batteries).

C9 - use phase	**BESS (83.7 kWh) – no replacement**					
Year	**1**	**2**	**3**	**4**	**5**	**6**
$El_{BESS \rightarrow BL}$ [kWh]	9,054.10	8,954.43	8,914.20	8,873.24	8,832.36	8,790.44
$El_{\eta loss}$ [kWh]	1,020.84	1,115.32	1,210.05	1,305.76	1,402.60	1,500.42
$El_{grid \rightarrow BL}$ [kWh]	7,707.59	7,810.51	7,857.86	7,906.08	7,954.32	8,003.73
$EL_{PV \rightarrow grid}$ [kWh]	6,174.67	6,067.75	5,922.45	5,777.03	5,630.50	5,484.18
Year	**7**	**8**	**9**	**10**	**11**	**12**
$El_{BESS \rightarrow BL}$ [kWh]	8,746.84	8,700.68	8,651.82	8,602.28	8,552.61	8,502.82
$El_{\eta loss}$ [kWh]	1,599.08	1,698.40	1,798.28	1,899.09	2,000.99	2,104.00
$El_{grid \rightarrow BL}$ [kWh]	8,054.96	8,108.87	8,165.55	8,222.98	8,280.62	8,338.40
$EL_{PV \rightarrow grid}$ [kWh]	5,338.82	5,195.48	5,054.36	4,913.05	4,770.88	4,627.72

Table 22. Energy model results in C10 (ten retired EV batteries).

C10 - use phase	**BESS (93 kWh) – no replacement**					
Year	**1**	**2**	**3**	**4**	**5**	**6**
$El_{BESS \rightarrow BL}$ [kWh]	9,178.23	9,070.69	9,029.86	8,988.01	8,942.93	8,897.19
$El_{\eta loss}$ [kWh]	1,034.02	1,129.72	1,225.67	1,322.58	1,420.11	1,518.59
$El_{grid \rightarrow BL}$ [kWh]	7,583.46	7,694.24	7,742.20	7,791.32	7,843.75	7,896.98
$EL_{PV \rightarrow grid}$ [kWh]	6,044.80	5,937.10	5,791.18	5,645.46	5,502.45	5,359.27
Year	**7**	**8**	**9**	**10**	**11**	**12**
$El_{BESS \rightarrow BL}$ [kWh]	8,850.35	8,803.84	8,757.71	8,708.54	8,657.20	8,605.99
$El_{\eta loss}$ [kWh]	1,617.96	1,718.49	1,820.25	1,922.52	2,025.43	2,129.50
$El_{grid \rightarrow BL}$ [kWh]	7,951.45	8,005.71	8,059.66	8,116.71	8,176.03	8,235.23
$EL_{PV \rightarrow grid}$ [kWh]	5,216.45	5,072.24	4,926.52	4,783.37	4,641.85	4,499.06

From data analysis results that the amount of electricity produced by the PV and delivered to the building through the BESS ($El_{BESS\rightarrow BL}$) increases as the BESS size increases. This is an expected outcome as higher is the size of the BESS higher is the amount of energy stored in and then available for the building. In each configuration, the $El_{BESS\rightarrow BL}$ decreases with time due to the battery capacity degradation and then to a reduced battery storage capacity (Figure 33). In detail in C1, the $El_{BESS\rightarrow BL}$ provided in the second and in the third year of BESS decreases, respectively, by 9.6% and 18% compared to the same value in the first year (Table 13). In C2 and C3, the $El_{BESS\rightarrow BL}$ in the last operation year of the BESS, respectively sixth and tenth year, decreases by around 20% compared to the first one. The rate of decrease of $El_{BESS\rightarrow BL}$ with time is lower in configurations with larger BESS size due to a lower battery stress that results in a lower battery degradation rate. In C5, the $El_{BESS\rightarrow BL}$ in the last operation year of the BESS decreases by around 13% compared to the first one and in C10 by around 12%.

With reference to $El_{\eta loss}$, it increases as the BESS size increases (Figure 37), since the electricity loss due to the BESS efficiency are higher in correspondence of higher consumption of electricity from the BESS (Figure 34). Moreover, in each configuration, $El_{\eta loss}$ increases with time due to the battery efficiency degradation. In this dissertation, the value of the cell charge/discharge efficiency is obtained from laboratory test. Due to a lack of data about charge/discharge efficiency degradation, it is assumed a linear degradation over time not related to the battery cycling (5 percentage points in 5 years) according to literature [89]. Then, in C1 and C2, the electricity loss due to the battery efficiency are lower since the BESS is replaced, respectively, after three and six operational years. In C3 the $El_{\eta loss}$, in the last operation year, increases of around 50% compared to the first one, in C5 by around 90%, and finally, in C10 by around 100%. Moreover, in the last the loss due to the battery efficiency accounts, in the last operation year, for about 6% of the overall electricity consumption. Then besides the battery capacity fade, also the battery efficiency fade, it is a relevant parameter of the battery operation phase. There is a paucity of performance data on charge/discharge efficiency for full EV pack [94] that takes into account additional loss due to the BMS. Therefore, further efforts to gather data about this parameter are needed in order to provide reliable estimation.

Concerning the electricity adsorbed from the electrical grid to feed the building load, it decreases with the increase of the capacity installed (Figure 37) since a higher share of the building load is match by the BESS. However, in each configuration, during the operational phase the amount of electricity taken from the grid increases due to the degradation of the BESS capacity.

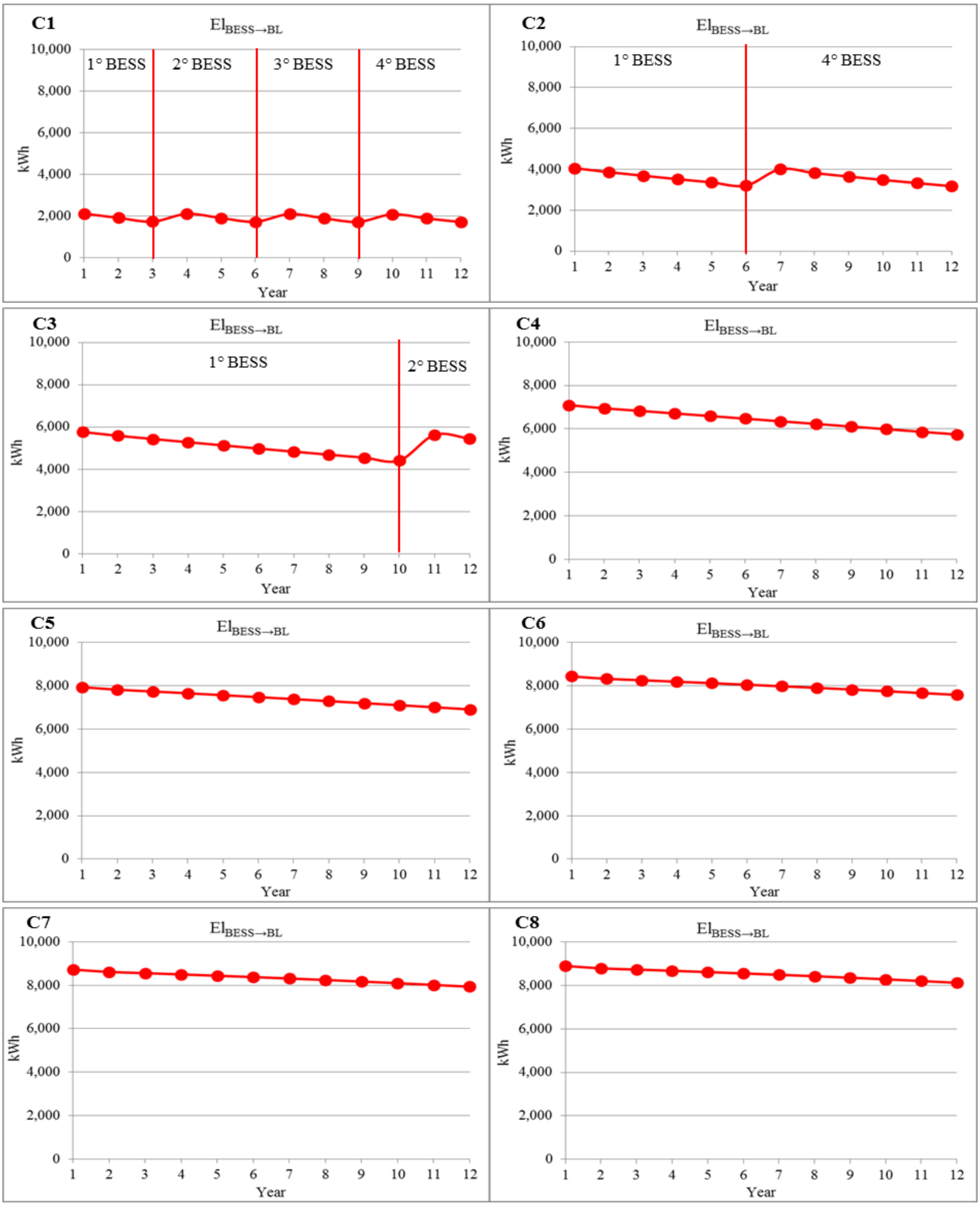

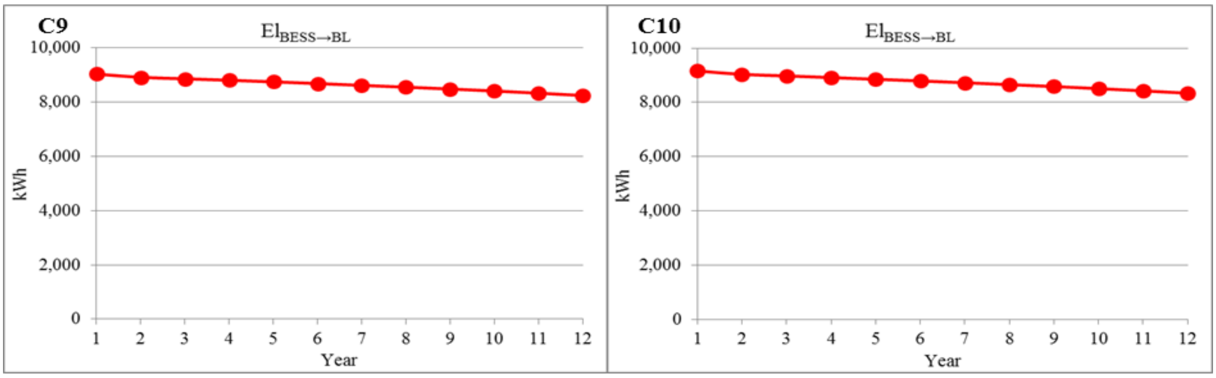

Figure 33. Trend of $EL_{BESS \rightarrow BL}$ in the timeframe examined in each configuration.

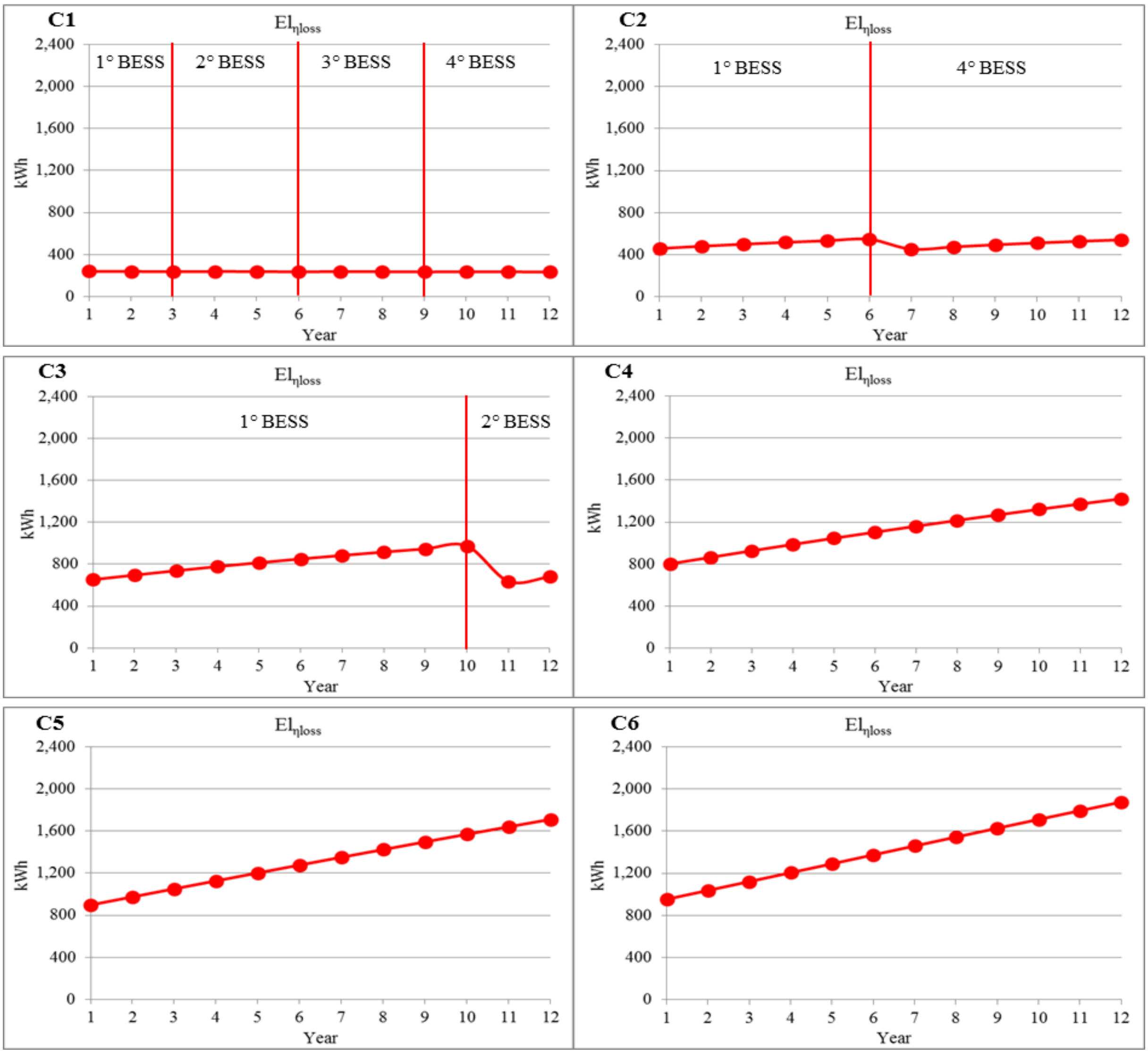

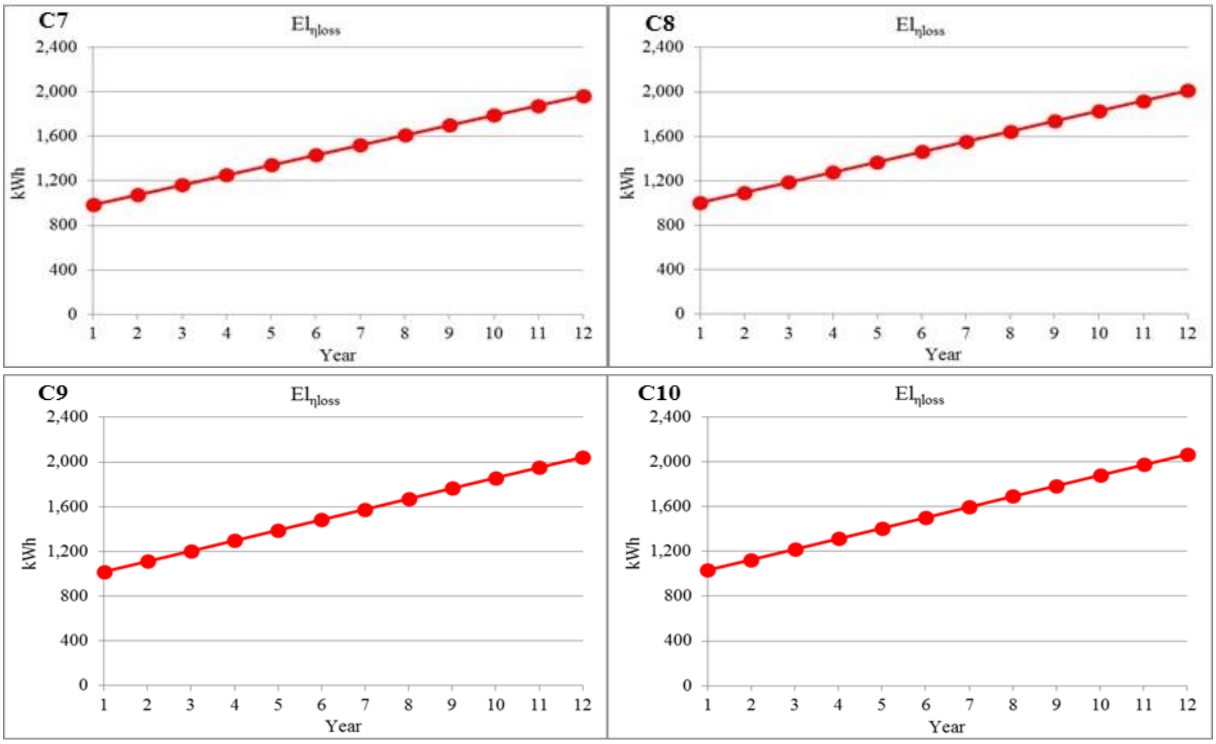

Figure 34. Trend of $El\eta_{loss}$ in the timeframe examined in each configuration.

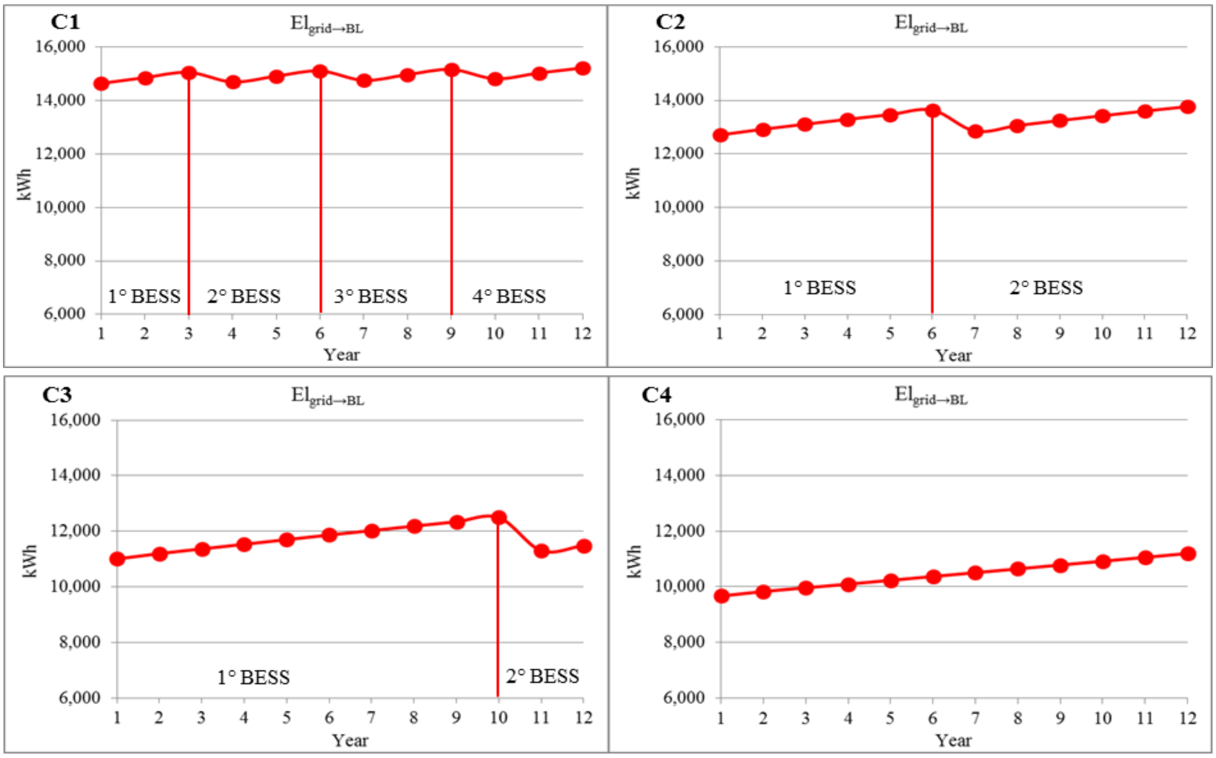

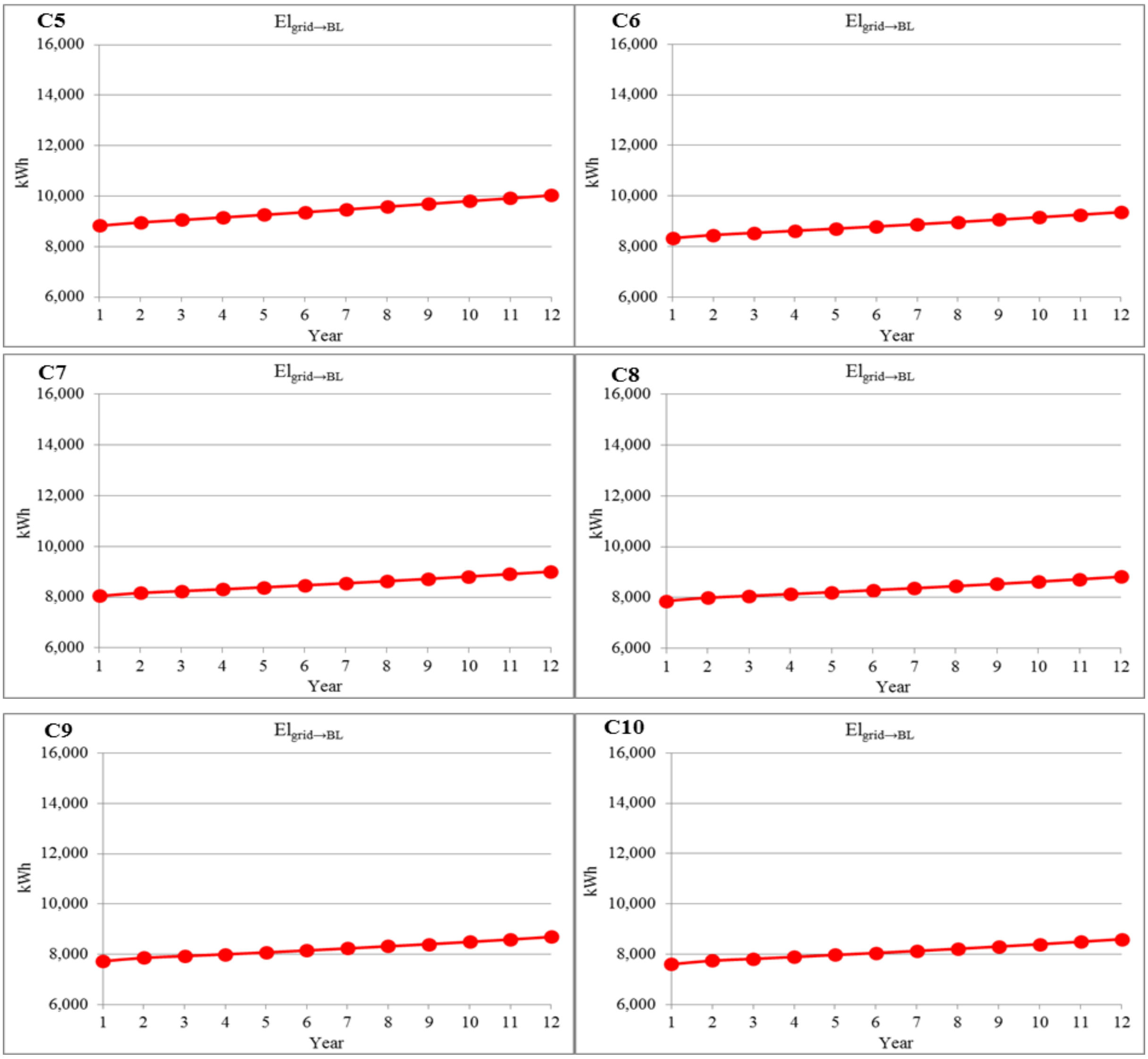

Figure 35. Trend of $EL_{grid\rightarrow BL}$ in the timeframe examined in each configuration.

The electricity fed into the grid decreases as the BESS increases (Figure 36 and Figure 37).

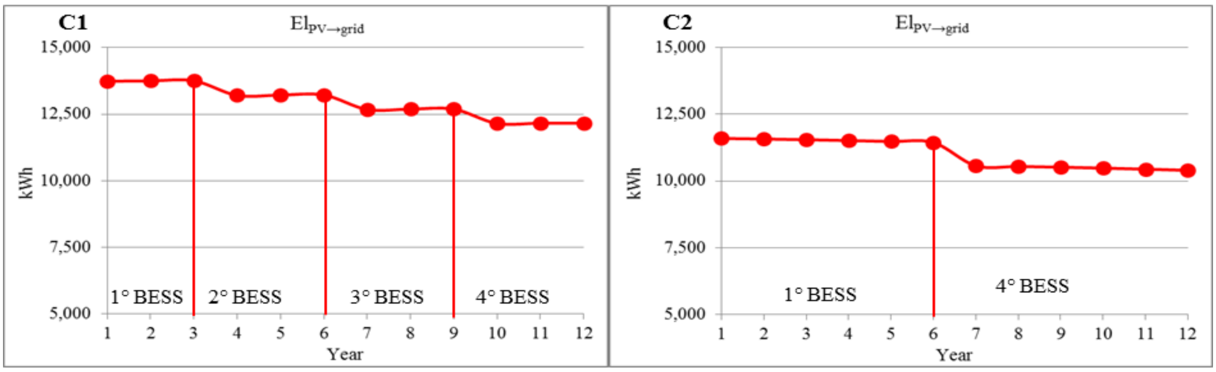

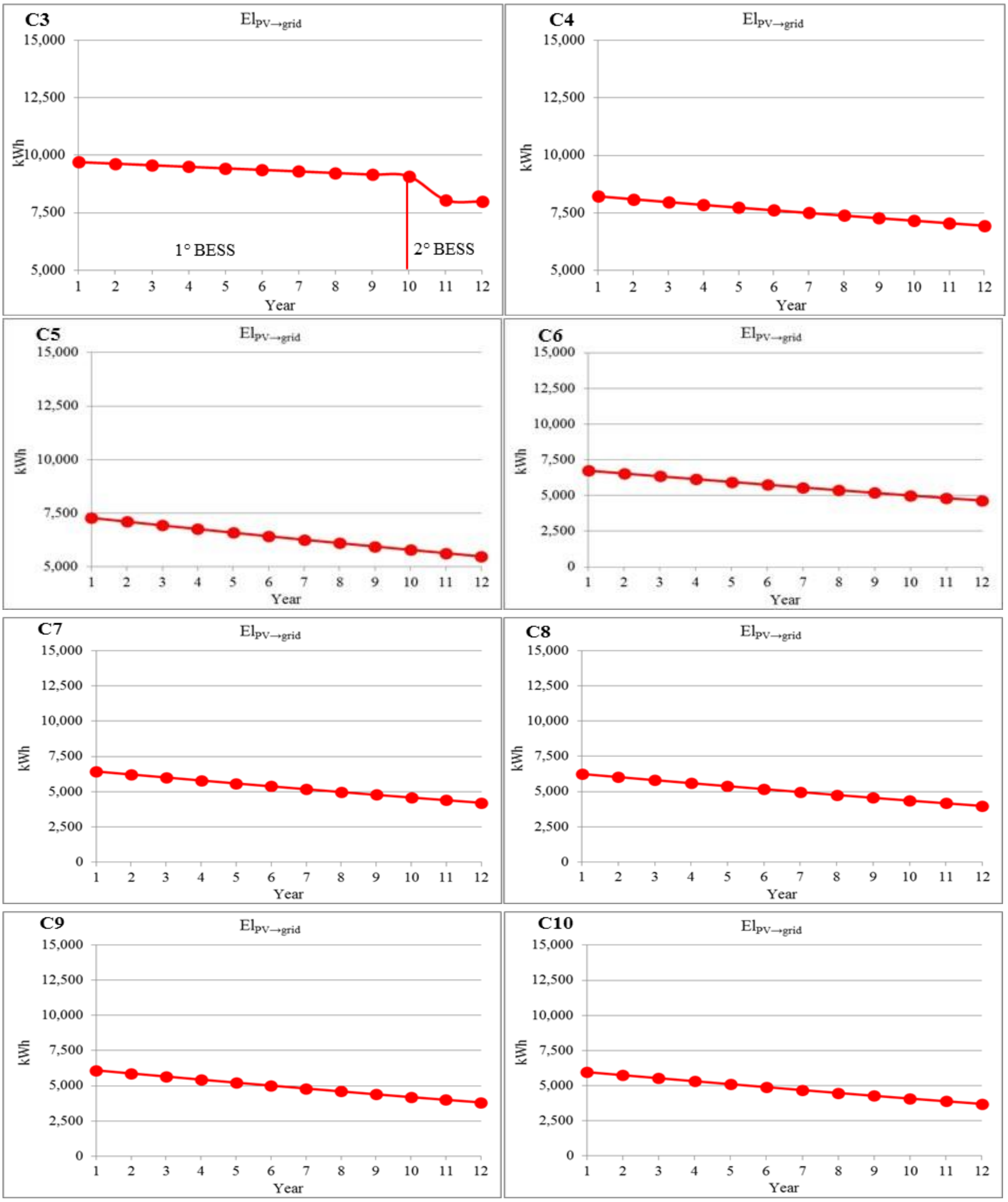

Figure 36. Trend of $EL_{PV \rightarrow grid}$ in the timeframe examined in each configuration.

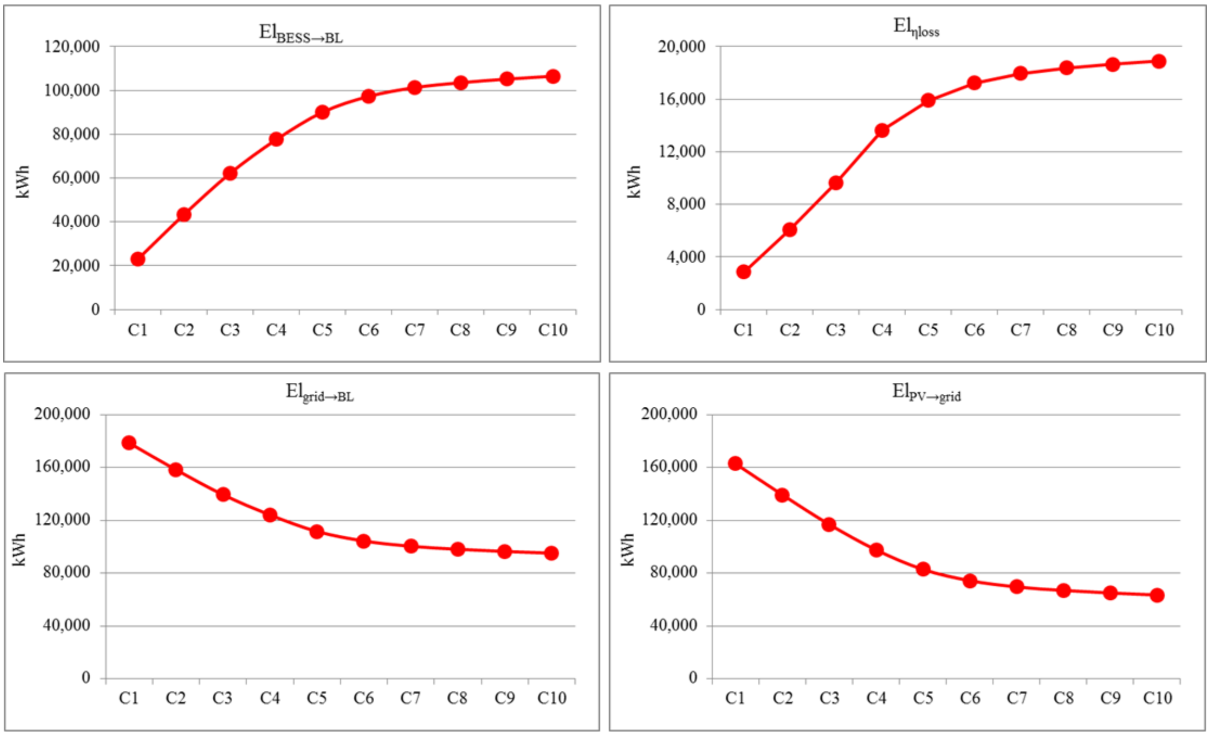

Figure 37. Trends of $EL_{BESS \rightarrow BL}$, $El\eta_{loss}$,$EL_{grid \rightarrow BL}$, $EL_{PV \rightarrow grid}$ with the increasing BESS size.

Table 23. PV – BESS – electrical grid system energy modelling overall results.

Parameter	C1	C2	C3	C4	C5
El_{PV} [kWh]	287,858.28	287,858.28	287,858.28	287,858.28	287,858.28
BL [kWh]	300,722.24	300,722.24	300,722.24	300,722.24	300,722.24
$El_{PV \rightarrow BL}$ [kWh]	99,134.97	99,134.97	99,134.97	99,134.97	99,134.97
$El_{BESS \rightarrow BL}$ [kWh]	23,069.82	43,403.33	62,217.77	77,580.54	90,033.34
$El_{\eta loss}$ [kWh]	2,855.44	6,083.95	9,640.12	13,627.09	15,905.11
$El_{grid \rightarrow BL}$ [kWh]	178,517.46	158,183.94	139,369.50	124,006.74	111,553.93
$EL_{PV \rightarrow grid}$ [kWh]	162,822.51	139,261.37	116,906.01	97,541.74	82,818.53
Parameter	**C6**	**C7**	**C8**	**C9**	**C10**
El_{PV} [kWh]	287,858.28	287,858.28	287,858.28	287,858.28	287,858.28
BL [kWh]	300,722.24	300,722.24	300,722.24	300,722.24	300,722.24
$El_{PV \rightarrow BL}$ [kWh]	99,134.97	99,134.97	99,134.97	99,134.97	99,134.97
$El_{BESS \rightarrow BL}$ [kWh]	97,257.41	103,537.72	105,175.80	105,175.80	106,490.54
$El_{\eta loss}$ [kWh]	17,227.03	18,364.00	18,654.82	18,654.82	18,884.83
$El_{grid \rightarrow BL}$ [kWh]	104,329.86	98,049.55	96,411.48	96,411.48	95,096.74
$EL_{PV \rightarrow grid}$ [kWh]	74,280.17	66,878.17	64,956.90	64,956.90	63,419.76

The energy analysis of the PV – BESS – electrical grid system highlights that the installation of an increasing energy storage capacity allows increasing the consumption of the electricity locally produced by PV and, consequently, to reduce the electricity imported from the grid. In particular, the last decreases by 46.7% in C10 compared to C1. However, starting from installed energy storage capacities between 46.5 kWh (C5) and 55.8 kWh (C6) any improvement can be considered negligible. This means that even though the self-consumption increases as the BESS size increases, it would not be by such a vast amount to justify the choice of a larger BESS.

Figure 38 shows how the percentage contribution of each energy system component changes with the installation of an increasing energy storage capacity.

The percentage contribution of $El_{PV \rightarrow BL}$ remains unchanged from C1 to C10 since the BESS does not affect this energy flow. The amount of electricity provided to the building through the BESS ranges from 7.7% in C1 to 35.4% in C10. Overall, it can be observed that starting from C5 the percentage breakdown among $El_{PV \rightarrow BL}$, $El_{grid \rightarrow BL}$ and $El_{BESS \rightarrow BL}$ shows negligible variations.

Figure 39 shows the percentage breakdown of the electricity generated by the PV plant with the installation of an increasing energy storage capacity. The amount of electricity fed to the electrical grid ranges from 56.6% in C1 to 22.0% in C10.

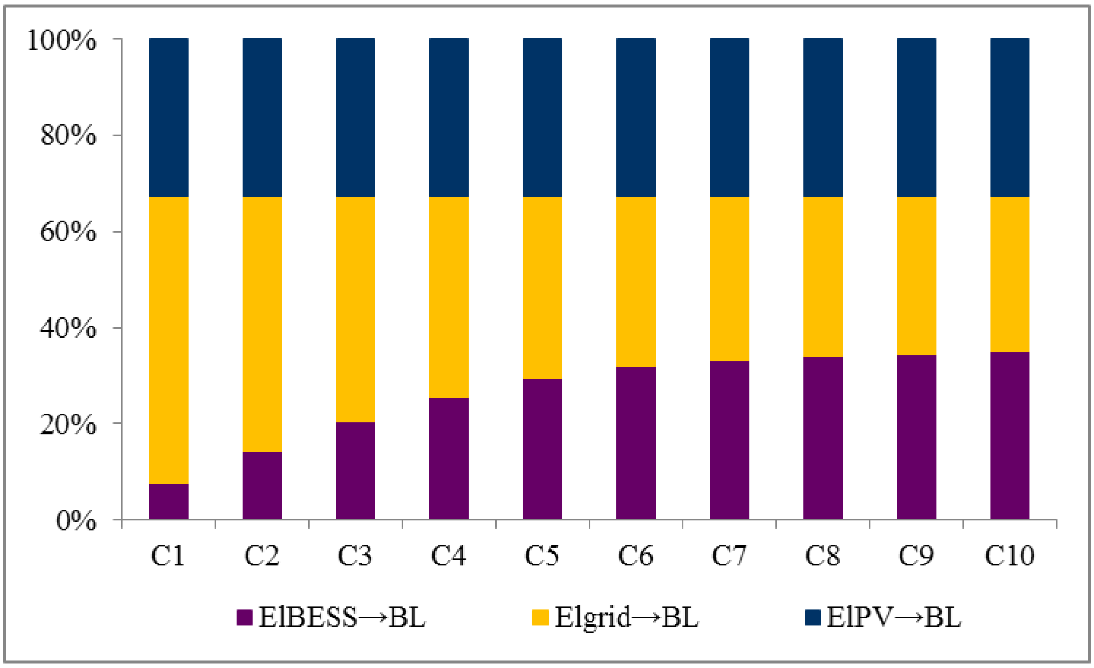

Figure 38. Percentage contribution of each energy system component with the installation of an increasing energy storage capacity.

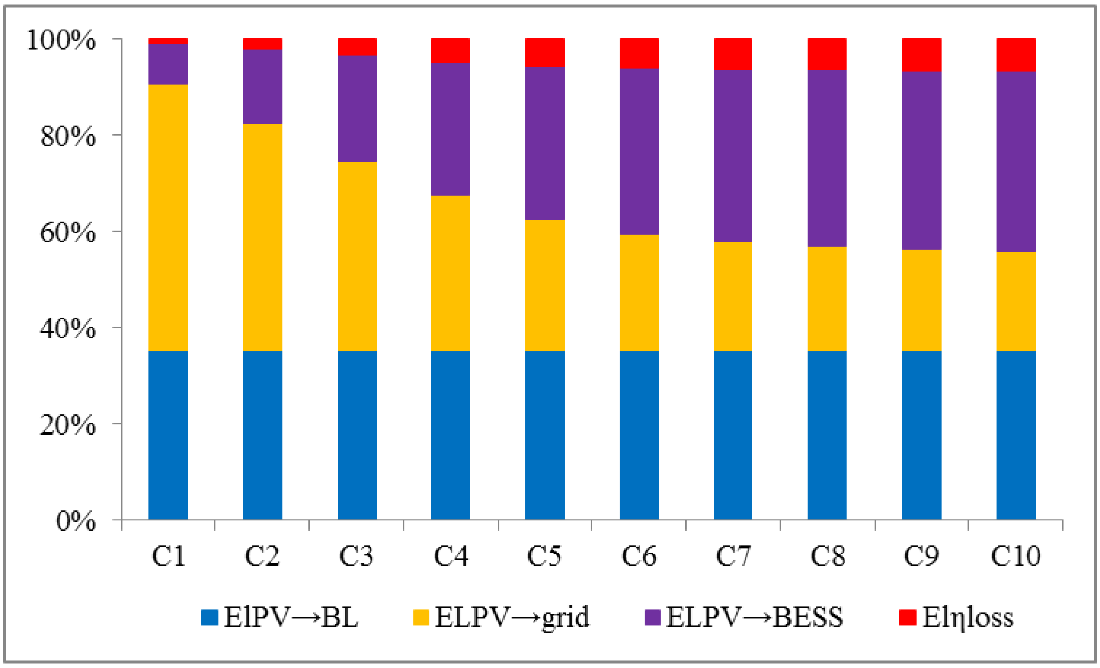

Figure 39. Percentage breakdown of the electricity generated by the PV plant with the installation of an increasing energy storage capacity.

5.2 PV – BESS – electrical grid system: load match and net exported analysis results

The load match between the on-site electricity generation and the building load is assessed through the γ_{load} indicator that describes the degree of matching of on-site energy generation to local energy demand. The building interaction with the energy infrastructure is evaluated through the ne factor that quantifies the amount of imported and exported energy.

In this section, the results of these factors are presented and discussed.

Table 24 illustrates the hourly γ_{load} values averaged on annual basis for each configuration examined and for each year simulated. Figure 40 shows the hourly γ_{load} values averaged over the examined period (12 years).

The results analysis highlights that γ_{load} grows together with the storage but after reaching the storage threshold of 46.5 kWh/55.8 kWh (corresponding, respectively, to the employment of five and six retired EV batteries), the effect of the storage on the γ_{load} is very limited (Figure 40). In fact, referring to the first year of simulation of each configuration, as an example, it results that γ_{load} in C2 increases by 17% compared to C1, but in C6 increases only by 3% compared to C5, and in C7 only by 2% compared to C6. Then, the γ_{load} is fairly steady starting from C5.

Table 24. Hourly γ_{load} values averaged on annual basis for each configuration examined.

Years	**Installed energy capacity [kWh]**									
	9.3	**18.6**	**27.9**	**37.2**	**46.5**	**55.8**	**65.1**	**74.4**	**83.7**	**93.0**
1	0.453	0.532	0.614	0.677	0.711	0.730	0.741	0.748	0.753	0.758
2	0.445	0.523	0.605	0.670	0.706	0.725	0.737	0.743	0.748	0.752
3	0.438	0.515	0.598	0.665	0.703	0.723	0.734	0.741	0.745	0.750
4	0.451	0.508	0.590	0.659	0.699	0.719	0.731	0.738	0.743	0.747
5	0.443	0.500	0.582	0.653	0.695	0.716	0.728	0.736	0.740	0.744
6	0.436	0.493	0.574	0.647	0.691	0.713	0.725	0.733	0.738	0.742
7	0.449	0.527	0.566	0.641	0.686	0.710	0.723	0.730	0.735	0.739
8	0.441	0.518	0.559	0.635	0.682	0.706	0.719	0.727	0.732	0.736
9	0.434	0.510	0.552	0.629	0.677	0.703	0.716	0.724	0.729	0.733
10	0.447	0.503	0.545	0.622	0.673	0.699	0.713	0.720	0.726	0.729
11	0.439	0.495	0.603	0.616	0.668	0.695	0.709	0.717	0.722	0.726
12	0.432	0.489	0.595	0.610	0.664	0.688	0.705	0.713	0.719	0.722

The results analysis highlights that γ_{load} grows together with the storage but after reaching the storage threshold of 46.5 kWh/55.8 kWh (corresponding, respectively, to the employment of five and six retired EV batteries), the effect of the storage on the γ_{load} is very limited (Figure 40). In fact, referring to the first year of simulation of each configuration, as an example, it results that γ_{load} in C2 increases by 17% compared to C1, but in C6 increases only by 3% compared to C5, and in C7 only by 2% compared to C6. Then, the γ_{load} is fairly steady starting from C5.

The γ_{load} values decrease during the time – frame examined due to both the BESS capacity and PV degradation. However, the rate of γ_{load} reduction decreases in correspondence of the higher BESS size. This is due, as explained in Section 5.3, to the fact that the installation of a higher energy storage capacity allows a lower stress for the BESS and a slightly energy capacity degradation (Figure 32).

Table 25 shows the hourly γ_{load} values averaged on monthly basis (γ_{load_m}) for three representative years for each configuration examined (the first, the medium and the last operation year of the BESS lifetime). The higher values of γ_{load} occur, for each configuration, in correspondence of June due to the higher maximum and average values for solar horizontal radiation (Figure 16), the lower ones in January. Moreover, the improvement of the hourly γ_{load} values averaged on monthly basis are significant until the C5. The percentage variations of the γ_{load_m} in C6 compared to C5 are always lower than 4%, with the exception of the July in which the increases by 6% respect the corresponding value in C5.

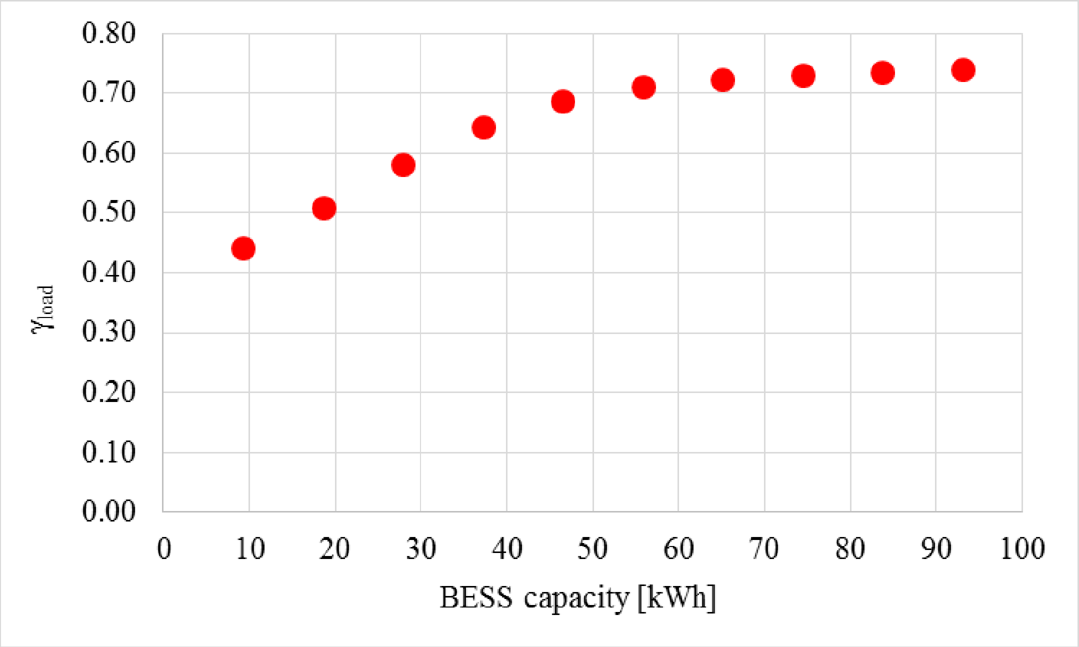

Figure 40. Hourly γ_{load} values averaged on annual basis over the examined period (12 years) for each configuration examined.

Table 25. Hourly γ_{load_m} values averaged on monthly basis for three representative years for each configuration examined.

Configuration	Year	January	February	March	April	May	June	July	August	September	October	November	December
	1Y	0.21907	0.32616	0.42563	0.50367	0.62404	0.64372	0.54394	0.55544	0.52748	0.44622	0.37095	0.25792
C1	2Y	0.21280	0.32197	0.41868	0.49255	0.61371	0.63358	0.53747	0.54728	0.51925	0.43776	0.36296	0.25392
	3Y	0.20977	0.31766	0.41218	0.48554	0.60434	0.62399	0.53143	0.53959	0.51172	0.42958	0.35604	0.24985
	1Y	0.24989	0.36505	0.49067	0.59530	0.76553	0.77791	0.60816	0.64286	0.63297	0.53290	0.43657	0.29299
C2	3Y	0.23700	0.35804	0.47927	0.57775	0.73554	0.75264	0.59716	0.62716	0.61358	0.51557	0.42470	0.28738
	6Y	0.23035	0.34802	0.46354	0.55836	0.69749	0.71682	0.58241	0.60535	0.58786	0.49263	0.41038	0.27963
	1Y	0.26929	0.39737	0.55806	0.69744	0.90690	0.91794	0.67971	0.73999	0.75648	0.64249	0.50206	0.31355
C3	5Y	0.25217	0.38408	0.53188	0.66048	0.87108	0.87812	0.65455	0.70737	0.71327	0.60398	0.47820	0.30549
	10Y	0.24575	0.37038	0.50566	0.62073	0.80857	0.82229	0.62857	0.66959	0.66516	0.55921	0.45221	0.29636
	1Y	0.28420	0.43147	0.62609	0.77596	0.95499	0.97916	0.76321	0.84110	0.87632	0.72465	0.55604	0.33440
C4	6Y	0.26138	0.41528	0.59790	0.74958	0.94297	0.96734	0.72969	0.80104	0.83372	0.69938	0.53338	0.32443
	12Y	0.25484	0.39872	0.56558	0.71042	0.91821	0.93391	0.69279	0.75596	0.77614	0.65333	0.50438	0.31209
	1Y	0.29724	0.45288	0.68040	0.80598	0.97798	0.98527	0.83567	0.91040	0.93308	0.75343	0.58154	0.34730
C5	6Y	0.27174	0.44246	0.66094	0.79509	0.96994	0.98347	0.81217	0.88921	0.92014	0.73921	0.56898	0.34007
	12Y	0.26495	0.42975	0.63335	0.78043	0.95614	0.98141	0.78099	0.85729	0.89390	0.72124	0.54639	0.33026
	1Y	0.30389	0.46766	0.70135	0.82520	0.98988	0.99026	0.88603	0.94987	0.94793	0.77376	0.60337	0.35273
C6	6Y	0.27705	0.46038	0.69397	0.81924	0.98531	0.98848	0.87275	0.93724	0.94066	0.76526	0.58867	0.34501
	12Y	0.27039	0.44922	0.68184	0.80908	0.97933	0.98578	0.85099	0.92016	0.93312	0.75093	0.56973	0.33588
	1Y	0.30700	0.47775	0.71554	0.83790	0.99194	0.99462	0.90387	0.96805	0.95904	0.79474	0.62189	0.35517
C7	6Y	0.27705	0.47038	0.70912	0.83235	0.99194	0.99366	0.89657	0.96288	0.95459	0.78433	0.60806	0.34792
	12Y	0.27070	0.46157	0.70078	0.82682	0.99148	0.99166	0.88509	0.95265	0.94848	0.77058	0.58944	0.33875
	1Y	0.31038	0.48570	0.72834	0.85083	0.99194	0.994624	0.91061	0.97881	0.96250	0.80633	0.63353	0.35517
C8	6Y	0.27705	0.47823	0.72211	0.84624	0.99194	0.994624	0.90436	0.97419	0.96105	0.80127	0.62043	0.34792
	12Y	0.27070	0.46891	0.71430	0.84128	0.99194	0.994624	0.89469	0.96833	0.95943	0.79294	0.60346	0.33875
	1Y	0.31500	0.48826	0.73828	0.86539	0.99194	0.994624	0.91392	0.98629	0.96672	0.81301	0.64210	0.35517
C9	6Y	0.27705	0.48105	0.73305	0.86065	0.99194	0.994624	0.90770	0.98349	0.96473	0.80899	0.62888	0.34792
	12Y	0.27070	0.47202	0.72589	0.85520	0.99194	0.994624	0.89853	0.97898	0.96237	0.80312	0.61129	0.33875
	1Y	0.31955	0.49055	0.74784	0.88041	0.99194	0.994624	0.91788	0.99019	0.97129	0.82049	0.65314	0.35517
C10	6Y	0.27705	0.48308	0.74142	0.87616	0.99194	0.994624	0.91169	0.98834	0.96921	0.81588	0.63929	0.34792
	12Y	0.27070	0.47220	0.73095	0.87056	0.99194	0.994624	0.90222	0.98597	0.96750	0.81058	0.61630	0.33875

In Table 26, the hourly ne values averaged on annual basis for each configuration examined are presented. The values of ne decrease with the increasing BESS size, since in correspondence of a higher energy storage capacity the amount of electricity fed into the grid decrease (Figure 41). Also for ne as γ_{load} the effect of the installation of an increasing energy storage capacity becomes negligible after the threshold of 46.5 kWh.

Table 26. Hourly ne values averaged on annual basis for each configuration examined.

Years	**Installed energy capacity [kWh]**									
	9.3	**18.5**	**27.8**	**37.1**	**46.3**	**55.6**	**64.9**	**74.2**	**83.4**	**92.7**
1	-0.079	-0.091	-0.102	-0.110	-0.114	-0.117	-0.118	-0.118	-0.118	-0.118
2	-0.081	-0.096	-0.110	-0.120	-0.127	-0.131	-0.134	-0.135	-0.136	-0.137
3	-0.082	-0.099	-0.115	-0.128	-0.136	-0.141	-0.143	-0.145	-0.146	-0.147
4		-0.102	-0.120	-0.135	-0.144	-0.150	-0.153	-0.155	-0.157	-0.158
5		-0.104	-0.125	-0.142	-0.153	-0.160	-0.163	-0.165	-0.167	-0.168
6		-0.107	-0.129	-0.148	-0.162	-0.169	-0.173	-0.176	-0.178	-0.179
7			-0.134	-0.155	-0.170	-0.179	-0.184	-0.187	-0.188	-0.190
8			-0.138	-0.162	-0.179	-0.189	-0.194	-0.197	-0.199	-0.201
9			-0.142	-0.168	-0.187	-0.198	-0.205	-0.208	-0.210	-0.212
10			-0.146	-0.174	-0.196	-0.208	-0.215	-0.219	-0.222	-0.224
11				-0.181	-0.204	-0.218	-0.226	-0.230	-0.233	-0.235
12				-0.187	-0.213	-0.228	-0.237	-0.242	-0.245	-0.247

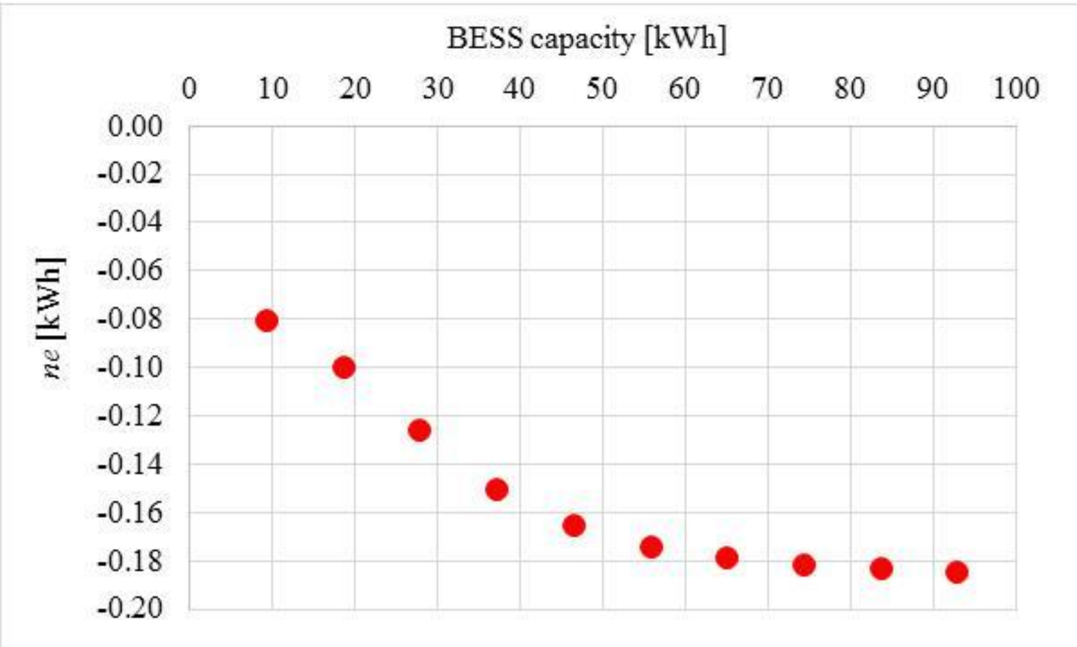

Figure 41. Hourly ne values averaged over the whole examined period (12 years) for each configuration examined.

Figure 42 and Figure 43 show, respectively, the coloured contour graphs of the γ_{load} and ne for the first and the last operation year of BESS lifetime, in all the configurations examined. The representation of the γ_{load} and *ne* in coloured contour graph gives significant information on when during the whole year the electricity demand of the building is supply by the electricity generated on – site and on when the electricity is imported in and exported from the grid. The x-axis reports the hours of the day (24) and the y-axis indicates the days of the year (1-365). The bars on the left associate the colours in the graph with the values assumed by the γ_{load} and *ne* in the whole period examined. Figure 42 shows that in C1 the γ_{load} follows the on-site PV generation for the most part of the year. In C2, due to the adoption of a higher energy capacity, the electricity stored in the BESS during periods with high PV generation and low load is able to supply electricity during the night for the greatest part of the year and in the summer season during the early morning hours. Starting from C5, the γ_{load} is equal to or close to one for a large part of the day during the whole year.

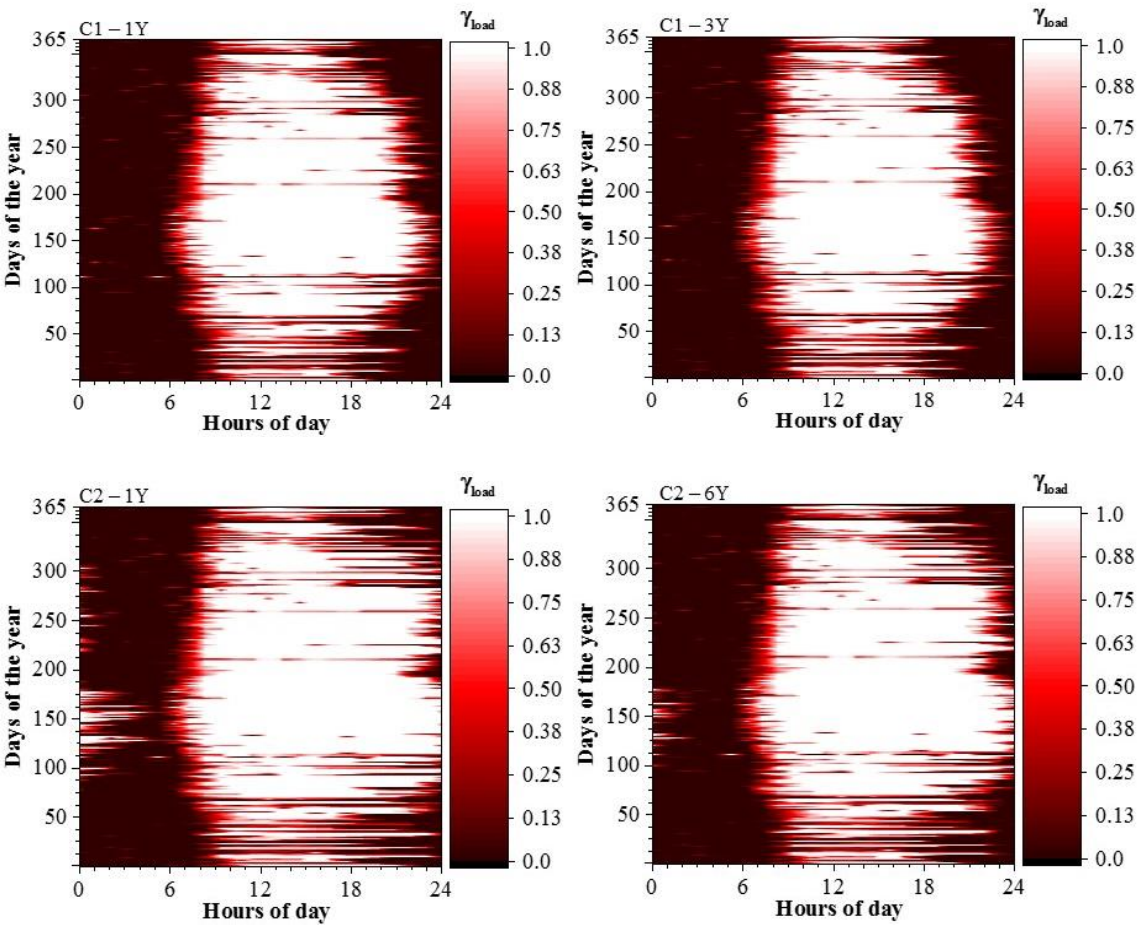

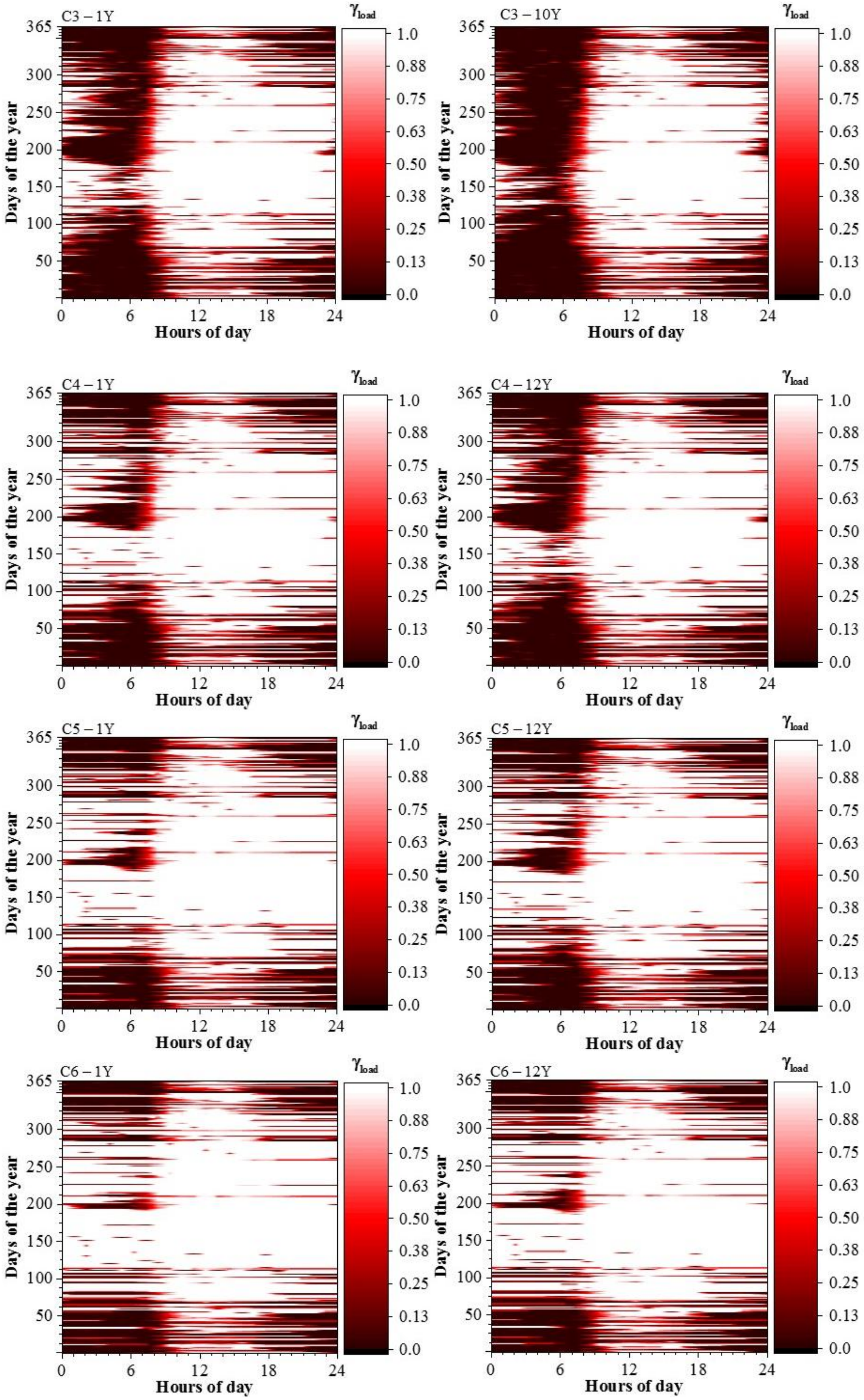
C3 – 1Y
C3 – 10Y
C4 – 1Y
C4 – 12Y
C5 – 1Y
C5 – 12Y
C6 – 1Y
C6 – 12Y
Days of the year
Hours of day
γ_{load}
365
300
250
200
150
100
50
0
6
12
18
24
1.0
0.88
0.75
0.63
0.50
0.38
0.25
0.13
0.0

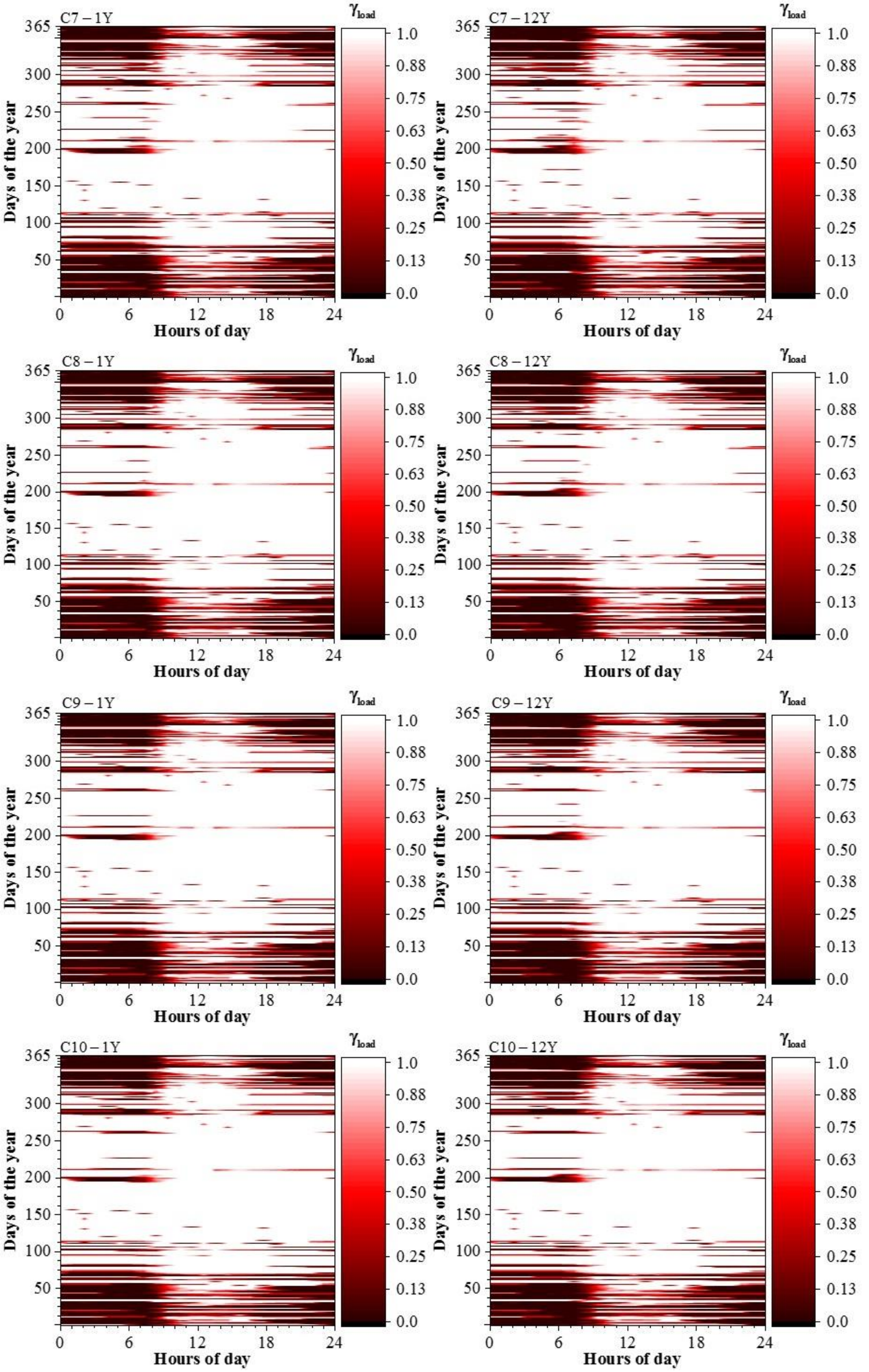

Figure 42. Coloured contour graph of the γ_{load} for the first and the last year of operation in each configuration examined.

The analysis of the coloured contour graph of the γ_{load} confirms that after reaching the threshold of 46.5 kWh any further increase in the storage energy capacity would yield only limited benefit. In Figure 42 it is also highlighted the effect of the BESS capacity degradation on the γ_{load}. In correspondence of each configuration analysed, the white area in the graph that represents the periods of the year with γ_{load} equal to one decreases in the last operation year of the BESS compared to the first one due to the capacity degradation that reduce the amount of energy dischargeable. However, the differences between the first and the last year of operation becomes negligible after C5. In fact, a higher installed energy capacity results in a lower stress for the BESS and then in a lower degradation of its performance.

Concerning to the *ne* indicator, the analysis highlights that the amount of electricity exported into the grid decreases as the BESS size increases, as it is able to store a larger amount of electricity. Also for the *ne* indicator, the improvement became negligible as the BESS energy capacity reaches the threshold of 46.5 kWh.

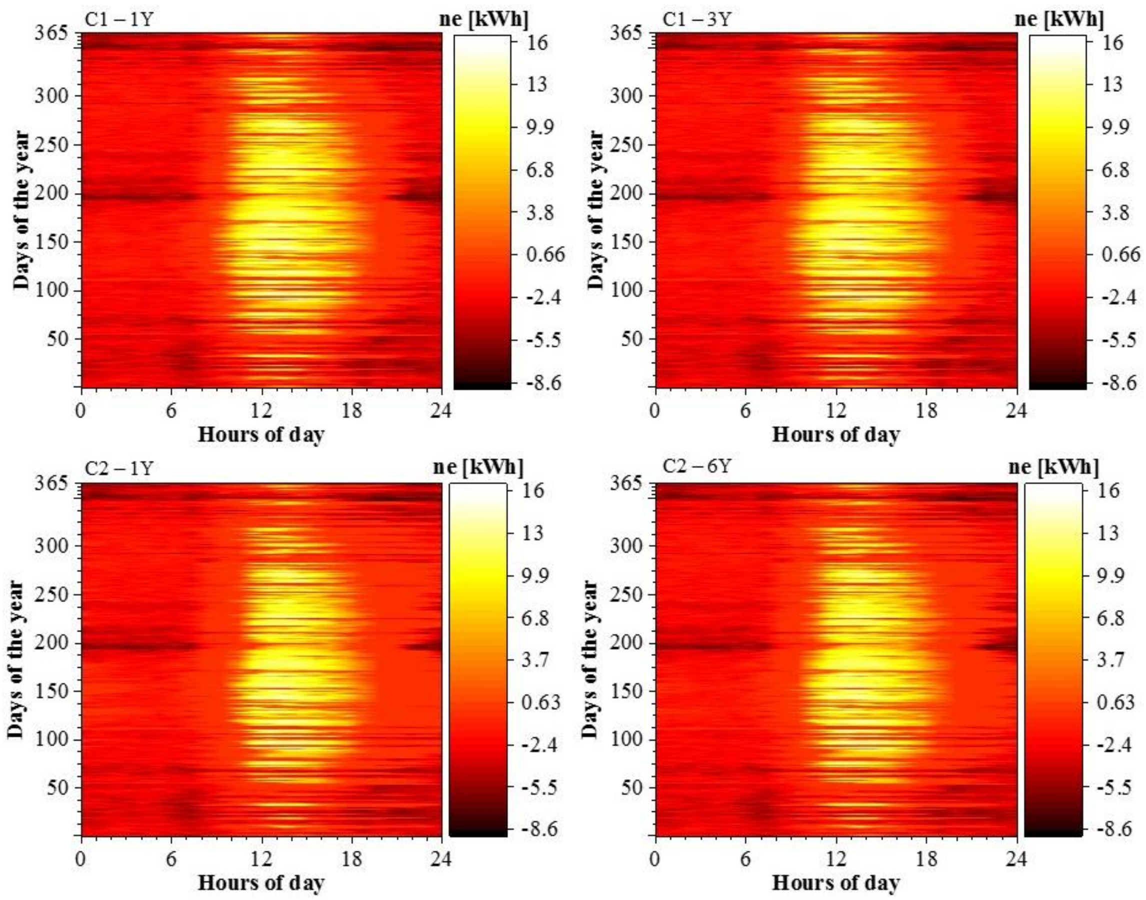

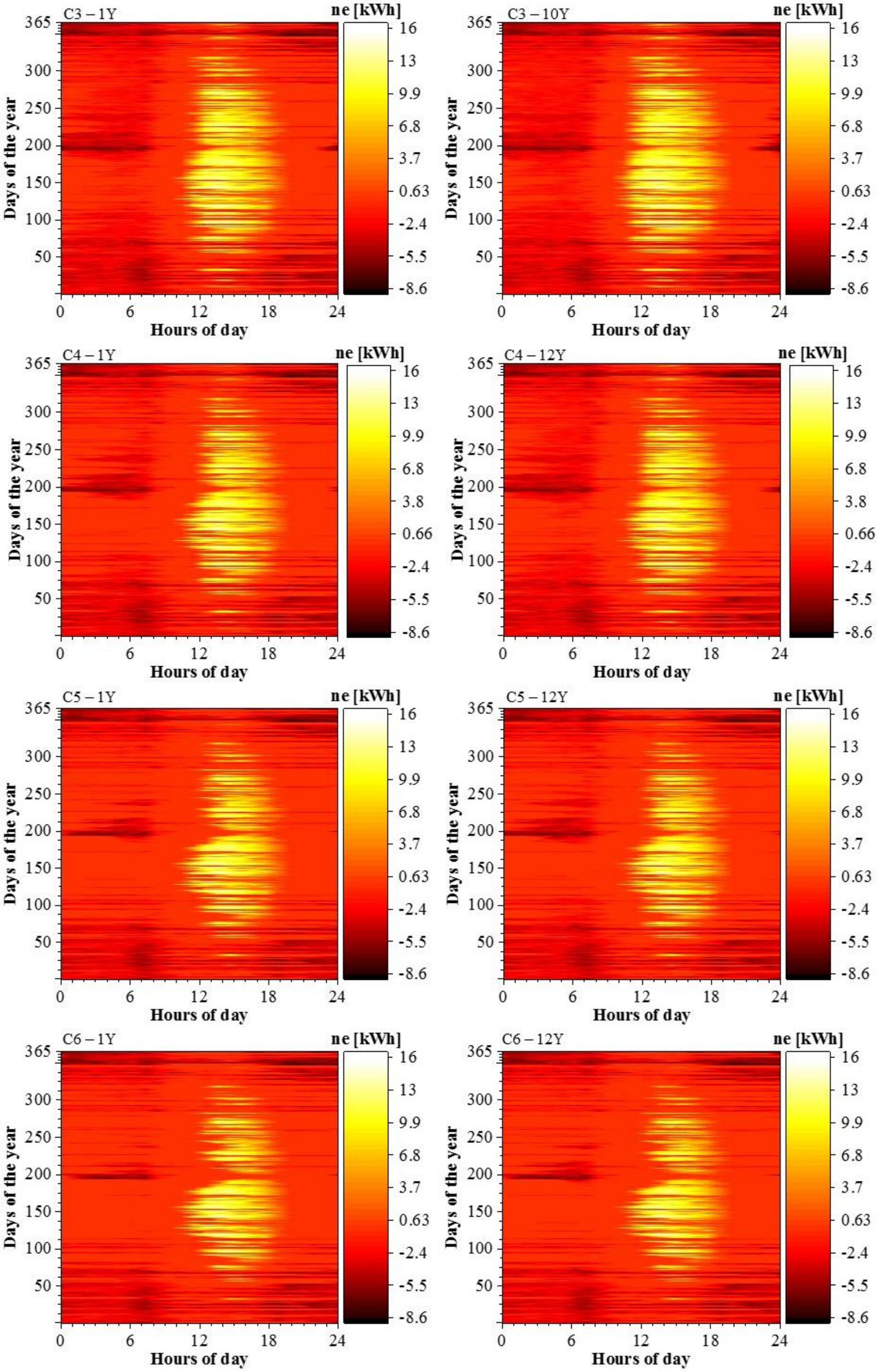
C3 – 1Y
ne [kWh]
16
13
9.9
6.8
3.7
0.63
-2.4
-5.5
-8.6
Days of the year
Hours of day
C3 – 10Y
ne [kWh]
C4 – 1Y
ne [kWh]
16
13
9.9
6.8
3.8
0.66
-2.4
-5.5
-8.6
C4 – 12Y
ne [kWh]
C5 – 1Y
ne [kWh]
C5 – 12Y
ne [kWh]
C6 – 1Y
ne [kWh]
C6 – 12Y
ne [kWh]
365
300
250
200
150
100
50
0
6
12
18
24

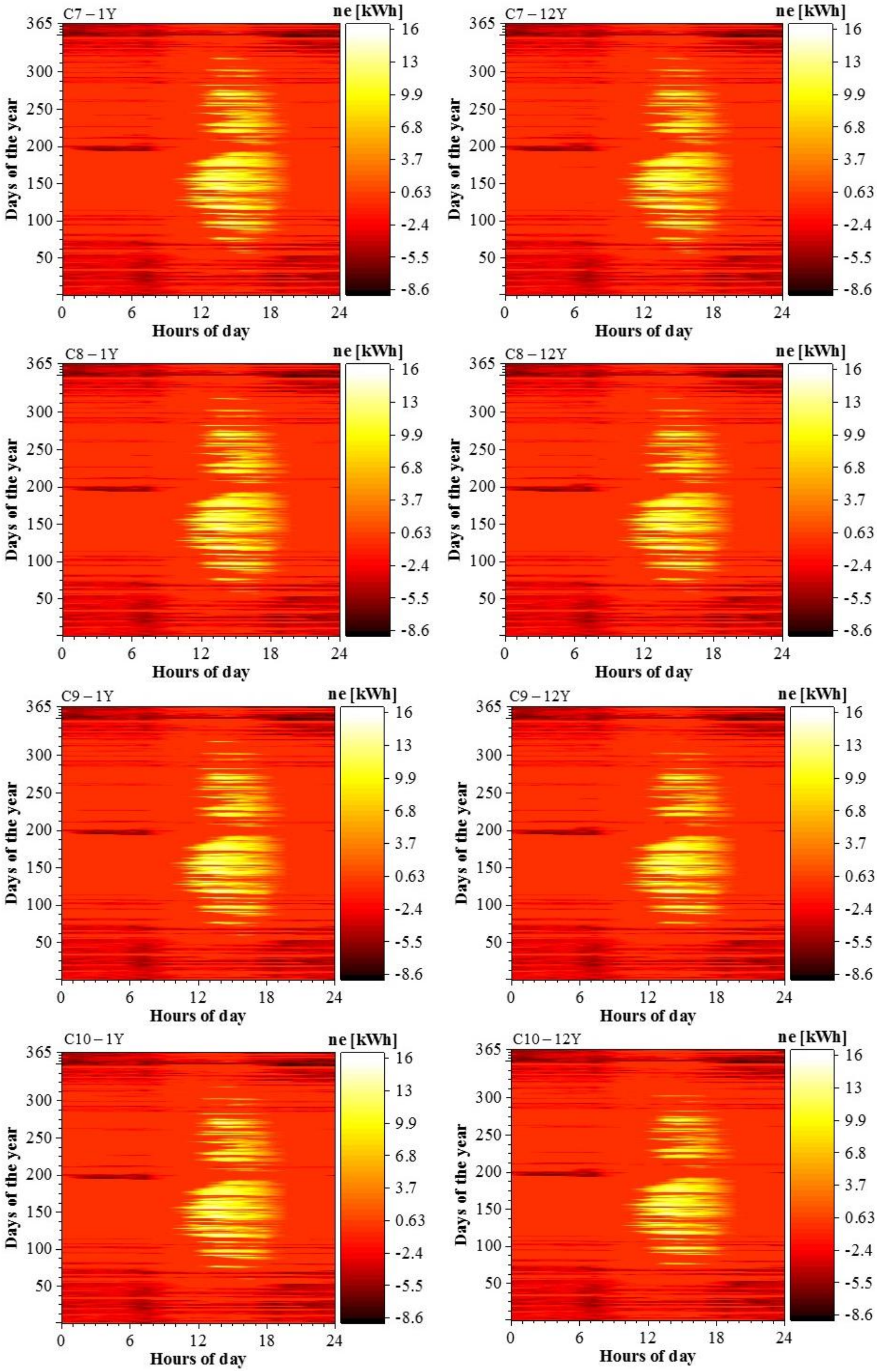

Figure 43. Coloured contour graph of the ne for the first and the last year of operation in each configuration examined.

5.3 Life cycle assessment of the traction lithium-ion battery pack

In this section, first the detailed LCA of the EV Li-ion battery production and use in the EV and recycling is presented. The use phase in the EV, although is out of the system boundaries of the examined case study, is modelled since the energy provided by the EV battery to perform this function is used to calculate the allocation factor for the partitioning of the impact of the battery production and EoL processes between the first and the second battery application. The results of this first LCA are input data for the LCA of the "PV – BESS – electrical grid", described in Chapter 3, where the Li-ion EV battery, examined in this section, is used as energy storage system after the first use in the EV.

5.3.1 Goal and scope definition

The goals of the LCA are:

- to provide the bill of material of the Lithium-ion battery cell based on the LMO–NMC technology described in Section 3.1;
- to estimate the potential life cycle environmental impacts of the LMO–NMC PHEV battery pack and to assess the contribution of each life cycle phase;
- to estimate the content of CRMs of the LMO–NMC battery cell technology examined;
- to assess the potential environmental impacts of and benefits from the production of secondary raw materials at the battery's EoL;
- to assess how the study assumptions affected the results obtained.

An attributional LCA approach is applied in accordance with the international standards of series ISO 14040 [113,114].

The functional unit selected as the reference for the LCA analysis is one LMO–NMC battery pack with a nominal capacity of 11.4 kWh, which guarantees 136,877 km of driving for a passenger car weighing 1860 kg before the battery capacity reduced about 81.31% [89].

The detailed description of the battery pack investigated is reported in Chapter 3.

The following phases are included in the analysis:

- the production phase (including raw material supply, material production, cell and battery pack assembly, transport and infrastructure);

- the use phase in the PHEV (including electricity consumed as a result of the battery's internal efficiency and by carrying the weight of the battery);
- the EoL phase (including the recycling of each component).

The impact assessment is based on the methods recommended by the European Product Environmental Footprint (PEF) [164], which provide a large set of environmental indicators consistent with the sustainability objective of avoiding burden-shifting among impact categories [165]. Because energy consumption is highly relevant to the evaluation of the studied system, the environmental impact categories recommended in the PEF are complemented by the cumulative energy demand (CED) method for energy impact estimation [166]. Moreover, in accordance with Bobba et al. [167] and Latunussa et al. [168], the land use and water resource depletion impact categories are excluded (as a result of the low availability and high uncertainty of LCI data). The abiotic depletion potential is calculated only for mineral resources (to avoid overlapping with the CED impact category).

The environmental impact categories investigated are listed in the following:

- Cumulative energy demand (CED) (MJ);
- Abiotic depletion potential (ADP) ($kgSb_{eq}$);
- Global warming potential (GWP) ($kgCO_{2eq}$);
- Ozone depletion potential (ODP) ($kgCFC\text{-}11_{eq}$);
- Human toxicity, non-cancer effects (HT-nce) (CTUh);
- Human toxicity, cancer effects (HT-ce) (CTUh);
- Particulate matter (PM) ($kgPM2.5_{eq}$);
- Ionizing radiation – human health (IR-hh) ($kBqU^{235}{}_{eq}$);
- Photochemical ozone formation potential (POFP) ($kgNMVOC_{eq}$);
- Acidification potential (AP) ($molcH^{+}{}_{eq}$);
- Terrestrial eutrophication (EU_T) ($molN_{eq}$);
- Freshwater eutrophication (EU_F) (kgP_{eq});
- Marine eutrophication (EU_M) (kgN_{eq});
- Freshwater ecotoxicity (E_{Fw}) (CTUe).

5.3.2 Life cycle inventory

In general, both primary and secondary data are used for the inventory of the battery pack. The LCI of the LMO-NMC cell is compiled based on the bill of material obtained at the JRC laboratory and literature studies. In detail, Majeau-Bettez et al. [65] and Ellingsen et al. [54] are the main sources of data for the upstream processes for the production of each cell component, the energy required for their assembly and the inventory of BMS, cooling system and battery packaging. Table 27 shows the main components of the battery pack and the correspondent weights for the examined battery pack. The weight of the battery is 175 kg. Approximately 64% of it is due to the battery cells, 28% to battery packaging and the remaining 8% to BMS and cooling system in equal weight.

Table 27. Weight of the main components of the battery.

Components	kg
Battery cell	111.70
Battery packaging	49.63
BMS	6.49
Cooling system	7.19
Total battery weight	**175**

Virgin materials are assumed for raw material inputs (e.g. aluminium, copper, plastics) which means that no environmental credits are considered to arise from recycled material content.

For the modelling of the EoL, the “recyclability substitution” approach has been applied. This assumes that the recycled materials produced at the EoL of the product will retain the properties of the original material input to the life cycle, and credits of the product with displacing virgin material production in proportion to the recyclability rate [141]. Then, recycled materials at EoL are assumed to displace virgin materials. Potential benefits from material recycling are credited to the EoL stage (in terms of “avoided primary materials”).

The eco-profiles of materials and energy sources used to produce the battery components are based on the Ecoinvent 3 database [169]. It is assumed that the production phase of the battery components occurred in Japan, and thus the Japanese electricity mix is used. The amount of electricity needed to assemble the cells and the battery pack is inferred from Ellingsen et al. [54]. Ellingsen et al. [54] presented three possible values for electricity consumption for cell manufacturing: 586 MJ/kWh, 960 MJ/kWh and 2318 MJ/kWh. In this dissertation, the value 586 MJ/kWh has been used since this is likely to better reflect large-scale production volumes according to Ellingsen et al. [54]. The operation phase and the EoL phase are assumed to take place in Europe, and thus the average European electricity mix is used to model these life cycle stages. Transport and infrastructure requirements during the manufacturing stage of the components are based on Ellingsen et al. [54].

In the following section, the authors describe the procedure and the assumptions used to compile the BoM of the LMO–NMC battery cell, by combining primary with literature data.

5.3.2.1 Cell material breakdown and life cycle inventory

A new LMO–NMC cell is disassembled in a glove box in an inert argon atmosphere, and a material breakdown analysis is performed. During all the disassembling steps, the weights of the detached elements and of the leftover material are recorded to keep track of evaporated electrolyte and any materials lost during dismantling. Electrolyte recollection can be challenging because of its volatility. A portion of liquid electrolyte is usually free inside the cell because it has not yet been completely absorbed by the active materials. The same behaviour has been observed in cells produced by other manufacturers [170]. The free electrolyte is first recollected through two holes drilled into the steel metal case. Then the metal case is removed, revealing two packages (jelly rolls) connected in parallel at the positive and negative terminals through a copper and aluminium current collector. Each of the two jelly rolls is made of three layers (cathode, anode and separator) rolled into a prismatic shape and wrapped with a soft plastic cover to keep the active materials soaking in the electrolyte. One package is then opened and unrolled to separate the three layers (see Figure 44). The dismantling and subsequent analysis are performed by carrying out a material breakdown, separating steel (external case, connectors and terminals), aluminium and copper (current collectors and electrode foils), polymer (wrapping, separator and tapes), cathode and anode active material, binder (for the anode and the cathode), carbon black (in the cathode) and, finally, electrolyte. One limit of the process lay in the impossibility to discriminate the fractions of binder and carbon black in the cathode composition and fraction of binder in the anode composition. To overcome such challenge an average value for the electrode composition is taken based on data available on literature for NMC and LMO cathodes [171] and graphite anodes [137,172]. Big scatter of the carbon black fraction results in a lower accuracy value. Eventually, assumption on the evaporated electrolyte during the dismantling process is made. These results of the cell material breakdown are shown in Table 28, where the average weight of all those elements is provided (% in weight and fraction in grams) including error estimation (+/– g).

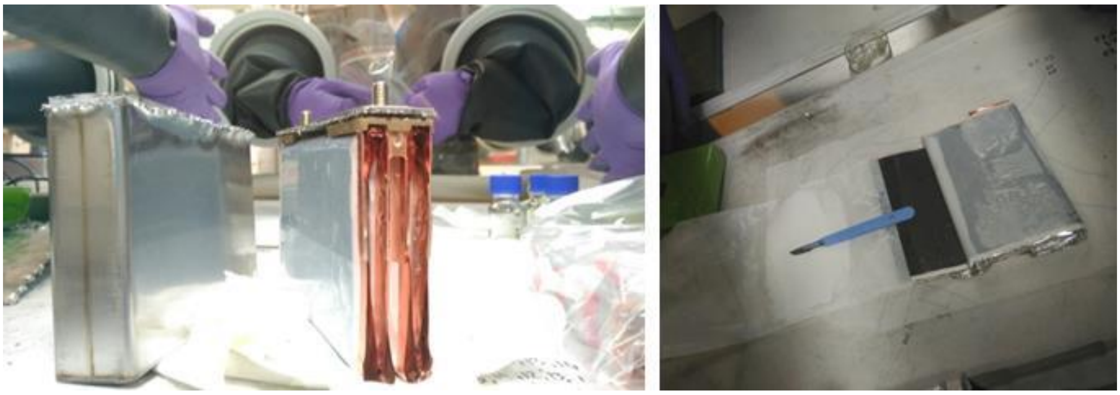

Figure 44. Left, components of a fresh LMO–NMC/graphite cell after opening and removing the cell casing in a glove box; right, unfolding of one of the two prismatic jelly rolls [118].

Table 28. Material breakdown of a fresh LMO–NMC/graphite cell as determined by dismantling and further analysis

LMO-NMC cell (total weight before opening: 1396.2 g)	**% in weight (%)**	**Fraction/g**	**Accuracy (g)**
Steel: external case, connectors	21.47	299.8	+/−2
Al: current collectors, electrode foils	3.74	52.2	+/−2
Cu: current collectors, electrode foils	10.03	140.0	+/−6
Polymer: wrapping, tapes, separator	5.99	83.6	+/−2
Anode active material: graphite	10.17	142.0	+/−12
Binder	2.68	37.4	+/−6
Cathode active material: LMO-NMC	27.47	383.5	+/−20
Carbon black in the cathode	3.38	47.2	+/−32
Electrolyte	13.75	192.0	+/−20
Uncounted materials lost in cutting/drilling/handling (steel, polymer, Cu, Al, active materials)	1.32	18.5	+/−5

The most difficult estimation is that of the composition of the active material, to distinguish the contributions of the binder and the remaining electrolyte for the anode and the cathode and the carbon black for the cathode. Carbon black resulted in the poorest accuracy due to the scarcity of available data in the literature.

The main assumption for the LMO-NMC cell modelling are described in the following:

Anode: The anode is composed of a copper current collector with a coat of negative electrode paste that consists of a negative active material and a small amount of binder. The specific compositions of the negative active material and of the binder are unknown, so they are assumed based on literature studies. Graphite can be divided into natural graphite and synthetic graphite. Based on Ellingsen et al. [54], in this study it is assumed that the anode consists on synthetic graphite. Concerning the binder, the most common compositions are made of polyvinylidene fluoride (PVDF), polytetrafluoroethylene (PTFE), poly acrylic acid (PAA) and carboxymethyl cellulose (CMC) [54,65]. According to Ellingsen et al. [54], in this study, the binder is assumed to be PAA and CMC. Both the required amounts of negative active material and binder are determined during battery cell dismantling. In anode manufacturing, a solvent is used to give the mixture a slurry texture. After the negative paste is applied to the current collector, the solvent evaporated. The information about solvent is not available, so its composition is modelled as N-methyl-2-pyrrolidone (NMP) in accordance with literature [54,65,127]. The required amount is taken from Ellingsen et al. [54].

Cathode: The cathode is composed of an aluminium current collector with a coat of positive electrode paste. The positive electrode paste is composed of the positive active material, the binder, and the carbon black which has the function to improve the conductivity. The specific composition of the positive active material was provided by the battery manufacturer. The active cathode material composition for the analysed battery is modelled as 52% of $LiMn_2O_4$ (LMO) and 48% of $Li(Ni_{0.4}Co_{0.2}Mn_{0.4})O_2$ (NMC). The LMO inventory is taken from the Ecoinvent database, while the NMC inventory is from Majeau-Bettez et al. [65]. Based on Ellingsen et al. [54], the binder is assumed to be PVDF, with the required amounts determined during battery cell dismantling. Similarly to the negative electrode paste, in the positive electrode paste manufacturing NMP is considered to be the solvent and the required amount was taken from Ellingsen et al. [54].

Electrolyte: the specific composition of the electrolyte is not detected during cell dismantling. Therefore, it is assumed that it is made of lithium salt (lithium hexafluorophosphate – $LiPF_6$) and a solvent, typically ethylene carbonate ($C_3H_4O_3$), in accordance with the literature [54,69,120,127]. The amount of electrolyte per battery cell is determined in the laboratory.

Separator: The specific material composition of the separator is not determined, so it is modelled made for 80% of polypropylene (PP) and 20% polyethylene (PE), in accordance with Nelson et al. [173]. The weight is determined in the laboratory.

Cell case: the cell case is made of steel. It contained the anode and cathode soaked with electrolyte and folded together with the separator in two jelly rolls that are properly connected to the two external negative and positive tabs. The composition of the case is obtained by combining the data determined in the laboratory with the LCI by Ellingsen et al. [54].

In Table 29 are summarized the type of data source (i.e. primary or secondary) and the mass of each cell component.

Table 29. BoM of the LMO–NMC cell and main assumptions for cell modelling.

Cell component	Mass (g)
Anode	**282.94*** (P*)**
Negative current collector: copper (P)	113.48 (P)
Negative active material: synthetic graphite (L**) [54]	162.24 (P)
Binder: 0.5 polyacrylic acid (PAA) + 0.5 carboxymethyl cellulose (CMC) (L)	7.22 (P)
Solvent: N-methyl-2-pyrrolidone (NMP) (L)	159.8 (L)
Cathode	**502.82*** (P)**
Positive current collector: aluminium (P)	40.36 (P)
Positive active material: LMO (P/L)	217.45 (P)
Positive active material: NMC (P/L)	200.73 (P)
Binder: polyvinylidene fluoride (PVDF) (L)	19.68 (P)
Carbon (P)	24.6 (P)
Solvent: NMP (L)	189.6 (L)
Electrolyte	**170.58 (P)**
Lithium hexafluorophosphate ($LiPF_6$) (L)	150.11 (L)
Ethylene carbonate ($C_3H_4O_3$) (L)	20.47 (L)
Separator	**67.4 (P)**
Polypropylene, granulate (PP) (L)	53.92 (L)
Polyethylene, granulate (PE) (L)	13.48 (L)
Cell case	**372.47 (P)**
Aluminium (P/L)	11.77 (P)
Copper (P/L)	26.38 (P)
Packaging film (P/L)	7.23 (P)
Polyethylene terephthalate, granulate (PETP) (P/L)	5.36 (P)
Polypropylene, granulate (PP) (L)	22 (P)
Steel (P/L)	299.72 (P)
Total	**1396.20*****

*Primary data, **Literature data, ***The amounts of NMP used in cathode and anode manufacturing are not included in the total.

In Table 30 the amounts of each battery cell components referred to the whole battery pack (80 cells) are summarized.

Table 30. LCI of the battery cells.

Cell components	**Amount [kg]**
Anode	
Cu foil	9.08E+00
Negative active material: synthetic graphite	1.30E+01
Poly acrylic acid (PAA)	2.88E-01
Carboxymethyl cellulose	2.88E-01
Cathode	
Al foil	3.23E+00
Positive active material: NMC	1.94E+01
Positive active material: LMO	1.41E+01
Binder (PVDF)	1.57E+00
carbon black	1.97E+00
Electrolyte	
Lithium hexafluorophosphate	1.64E+00
Ethylene carbonate	1.20E+01
Separator	
Polymer	5.39E+00
Cell case	
Aluminium	9.42E-01
Copper	2.11E+00
Steel	2.40E+01
PETP	4.29E-01
FILM	5.78E-01
PP	1.76E+00
Total	**1.12E+02**

A detailed description of the BMS, battery packaging and cooling system is available in Ellingsen et al. [54]. In Table 31 the LCIs of these components, resulting by the own elaboration of the LCIs presented by Ellingsen et al. [54] are illustrated.

Table 31. LCI of the BMS, packaging and cooling system.

Component	**BMS [kg]**	**Packaging [kg]**	**Cooling system [kg]**
Acrylonitrile-butadiene-styrene copolymer	2.44E-03	1.02E+00	8.70E-02
Al	2.34E-01	1.78E+01	6.53E+00
Brass	1.94E-02		
Butyl acrylate		4.07E-03	
Cable, ribbon cable, 20-pin, with plugs	8.76E-01		
Copper	5.28E-01	7.36E-01	
Electric connector, wire clamp	6.70E-02		
Electronic component, passive	8.16E-01		
Ethylene glycol			3.45E-01
Glass fibre			1.45E-02
Integrated circuit, logic type	1.74E-03		
Nylon 6-6	1.19E-01	1.19E-01	
Packaging film, low density polyethylene		8.32E+00	
Polyethylene terephthalate, granulate, amorphous	1.35E-01		
Polyphenylene sulfide	6.33E-02		
Polypropylene, granulate		3.31E+00	
Polyvinylidenchloride, granulate			5.03E-03
Printed wiring board, through-hole mounted, Pb free	9.19E-01		
Silicon, electronics grade			4.35E-02
Steel	2.67E+00	1.78E+01	1.65E-01
Synthetic rubber	8.08E-03	5.50E-01	1.68E-03
Tin	3.22E-02		
Total	**6.49E+00**	**4.96E+01**	**7.19E+00**

5.3.2.2 The battery operation phase

According to several literature studies [59,131,136], the battery operation phase accounts for electricity losses in the battery during use (i.e. to power the car for transport) and the extra electricity needed by the vehicle to carry the battery. The electricity consumed by the battery during operation is calculated using the following assumptions:

- the PHEV runs on electric mode for 75% (El_{drm}) and on petrol mode for the remaining 25% (P_{drm}) [64];
- the car consumes 0.192 kWh electricity per kilometre in electric mode (CEl_{drm}) [174];
- 30% of the vehicle's energy consumption can be related to battery transport (30% weight–energy relationship) (CEl_{w}).

The traction Lithium-ion battery examined is driven for about 136,877 km (D_{dr}) during the PHEV's lifetime at 80% maximum DoD and with 95% charging efficiency (η_c) [89]. The kerb weight of the car is inferred from the technical specification reported in the Mitsubishi catalogue for Outlander PHEV, i.e. 1860 kg [174].

Electricity losses due to internal battery efficiency (El_{be}) are calculated using the following equation (Eq. 5.1):

$$El_{be} = D_{dr} \cdot El_{drm} \cdot CEl_{drm} \cdot (1-\eta_c) = 136,877 \text{ km} \cdot 75\% \cdot 0.192 \frac{\text{kWh}}{\text{km}} \cdot 5\% = 986 \text{ kWh} \quad (5.1)$$

The extra electricity needed to carry the battery (El_{bw}) is calculated using the following equation (Eq. 5.2):

$$El_{bw} = \frac{W_b}{W_c} \cdot CEl_w \cdot \frac{CEl_{drm}}{\eta_c} \cdot D_{dr} \cdot El_{drm} = \frac{175 \text{ kg}}{1860} \cdot 30\% \cdot \frac{0.192 \text{ kWh}}{95\%} \cdot 136,877 \text{ km} \cdot 75\% = 586 \text{ kWh} \quad (5.2)$$

5.3.2.3 Battery end of life

In accordance with the Waste Batteries Directive (Directive 2006/66/EC) [75], when traction batteries in EVs reach their EoL, they have to be properly collected and recycled. In this section, the environmental impacts of and the potential environmental credits associated with battery pack recycling are assessed. In accordance with the PEFCRs on rechargeable batteries [175], the battery pack is assumed to be dismantled at EoL to separate the main components and maximise the recovery of the various material fractions. Regarding the battery cells, in accordance with Chagnes and Pospiech [76] and PEFCRs on rechargeable batteries [175], it is assumed that these are recycled through a pyrometallurgical process, since this is commonly used in Europe for battery recycling [70,176,177]. The concentrated and relatively clean metal alloy and the slag obtained are then treated through a hydrometallurgical process to extract valuable metals from both the metal alloy and the slag [175,178]. Pyrometallurgical recovery relies on high-temperature smelting to recover the metals and other materials [125]. Through smelting, the metal oxides are converted to their metallic form, a molten metal alloy, containing, in the case of the battery cell examined, nickel, cobalt, copper and steel [67,80,179,180]. This process does not allow the recovery of graphite, plastic materials, aluminium, lithium or manganese. The last three elements are entrained in the slag produced during the process [80]. The plastic materials are burned and not recyclable [80,181]. Moreover, carbon black, binder, CMC, PAA, electrolyte and graphite (which account for 37.8% of the total mass of the cells) are currently not recyclable and therefore lost during recycling (burned, evaporated or dispersed in the slag) [81,182]. It is assumed that the metal alloy and the slag resulting from the pyrometallurgical process are refined with a hydrometallurgical process to recover metal sulphate, which can be used again to manufacture batteries' active materials [175]. The recoverable products, depending on the composition of the battery cell examined, may include cobalt, nickel and manganese sulphates, copper and steel. Then, for the LCA model, the environmental credits for avoiding the production of an equivalent amount of primary materials are considered.

The inventories for the pyrometallurgical and hydrometallurgical treatments are based on the Ecoinvent database [169]. Regarding the plastic in the cell, the original Ecoinvent pyrometallurgical process is modified according to the Batteries 2020 project [183] and Fisher and Wallén [82]; therefore, instead of the original average treatment process for plastic mixtures that considers disposal in landfill, incineration and use as an alternative fuel and raw material in clinker production, only incineration is considered for plastics.

The BMS, the cooling system and the battery packaging are further dismantled into, for example, metal fractions, plastic fractions, printed wiring board (PWB) fractions, used cable, plastic materials and electronic scraps through a combination of manual dismantling and mechanical separation and sorting [169]. It is hypothesized that the copper fraction is recycled in a non-ferrous metal smelter, that the steel fraction is recycled in an electric arc furnace and that the process included steel making and casting. Finally, for the recycling of the aluminium fraction, an average European melting, alloying and casting technology is assumed.

The inventories for the EoL of the battery cells, the BMS, the packaging and the cooling system are detailed in Table 32. The eco-profiles of the materials and energy sources used in battery recycling are based on the Ecoinvent database [126,169]. The recycling rates of the recoverable materials embedded both in the cells and in other battery components are inferred from Chancerel and Marwede [184] and are summarized in Table 33.

Table 32. Inventory data used for the battery cells, BMS, packaging and cooling system EoL treatment modelling.

Reference product	**1 kg of cell**	**1 kg of molten metal alloy + slag**	**1 kg of BMS**	**1 kg of packaging**	**1 kg of cooling system**	**Ecoinvent processes used for the EoL treatment**
Inputs from nature						
Water (m^3)	1.00E–03	7.2E–04				
Inputs from technosphere						
Aluminium scrap preparation (kg)			0.04	0.36	0.91	Aluminium scrap, post-consumer, prepared for melting; treatment of aluminium scrap, post-consumer, by collecting, sorting, cleaning, pressing
Blister copper conversion facility (p)	5.00E–10		–	–	–	Blister copper conversion facility
Copper scrap preparation (kg)			0.08	0.01		Copper, treatment of scrap by electrolytic refining
Sodium hydroxide (kg)	0.35		–	–	–	Sodium hydroxide, without water, in 50% solution state
Sulfuric acid (kg)		0.23				Sulfuric acid production
Chemical inorganic		0.025				Chemical inorganic
Lime, hydrated		0.116				Lime, hydrated, packed
Chemical factory, organic		4.0E–10				Chemical factory, organic
Steel scrap preparation (kg)			0.41	0.36	0.02	Iron scrap, sorted, pressed, sorting and pressing of iron scrap
Electricity, medium voltage (kWh)	0.80	0.14	0.18	0.25	0.27	Electricity, medium voltage
Electricity, high voltage (kWh)			0.09	0.01		Electricity, high voltage
Heat, natural gas (MJ)			0.30	2.96	7.51	Heat production, natural gas, at boiler condensing modulating > 100 kW
Heat, heavy fuel (MJ)			0.02	0.04	0.47	Heat production, heavy fuel oil, at industrial furnace 1 MW
Heat, hard coal (MJ)			0.50	0.10		Heat production, at hard coal industrial furnace 1–10 MW
Emissions to air (for details about emissions to air please consult Ecoinvent 3 database)						
Emissions to water (for details about emissions to air please consult Ecoinvent 3 database)						
Output to technosphere (waste for further treatment)						
Electronic scrap (kg)	–		0.14	–	–	Treatment of electronics scrap from control unit
Non-Fe-Co metals** (kg)		0.18*	–	–	–	Non-Fe-Co metals, treatment of used Li-ion battery, hydrometallurgical processing
PWB (kg)	–		0.14	–	–	Used printed wiring boards, treatment of scrap printed wiring

						boards, shredding and separation
Used cable (kg)	–		0.14	–	–	Used cable
Waste graphical paper (kg)		0.065				Waste graphical paper
Waste gypsum		0.339				Waste gypsum
Plastic material in the cells	0.07*	–***	–	–	–	Waste plastic to municipal incinerator
Plastic materials (kg)	–		0.04	0.24	–	Waste plastic, mixture
Avoided product						
Aluminium (kg)			0.04	0.35	0.89	Aluminium, primary, ingot
Cobalt sulphate (kg)		0.02				Cobalt sulphate [65]
Copper (kg)		0.10	0.08	0.01	–	Copper production, primary
Nickel sulphate (kg)		0.04				Nickel sulphate [65]
Manganese sulphate (kg)		0.13				Manganese sulphate [65]
Steel (kg)		0.21	0.40	0.35	0.02	Steel, low-alloyed, hot rolled production

*The amounts are adapted to match the input of materials specific to the composition of the analysed battery cell; **The output of this process is the production of copper; ***It is assumed that all plastic materials are burned during the pyrometallurgical recycling process.

Table 33. Recoverable materials from battery pack components and corresponding recycling rates.

Materials	**Recycling rate (%)**	**Material recovered from the cells**	**Material recovered from other components**
Aluminium	98	NR*	R**
Cobalt (as cobalt sulphate)	90	R	NP***
Copper	95	R	R
Nickel (as nickel sulphate)	90	R	NP
Manganese (as manganese sulphate)	90	R	NP
Steel	98	R	R

*NR, not recovered; **R, recovered; ***NP, not present

The recycling processes of the BMS, cooling system and battery packaging are modelled taking into account the preparation of the aluminium, iron and copper scraps for recycling and the energy required to recycle each recoverable fraction. PWB, electronic scrap, plastic materials and used cable are considered waste for further treatment. Specifically, for PWB treatment for the recovery of precious metals using a metallurgical process is considered. This included infrastructure for weighting, shredding and sampling the PWB, energy consumption and an estimation of the energy required to transport it. For electronic scrap, the dismantling of the electronic control equipment is considered.

Finally, for used cable the treatment process included infrastructure (a shredder, followed by a modern grinding machine with current separation technology), energy consumption and an estimation of the energy required to transport waste cable from electric and electronic devices. For the plastic fraction, an average treatment is considered, such as disposal in landfill, incineration or use as an alternative fuel or as a raw material in clinker production.

Figure 45 shows a diagram of the battery components' EoL treatments.

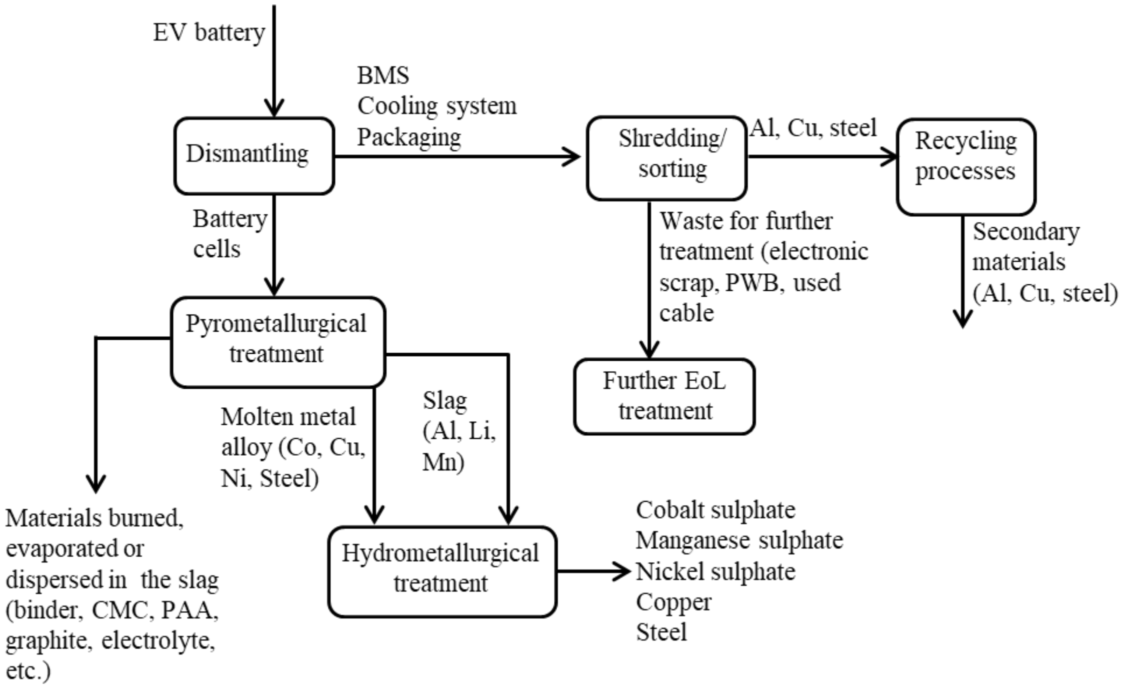

Figure 45. Diagram of the battery components' EoL treatments.

5.3.3 Life cycle impact assessment and interpretation

The life cycle impact assessment (LCIA) of the FU is illustrated in Table 34. The impacts due to recycling have been separated from the environmental credits arising from avoiding the production of primary materials. The contribution of each life cycle phase is detailed in Table 35.

Battery production is the phase mainly responsible for almost all the impacts considered. In fact, with the exception of the categories ionizing radiation – human health and freshwater eutrophication, the contribution of battery production is always higher than 60%. This trend is consistent with previous LCA studies that have estimated the life cycle impacts of Li-ion traction batteries [51,136,185]. This outcome confirms the importance of understanding the environmental impacts of battery production when assessing the environmental sustainability of electric mobility.

Table 34. Life cycle environmental impacts – impacts refer to the defined FU (one LMO–NMC battery pack).

Impact category	Total (without credits)	Recycling credits
CED (MJ)	6.32E+04	-5.54E+03
ADP ($kgSb_{eq}$)	7.73E-02	-1.27E-02
GWP ($kgCO_{2eq}$)	3.63E+03	-3.45E+02
ODP ($kgCFC\text{-}11_{eq}$)	3.23E-04	-2.38E-05
HT-nce (CTUh)	2.49E-03	-5.21E-04
HT-ce (CTUh)	4.35E-04	-1.73E-04
PM (kg $PM2.5_{eq}$)	2.59E+00	-4.11E-01
IR-hh ($kBqU^{235}{}_{eq}$)	6.54E+02	-4.15E+01
POFP ($kgNMVOC_{eq}$)	1.10E+01	-1.35E+00
AP ($molH^{+}{}_{eq}$)	3.16E+01	-4.70E+00
EU_T ($molN_{eq}$)	3.57E+01	-4.47E+00
EU_F (kgP_{eq})	2.54E+00	-3.85E-01
EU_M (kgN_{eq})	6.32E+00	-1.86E+00
E_{Fw} (CTUe)	1.91E+05	-1.53E+04

Table 35. Life cycle environmental impacts – impacts refer to the defined FU (one LMO–NMC battery pack)

Impact category	Battery pack production (%)	Battery operation (%)	Battery pack EoL (%)	Total (without credits)	Recycling credits* (%)
CED (MJ)	67.4	27.6	5.0	6.32E+04	-8.8
ADP ($kgSb_{eq}$)	97.6	1.2	1.2	7.73E-02	-16.4
GWP ($kgCO_{2eq}$)	73.6	21.3	5.1	3.63E+03	-9.5
ODP ($kgCFC\text{-}11_{eq}$)	62.9	24.3	12.8	3.23E-04	-7.4
HT-nce (CTUh)	86.7	9.2	4.1	2.49E-03	-20.9
HT-ce (CTUh)	84.3	13.0	2.7	4.35E-04	-39.9
PM (kg $PM2.5_{eq}$)	83.8	11.0	5.2	2.59E+00	-15.8
IR-hh ($kBqU^{235}{}_{eq}$)	35.5	57.2	7.3	6.54E+02	-6.3
POFP ($kgNMVOC_{eq}$)	82.7	13.9	3.3	1.10E+01	-12.3
AP ($molH^{+}{}_{eq}$)	83.4	13.5	3.1	3.16E+01	-14.9
EU_T ($molN_{eq}$)	81.4	15.0	3.6	3.57E+01	-12.5
EU_F (kgP_{eq})	67.9	27.3	4.8	2.54E+00	-15.1
EU_M (kgN_{eq})	87.7	10.0	2.2	6.32E+00	-29.4
E_{Fw} (CTUe)	30.9	9.7	59.5	1.91E+05	-8.0

*Expressed as a percentage of the "Total" burden, including "Battery pack production", "Battery operation" and "Battery pack EoL"

The battery operation phase has a large impact only on ionizing radiation – human health (57.2%). In the use phase, the impacts of the electricity lost from battery efficiency are about twice those of the electricity lost from battery transport.

Battery recycling has a large impact on freshwater ecotoxicity (60%). Besides generating potential environmental impacts, recycling results in environmental credits due to recoverable products, presented as negative values in Table 34 and Table 35 and negative bars in Figure 46, for the various impact categories. The environmental credits associated with materials recovered through battery recycling processes exceed the associated environmental impacts in all the impact categories examined, with the exception of ozone depletion potential, ionizing radiation and freshwater ecotoxicity.

The environmental credits are particularly relevant to the impact categories of marine eutrophication (–29.4%), human toxicity (about – 40% for both human toxicity – cancer effect and -20% for human – toxicity – non cancer effect), abiotic resource depletion (–16.4%), particulate matter (-15.8%) and freshwater eutrophication (-15%). This outcome confirms the environmental benefits of recovering Li-ion battery materials, as reported in previous studies [4,78,79,125,186].

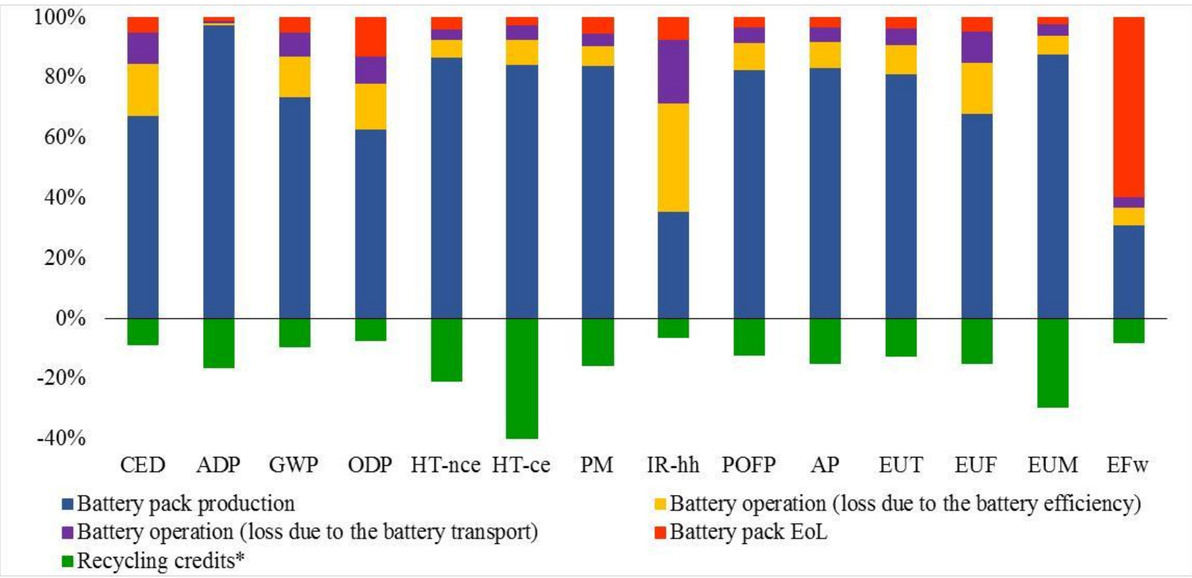

*Expressed as a percentage of the "Total" burden, including "Battery pack production", "Battery operation" and "Battery pack EoL"

Figure 46. Life cycle environmental impacts – impacts refer to the defined FU (one LMO–NMC battery pack).

The main contribution to the battery pack recycling impacts is from the cells recycling process that accounts for more than 80% in almost all the examined impact categories. The exception is the freshwater ecotoxicity impact category in which battery packaging and cooling system recycling process account, respectively, for 69% and 27% (Figure 47).

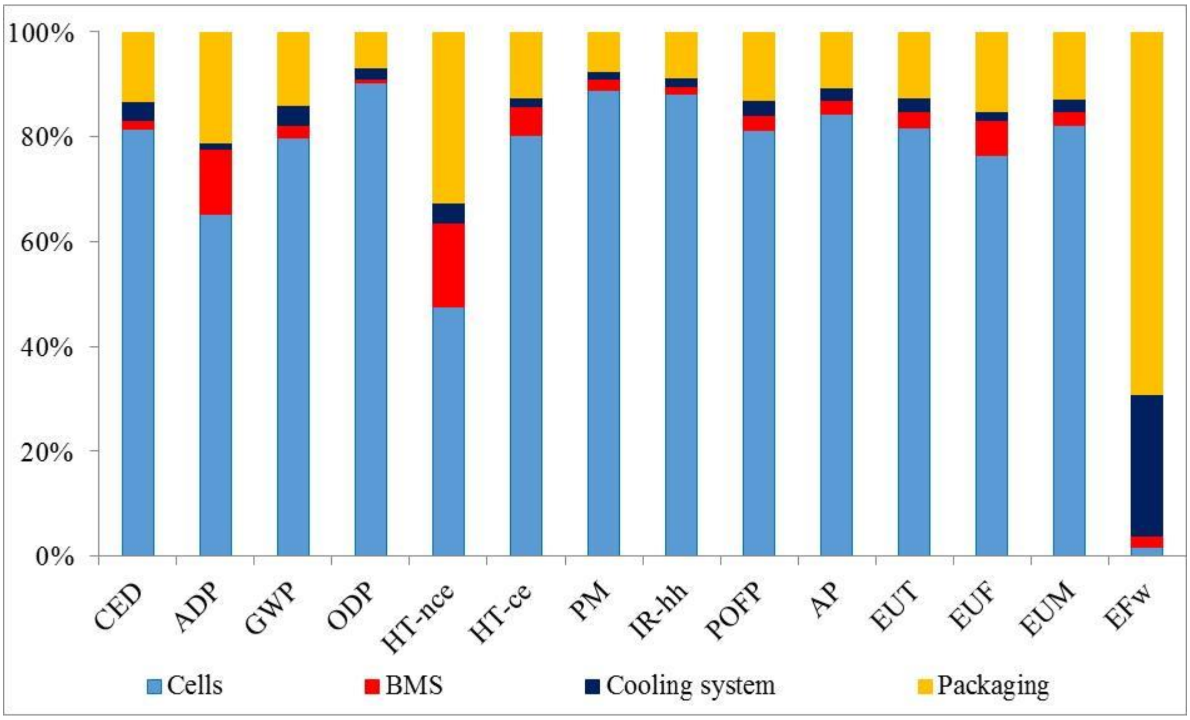

Figure 47. Impact related to battery pack recycling treatment – process contribution.

Figure 48 illustrates the process contribution to the environmental credits related to battery pack recycling treatment.

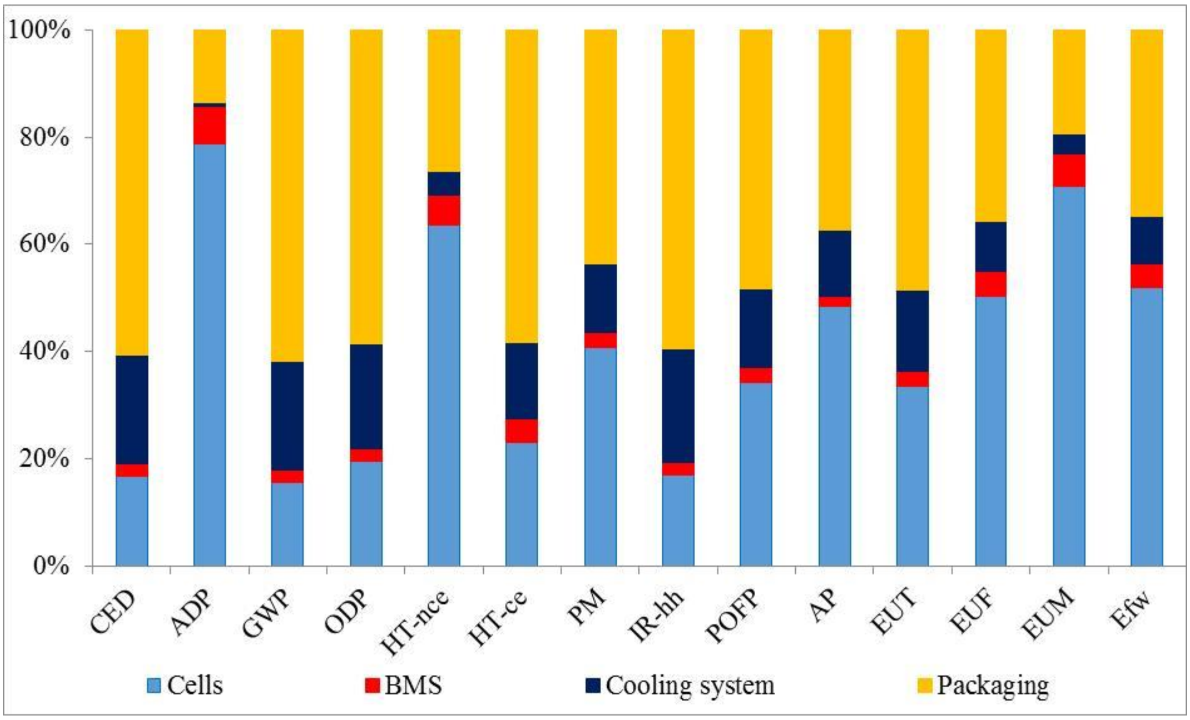

Figure 48. Environmental credits related to the battery pack recycling treatment – process contribution.

In terms of the production phase, a more in-depth analysis of the impacts associated to the battery production phase is carried out. The obtained results are illustrated in Table 36, while in Figure 49 the contribution analysis related to each battery components is shown.

Table 36. Life cycle environmental impacts – impacts refer to the battery pack production phase.

Impact category	**Battery cells**	**Battery packaging**	**BMS**	**Cooling system**	**Transport, electricity*, infrastructure**	**Total**
CED (MJ)	3.23E+04	6.10E+03	2.65E+03	1.35E+03	2.02E+02	4.26E+04
ADP ($kgSb_{eq}$)	2.37E-02	3.11E-03	4.83E-02	8.14E-05	2.21E-04	7.55E-02
GWP ($kgCO_{2eq}$)	2.08E+03	3.21E+02	1.81E+02	7.50E+01	1.39E+01	2.67E+03
ODP ($kgCFC\text{-}11_{eq}$)	1.57E-04	2.42E-05	1.36E-05	6.38E-06	1.93E-06	2.03E-04
HT-nce (CTUh)	1.13E-03	2.04E-04	7.92E-04	2.55E-05	4.09E-06	2.16E-03
HT-ce (CTUh)	1.67E-04	1.20E-04	5.45E-05	2.47E-05	9.36E-07	3.67E-04
PM (kg $PM2.5_{eq}$)	1.63E+00	2.49E-01	2.29E-01	4.95E-02	1.45E-02	2.18E+00
IR-hh ($kBqU^{235}_{eq}$)	1.37E+02	5.92E+01	1.79E+01	1.74E+01	1.03E+00	2.33E+02
POFP ($kgNMVOC_{eq}$)	6.86E+00	9.92E-01	9.75E-01	1.93E-01	9.36E-02	9.11E+00
AP ($molH^{+}_{eq}$)	2.14E+01	2.27E+00	1.94E+00	5.33E-01	2.03E-01	2.64E+01
EU_T ($molN_{eq}$)	2.20E+01	3.13E+00	2.95E+00	6.50E-01	3.78E-01	2.91E+01
EU_F (kgP_{eq})	9.75E-01	2.16E-01	4.88E-01	4.69E-02	2.18E-03	1.73E+00
EU_M (kgN_{eq})	4.50E+00	5.60E-01	3.90E-01	6.97E-02	2.98E-02	5.55E+00
E_{Fw} (CTUe)	3.15E+04	7.36E+03	1.85E+04	1.41E+03	1.47E+02	5.90E+04

*Electricity for battery pack assembly

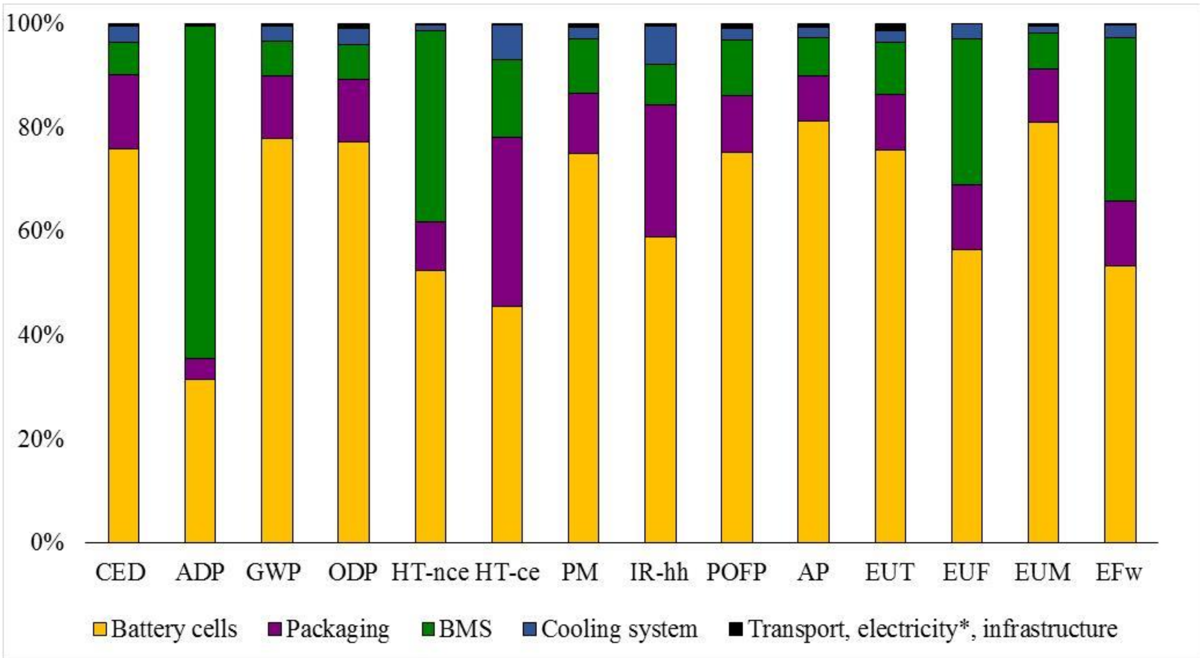

*Electricity for battery pack assembly

Figure 49. Environmental impacts – battery production phase

From data analysis results that battery cells production makes the largest contribution to all of the environmental impact categories examined. In detail its contribution is ranging from a minimum of about 31.4% (for the abiotic depletion potential) up to 81.2% (for acidification potential). In eight out fourteen impact categories battery cells account for more than 70% of the overall impact. In detail, battery cells production account for 81% in marine eutrophication, 77.9% in global warming potential, 77.3% in the ozone depletion potential, 75.8%, in cumulative energy demand, 75,6% in terrestrial eutrophication 75.3% in photochemical ozone formation and 75.1% in particulate matter.

The global warming potential of the battery production, calculated per kilowatt hour of battery energy capacity, for ease of comparison with previous studies, is 182 $kgCO_{2eq}$ per kWh of battery energy capacity. This value is in the mid-range of estimates found in the literature review summarized in Table 3 and in the study by Ellingsen et al. [117]. Thus, it can be concluded that the LMO–NMC composite cathode technology could represent, besides a good compromise between the higher and the lower energy performance of the NMC and LMO parts, respectively, also a good environmental compromise in terms of global warming potential.

According to Ellingsen et al. [117], large differences in the global warming potential of the production phase can be due to the different energy demands for cell manufacturing and pack assembly. Owing to a dearth of primary data, the greenhouse gas emissions from cell manufacturing are the most difficult aspect of battery production to analyse [120]. For this reason, energy consumption is a relevant parameter in the sensitivity analysis (Section 5.3.4).

As the cells are responsible for the main energy and environmental contributions in almost all the impact categories examined and they are the battery components for which primary data are available, a detailed process contribution analysis is carried out in Section 5.3.3.1.

Concerning the BMS, the impact is particular relevant for impact categories as: abiotic depletion potential in which it accounts for 64% mainly due to the electronic components, printed wiring board (PWB) and cable production. The detailed process contribution of the BMS to the abiotic depletion potential impact category is illustrated in Figure 50. The BMS presents also relevant contributes in the human toxicity – non cancer effect, in which it accounts for around 40%, and in the freshwater ecotoxicity and eutrophication, in which it represents 31.5% and 28%, respectively, of the total impacts. The detailed process contribution of the BMS in human toxicity – non cancer effect is illustrated in Figure 51.

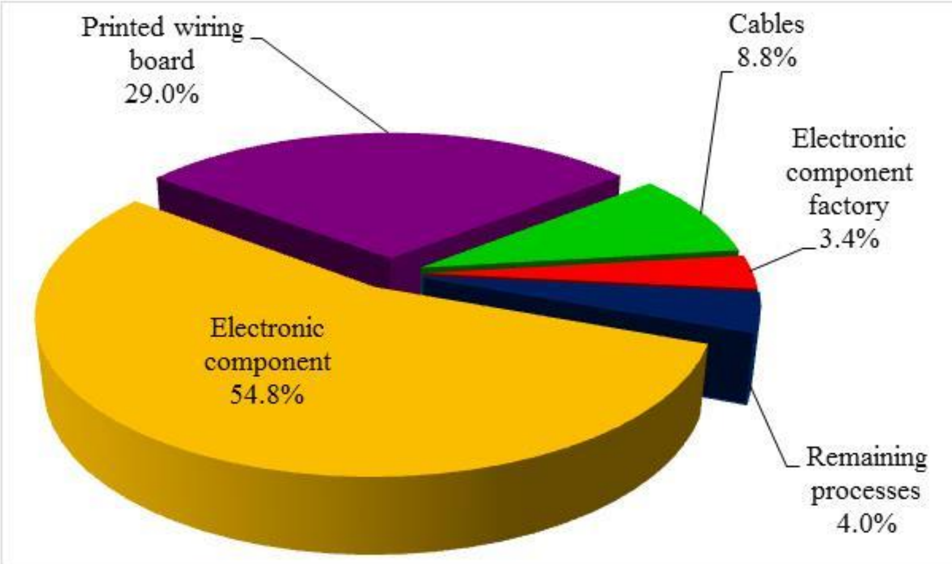

*Remaining processes: sum of the processes with a percentage contribution lower than 3%

Figure 50. BMS production: process contribution to the abiotic depletion potential impact category.

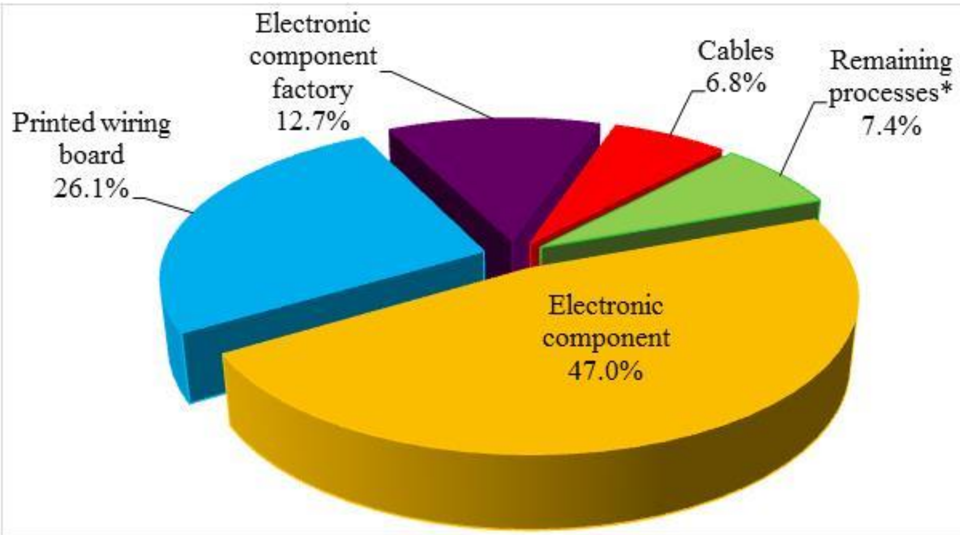

*Remaining processes: sum of the processes with a percentage contribution lower than 3%

Figure 51. BMS production: process contribution to the human toxicity – non cancer effect impact category.

Electronic component and printed wiring board production processes are responsible for around 70% of the total impact on the BMS. These processes are also responsible of the highest impact on freshwater eutrophication (Figure 52) and freshwater eco-toxicity (Figure 53).

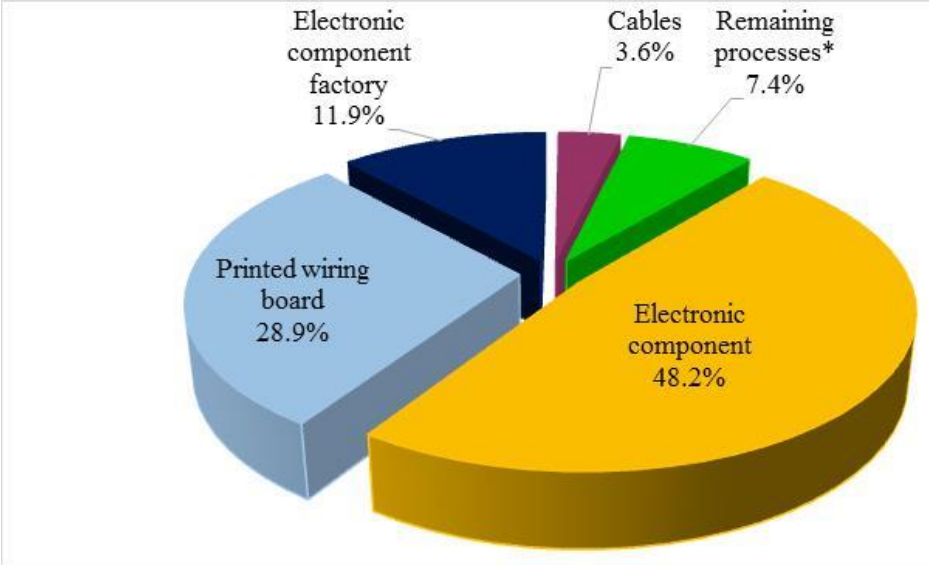

*Remaining processes: sum of the processes with a percentage contribution lower than 3%

Figure 52. BMS production: process contribution to the freshwater eutrophication impact category.

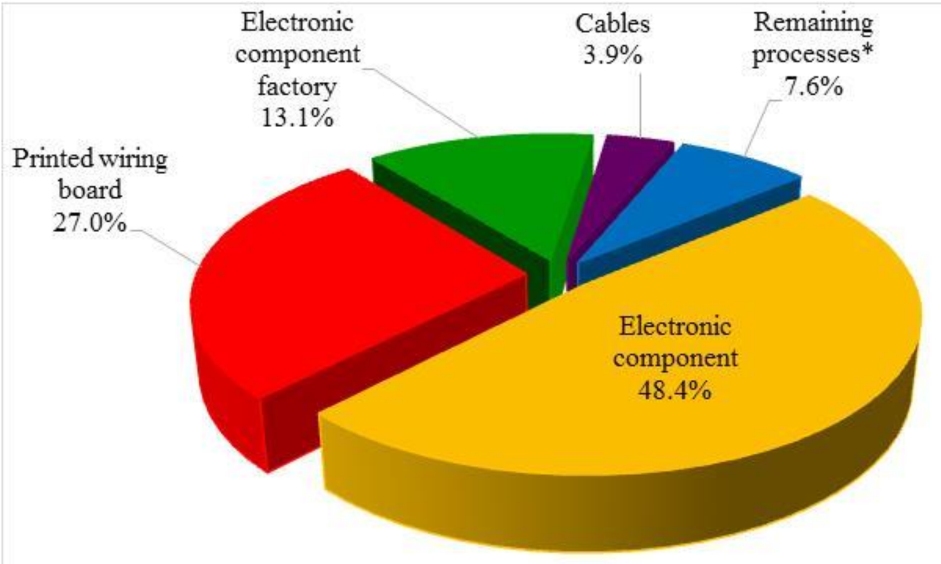

*Remaining processes: sum of the processes with a percentage contribution lower than 3%

Figure 53. BMS production: process contribution to the freshwater eco-toxicity impact category.

Battery packaging never exceeds 33.5%, with the highest contribution made to the human toxicity – non cancer effect impact category. For this category, the production of aluminium, steel and copper is responsible for 80% of the overall impact (Figure 54).

The production of the cooling system accounts for about 7.5% of the ionizing radiation – human health categories and 7% to the human toxicity – non cancer effect, and contributes less than 3% to all other impact categories. Transport, electricity needed for battery pack assembly and infrastructure contribute less than 1.5% to all the categories examined.

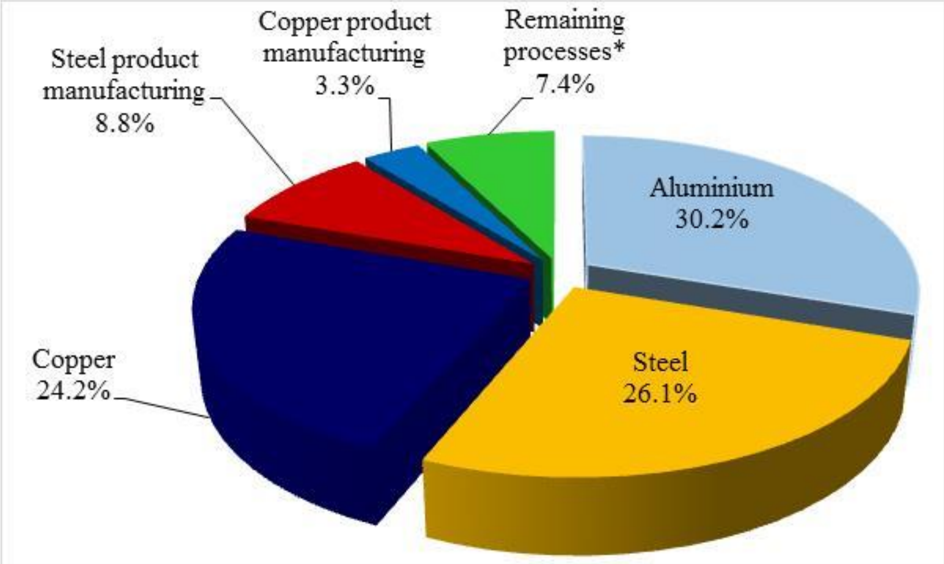

*Remaining processes: sum of the processes with a percentage contribution lower than 3%

Figure 54. Packaging production: process contribution to the human toxicity – non cancer effect impact category.

5.3.3.1 Life cycle impact contribution analysis of battery cells production process

As the cells are responsible for the main energy and environmental contributions, and they are the battery components for which the authors have primary data, the production process of one cell (energy capacity 142.5 Wh; weight 1396.20 g) is examined in detail.

The LCIA results are summarized in Table 37. While the contribution of the different battery cell components are illustrated in Figure 55.

The analysis of the results obtained shows that in cell production the cell assembly process is responsible for the greatest impacts in almost all of the impact categories investigated. For example, it accounts for about 66.8% of global warming potential (Figure 56), and 60% of cumulative energy demand (Figure 57) and ozone depletion potential (Figure 58).

Table 37. Life cycle impacts of one battery cell production process.

Impact category	Anode	Cathode	Electrolyte	Separator	Cell case	Assembly	Transport, infrastructure, process water	Total
CED (MJ)	3.65E+01	8.18E+01	1.63E+01	6.93E+00	1.70E+01	2.44E+02	9.40E-01	4.03E+02
ADP ($kgSb_{eq}$)	1.99E-04	1.94E-05	1.78E-05	4.93E-07	5.41E-05	4.35E-06	1.71E-06	2.97E-04
GWP ($kgCO_{2eq}$)	1.83E+00	4.61E+00	8.59E-01	2.09E-01	1.04E+00	1.74E+01	6.75E-02	2.60E+01
ODP ($kgCFC\text{-}11_{eq}$)	1.66E-07	4.10E-07	9.49E-08	1.15E-08	7.14E-08	1.20E-06	6.85E-09	1.96E-06
HT-nce (CTUh)	5.63E-06	4.21E-06	4.19E-07	4.26E-08	2.22E-06	1.62E-06	2.76E-08	1.42E-05
HT-ce (CTUh)	2.76E-07	5.18E-07	5.22E-08	9.74E-09	8.36E-07	3.85E-07	8.66E-09	2.09E-06
PM (kg $PM2.5_{eq}$)	2.64E-03	8.32E-03	8.52E-04	9.29E-05	1.15E-03	7.29E-03	5.36E-05	2.04E-02
IR-hh ($kBqU^{235}{}_{eq}$)	1.58E-01	6.40E-01	1.01E-01	2.51E-02	9.87E-02	6.83E-01	6.94E-03	1.71E+00
POFP ($kgNMVOC_{eq}$)	9.64E-03	2.25E-02	2.97E-03	7.04E-04	4.42E-03	4.50E-02	3.59E-04	8.57E-02
AP ($molH^{+}{}_{eq}$)	2.08E-02	1.21E-01	8.23E-03	9.76E-04	8.30E-03	1.08E-01	5.06E-04	2.67E-01
EU_T ($molN_{eq}$)	2.80E-02	7.08E-02	9.43E-03	1.65E-03	1.36E-02	1.49E-01	1.68E-03	2.75E-01
EU_F (kgP_{eq})	3.65E-03	3.81E-03	4.26E-04	6.31E-05	1.38E-03	2.83E-03	1.97E-05	1.22E-02
EU_M (kgN_{eq})	2.66E-02	7.42E-03	1.05E-03	1.59E-04	6.65E-03	1.42E-02	1.20E-04	5.62E-02
E_{Fw} (CTUe)	1.30E+02	1.31E+02	1.18E+01	1.40E+00	5.73E+01	6.18E+01	1.12E+00	3.94E+02

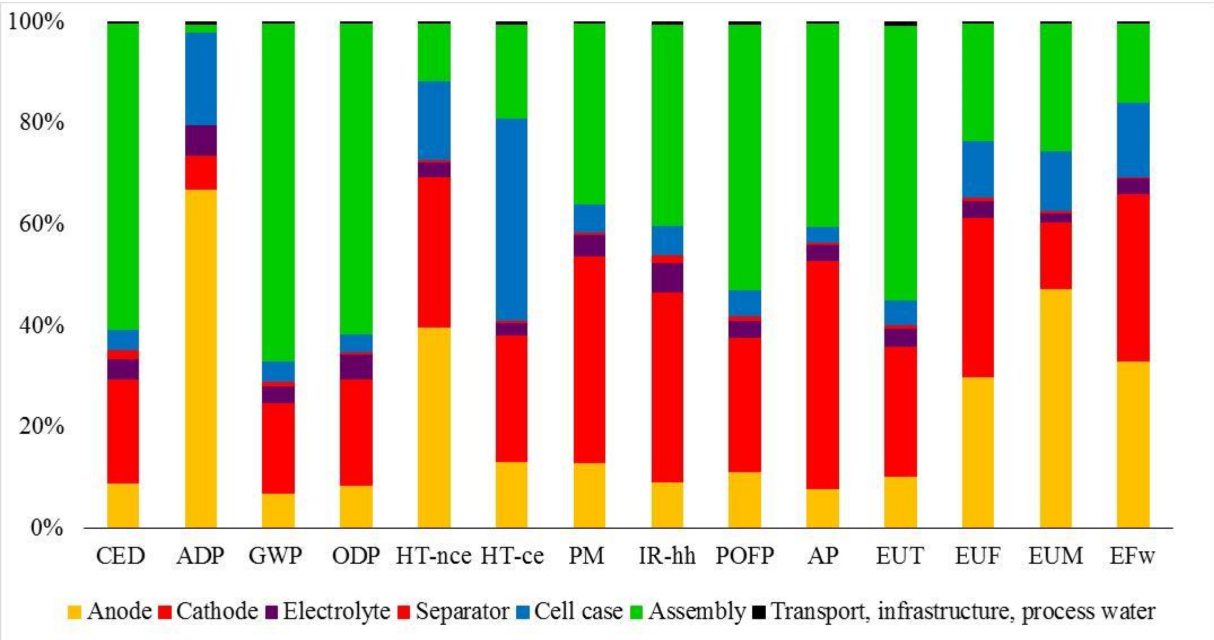

Figure 55. Environmental impacts – battery cell production phase.

Therefore, to increase the sustainability of battery production it is necessary to reduce the impacts of the energy consumed during cell assembly by adopting more efficient processes and technologies and by increasing the use of cleaner energy sources (e.g. RESs).

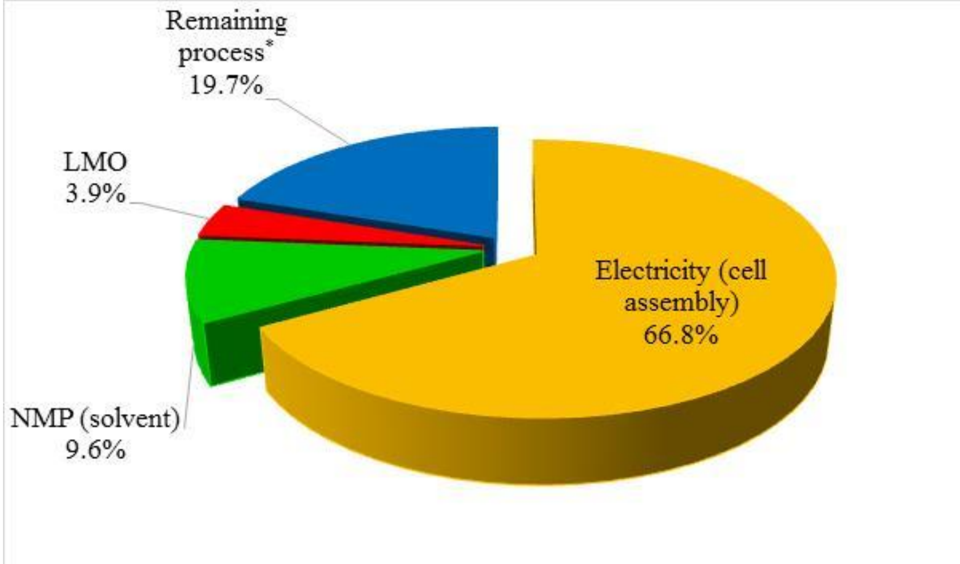

*Remaining processes: sum of the processes with a percentage contribution lower than 3%

Figure 56. Battery cell production: process contribution to the global warming potential impact category.

In the abiotic depletion potential, the highest contribution (67%) is from anode. It is worth mentioning that, although cobalt (contained in the cathode) is designated as critical raw material, the greatest impact on abiotic resource depletion is attributable to the anode production process and, specifically, copper primary production, which accounts for 77% of the total impact of cell production on this category (Figure 59). In fact, the criticality of cobalt is mainly attributable to political and economic reasons that are not captured by an environmental impact category. Abiotic depletion potential is one of the few indicators that relates to the consumption of non-energy resources [187]. However, its characterization factors do not reflect regional differences in resource consumption, or quality losses during, for example, material use and EoL treatments [188].

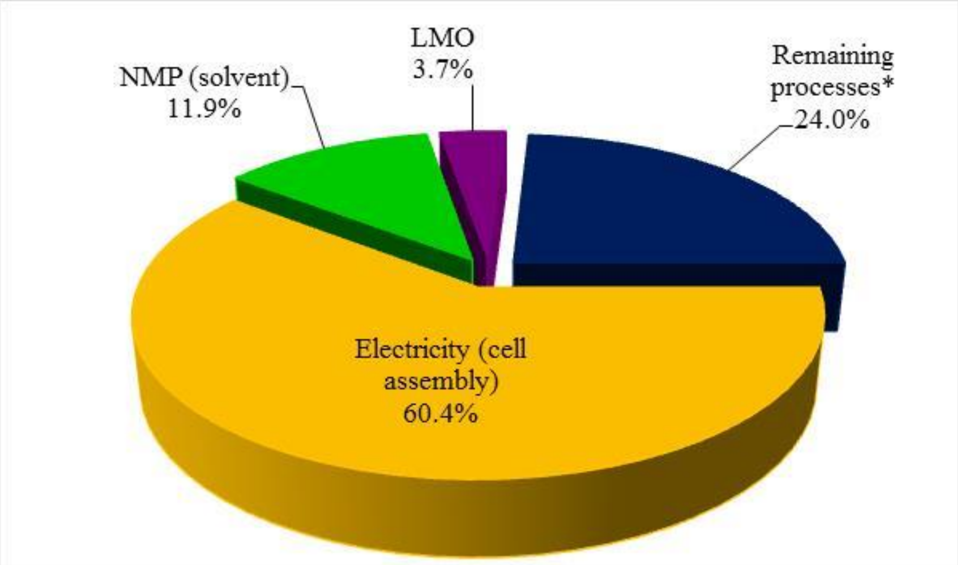

*Remaining processes: sum of the processes with a percentage contribution lower than 3%

Figure 57. Battery cell production: process contribution to the cumulative energy demand impact category.

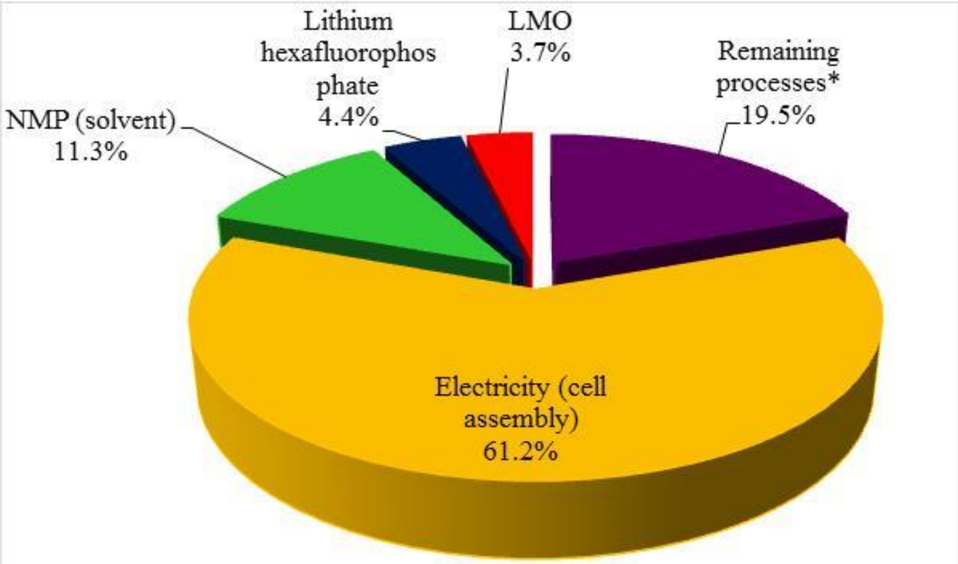

*Remaining processes: sum of the processes with a percentage contribution lower than 3%

Figure 58. Battery cell production: process contribution to the ozone depletion impact category.

Cathode and anode contribute, overall, for more than 60% in human toxicity – non cancer effect in which the highest contribution is due to steel production (Figure 60); particulate matter (Figure 61), freshwater eutrophication (Figure 62) and marine eutrophication (Figure 63), and freshwater eco-toxicity (Figure 64) impact categories.

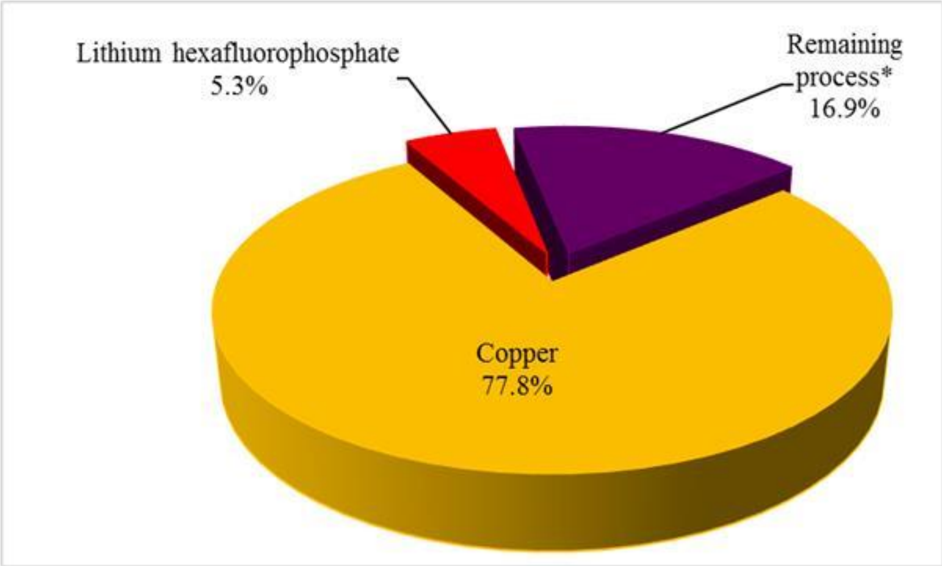

*Remaining processes: sum of the processes with a percentage contribution lower than 3%

Figure 59. Battery cell production: process contribution to the abiotic depletion potential impact category.

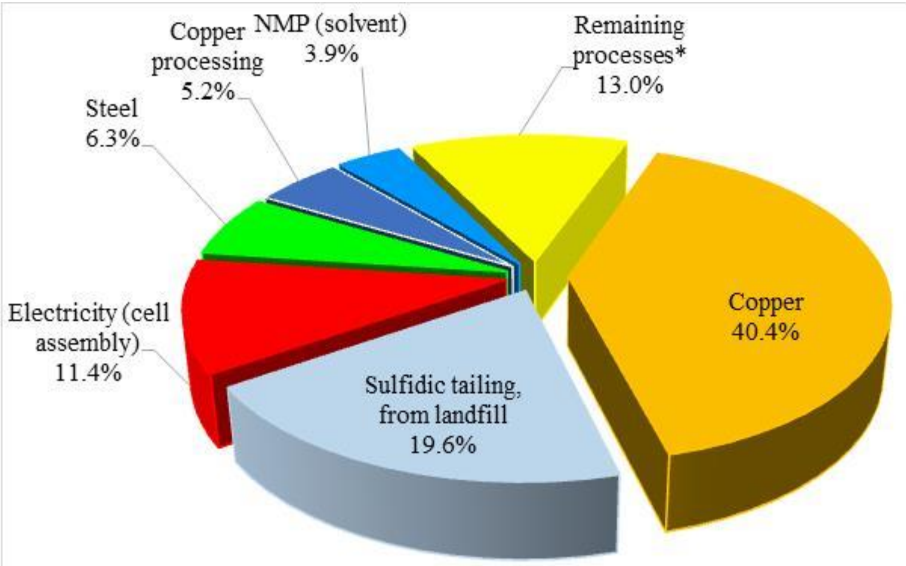

*Remaining processes: sum of the processes with a percentage contribution lower than 3%

Figure 60. Battery cell production: process contribution to the human toxicity – non cancer effect impact category.

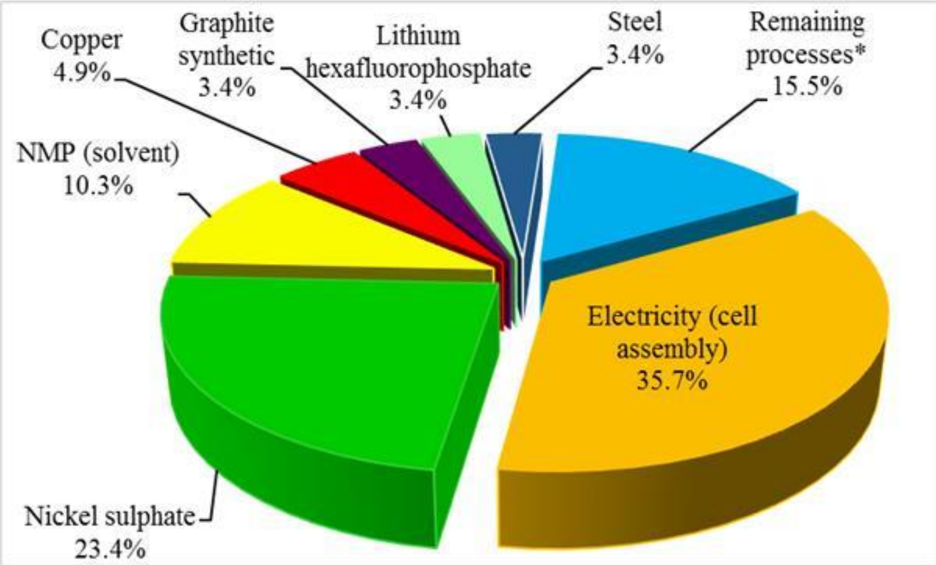

*Remaining processes: sum of the processes with a percentage contribution lower than 3%

Figure 61. Battery cell production: process contribution to the particulate matter impact category.

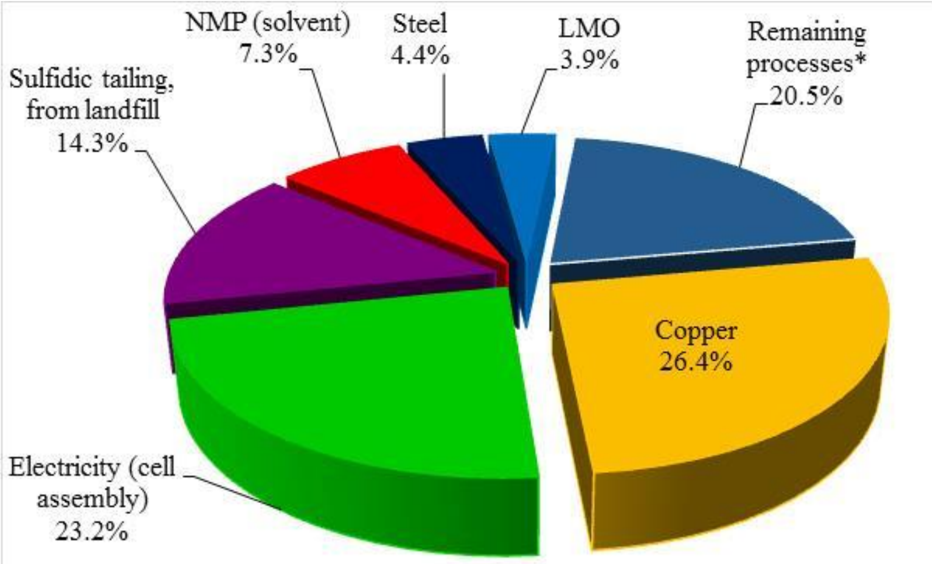

*Remaining processes: sum of the processes with a percentage contribution lower than 3%

Figure 62. Battery cell production: process contribution to the freshwater eutrophication impact category.

The detailed contribution analysis of the cell sub – components highlights that the NMP production is the main contributor, after the cell assembly process, to several impact categories examined. For this reason, the NMP has been identified as a potential relevant parameter for the sensitivity analysis.

The electrolyte production presents a contribution lower than 6%, the separator and the “transport, infrastructure, process water production” account for less than 2% and 0.6%, respectively, in all the examined impact categories. The contribution of the cell case to the different impact categories ranges from 3% (for acidification potential) to 40% in human toxicity – cancer effect.

Finally, in Table 38 the CRMs content referred to the examined battery pack is illustrated.

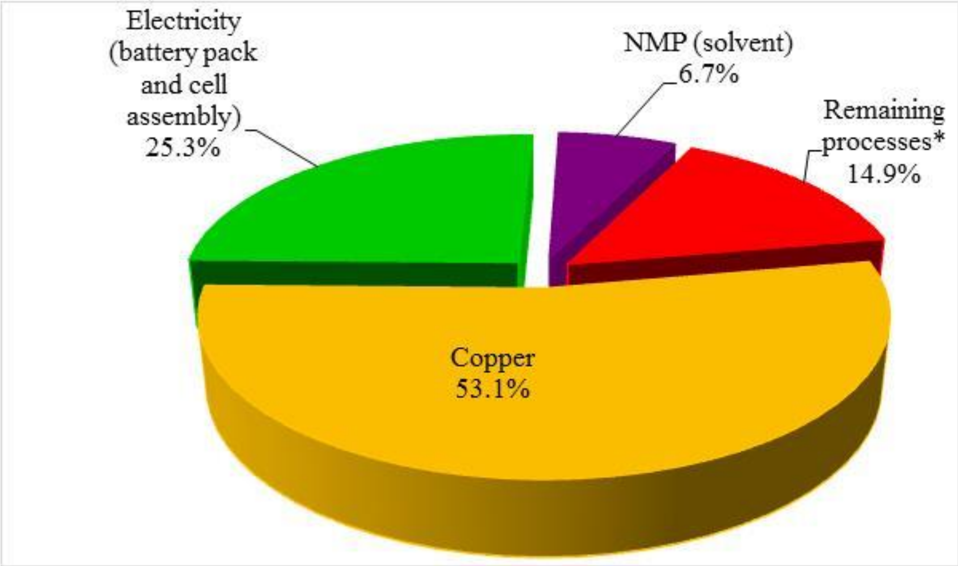

*Remaining processes: sum of the processes with a percentage contribution lower than 3%

Figure 63. Battery cell production: process contribution to the marine eutrophication impact category.

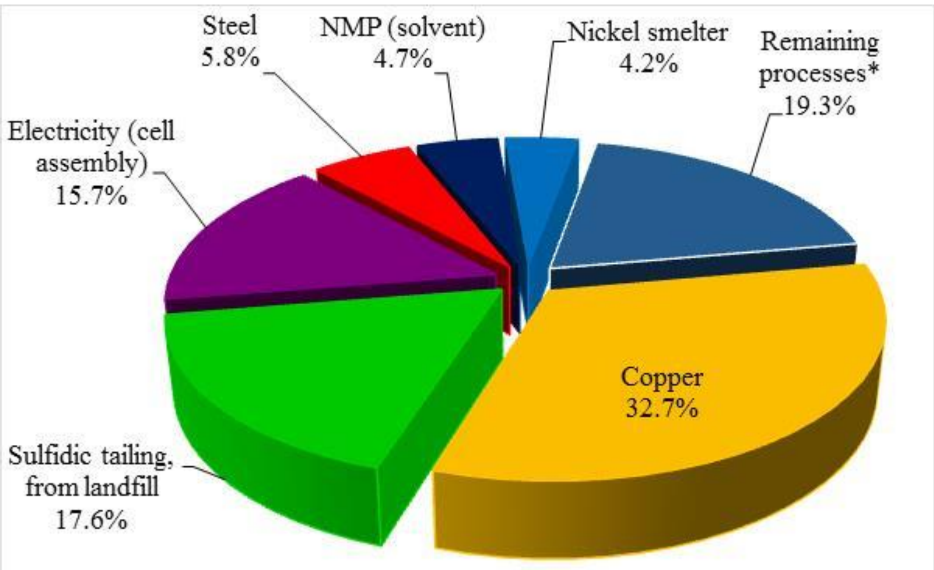

*Remaining processes: sum of the processes with a percentage contribution lower than 3%

Figure 64. Battery cell production: process contribution to the freshwater eco-toxicity impact category.

Table 38. CRMs content per battery pack.

CRM	Unit of measure	Value referred to 80 cells (one battery pack)
Barite	g	830.23
Cobalt	kg	2.59
Fluorspar	kg	17.39
Gallium	ng	7.71
Heavy rare earths	ng	1.75
Indium	mg	110.91
Light rare earths	ng	345.45
Magnesite	g	919.99
Phosphorus	g	967.34
Phosphorus, 18% in apatite, 4% in crude ore	kg	1.31
Platinum group metals	µg	1380.46
Tantalum	mg	72.80

5.3.3.2 Battery pack recycling: contribution analysis

In this section, the detailed LCIA results of the impacts and environmental credits related to the recycling process of each battery components are illustrated and discussed.

In Table 39, the life cycle impacts and credits of battery cells recycling are summarized. Cell recycling using a pyrometallurgical-hydrometallurgical process results in environmental credits in almost all the impact categories examined, with the exceptions of cumulative energy demand, global warming potential, ozone depletion potential and ionizing radiation impact categories.

The main contributions to the recycling impacts relate to electricity consumption, sodium hydroxide production and waste treatment, which overall account for more than 44% in all the impact categories examined (Figure 65). Concerning the electricity, its contribution to the overall impacts ranges from 2.7% (for abiotic depletion potential) to 53.6% (for ionizing radiation); sodium hydroxide production account for a minimum of 15.6% (in particulate matter) up to 78.4% (in ozone depletion potential); waste treatment contribution ranges from 3.6% (for ozone depletion potential) up to 34.3% (for global warming potential).

Concerning the environmental credits, they represent a percentage of the total burden associated to the whole battery pack production equal to 20% in marine eutrophication impact category and 13% in both abiotic depletion and human toxicity – non cancer effect, and ranging from 1% (ionizing radiation) to 9% (human toxicity – cancer effect) in the other impact categories.

The environmental credits related to the cell recycling process are higher than the correspondent impacts in almost all the environmental categories examined with the exception of cumulative energy demand, global warming potential, ozone depletion potential and ionizing radiation. However, the environmental benefits of recycling could be increased if the other cell components/materials, such as graphite, electrolyte and aluminium, were recovered, i.e. by designing battery cells to make disassembling and separating the cell components easier and more secure [189]. Moreover, if reuse in stationary energy storage applications is envisaged, this strategy could be useful to guarantee easy disassembly of modules into cells to test the failure rate of the cells [89,111].

The processes contribution to the environmental credits is illustrated in Figure 66. Copper recycling accounts for the highest environmental credits in almost all the environmental impact categories investigated. It represents a percentage ranging from about 20% in acidification potential to 96% in abiotic depletion potential.

Table 39. Life cycle impacts and credits of battery cells recycling.

Impact category	Recycling impacts - cell	Recycling credits - cell
CED (MJ)	2.57E+03	-9.26E+02
ADP ($kgSb_{eq}$)	6.19E-04	-1.00E-02
GWP ($kgCO_{2eq}$)	1.48E+02	-5.35E+01
ODP ($kgCFC\text{-}11_{eq}$)	3.73E-05	-4.63E-06
HT-nce (CTUh)	4.82E-05	-3.31E-04
HT-ce (CTUh)	9.33E-06	-4.01E-05
PM ($kg\ PM2.5_{eq}$)	1.20E-01	-1.67E-01
IR-hh ($kBqU^{235}{}_{eq}$)	4.20E+01	-7.00E+00
POFP ($kgNMVOC_{eq}$)	2.99E-01	-4.63E-01
AP ($molH^{+}{}_{eq}$)	8.37E-01	-2.27E+00
EU_T ($molN_{eq}$)	1.05E+00	-1.50E+00
EU_F (kgP_{eq})	9.24E-02	-1.94E-01
EU_M (kgN_{eq})	1.16E-01	-1.32E+00
E_{Fw} (CTUe)	1.94E+03	-7.96E+03

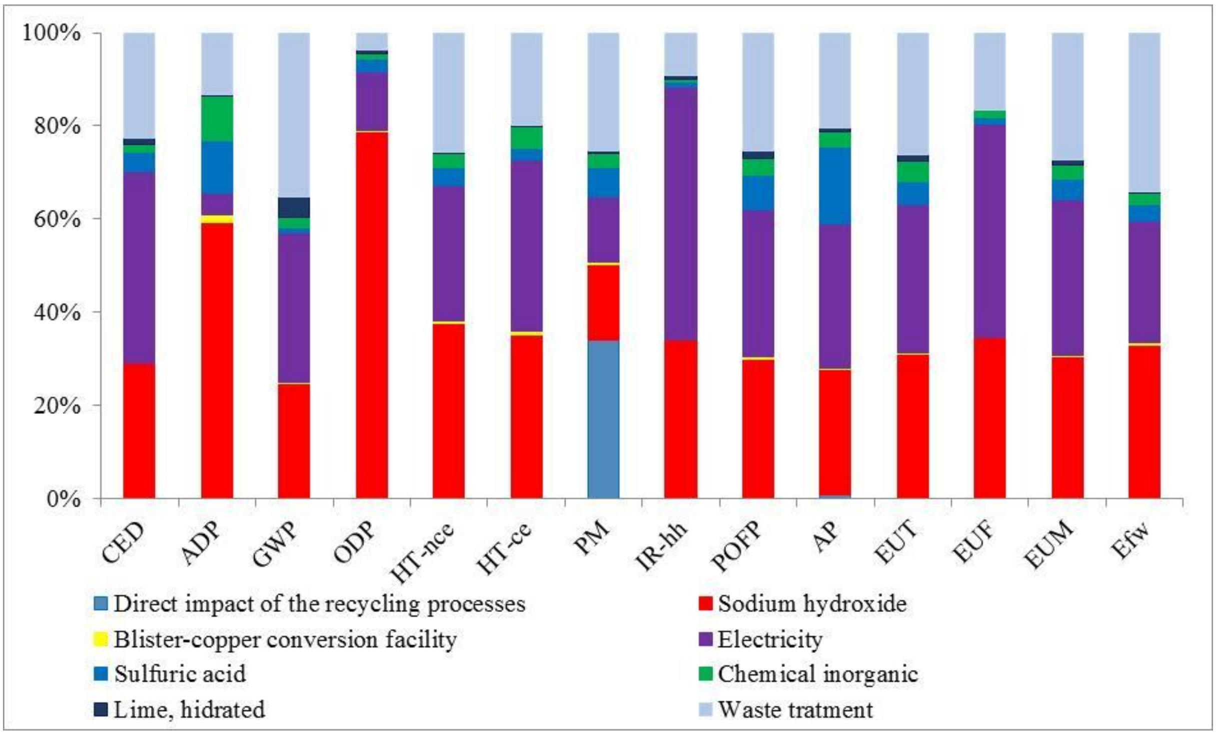

Figure 65. Impact related to battery cell recycling treatment – process contribution.

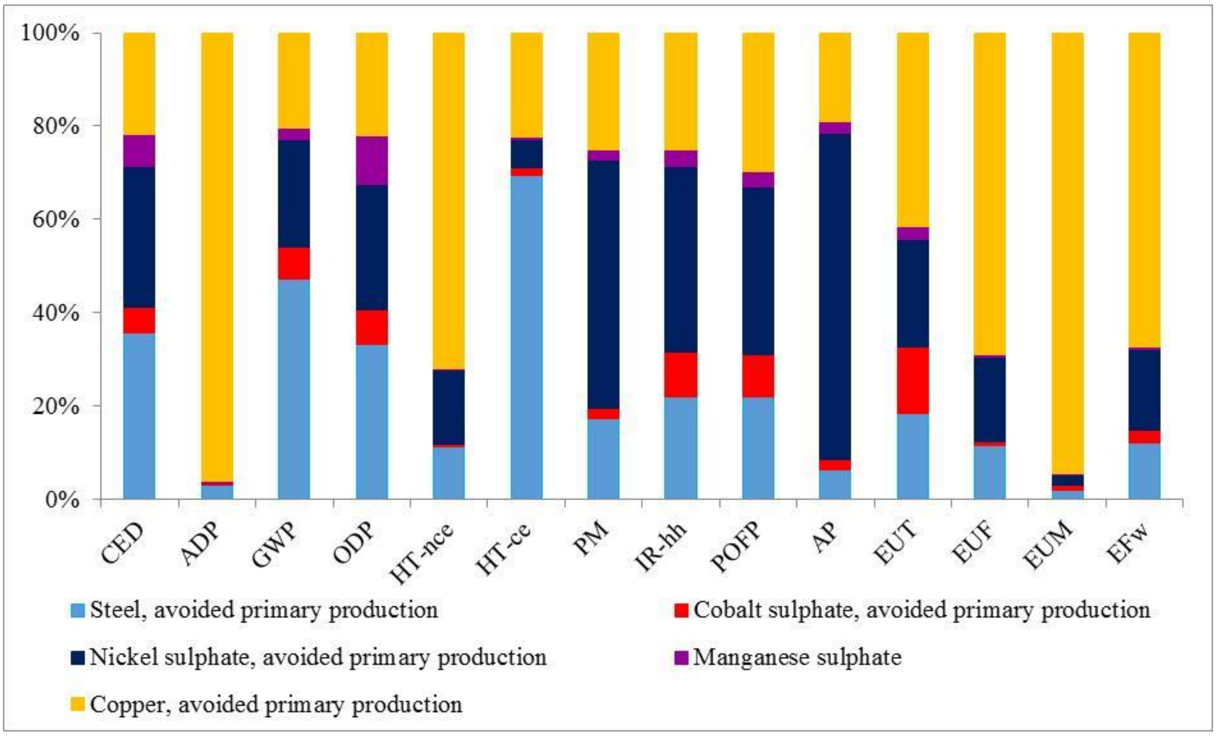

Figure 66. Environmental credits related to battery cell recycling treatment – process contribution.

Regarding the other battery components, Table 40, Table 41 Table 42 illustrate, respectively, the environmental impacts and credits related to the BMS, cooling system and packaging. The LCIA results highlight that the largest contributions to the recycling impacts of each components are associated with energy consumption (heat and electricity) and with preparing copper scraps for recycling (Figure 66, Figure 67 and Figure 68).Overall, these contribute more than 50% to all the impact categories examined, with the exception of freshwater ecotoxicity, in which the preparation of aluminium scraps for recycling accounts for more than 99% in the cooling system and packaging recycling processes and for 45% in the BMS recycling process.

The environmental credits, related to the avoidance of the production of the copper, aluminium and steel recovered from the BMS, cooling system and packaging, are significant in the cumulative energy demand, global warming potential, ozone depletion potential, ionizing radiation and human toxicity – cancer effect impact categories, in which they account for 83%, 84%, 81%, 83% and 77%, respectively, of the total environmental credits. While they represent a percentage of the total burden associated to the whole battery production of about 30% in human toxicity – cancer effect and lower than 10% in the other impact categories.

Concerning the BMS, the environmental credits related to the secondary material recovered are higher than the environmental impacts related to the recycling process in all the examined environmental categories with the exception of freshwater eco-toxicity, in which the highest recycling impact (44%) (Table 40) is due to the preparation of the aluminium scraps (Figure 67). The highest environmental credits are mainly related to the avoidance of the production of the copper (Figure 68).

Table 40. Life cycle impacts and credits of BMS recycling.

Impact category	Recycling impacts - BMS	Recycling credits - BMS
CED (MJ)	4.75E+01	-1.27E+02
ADP ($kgSb_{eq}$)	1.17E-04	-8.90E-04
GWP ($kgCO_{2eq}$)	4.41E+00	-8.40E+00
ODP ($kgCFC\text{-}11_{eq}$)	2.31E-07	-5.94E-07
HT-nce (CTUh)	1.61E-05	-2.91E-05
HT-ce (CTUh)	6.32E-07	-7.34E-06
PM ($kg\ PM2.5_{eq}$)	2.89E-03	-1.11E-02
IR-hh ($kBqU^{235}{}_{eq}$)	6.39E-01	-1.02E+00
POFP ($kgNMVOC_{eq}$)	1.03E-02	-3.86E-02
AP ($molH^{+}{}_{eq}$)	2.60E-02	-8.45E-02
EU_T ($molN_{eq}$)	4.02E-02	-1.30E-01
EU_F (kgP_{eq})	8.14E-03	-1.75E-02
EU_M (kgN_{eq})	3.95E-03	-1.14E-01
E_{Fw} (CTUe)	2.33E+03	-7.05E+02

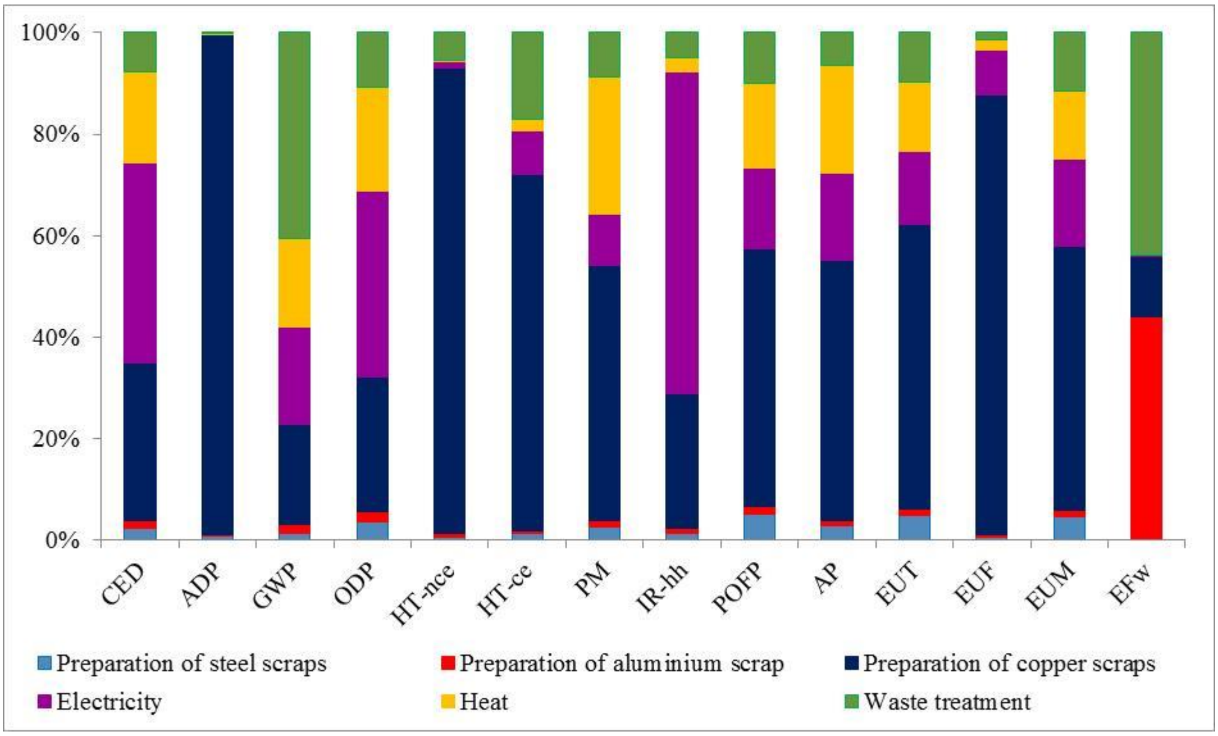

Figure 67. Impact related to BMS recycling treatment – process contribution.

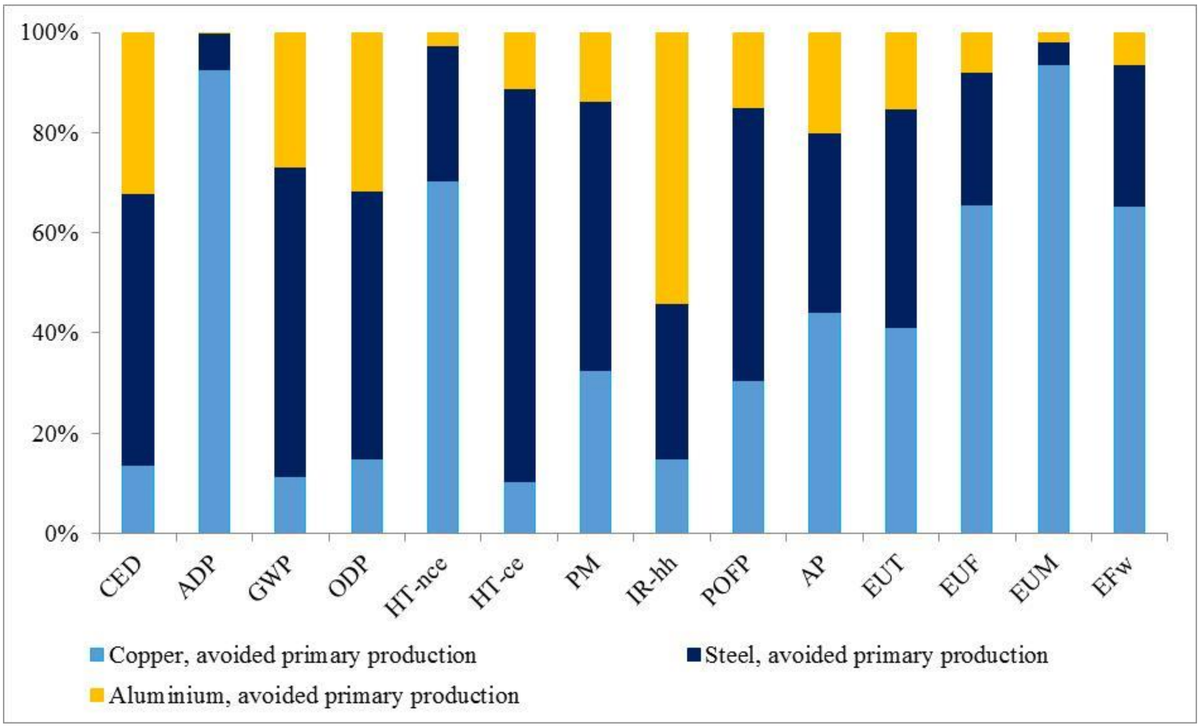

Figure 68. Environmental credits related to BMS recycling treatment – process contribution.

Regarding the cooling system, the environmental credits related to the secondary material recovered are higher than the environmental impacts related to the recycling process in all the examined environmental categories with the exception of freshwater eco-toxicity, in which the preparation of the aluminium scraps accounts for more than 99% (Figure 69). The highest environmental credits are mainly related to the avoidance of the production of the aluminium (Figure 70).

Table 41. Life cycle impacts and credits of cooling system recycling.

Impact category	Recycling impacts - Cooling system	Recycling credits - Cooling system
CED (MJ)	1.16E+02	-1.13E+03
ADP ($kgSb_{eq}$)	1.20E-05	-6.64E-05
GWP ($kgCO_{2eq}$)	7.40E+00	-6.99E+01
ODP ($kgCFC\text{-}11_{eq}$)	8.92E-07	-4.62E-06
HT-nce (CTUh)	3.98E-06	-2.30E-05
HT-ce (CTUh)	1.96E-07	-2.47E-05
PM ($kg\ PM2.5_{eq}$)	2.02E-03	-5.31E-02
IR-hh ($kBqU^{235}{}_{eq}$)	7.73E-01	-8.81E+00
POFP ($kgNMVOC_{eq}$)	1.06E-02	-1.97E-01
AP ($molH^{+}{}_{eq}$)	2.17E-02	-5.90E-01
EU_T ($molN_{eq}$)	3.27E-02	-6.77E-01
EU_F (kgP_{eq})	1.83E-03	-3.59E-02
EU_M (kgN_{eq})	3.30E-03	-6.95E-02
E_{Fw} (CTUe)	3.08E+04	-1.34E+03

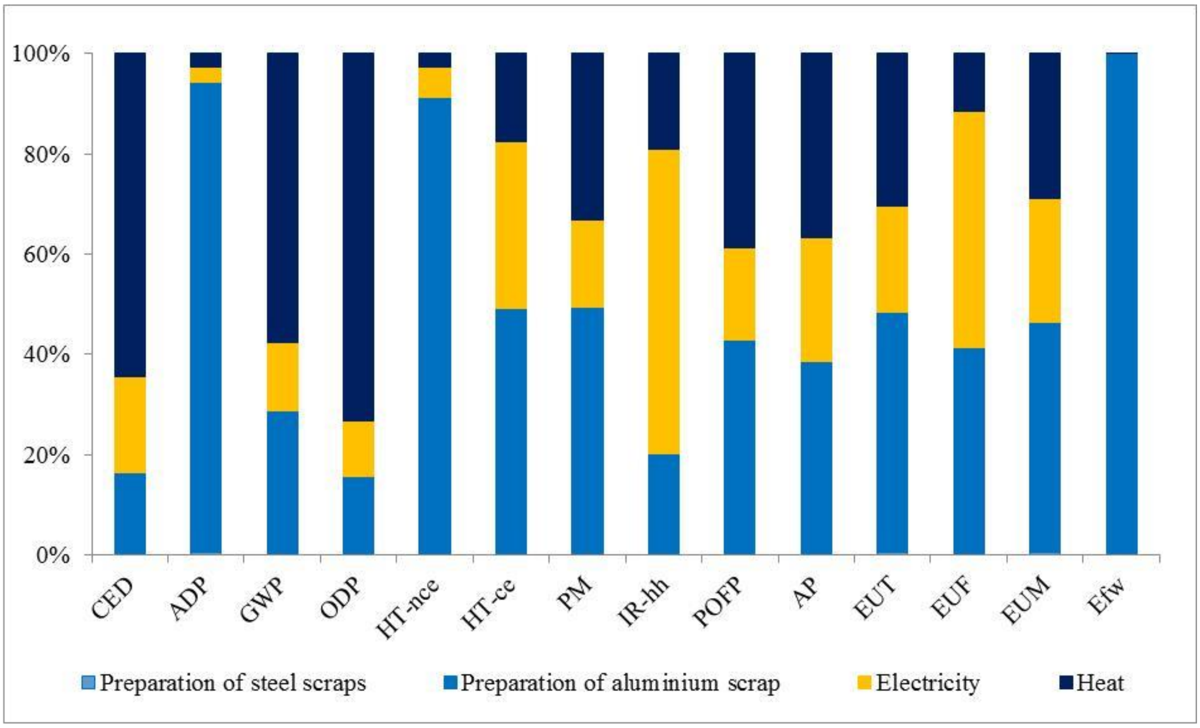

Figure 69. Impact related to cooling system recycling treatment – process contribution.

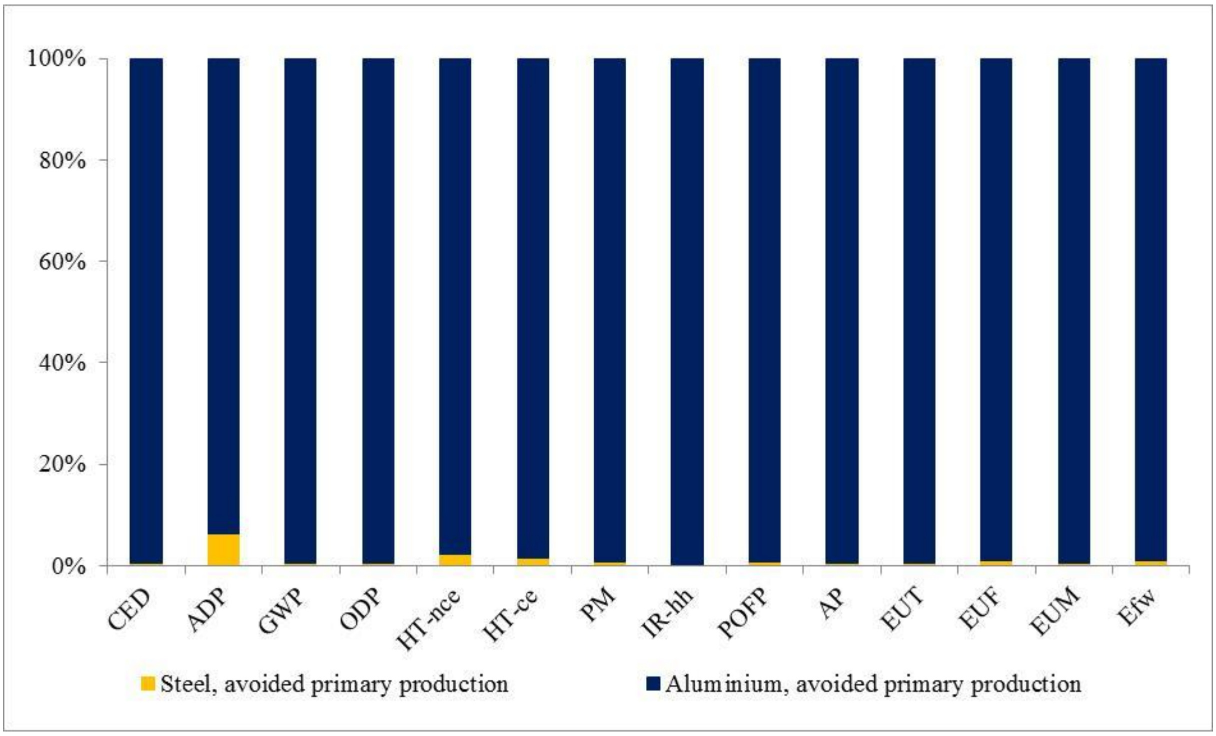

Figure 70. Environmental credits related to cooling system recycling treatment – process contribution.

Table 42. Life cycle impacts and credits of battery packaging recycling..

Impact category	Recycling impacts - Battery packaging	Recycling credits - Battery packaging
CED (MJ)	4.18E+02	-3.35E+03
ADP ($kgSb_{eq}$)	2.00E-04	-1.73E-03
GWP ($kgCO_{2eq}$)	2.58E+01	-2.13E+02
ODP ($kgCFC\text{-}11_{eq}$)	2.85E-06	-1.40E-05
HT-nce (CTUh)	3.30E-05	-1.38E-04
HT-ce (CTUh)	1.46E-06	-1.01E-04
PM ($kg\ PM2.5_{eq}$)	1.01E-02	-1.79E-01
IR-hh ($kBqU^{235}{}_{eq}$)	4.19E+00	-2.47E+01
POFP ($kgNMVOC_{eq}$)	4.77E-02	-6.55E-01
AP ($molH^{+}{}_{eq}$)	1.06E-01	-1.75E+00
EU_T ($molN_{eq}$)	1.62E-01	-2.17E+00
EU_F (kgP_{eq})	1.84E-02	-1.38E-01
EU_M (kgN_{eq})	1.80E-02	-3.60E-01
E_{Fw} (CTUe)	7.87E+04	-5.34E+03

Regarding the packaging, the environmental credits related to the secondary material recovered are higher than the environmental impacts related to the recycling process in all the examined environmental categories with the exception of freshwater eco-toxicity, in which the preparation of the aluminium scraps accounts for more than 99% (Figure 71).

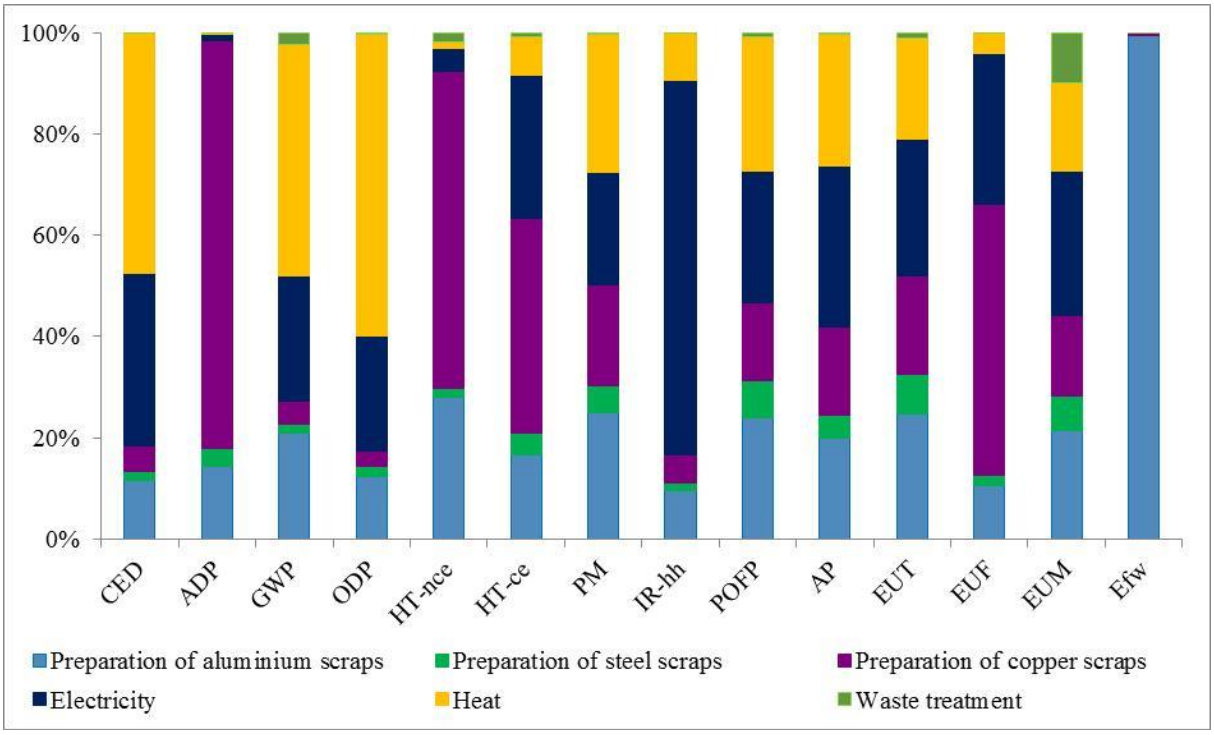

Figure 71. Impact related to packaging recycling treatment – process contribution.

The highest environmental credits are mainly related to the avoidance of the production of the aluminium in all the examined impact categories with the exception on the abiotic depletion potential in which the highest contribution is due to the avoidance of the copper production (Figure 72).

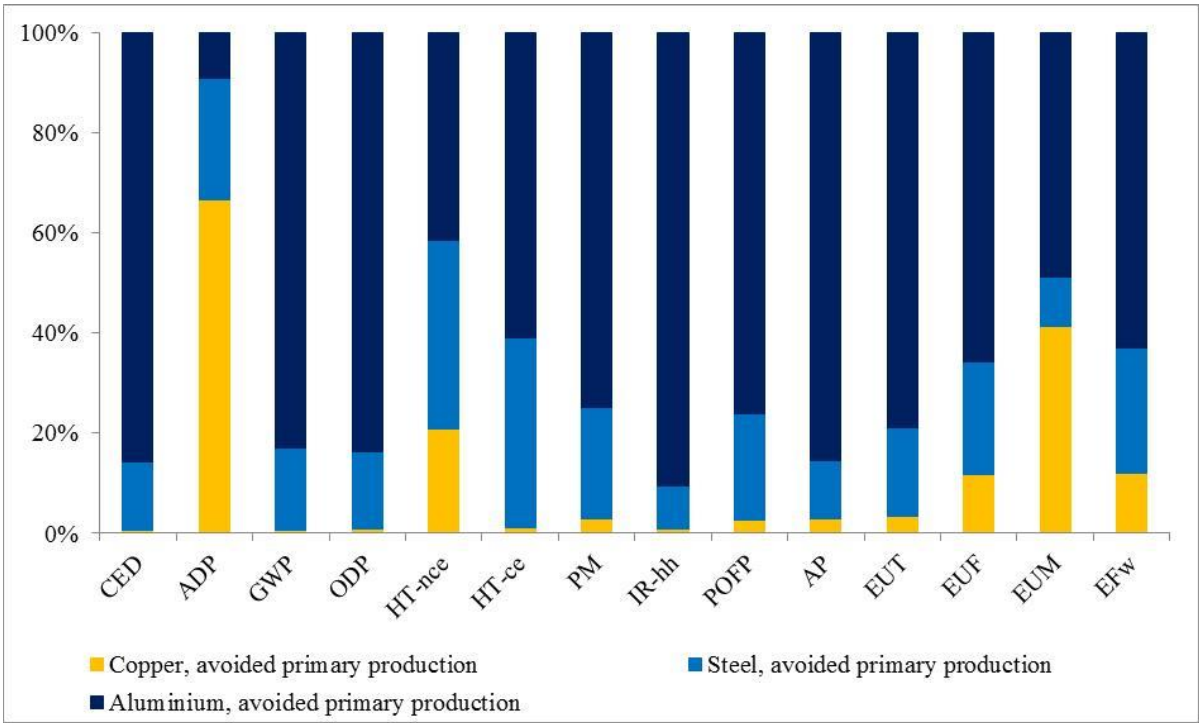

Figure 72. Environmental credits related to packaging recycling treatment – process contribution.

The results obtained show that, although the most valuable metals (cobalt, nickel and copper) are contained in the cathode, the recycling of other materials, such as aluminium, copper and steel, contained in the other battery components increases the environmental benefits of battery recycling. Appropriate battery design could make it easier to separate the battery components and thereby optimize the recovery of the various metal fractions.

5.3.4 Sensitivity analysis

Although the LCA is a useful tool for estimating the effective energy and environmental impacts of a product or service, its reliability strictly depends on complete and precise data, which are not always available [190,191]. Because of the lack of primary data from industry, several assumptions have been made in this study. Hence, a sensitivity analysis is performed, based on a scenario analysis, to assess the influence of the assumptions on the results obtained. As discussed by Igos et al. (2018), this approach also allows the uncertainty resulting from input data to be embodied and modelled.

Compared with the “base case” analysis (as described in previous sections), “worst” and “best” scenarios are set by assuming one-at-a-time parameter change. Relevant parameters for the scenario analysis are identified according to the LCIA outcomes. The values of these parameters for the “worst” and “best” scenarios are decided on using data from the literature. With regard to the production stage, the sensitivity analysis is performed for the battery cells only, as details on the other battery components were inferred from literature studies.

The assessment of battery cell production is based on inputs of materials obtained from disassembly experiments performed on a case-study battery cell, while the energy required for cell assembly is inferred from literature data [54].

As discussed in Section 5.3.2.1 and highlighted in Table 43, for the negative active material, the binder, the solvent, the electrolyte and the cell case assumptions are made about the amount used in the cell and in the specific material composition; moreover, the electricity required for cell assembly is another input to the LCA model affected by high uncertainty.

The main assumptions about the cell production process are detailed in Table 43.

Table 43. Main assumptions related to the cell production process.

Cell component/energy requirement	**Assumptions for the LCA**
Negative active material	Material composition: synthetic graphite
Binder	Material composition: in the cathode, PAA+CMC; in the anode, PVDF
Solvent	Material composition and weight: NMP, 0.4 kg/kg of positive electrode paste; 0.94 kg/kg of negative electrode paste
Electrolyte	Material composition: $LiPF_6$ + $C_3H_4O_3$
Separator	Material composition: PP granulate + PE granulate
Cell case	Material composition of plastic fraction: PP granulate + PE granulate
Cell assembly	Amount: 586 MJ/kWh of battery cell capacity

The LCIA results show that the negative active material, the binder and the cell case were not major contributors to battery cell production, as their incidences are less than 3% in all the impact categories examined; therefore, they are not taken into account in the sensitivity analysis. With regard to the electrolyte, its composition is based on previous studies; however, it is not possible to identify a detailed composition in the literature that differed from that assumed in the present study (including the option of using water, as mentioned by Zackrisson et al. [136]).

Concerning the solvent, it is not possible to identify in the literature a composition different from that assumed in the present study. Therefore, the sensitivity analysis is therefore carried out for two parameters: the amount of solvent and the electricity required for cell assembly.

For the use phase, a sensitivity analysis was performed to assess how the battery efficiency and weight–energy relationship influenced the results obtained.

For the EoL phase, the goal of the sensitivity analysis was to assess how lower recycling rates (than the values in Table 33 considered as the base case could affect the overall life cycle impacts.

The main assumptions of the scenario analysis are shown in Table 44.

Table 44. Main assumptions of the sensitivity analysis.

Life cycle phase	Parameters	Base case	Worst scenario	Best scenario
Production	• NMP	• NMP, 0.4 kg/kg of positive electrode paste; 0.94 kg/kg of negative electrode paste [54]	• 0.82 kgNMP/kg for both positive and negative electrode paste [193].	• 0.28 kgNMP/kg for both positive and negative electrode paste [65];
	• Electricity for cell assembly	• 586 MJ/kWh of battery cell capacity [54]	• 960 MJ/kWh of battery capacity [54]	• 309 MJ/kWh of battery capacity [193]
Use	• Battery charging efficiency	• 95% [89]	• 90% [136]	• 98% [89]
	• Weight–energy relationship	• 30% [136]	• 50% (higher electricity Consumption for battery transport) [136]	• 15% (lower electricity Consumption for battery transport) [136]
	• Driven range (km)	• 136,877 (own primary data)	• 96,000 (–30% compared with base case)	• 180,000 (+30% compared with base case
EoL	• Recycling rate	• Table 33 [184]	• –30%	–

For each parameter (according to both the LCIA outcomes and the uncertainty at input level) a worst and a best scenario were defined with respect to the base case by using data from the literature or the authors making their own arbitrary variations [192]. This scenario analysis permitted, in accordance with Igos et al. (2018), to perform a sensitivity analysis including a rough estimation consideration of the uncertainty related to the input data.

With regard to the production phase, the sensitivity analysis highlights that varying the NMP amount in the range examined does not affect the results obtained significantly, as the percentage variation of the impacts in the worst and best scenarios, if compared with the base case, are lower than +/–5% in all the impact categories examined (Table 45).

In terms of the electricity consumed during cell assembly, in both scenarios (worst and best) battery production remains the life cycle phase responsible for the highest impacts in almost all the categories examined (Table 46 and Table 47).

Table 45. Sensitivity analysis results – NMP, percentage variations between the scenarios examined and the base case.

Impact category	**Base case**	**Worst scenario (%)**	**Best scenario (%)**
CED (MJ)	4.26E+04	4.5	-4.3
ARD ($kgSb_{eq}$)	7.55E-02	0.4	-0.4
GWP ($kgCO_{2eq}$)	2.67E+03	3.7	-3.6
ODP ($kgCFC\text{-}11_{eq}$)	2.03E-04	4.4	-4.2
HT-nce (CTUh)	2.16E-03	1.0	-1.0
HT-ce (CTUh)	3.67E-04	1.1	-1.0
PM (kg $PM2.5_{eq}$)	2.17E+00	3.9	-3.7
IR-hh ($kBqU^{235}{}_{eq}$)	2.32E+02	3.8	-3.6
POFP ($kgNMVOC_{eq}$)	9.10E+00	3.1	-3.0
AP ($molH^{+}{}_{eq}$)	2.63E+01	2.5	-2.4
EU_T ($molN_{eq}$)	2.91E+01	2.9	-2.8
EU_F (kgP_{eq})	1.73E+00	2.1	-2.0
EU_M (kgN_{eq})	5.55E+00	2.7	-2.6
E_{Fw} (CTUe)	5.90E+04	1.3	-1.2

Table 46. Sensitivity analysis results – cell assembly (worst scenario).

Impact category	**Battery pack production (%)**	**Battery operation (%)**	**Battery pack EoL (%)**	**Total (without credits) (%)**	**Recycling credits* (%)**
CED (MJ)	72.8	23.5	3.7	7.43E+04	-3.8
ADP ($kgSb_{eq}$)	97.8	1.2	1.0	7.74E-02	-14.4
GWP ($kgCO_{2eq}$)	78.8	17.5	3.6	4.42E+03	-3.8
ODP ($kgCFC\text{-}11_{eq}$)	68.9	20.8	10.3	3.77E-04	-3.4
HT-nce (CTUh)	88.1	9.0	2.8	2.54E-03	-17.8
HT-ce (CTUh)	85.2	12.5	2.3	4.52E-04	-18.9
PM (kg $PM2.5_{eq}$)	86.0	9.7	4.3	2.93E+00	-11.7
IR-hh ($kBqU^{235}{}_{eq}$)	38.8	54.8	6.4	6.82E+02	-3.3
POFP ($kgNMVOC_{eq}$)	85.8	11.7	2.5	1.31E+01	-7.4
AP ($molH^{+}{}_{eq}$)	85.9	11.6	2.4	3.66E+01	-13.0
EU_T ($molN_{eq}$)	84.7	12.6	2.7	4.26E+01	-7.2
EU_F (kgP_{eq})	70.0	26.1	3.9	2.66E+00	-11.2
EU_M (kgN_{eq})	89.1	9.1	1.8	6.97E+00	-22.6
E_{Fw} (CTUe)	50.2	15.0	34.8	1.23E+05	-9.8

*Expressed as a percentage of the "Total" burden, including "Battery pack production", "Battery operation" and "Battery pack EoL"

The electricity consumption during cell assembly has a large effect on the environmental assessment (Table 48). The results prove overall the relevance of further investigating this aspect in future studies, possibly using primary data from industry.

Table 47. Sensitivity analysis results – cell assembly (best scenario)

Impact category	Battery pack production (%)	Battery operation (%)	Battery pack EoL (%)	Total (without credits)	Recycling credits* (%)
CED (MJ)	62.3	32.6	5.2	5.36E+04	-5.3
ADP ($kgSb_{eq}$)	97.8	1.2	1.0	7.70E-02	-14.5
GWP ($kgCO_{2eq}$)	68.3	26.2	5.5	2.95E+03	-5.7
ODP ($kgCFC\text{-}11_{eq}$)	57.4	28.5	14.1	2.75E-04	-4.6
HT-nce (CTUh)	87.5	9.6	3.0	2.40E-03	-18.8
HT-ce (CTUh)	84.1	13.5	2.4	4.19E-04	-20.4
PM (kg $PM2.5_{eq}$)	82.3	12.3	5.4	2.31E+00	-14.8
IR-hh ($kBqU^{235}{}_{eq}$)	33.1	59.9	7.0	6.24E+02	-3.6
POFP ($kgNMVOC_{eq}$)	80.0	16.5	3.5	9.26E+00	-10.4
AP ($molH^{+}{}_{eq}$)	81.2	15.5	3.2	2.74E+01	-17.3
EU_T ($molN_{eq}$)	78.3	17.9	3.8	2.99E+01	-10.2
EU_F (kgP_{eq})	67.0	28.7	4.3	2.42E+00	-12.3
EU_M (kgN_{eq})	86.8	11.0	2.2	5.77E+00	-27.4
E_{Fw} (CTUe)	48.0	15.7	36.3	1.18E+05	-10.3

*Expressed as a percentage of the “Total” burden, including “Battery pack production”, “Battery operation” and “Battery pack EoL”

Table 48. Sensitivity analysis results – cell assembly, percentage variations between the scenarios examined and the base case

Impact category	Base case	Worst scenario (%)	Best scenario (%)
CED (MJ)	6.32E+04	18.2	-14.5
ARD ($kgSb_{eq}$)	7.73E-02	0.3	-0.2
GWP ($kgCO_{2eq}$)	3.63E+03	22.5	-18.0
ODP ($kgCFC\text{-}11_{eq}$)	3.23E-04	17.5	-14.0
HT-nce (CTUh)	2.49E-03	3.1	-2.4
HT-ce (CTUh)	4.35E-04	4.2	-3.3
PM (kg $PM2.5_{eq}$)	2.59E+00	13.2	-10.6
IR-hh ($kBqU^{235}{}_{eq}$)	6.54E+02	4.9	-3.9
POFP ($kgNMVOC_{eq}$)	1.10E+01	19.3	-15.4
AP ($molH^{+}{}_{eq}$)	3.16E+01	16.1	-12.9
EU_T ($molN_{eq}$)	3.57E+01	19.7	-15.7
EU_F (kgP_{eq})	2.54E+00	5.2	-4.2
EU_M (kgN_{eq})	6.32E+00	10.6	-8.5
E_{Fw} (CTUe)	1.91E+05	1.5	-1.2

With regard to the operation phase, the sensitivity analysis highlights that the weight–energy relationship, this parameter only slightly affected the results obtained. Moreover, the impacts of electricity losses due to battery efficiency are larger than those caused by the electricity consumed by battery transport in both scenarios examined (Table 49 and Table 50), although in the worst scenario they become more similar.

Table 49. Sensitivity analysis results – weight–energy relationship (worst scenario)

Impact category	Battery pack production (%)	Battery operation (loss due to the battery efficiency) (%)	Battery operation (loss due to the battery transport) (%)	Battery pack EoL (%)	Total	Recycling credits* (%)
CED (MJ)	63.1	16.2	16.1	4.7	6.75E+04	-8.2
ADP ($kgSb_{eq}$)	97.3	0.7	0.7	1.2	7.76E-02	-16.4
GWP ($kgCO_{2eq}$)	69.9	12.7	12.6	4.8	3.82E+03	-9.0
ODP (kgCFC-11_{eq})	59.3	14.4	14.2	12.0	3.42E-04	-7.0
HT-nce (CTUh)	84.8	5.6	5.6	4.0	2.55E-03	-20.5
HT-ce (CTUh)	81.7	7.9	7.8	2.6	4.49E-04	-38.7
PM (kg $PM2.5_{eq}$)	81.6	6.7	6.6	5.1	2.66E+00	-15.4
IR-hh ($kBqU^{235}{}_{eq}$)	31.1	31.4	31.1	6.4	7.47E+02	-5.6
POFP ($kgNMVOC_{eq}$)	80.0	8.4	8.4	3.2	1.14E+01	-11.9
AP ($molH^{+}{}_{eq}$)	80.7	8.2	8.1	3.0	3.26E+01	-14.4
EU_T ($molN_{eq}$)	78.5	9.1	9.0	3.5	3.71E+01	-12.1
EU_F (kgP_{eq})	63.6	16.0	15.9	4.4	2.71E+00	-14.2
EU_M (kgN_{eq})	85.6	6.1	6.1	2.2	6.48E+00	-28.7
E_{Fw} (CTUe)	30.1	5.9	5.9	58.1	1.96E+05	-7.8

*Expressed as a percentage of the “Total” burden, including “Battery pack production”, “Battery operation” and “Battery pack EoL”.

Table 50. Sensitivity analysis results – weight–energy relationship (best scenario)

Impact category	Battery pack production (%)	Battery operation (loss due to the battery efficiency) (%)	Battery operation (loss due to the battery transport) (%)	Battery pack EoL (%)	Total	Recycling credits* (%)
CED (MJ)	71.0	18.3	5.4	5.3	5.99E+04	-9.2
ADP ($kgSb_{eq}$)	97.8	0.7	0.2	1.2	7.72E-02	-16.4
GWP ($kgCO_{2eq}$)	76.6	13.9	4.1	5.3	3.48E+03	-9.9
ODP (kgCFC-11_{eq})	65.9	16.0	4.7	13.4	3.08E-04	-7.7
HT-nce (CTUh)	88.2	5.9	1.7	4.1	2.45E-03	-21.3
HT-ce (CTUh)	86.4	8.4	2.5	2.7	4.24E-04	-40.9
PM (kg $PM2.5_{eq}$)	85.6	7.0	2.1	5.3	2.54E+00	-16.2
IR-hh ($kBqU^{235}{}_{eq}$)	39.8	40.1	11.9	8.2	5.84E+02	-7.1
POFP ($kgNMVOC_{eq}$)	84.9	9.0	2.7	3.4	1.07E+01	-12.6
AP ($molH^{+}{}_{eq}$)	85.5	8.7	2.6	3.2	3.08E+01	-15.3
EU_T ($molN_{eq}$)	83.7	9.7	2.9	3.7	3.47E+01	-12.9
EU_F (kgP_{eq})	71.6	18.0	5.4	5.0	2.41E+00	-16.0
EU_M (kgN_{eq})	89.4	6.4	1.9	2.3	6.20E+00	-30.0
E_{Fw} (CTUe)	31.4	6.2	1.8	60.6	1.88E+05	-8.2

*Expressed as a percentage of the “Total” burden, including “Battery pack production”, “Battery operation” and “Battery pack EoL”.

The weight–energy relationship has a small e effect on the results obtained (Table 51).

Table 51. Sensitivity analysis results – weight–energy relationship, percentage variations between the scenarios examined and the base case

Impact category	Base case	Worst scenario (%)	Best scenario (%)
CED (MJ)	6.32E+04	6.9	-5.1
ARD ($kgSb_{eq}$)	7.73E-02	0.3	-0.2
GWP ($kgCO_{2eq}$)	3.63E+03	5.3	-4.0
ODP ($kgCFC\text{-}11_{eq}$)	3.23E-04	6.0	-4.5
HT-nce (CTUh)	2.49E-03	2.3	-1.7
HT-ce (CTUh)	4.35E-04	3.2	-2.4
PM (kg $PM2.5_{eq}$)	2.59E+00	2.7	-2.0
IR-hh ($kBqU^{235}{}_{eq}$)	6.54E+02	14.2	-10.7
POFP ($kgNMVOC_{eq}$)	1.10E+01	3.5	-2.6
AP ($molH^{+}{}_{eq}$)	3.16E+01	3.3	-2.5
EU_T ($molN_{eq}$)	3.57E+01	3.7	-2.8
EU_F (kgP_{eq})	2.54E+00	6.8	-5.1
EU_M (kgN_{eq})	6.32E+00	2.5	-1.9
E_{Fw} (CTUe)	1.91E+05	2.4	-1.8

The impact of battery transport becomes larger than that of battery efficiency when the latter is 98% (Table 53). Battery efficiency has a large effect on the results obtained (Table 52, Table 53 and Table 54).

Table 52. Sensitivity analysis results – battery efficiency (worst scenario)

Impact category	Battery pack production	Battery operation (loss due to the battery efficiency)	Battery operation (loss due to the battery transport)	Battery pack EoL	Total (without credits)	Recycling credits* (%)
CED (MJ)	57.2	29.4	9.2	4.2	7.45E+04	-7.4
ADP ($kgSb_{eq}$)	96.9	1.5	0.5	1.2	7.79E-02	-16.3
GWP ($kgCO_{2eq}$)	64.6	23.5	7.4	4.5	4.13E+03	-8.4
ODP ($kgCFC\text{-}11_{eq}$)	54.4	26.3	8.3	11.0	3.74E-04	-6.4
HT-nce (CTUh)	81.8	10.9	3.4	3.8	2.64E-03	-19.8
HT-ce (CTUh)	77.8	15.0	4.7	2.5	4.71E-04	-36.8
PM (kg $PM2.5_{eq}$)	78.3	12.9	4.0	4.8	2.78E+00	-14.8
IR-hh ($kBqU^{235}{}_{eq}$)	25.9	52.3	16.4	5.3	8.96E+02	-4.6
POFP ($kgNMVOC_{eq}$)	75.9	16.0	5.0	3.1	1.20E+01	-11.3
AP ($molH^{+}{}_{eq}$)	76.7	15.5	4.9	2.9	3.43E+01	-13.7
EU_T ($molN_{eq}$)	74.2	17.2	5.4	3.3	3.92E+01	-11.4
EU_F (kgP_{eq})	57.7	29.1	9.1	4.0	2.99E+00	-12.9
EU_M (kgN_{eq})	82.4	11.8	3.7	2.1	6.73E+00	-27.6
E_{Fw} (CTUe)	29.0	11.4	3.6	56.0	2.03E+05	-7.6

*Expressed as a percentage of the "Total" burden, including "Battery pack production", "Battery operation" and "Battery pack EoL".

Table 53. Sensitivity analysis results – battery efficiency (best scenario)

Impact category	Battery pack production	Battery operation (loss due to the battery efficiency)	Battery operation (loss due to the battery transport)	Battery pack EoL	Total (without credits)	Recycling credits* (%)
CED (MJ)	76.3	6.8	11.3	5.7	5.58E+04	-9.9
ADP ($kgSb_{eq}$)	98.1	0.3	0.4	1.2	7.70E-02	-16.5
GWP ($kgCO_{2eq}$)	80.8	5.1	8.5	5.6	3.30E+03	-10.4
ODP ($kgCFC\text{-}11_{eq}$)	70.1	5.9	9.8	14.2	2.90E-04	-8.2
HT-nce (CTUh)	90.2	2.1	3.5	4.2	2.39E-03	-21.8
HT-ce (CTUh)	89.2	3.0	5.0	2.8	4.11E-04	-42.2
PM ($kg\ PM2.5_{eq}$)	87.9	2.5	4.2	5.4	2.47E+00	-16.6
IR-hh ($kBqU^{235}{}_{eq}$)	46.8	16.4	27.2	9.6	4.96E+02	-8.4
POFP ($kgNMVOC_{eq}$)	87.9	3.2	5.3	3.5	1.04E+01	-13.1
AP ($molH^{+}{}_{eq}$)	88.4	3.1	5.2	3.3	2.98E+01	-15.8
EU_T ($molN_{eq}$)	86.9	3.5	5.8	3.8	3.35E+01	-13.4
EU_F (kgP_{eq})	76.8	6.7	11.1	5.4	2.25E+00	-17.1
EU_M (kgN_{eq})	91.6	2.3	3.8	2.3	6.05E+00	-30.7
E_{Fw} (CTUe)	32.2	2.2	3.6	62.0	1.83E+05	-8.4

*Expressed as a percentage of the "Total" burden, including "Battery pack production", "Battery operation" and "Battery pack EoL".

Finally, the sensitivity analysis of the driving range shows that the environmental impacts, expressed per kilometre, increase by about 35% (average value) in the worst scenario, while in the best scenario they decrease by about 20% (average value) compared with the base case (Table 55). Therefore, increasing the lifetime of batteries could significantly improve the environmental sustainability of electric mobility.

Table 54. Sensitivity analysis results – battery efficiency, percentage variations between the scenarios examined and the base case

Impact category	Base case	Worse case (%)	Best case (%)
CED (MJ)	6.32E+04	17.9	-11.6
ADP ($kgSb_{eq}$)	7.73E-02	0.8	-0.5
GWP ($kgCO_{2eq}$)	3.63E+03	13.8	-9.0
ODP ($kgCFC\text{-}11_{eq}$)	3.23E-04	15.7	-10.2
HT-nce (CTUh)	2.49E-03	6.0	-3.9
HT-ce (CTUh)	4.35E-04	8.4	-5.5
PM ($kg\ PM2.5_{eq}$)	2.59E+00	7.1	-4.6
IR-hh ($kBqU^{235}{}_{eq}$)	6.54E+02	37.0	-24.1
POFP (kgNMVOCeq)	1.10E+01	9.0	-5.9
AP ($molH^{+}{}_{eq}$)	3.16E+01	8.7	-5.7
EU_T ($molN_{eq}$)	3.57E+01	9.7	-6.3
EU_F (kgP_{eq})	2.54E+00	17.7	-11.5
EU_M (kgN_{eq})	6.32E+00	6.5	-4.2
E_{Fw} (CTUe)	1.91E+05	6.3	-4.1

Table 55.Sensitivity analysis results – battery efficiency, percentage variations between the scenarios examined and the base case

Impact category	Base case	Worst case (%)	Best case (%)
CED (MJ/km)	4.62E-01	38.2	-21.5
ADP ($kgSb_{eq}$/km)	5.65E-07	42.4	-23.9
GWP ($kgCO_{2eq}$/km)	2.65E-02	39.2	-22.1
ODP ($kgCFC\text{-}11_{eq}$/km)	2.36E-09	38.7	-21.8
HT-nce (CTUh/km)	1.82E-08	41.1	-23.1
HT-ce (CTUh/km)	3.18E-09	40.5	-22.8
PM (kg $PM2.5_{eq}$/km)	1.89E-05	40.8	-23.0
IR-hh ($kBqU^{235}{}_{eq}$/km)	4.78E-03	33.5	-18.9
POFP ($kgNMVOC_{eq}$)	8.04E-05	40.4	-22.7
AP ($molH^{+}{}_{eq}$/km)	2.31E-04	40.4	-22.8
EU_T ($molN_{eq}$/km)	2.61E-04	40.2	-22.6
EU_F (kgP_{eq}/km)	1.86E-05	38.2	-21.5
EU_M (kgN_{eq}/km)	4.62E-05	41.0	-23.1
E_{Fw} (CTUe/km)	1.40E+00	41.0	-23.1

The results of the sensitivity analysis of EoL treatment are illustrated in Table 56. Although the material recoverable rates are reduced, recycling results in environmental credits in the same impact categories of the base case (Table 34). However, the environmental credits are significantly reduced (Figure 73) compared to the reference case (Figure 45). This proves the importance of ensuring high recovery levels for the various material fractions, for example through appropriate design of batteries' EoL, and proper dismantling and sorting of the waste battery components for recycling.

Table 56. Sensitivity analysis results – recycling rates in EoL treatments.

Impact category	Total (without credits)	Recycling credits
CED (MJ)	6.32E+04	-3.90E+03
ADP ($kgSb_{eq}$)	7.73E-02	-8.94E-03
GWP ($kgCO_{2eq}$)	3.63E+03	-2.43E+02
ODP ($kgCFC\text{-}11_{eq}$)	3.23E-04	-1.68E-05
HT-nce (CTUh)	2.49E-03	-3.67E-04
HT-ce (CTUh)	4.35E-04	-1.22E-04
PM (kg $PM2.5_{eq}$)	2.59E+00	-2.89E-01
IR-hh ($kBqU^{235}{}_{eq}$)	6.54E+02	-2.92E+01
POFP (kgNMVOCeq)	1.10E+01	-9.52E-01
AP ($molH^{+}{}_{eq}$)	3.16E+01	-3.30E+00
EU_T ($molN_{eq}$)	3.57E+01	-3.14E+00
EU_F (kgP_{eq})	2.54E+00	-2.71E-01
EU_M (kgN_{eq})	6.32E+00	-1.31E+00
E_{Fw} (CTUe)	1.91E+05	-1.08E+04

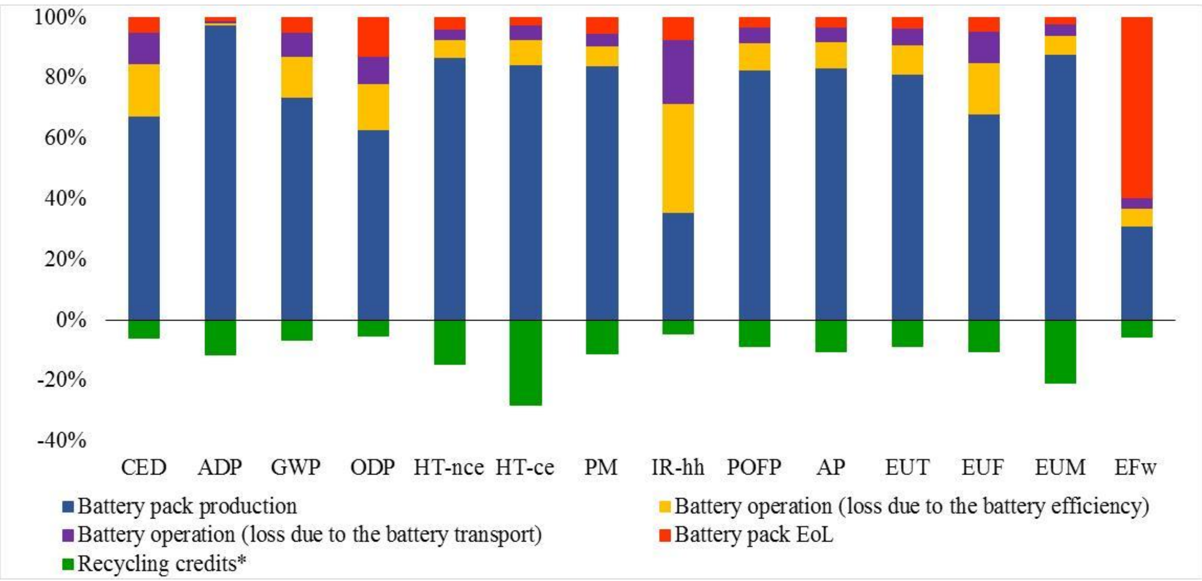

*Expressed as a percentage of the "Total" burden, including "Battery pack production", "Battery operation" and "Battery pack EoL"

Figure 73. Sensitivity analysis results – recycling rates in EoL treatments - Life cycle environmental impacts contribution processes

The sensitivity analysis confirms that adopting a more renewable electricity mix can significantly improve the impacts relates to the battery use phase. Moreover, it confirms that battery efficiency, more than battery weight, is a key factor in reducing the impacts of the battery use phase. Finally, a greater driving range significantly improves the environmental sustainability of electric mobility.

5.4 LCA of the PV + BESS + electrical grid system – modelling and assumptions

This section describes the LCA of the energy system (PV + BESS + electrical grid) providing the electricity to the building.

The goal of the LCA is to estimate, for each configuration examined, the potential life cycle energy and environmental impacts connected to the PV – BESS – electrical grid system and to assess the contribution of each system component to the whole life cycle impacts.

The LCA is performed following an attributional approach according to the international standards of series ISO 14040 [113,114].

The FU, selected as reference for the LCA, is the electricity required by the building in a time scale of 12 years. As previously explained (Section 5.1), this time scale is selected considering a maximum service life of 20 years for the battery (first and second life), a service life in the EV of about 8 years and a potential maximum residual lifetime[7] of about 12 years for a less demanding stationary application [104,194].

The reference flow includes all components that provide the function described by the FU:

1. the PV – system installed in the building (described in Chapter 3);
2. the BESS (described in Section 3);
3. the electrical grid.

The energy and environmental impacts associated to each component of the energy system are assessed following a "from cradle to consumer" approach.

The environmental impact categories and impact assessment methods are illustrated in Section 5.3.1.

For each energy system component, the most relevant modelling assumptions and data needed are included in the following. The eco – profiles of materials and energy sources used to produce the battery components were based on Ecoinvent 3 database [169].

PV system

This component accounts for the energy and environmental impacts related to the electricity produced by the PV power plant and directly consumed in the building.

The life cycle energy and environmental impacts for this component are calculated as:

$$I_{PVsystem,i} = El_{PV \rightarrow Bl} \cdot i_{PV,i} \tag{5.1}$$

where:

$I_{PVsystem,i}$ = overall impact on impact category "i" associated to the electricity produced by the PV system and directly consumed in the building. This impact includes the PV manufacturing and EoL disposal [unit[8]].

$El_{PV \rightarrow Bl}$ = PV electricity generated on-site and directly consumed by the building [kWh].

$i_{PV,i}$ = specific impact on the impact category "i" of the electricity generated by the PV system, in each examined impact category. The impact related to the PV production and EoL disposal is quantified per kWh of electricity generated [unit/kWh].

[7] The residual lifetime depends on both batteries applications in first and second uses.
[8] Unit: unit of measure of each investigated impact category.

i = examined impact category.

Battery Energy Storage System

The BESS accounts for the energy and environmental impacts associated to the EV battery pack production, to the preparation of the battery pack for reuse (repurposing), to the electricity produced by the PV system and provided to the building through the BESS, to the electricity loss due to the battery efficiency and to the battery pack EoL treatment.

EV Lithium – ion production and recycling processes modelling

The impact related to the battery pack production and EoL are described in Section 5.4. As the EV traction battery provided two functions, one in the EV and another in the stationary energy storage system, a multi-functionality [195] problem occurs and the energy and environmental impacts of the battery manufacturing and EoL affect both the first and the second applications [89].

In order to quantify the impacts of the battery manufacturing and EoL treatment for each function, the allocation approach is applied. In detail, the impacts between the co-functions are allocated using a quality – based allocation factor, calculated considering the electricity delivered during the first life in the EV and the electricity delivered during the second life in the building.

The electricity needed to provide the first function (El_{EV}) is calculated as:

$$El_{EV} = D_{dr} \cdot El_{drm} \cdot CEl_{drm} \quad (5.2)$$

where:

D_{dr} = kilometres driven during the first life (km);

El_{drm} = kilometres driven in electric mode (%);

CEl_{drm} = electricity delivered by the EV traction battery per km driven in “electric mode” (kWh/km).

The El_{EV} is equal to 26,280 kWh.

The electricity delivered during the stationary second life application, $El_{BESS \rightarrow Bl}$, is calculated through the energy balance model described in Section 4.1.

The allocation factor for the second life application (α_{fII}) is calculated for each configuration as in Equation 5.3:

$$\alpha_{fII} = \frac{El_{BESS \to Bl}}{(El_{EV} + El_{BESS \to Bl})} \tag{5.3}$$

According to Richa et al. [104] and to Bobba et al. [89], for allocating impacts of EV battery manufacturing and EoL treatments, only those component that are considered for reuse (i.e. battery cells, BMS, cooling system and module casing) are accounted for. The impacts of the components that are recycled or landfilled after the first service life (i.e. battery casing) are not allocated to the second service life.

The life cycle energy and environmental impacts of the battery production and recycling and potential benefits related to material recycling (in terms of "avoided primary materials") attributable to the stationary second life application are calculated as in Equations 5.4, 5.5 and 5.6:

$$I_{BP,i^*} = \alpha_{fII} \cdot n_B \cdot \ i_{BP,i} \tag{5.4}$$

$$I_{BR,i^*} = \alpha_{fII} \cdot n_B \cdot \ i_{BR,i} \tag{5.5}$$

$$EC_{BR,i^*} = \alpha_{fII} \cdot n_B \cdot \ ec_{BR,i} \tag{5.6}$$

where:

$I_{BP,i}^*$ = overall impact on the impact category "i" of the battery manufacturing, allocated to the stationary second life application [unit];

$I_{BR,i}^*$ = overall impact on the impact category "i" of the battery recycling, allocated to the stationary second life application [unit];

$EC_{BR,i,j}^*$ = overall environmental credit on the impact category "i" related to the avoided primary materials [unit];

n_B = number of batteries employed in the examined configuration;

$i_{BP,i}$ = specific impact on the impact category "i" of the battery manufacturing process [unit/kWh] [118];

$i_{BR,i}$ = specific impact on the impact category "i" of the battery recycling process [unit/kWh] [118];

$ec_{BR,I}$ = specific environmental credit on the impact category "i" related to the avoided primary materials [unit/kWh] [118].

Concerning the recycling process, it is assumed that the recoverable products are re-used within the investigated system (closed loop recycling) then, both the impacts related to the recycling and the environmental credits are entirely attributed to it.

The allocation factor for partitioning the impacts to the second life application, calculated with the Equation 5.3, are illustrated in Table 57. For each configuration, the amount of electricity delivered to the building through the BESS is summarized in Table 23. While the electricity delivered by the reused batteries during their first life in the EV is calculated for each configuration with Equation 5.2.

In C1, where the BESS is replaced every three years, four different values of α_{fII} are obtained since although the BESS is substituted with an equivalent BESS, the electricity generation from PV decreases every years due to the PV efficiency degradation. Consequently, the electricity delivered from the BESS to feed the building load ($El_{BESS \rightarrow BL}$ in Equation 5.3) decreases from one year to the next one. The same consideration are valid for C2 and C3. However, in C3 another aspect has to be taken into account to allocate the impact of the battery production and EoL treatment between the first (in the EV) and the second application. In fact, in C3 the BESS has a lifetime equal to 10 years in the examined application, then the first battery group installed works for 10 years before to reach its EoL. Than the α_{fII} calculated for the 2° BESS in C3, besides the electricity delivered the first (El_{EV}) and the second application ($El_{BESS \rightarrow BL}$), considers that the second group of EV batteries installed at the eleventh year are used only for two years out of the BESS lifetime to cover the examined timeframe (12 years) as shown in the Equation 5.4:

$$\alpha_{fII} = \frac{El_{BESS \rightarrow Bl}}{(El_{EV} + El_{BESS \rightarrow Bl})} \cdot \frac{T_{empl\_Cx}}{Lt_{Cx}} \tag{5.4}$$

where:

T_{empl_Cx}: years of use of a BESS in a specific configuration [year];

Lt_{Cx}: effective lifetime of a BESS in a specific configuration [year];

x: examined configuration (x: 1, 2,…,10).

Table 57. Allocation factor for the configurations examined

Configuration	α_{fII}			
C1	**1° BESS (3 years)**	**2° BESS (3 years)**	**3° BESS (3 years)**	**4° BESS (3 years)**
	0.1805	0.1801	0.1798	0.1795
C2	**1° BESS (6 years)**		**2° BESS (6 years)**	
	0.3557		0.3544	
C3	**1° BESS (10 years)**		**2° BESS (2years)**	
	0.4630		0.1598	
C4 ÷ C10	**1° BESS (12 years)**			
C4	0.4960			
C5	0.4774			
C6	0.4513			
C7	0.4233			
C8	0.3964			
C9	0.3722			
C10	0.3508			

EV Lithium – ion repurposing process modelling

The impacts due to the repurposing (I_{BRep}) phase is modelled according literature studies [89,92,95,196].

The repurposing phase involves:

- battery pack disassembly up to modules as a deeper disassembly is not technically/economically feasible. It is hypothesized a manually disassembly of the battery pack then, no impacts are considered for the battery disassembling process;
- energy consumption for battery testing to evaluate the state of health of the battery pack [92] (electricity consumption for 1 cycle of charge/discharge);
- manufacture of new casing for the battery pack in order to guarantee safety conditions.

The impacts related to the manufacture and EoL of the new casing are fully allocated to the second life application.

The life cycle energy and environmental impacts related to the repurposing phase are calculated with the following Equation 5.7:

$$I_{BRep,i} = n_B \cdot i_{BRep,i} \quad (5.7)$$

where:

$I_{BRep,i}$ = overall impact on the impact category "i" of the battery repurposing phase [unit];

$I_{BRep,i}$ = specif impact on the impact category "i" of the battery repurposing phase (including both the impacts related to the production of the new component and the electricity consumed to test one battery pack) [unit] [89].

PV electricity provided to the building through the BESS

The electricity produced by the PV and provided to the building through the BESS and the related electricity loss due to battery efficiency are calculate as explained in Section 4.1. The associated impacts are calculated with the following Equations 5.8 and 5.9, respectively:

$$I_{El_{BESS\rightarrow Bl},i} = El_{BESS\rightarrow BL} \cdot i_{PV,i} \quad (5.8)$$

$$I_{El_{\eta loss},i} = El_{\eta loss} \cdot i_{PV,i} \quad (5.9)$$

Electrical grid

The electrical grid included the impact associated to the electricity imported from the national electrical grid. The imported electricity is calculated as explained in Section 4.1. The impacts for this component are calculated as in Equation 5.10:

$$I_{Elgrid,i} = El_{grid\rightarrow BL} \cdot i_{Elgrid,i} \quad (5.10)$$

where:

$I_{Elgrid,i}$ = overall impact on the impact category "i" associated to the electricity imported from the electrical grid [unit];

$El_{grid\rightarrow BL}$ = amount of electricity imported from the electrical grid [kWh];

$i_{Elgrid,i}$ = specific impact on the impact category "i" associated to the electricity imported from the national electrical grid [unit/kWh].

Finally, the potential benefits related to the PV electricity fed into the grid (in terms of "avoided electricity from the grid") are assessed as in Equation 5.11:

$$EC_{EL_{PV\rightarrow grid,i}} = -\left(El_{PV\rightarrow grid} \cdot i_{Elgrid,i}\right) \quad (5.11)$$

where:

$EC_{EL_{PV \rightarrow grid,i}}$ = overall environmental credit on the impact category “i” related to the avoided electricity taken from the electrical grid [unit];

$i_{Elgrid,i}$ = specific environmental impact on the impact category “i” of the electricity imported from the national electrical grid [169] [unit/kWh].

5.4.1 Life cycle impact assessment and interpretation - PV + BESS + electrical grid system

The life cycle impacts assessment (LCIA) results referred to the FU are illustrated in Table 58. The environmental credits for avoiding production of primary materials and avoided electricity from the electrical grid are separated from the life cycle impacts according to the UNI EN 15978: 2011 standard [197].

The installation of an increasing energy storage capacity causes an improvement of the PV-BESS-electrical grid system environmental performance in almost all the examined impact categories with the exception of the abiotic depletion potential, human toxicity – cancer and non cancer effect and freshwater ecotoxicity.

The impact categories can be grouped in three clusters depending on three different trends traceable with the increasing installed capacity in order to generalize the results and draw some more general conclusions. The first cluster, composed of the global warming potential, ozone depletion potential and ionizing radiation, shows a continuous decrease from C1 to C10. In detail, they decrease on average of 27% in C10 compared with C1. However, the marginal benefits obtainable within the scenarios become negligible (lower than 3%) past the threshold of 46.5 kWh of installed capacity (C5) (Figure 74). The percentage variation between the impacts in C6 and in C5 is -2.7% for the global warming potential, -2.4% for the ozone depletion potential and -3.5% for ionizing radiation-human health. The second cluster, composed by the abiotic depletion potential, human toxicity – cancer effect and non cancer effect and freshwater ecotoxicity, shows an increasing trend from configuration 1 to 10 (Figure 75). In C10 the impact on abiotic depletion potential increases by around 80%, in human toxicity non cancer effect by 31.6%, in human toxicity cancer effect by 15.6%, and finally in freshwater ecotoxicity by 14.8%.

Table 58. Life cycle environmental impacts – referred to the FU (electricity required by the building in a time scale of 12 years).

Impact category	C1		C2		C3		C4		C5	
	Life cycle impacts	**Environmental credits***	**Life cycle impacts**	**Environmental credits***	**Life cycle impacts**	**Environmental credits***	**Life cycle impacts**	**Environmental credits***	**Life cycle impacts**	**Environmental credits***
CED (MJ)	2.251E+06	-64.7%	2.218E+06	-56.4%	2.172E+06	-48.4%	2.146E+06	-41.1%	2.127E+06	-35.4%
ADP (kgSb$_{eq}$)	5.151E-01	-23.3%	6.178E-01	-18.3%	6.838E-01	-14.7%	7.498E-01	-12.2%	8.124E-01	-10.7%
GWP (kgCO$_{2eq}$)	1.028E+05	-81.4%	9.600E+04	-74.8%	8.865E+04	-68.2%	8.311E+04	-60.9%	7.902E+04	-54.7%
ODP (kgCFC-11$_{eq}$)	1.162E-02	-78.4%	1.093E-02	-71.5%	1.020E-02	-64.4%	9.645E-03	-57.0%	9.225E-03	-50.8%
HT-nce (CTUh)	2.657E-02	-50.3%	2.850E-02	-41.5%	2.943E-02	-34.6%	3.058E-02	-28.8%	3.180E-02	-24.8%
HT-ce (CTUh)	4.906E-03	-63.5%	5.024E-03	-55.7%	4.987E-03	-48.6%	5.041E-03	-42.4%	5.155E-03	-38.1%
PM (kg PM2.5$_{eq}$)	4.503E+01	-68.2%	4.466E+01	-59.5%	4.345E+01	-51.8%	4.286E+01	-44.4%	4.268E+01	-38.6%
IR-hh (kBqU$^{235}_{eq}$)	1.407E+04	-83.7%	1.297E+04	-77.8%	1.185E+04	-71.7%	1.099E+04	-64.8%	1.032E+04	-58.8%
POFP (kgNMVOC$_{eq}$)	2.277E+02	-75.1%	2.193E+02	-67.1%	2.080E+02	-59.7%	2.002E+02	-52.2%	1.953E+02	-46.0%
AP (molH$^{+}_{eq}$)	5.542E+02	-76.6%	5.339E+02	-68.7%	5.046E+02	-61.4%	4.847E+02	-54.0%	4.723E+02	-47.7%
EU$_{T}$ (molN$_{eq}$)	7.211E+02	-76.4%	6.917E+02	-68.6%	6.528E+02	-61.4%	6.260E+02	-53.8%	6.084E+02	-47.6%
EU$_{F}$ (kgP$_{eq}$)	3.511E+01	-67.0%	3.501E+01	-58.3%	3.422E+01	-50.6%	3.390E+01	-43.3%	3.387E+01	-37.7%
EU$_{M}$ (kgN$_{eq}$)	7.441E+01	-74.4%	7.365E+01	-66.3%	7.072E+01	-59.2%	6.913E+01	-52.1%	6.864E+01	-46.5%
E$_{Fw}$ (CTUe)	2.927E+06	-56.7%	3.028E+06	-47.3%	3.056E+06	-39.6%	3.109E+06	-32.7%	3.171E+06	-27.6%

Impact category	C6		C7		C8		C9		C10	
	Life cycle impacts	**Environmental credits***	**Life cycle impacts**	**Environmental credits***	**Life cycle impacts**	**Environmental credits***	**Life cycle impacts**	**Environmental credits***	**Life cycle impacts**	**Environmental credits***
CED (MJ)	2.121E+06	-32.0%	2.122E+06	-30.1%	2.125E+06	-29.0%	2.130E+06	-28.2%	2.134E+06	-27.5%
ADP (kgSb$_{eq}$)	8.555E-01	-10.0%	8.856E-01	-9.7%	9.077E-01	-9.6%	9.261E-01	-9.5%	9.420E-01	-9.5%
GWP (kgCO$_{2eq}$)	7.692E+04	-50.7%	7.600E+04	-48.3%	7.571E+04	-46.8%	7.559E+04	-45.7%	7.556E+04	-44.8%
ODP (kgCFC-11$_{eq}$)	9.004E-03	-46.8%	8.902E-03	-44.5%	8.863E-03	-43.1%	8.843E-03	-42.0%	8.831E-03	-41.1%
HT-nce (CTUh)	3.273E-02	-22.6%	3.345E-02	-21.5%	3.402E-02	-21.0%	3.452E-02	-20.6%	3.496E-02	-20.3%
HT-ce (CTUh)	5.269E-03	-35.8%	5.379E-03	-34.8%	5.483E-03	-34.3%	5.580E-03	-34.1%	5.673E-03	-34.0%
PM (kg PM2.5$_{eq}$)	4.281E+01	-35.1%	4.309E+01	-33.1%	4.343E+01	-32.0%	4.376E+01	-31.2%	4.407E+01	-30.5%
IR-hh (kBqU$^{235}_{eq}$)	9.963E+03	-54.9%	9.789E+03	-52.5%	9.712E+03	-51.1%	9.667E+03	-50.0%	9.637E+03	-49.0%
POFP (kgNMVOC$_{eq}$)	1.933E+02	-42.1%	1.931E+02	-39.8%	1.936E+02	-38.5%	1.944E+02	-37.4%	1.952E+02	-36.6%
AP (molH$^{+}_{eq}$)	4.677E+02	-43.8%	4.674E+02	-41.5%	4.692E+02	-40.1%	4.714E+02	-39.1%	4.736E+02	-38.3%
EU$_{T}$ (molN$_{eq}$)	6.011E+02	-43.7%	5.997E+02	-41.3%	6.012E+02	-39.9%	6.033E+02	-38.9%	6.056E+02	-38.1%
EU$_{F}$ (kgP$_{eq}$)	3.403E+01	-34.3%	3.429E+01	-32.5%	3.457E+01	-31.4%	3.484E+01	-30.6%	3.509E+01	-30.0%
EU$_{M}$ (kgN$_{eq}$)	6.887E+01	-43.2%	6.947E+01	-41.2%	7.021E+01	-40.1%	7.092E+01	-39.3%	7.159E+01	-38.7%
E$_{Fw}$ (CTUe)	3.223E+06	-24.7%	3.266E+06	-23.0%	3.302E+06	-22.1%	3.333E+06	-21.4%	3.361E+06	-20.9%

*Expressed as percentage of the "Life cycle impacts" including the impacts associated to the "PV system", "BESS" and "Electrical grid".

The third cluster of impact categories presents a mixed trend and includes global energy requirement, acidification potential, particulate matter, marine eutrophication, photochemical ozone formation, terrestrial eutrophication and freshwater eutrophication (Figure 76). The impacts on global energy requirement decreases until C6 (55.8 kWh of installed capacity); those on particulate matter and marine eutrophication until C5 (46.5 kWh of installed capacity); those on acidification potential, photochemical ozone formation and terrestrial eutrophication until C7 (65.1 kWh of installed capacity); those on freshwater eutrophication until C3 (27.9 kWh of installed capacity). After these values of capacity installed, the impacts increase.

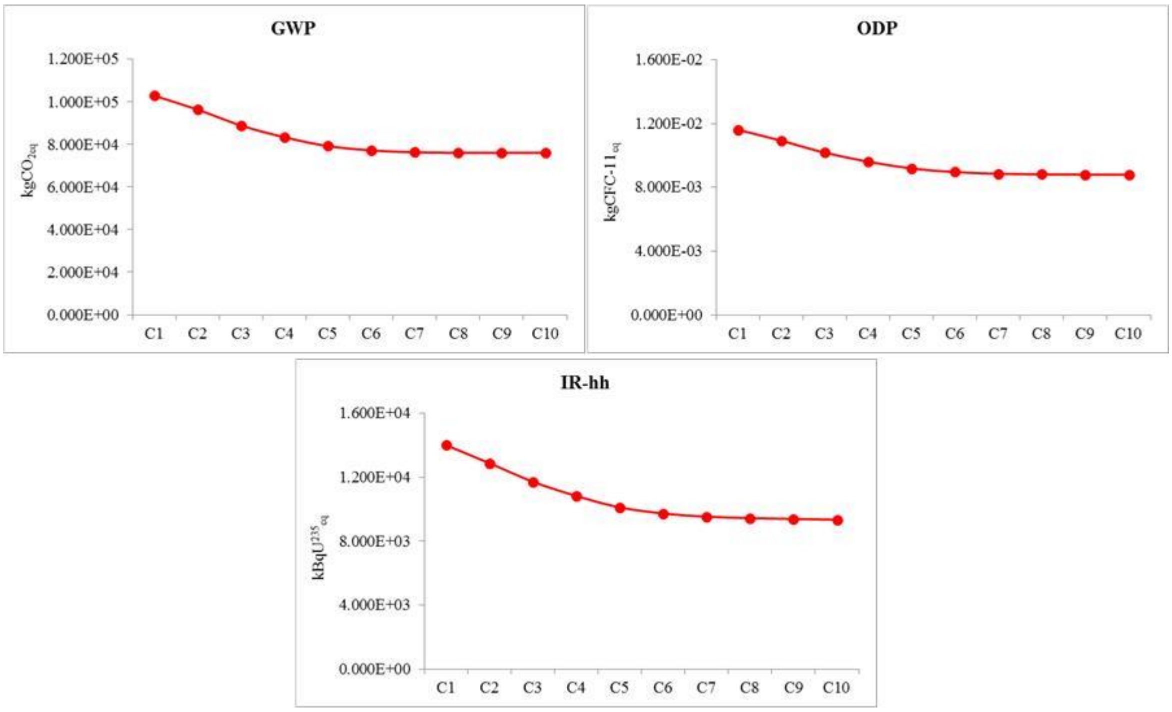

Figure 74. Trend of the impact categories belonging to cluster 1 with the increase of the BESS size.

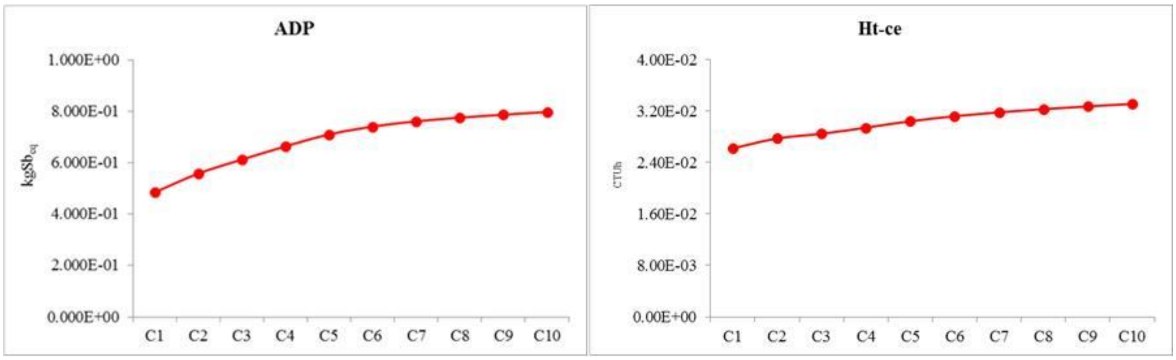

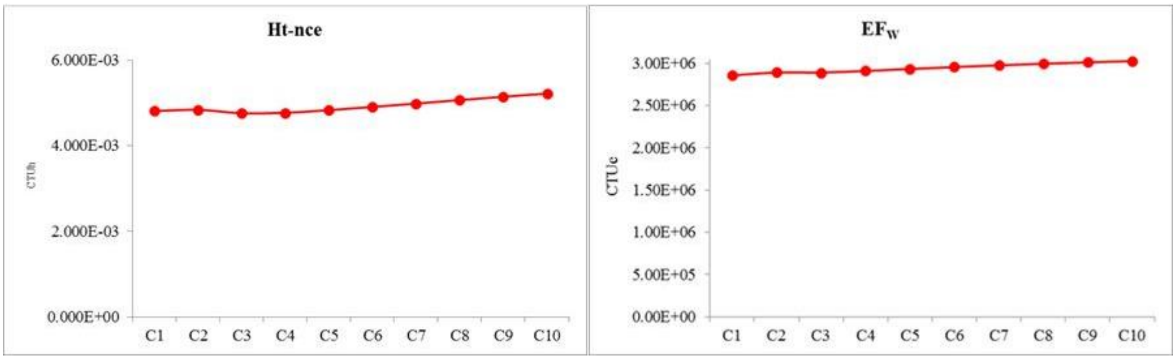

Figure 75. Trend of the impact categories belonging to cluster 2 with the increase of the BESS size.

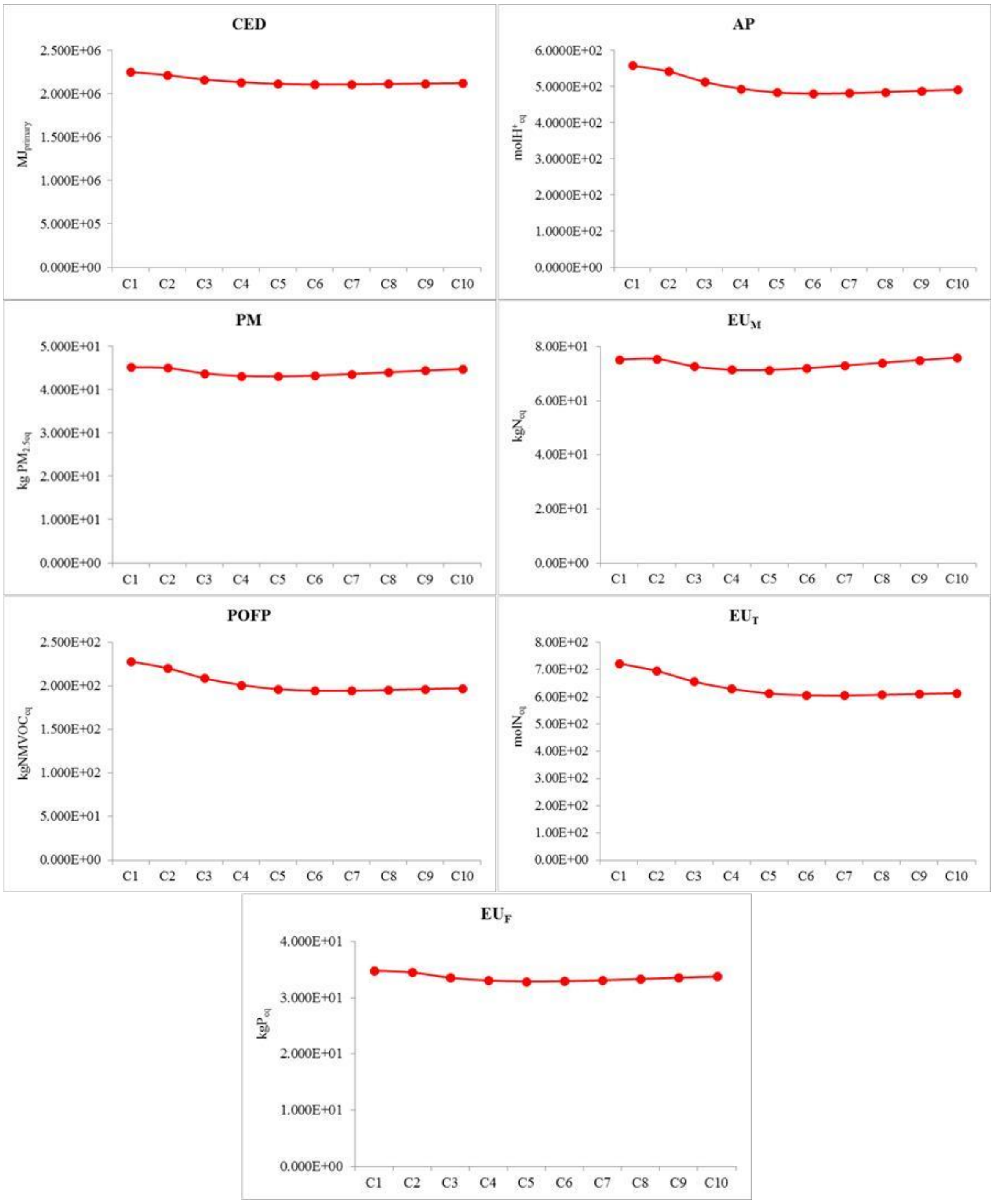

Figure 76. Trend of the impact categories belonging to cluster 3 with the increase of the BESS size.

In order to provide an interpretation of the LCIA results illustrated in Table 58 and in Figure 74, Figure 75 and Figure 76, a detailed contribution analysis of each component (PV + BESS + electrical grid) of the energy system examined to the total impacts in all the examined configurations is carried out. Moreover, also the breakdown of the impacts associated to each component of the BESS is illustrated. The impacts related to the PV system (electricity produced by the PV power plant and directly consumed in the building) are summarized in Table 59.

Table 59. Life cycle environmental impacts of the PV system.

Impact category	PV system impact in the examined timeframe
CED (MJ)	4.93E+05
ADP (kgSb$_{eq}$)	2.67E-01
GWP (kgCO$_{2eq}$)	7.21E+03
ODP (kgCFC-11$_{eq}$)	1.16E-03
HT-nce (CTUh)	8.42E-03
HT-ce (CTUh)	1.04E-03
PM (kg PM2.5$_{eq}$)	7.83E+00
IR-hh (kBqU$^{235}_{eq}$)	7.68E+02
POFP (kgNMVOC$_{eq}$)	2.69E+01
AP (molH$^{+}_{eq}$)	5.69E+01
EU$_T$ (molN$_{eq}$)	7.69E+01
EU$_F$ (kgP$_{eq}$)	6.50E+00
EU$_M$ (kgN$_{eq}$)	8.66E+00
E$_{Fw}$ (CTUe)	7.86E+05

The life cycle impacts associated to the BESS and to the electrical grid are illustrated in Table 60 and in Table 61.

The impacts associated to the PV are the same in all the examined configurations, as the electricity generated on-site and directly consumed remained unchanged from C1 to C10, since it is not affected by the BESS size (Table 23). Then, as highlighted in Figure 77, in which is illustrated the contribution of each energy system component to the examined impact categories in all configurations investigated, the contribution of the PV system remains unchanged. The contribution of the BESS increased in all the impact categories in all the examined configurations due to the increased impacts related to the production and recycling of a larger BESS and to the amount of PV electricity provided to the building through the BESS. Consequently, the contribution to the total impacts of the electrical grid decreases in all the examined impact categories and configurations due to the reduced import of electricity from the grid.

Table 60. Life cycle environmental impacts of the BESS system.

Impact category	C1	C2	C3	C4	C5
CED (MJ)	1.67E+05	3.15E+05	4.36E+05	5.47E+05	6.40E+05
ADP ($kgSb_{eq}$)	1.27E-01	2.44E-01	3.22E-01	3.99E-01	4.70E-01
GWP ($kgCO_{2eq}$)	4.24E+03	7.88E+03	1.02E+04	1.25E+04	1.48E+04
ODP ($kgCFC\text{-}11_{eq}$)	4.99E-04	9.42E-04	1.26E-03	1.56E-03	1.84E-03
HT-nce (CTUh)	4.07E-03	7.60E-03	1.00E-02	1.24E-02	1.46E-02
HT-ce (CTUh)	6.99E-04	1.18E-03	1.47E-03	1.80E-03	2.14E-03
PM (kg $PM2.5_{eq}$)	3.99E+00	7.40E+00	9.69E+00	1.20E+01	1.41E+01
IR-hh ($kBqU^{235}{}_{eq}$)	4.34E+02	8.06E+02	1.04E+03	1.28E+03	1.51E+03
POFP ($kgNMVOC_{eq}$)	1.49E+01	2.77E+01	3.59E+01	4.42E+01	5.22E+01
AP ($molH^{+}{}_{eq}$)	3.63E+01	6.85E+01	8.78E+01	1.08E+02	1.27E+02
EU_T ($molN_{eq}$)	4.49E+01	8.38E+01	1.08E+02	1.33E+02	1.57E+02
EU_F (kgP_{eq})	3.22E+00	6.01E+00	7.90E+00	9.76E+00	1.15E+01
EU_M (kgN_{eq})	6.64E+00	1.26E+01	1.59E+01	1.94E+01	2.30E+01
EF_w (CTUe)	3.37E+05	6.43E+05	8.62E+05	1.07E+06	1.26E+06
Impact category	**C6**	**C7**	**C8**	**C9**	**C10**
CED (MJ)	6.98E+05	7.34E+05	7.58E+05	7.77E+05	7.93E+05
ADP ($kgSb_{eq}$)	5.18E-01	5.51E-01	5.74E-01	5.94E-01	6.11E-01
GWP ($kgCO_{2eq}$)	1.63E+04	1.75E+04	1.83E+04	1.91E+04	1.97E+04
ODP ($kgCFC\text{-}11_{eq}$)	2.02E-03	2.14E-03	2.23E-03	2.30E-03	2.36E-03
HT-nce (CTUh)	1.61E-02	1.71E-02	1.79E-02	1.85E-02	1.90E-02
HT-ce (CTUh)	2.38E-03	2.56E-03	2.70E-03	2.83E-03	2.95E-03
PM (kg $PM2.5_{eq}$)	1.56E+01	1.66E+01	1.74E+01	1.80E+01	1.85E+01
IR-hh ($kBqU^{235}{}_{eq}$)	1.68E+03	1.79E+03	1.88E+03	1.95E+03	2.02E+03
POFP ($kgNMVOC_{eq}$)	5.77E+01	6.17E+01	6.46E+01	6.71E+01	6.92E+01
AP ($molH^{+}{}_{eq}$)	1.41E+02	1.52E+02	1.59E+02	1.66E+02	1.71E+02
EU_T ($molN_{eq}$)	1.74E+02	1.86E+02	1.95E+02	2.03E+02	2.10E+02
EU_F (kgP_{eq})	1.27E+01	1.35E+01	1.41E+01	1.46E+01	1.51E+01
EU_M (kgN_{eq})	2.57E+01	2.76E+01	2.91E+01	3.03E+01	3.14E+01
EF_w (CTUe)	1.38E+06	1.47E+06	1.52E+06	1.57E+06	1.61E+06

Table 61. Life cycle environmental impacts of the electrical grid.

Impact category	C1	C2	C3	C4	C5
CED (MJ)	1.59E+06	1.41E+06	1.24E+06	1.11E+06	9.95E+05
ADP ($kgSb_{eq}$)	1.21E-01	1.07E-01	9.42E-02	8.38E-02	7.54E-02
GWP ($kgCO_{2eq}$)	9.13E+04	8.09E+04	7.13E+04	6.34E+04	5.71E+04
ODP ($kgCFC\text{-}11_{eq}$)	9.96E-03	8.83E-03	7.78E-03	6.92E-03	6.23E-03
HT-nce (CTUh)	1.41E-02	1.25E-02	1.10E-02	9.79E-03	8.80E-03
HT-ce (CTUh)	3.17E-03	2.81E-03	2.47E-03	2.20E-03	1.98E-03
PM ($kg\ PM2.5_{eq}$)	3.32E+01	2.94E+01	2.59E+01	2.31E+01	2.08E+01
IR-hh ($kBqU^{235}{}_{eq}$)	1.29E+04	1.14E+04	1.00E+04	8.94E+03	8.04E+03
POFP ($kgNMVOC_{eq}$)	1.86E+02	1.65E+02	1.45E+02	1.29E+02	1.16E+02
AP ($molH^{+}{}_{eq}$)	4.61E+02	4.09E+02	3.60E+02	3.20E+02	2.88E+02
EU_T ($molN_{eq}$)	5.99E+02	5.31E+02	4.68E+02	4.16E+02	3.75E+02
EU_F (kgP_{eq})	2.54E+01	2.25E+01	1.98E+01	1.76E+01	1.59E+01
EU_M (kgN_{eq})	5.91E+01	5.24E+01	4.61E+01	4.11E+01	3.69E+01
EF_w (CTUe)	1.80E+06	1.60E+06	1.41E+06	1.25E+06	1.13E+06
Impact category	**C6**	**C7**	**C8**	**C9**	**C10**
CED (MJ)	9.30E+05	8.94E+05	8.74E+05	8.60E+05	8.48E+05
ADP ($kgSb_{eq}$)	7.05E-02	6.78E-02	6.63E-02	6.52E-02	6.43E-02
GWP ($kgCO_{2eq}$)	5.34E+04	5.13E+04	5.02E+04	4.93E+04	4.86E+04
ODP ($kgCFC\text{-}11_{eq}$)	5.82E-03	5.60E-03	5.47E-03	5.38E-03	5.31E-03
HT-nce (CTUh)	8.23E-03	7.92E-03	7.74E-03	7.61E-03	7.51E-03
HT-ce (CTUh)	1.85E-03	1.78E-03	1.74E-03	1.71E-03	1.69E-03
PM ($kg\ PM2.5_{eq}$)	1.94E+01	1.87E+01	1.82E+01	1.79E+01	1.77E+01
IR-hh ($kBqU^{235}{}_{eq}$)	7.52E+03	7.23E+03	7.07E+03	6.95E+03	6.85E+03
POFP ($kgNMVOC_{eq}$)	1.09E+02	1.04E+02	1.02E+02	1.00E+02	9.90E+01
AP ($molH^{+}{}_{eq}$)	2.69E+02	2.59E+02	2.53E+02	2.49E+02	2.46E+02
EU_T ($molN_{eq}$)	3.50E+02	3.37E+02	3.29E+02	3.24E+02	3.19E+02
EU_F (kgP_{eq})	1.48E+01	1.43E+01	1.39E+01	1.37E+01	1.35E+01
EU_M (kgN_{eq})	3.45E+01	3.32E+01	3.25E+01	3.19E+01	3.15E+01
EF_w (CTUe)	1.05E+06	1.01E+06	9.91E+05	9.74E+05	9.61E+05

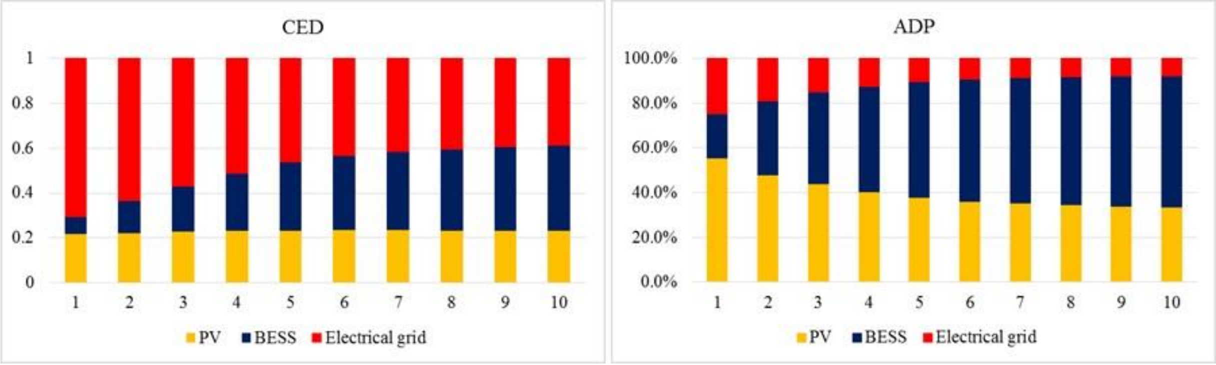


GWP
ODP
HT-ce
HT-nce
PM
IR-hh
POFP
AP
EU_T
EU_F
100.0%
80.0%
60.0%
40.0%
20.0%
0.0%
1 2 3 4 5 6 7 8 9 10
PV BESS Electrical grid

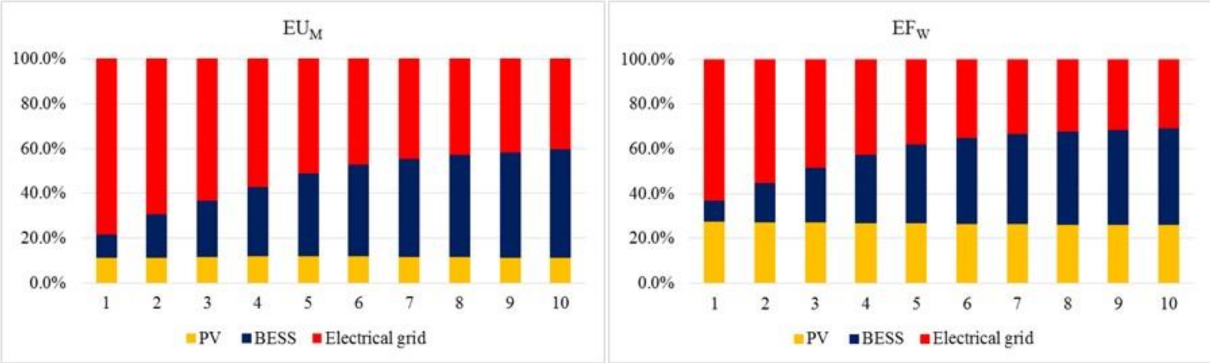

Figure 77. LCIA – PV – BESS – electrical grid process contribution analysis.

The detailed analysis of the impacts associated to each BESS component for the impacts category belonging to the first class are illustrated in Table 62,

and Table 64.

Concerning the cluster 1, the reduction of the impacts is mainly due to the decrease of the electricity imported from the electrical grid due to the installation of an increasing BESS size that allow to increase the self-consumption of the electricity from PV. In these impact categories, the electricity from the grid performs worse than the electricity from PV resulting in the improvement of the environmental performance.

Table 62. Life cycle impact assessment – process contribution analysis of BESS components on GWP.

Configuration	PV electricity provided through the BESS ($kgCO_{2eq}$)	Loss due to the BESS efficiency ($kgCO_{2eq}$)	BESS production ($kgCO_{2eq}$)	BESS repurposing ($kgCO_{2eq}$)	BESS recycling ($kgCO_{2eq}$)
C1	1.68E+03	2.08E+02	1.87E+03	3.40E+02	1.44E+02
C2	3.15E+03	4.42E+02	3.67E+03	3.40E+02	2.72E+02
C3	4.52E+03	7.01E+02	4.31E+03	3.06E+02	3.15E+02
C4	5.64E+03	9.91E+02	5.13E+03	3.40E+02	3.74E+02
C5	6.54E+03	1.16E+03	6.18E+03	4.25E+02	4.51E+02
C6	7.07E+03	1.25E+03	7.00E+03	5.10E+02	5.12E+02
C7	7.36E+03	1.31E+03	7.67E+03	5.94E+02	5.62E+02
C8	7.53E+03	1.33E+03	8.20E+03	6.79E+02	6.03E+02
C9	7.64E+03	1.36E+03	8.67E+03	7.64E+02	6.39E+02
C10	7.74E+03	1.37E+03	9.07E+03	8.49E+02	6.71E+02

Table 63. Life cycle impact assessment – process contribution analysis of BESS components on ODP.

Configuration	PV electricity provided through the BESS (kgCFC-11$_{eq}$)	Loss due to the BESS efficiency (kgCFC-11$_{eq}$)	BESS production (kgCFC-11$_{eq}$)	BESS repurposing (kgCFC-11$_{eq}$)	BESS recycling (kgCFC-11$_{eq}$)
C1	2.70E-04	3.34E-05	1.43E-04	2.19E-05	3.08E-05
C2	5.08E-04	7.12E-05	2.81E-04	2.19E-05	5.95E-05
C3	7.28E-04	1.13E-04	3.30E-04	1.97E-05	6.94E-05
C4	9.08E-04	1.59E-04	3.93E-04	2.19E-05	8.25E-05
C5	1.05E-03	1.86E-04	4.73E-04	2.74E-05	9.94E-05
C6	1.14E-03	2.02E-04	5.37E-04	3.29E-05	1.13E-04
C7	1.19E-03	2.10E-04	5.87E-04	3.84E-05	1.24E-04
C8	1.21E-03	2.15E-04	6.28E-04	4.38E-05	1.32E-04
C9	1.23E-03	2.18E-04	6.64E-04	4.93E-05	1.40E-04
C10	1.25E-03	2.21E-04	6.95E-04	5.48E-05	1.47E-04

Table 64. Life cycle impact assessment – process contribution analysis of BESS components on IR-hh.

Configuration	PV electricity provided through the BESS (kBqU$^{235}_{eq}$)	Loss due to the BESS efficiency (kBqU$^{235}_{eq}$)	BESS production (kBqU$^{235}_{eq}$)	BESS repurposing (kBqU$^{235}_{eq}$)	BESS recycling (kBqU$^{235}_{eq}$)
C1	1.79E+02	2.21E+01	1.62E+02	3.19E+01	3.89E+01
C2	3.36E+02	4.71E+01	3.20E+02	3.19E+01	7.13E+01
C3	4.82E+02	7.47E+01	3.75E+02	2.87E+01	8.21E+01
C4	6.01E+02	1.06E+02	4.46E+02	3.19E+01	9.74E+01
C5	6.97E+02	1.23E+02	5.37E+02	3.99E+01	1.17E+02
C6	7.53E+02	1.33E+02	6.09E+02	4.79E+01	1.34E+02
C7	7.85E+02	1.39E+02	6.67E+02	5.58E+01	1.47E+02
C8	8.02E+02	1.42E+02	7.13E+02	6.38E+01	1.58E+02
C9	8.15E+02	1.45E+02	7.54E+02	7.18E+01	1.68E+02
C10	8.25E+02	1.46E+02	7.89E+02	7.98E+01	1.76E+02

Concerning the battery production phase, the associated impacts accounts for a contribution ranging from 1.8% (in C1) to 12.2% (in C10) to the life cycle global warming potential, from 1.2% (in C1) to 8% (in C10) to the life cycle ozone depletion potential, and from 1.2% (in C1) to 8.3% (in C10) to the life cycle ionizing radiation – human health. The increase in impacts, due to battery production caused by a growing installed capacity, has not enough relative weight to offset the obtained environmental improvements. In cluster 1, the impact due to the electricity imported from the grid is responsible for the highest contribution in all the examined configurations. It accounts for a share ranging from around 85% (in C1) to 60% (in C10) in global warming potential and ozone depletion potential and from 91.4% (in C1) to 70.8% (in C10) in ionizing radiation – human health. The contribution analysis highlights that battery repurposing, recycling and loss due to the efficiency account for a contribution lower than 3% in all the impact categories examined.

Figure 78 shows, on the left the percentage variation of the impacts due to the BESS and to the electrical grid between each configuration and the previous one, and on the right the absolute difference one. The benefits associated to the reduced electricity import from the grid surpass significantly the increase of the impacts associated to the BESS (including EV battery production, repurposing and recycling and the impacts associated to the electricity loss due to the battery efficiency). However, the reduction of the impacts with the increasing installed capacity becomes negligible after the threshold of 46.5 kWh of installed capacity (C5) is surpassed.

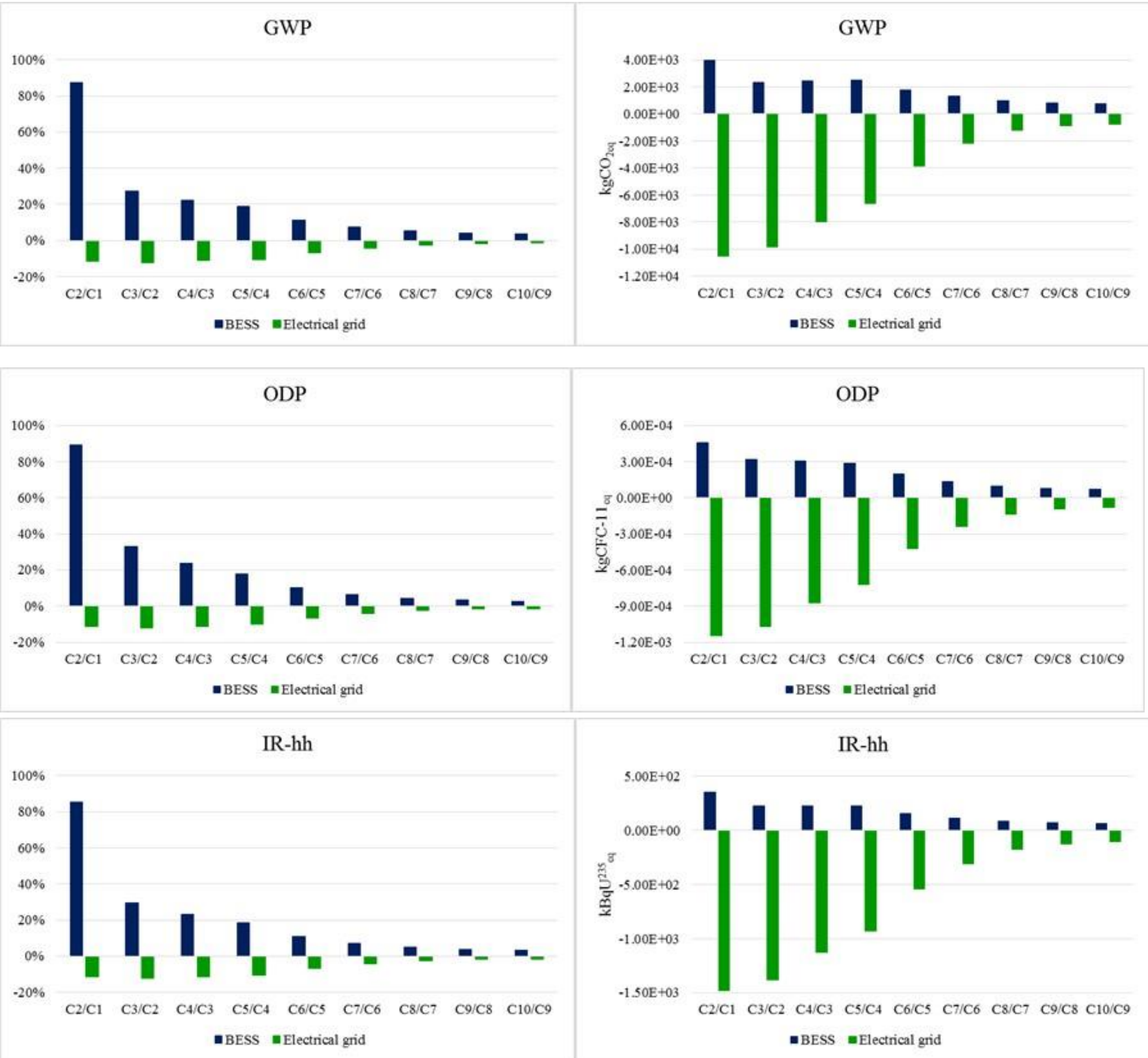

Figure 78. Cluster 1 - Left: Percentage variations of the impacts due to the BESS and to the electrical grid in each configuration compared with the pervious one ((I_{Cn}-I_{Cn-1})/I_{Cn-1}); Right: Absolute differences of the impacts associated with the BESS and the electrical grid between each configuration and the previous one (I_{Cn}-$I_{(Cn-1)}$).

In the environmental categories belonging to the cluster 2, the increase of the impacts is mainly due to the increased share of the electricity generated from the PV plant in building load supply and to the production of a larger BESS. In abiotic depletion potential, the electricity from PV (directly consumed and provided through the BESS) is responsible for the highest contribution (higher than 60%) in all the examined configurations. In freshwater ecotoxicity, the contribution of the electricity from PV ranges from 33% in C1 to 49% in C10; in human toxicity – non cancer effect from 40% (in C1) to 50% (in C10), and in human toxicity – cancer effect from 26% (in C1) to 38% (in C10). The contribution of the battery production with the increasing BESS size is significant in all the impact categories belonging to cluster 2 with the exception of freshwater ecotoxicity. In abiotic depletion potential, battery production contribution ranges from around 10.5% (in C1) to 28% in C10, in human toxicity – non cancer effect from around 6% (in C1) to around 21% (in C10), and human toxicity – cancer effect from around 6% (in C1) to around 15% (in C10). In freshwater ecotoxity, battery production represents a percentage lower than 7% in all the configurations examined. The repurposing process accounts for a percentage lower than 4%, with the exception of human toxicity – cancer effect in which is responsible for a contribution ranging from 4% (in C1) to 9% (in C10). The impact associated to the electricity losses due to the BESS efficiency accounts always for less than 5%.

Table 65. Life cycle impact assessment – process contribution analysis of BESS components on ADP.

Configuration	PV electricity provided through the BESS ($kgSb_{eq}$)	Loss due to the BESS efficiency ($kgSb_{eq}$)	BESS production ($kgSb_{eq}$)	BESS repurposing ($kgSb_{eq}$)	BESS recycling ($kgSb_{eq}$)
C1	6.22E-02	7.70E-03	5.40E-02	2.77E-03	7.04E-04
C2	1.17E-01	1.64E-02	1.06E-01	2.77E-03	1.36E-03
C3	1.68E-01	2.60E-02	1.25E-01	2.49E-03	1.59E-03
C4	2.09E-01	3.67E-02	1.48E-01	2.77E-03	1.89E-03
C5	2.43E-01	4.29E-02	1.79E-01	3.46E-03	2.28E-03
C6	2.62E-01	4.64E-02	2.03E-01	4.15E-03	2.59E-03
C7	2.73E-01	4.84E-02	2.22E-01	4.84E-03	2.83E-03
C8	2.79E-01	4.95E-02	2.37E-01	5.53E-03	3.04E-03
C9	2.83E-01	5.03E-02	2.51E-01	6.22E-03	3.21E-03
C10	2.87E-01	5.09E-02	2.62E-01	6.92E-03	3.37E-03

Table 66. Life cycle impact assessment – process contribution analysis of BESS components on HT – nce.

Configuration	PV electricity provided through the BESS (CTUh)	Loss due to the BESS efficiency (CTUh)	BESS production (CTUh)	BESS repurposing (CTUh)	BESS recycling (CTUh)
C1	1.96E-03	2.43E-04	1.51E-03	2.78E-04	7.74E-05
C2	3.69E-03	5.17E-04	2.97E-03	2.78E-04	1.47E-04
C3	5.28E-03	8.19E-04	3.48E-03	2.50E-04	1.71E-04
C4	6.59E-03	1.16E-03	4.15E-03	2.78E-04	2.04E-04
C5	7.65E-03	1.35E-03	4.99E-03	3.47E-04	2.45E-04
C6	8.26E-03	1.46E-03	5.66E-03	4.16E-04	2.79E-04
C7	8.60E-03	1.53E-03	6.19E-03	4.86E-04	3.06E-04
C8	8.79E-03	1.56E-03	6.63E-03	5.55E-04	3.28E-04
C9	8.93E-03	1.58E-03	7.00E-03	6.25E-04	3.47E-04
C10	9.04E-03	1.60E-03	7.33E-03	6.94E-04	3.64E-04

Table 67. Life cycle impact assessment – process contribution analysis of BESS components on HT – ce.

Configuration	PV electricity provided through the BESS (CTUh)	Loss due to the BESS efficiency (CTUh)	BESS production (CTUh)	BESS repurposing (CTUh)	BESS recycling (CTUh)
C1	2.42E-04	2.99E-05	2.31E-04	1.87E-04	9.13E-06
C2	4.55E-04	6.37E-05	4.55E-04	1.87E-04	1.71E-05
C3	6.52E-04	1.01E-04	5.34E-04	1.68E-04	1.98E-05
C4	8.13E-04	1.43E-04	6.35E-04	1.87E-04	2.35E-05
C5	9.43E-04	1.67E-04	7.64E-04	2.34E-04	2.83E-05
C6	1.02E-03	1.80E-04	8.67E-04	2.80E-04	3.22E-05
C7	1.06E-03	1.88E-04	9.49E-04	3.27E-04	3.54E-05
C8	1.08E-03	1.92E-04	1.02E-03	3.74E-04	3.80E-05
C9	1.10E-03	1.95E-04	1.07E-03	4.20E-04	4.02E-05
C10	1.12E-03	1.98E-04	1.12E-03	4.67E-04	4.23E-05

Table 68. Life cycle impact assessment – process contribution analysis of BESS components on E_{FW}.

Configuration	PV electricity provided through the BESS (CTUe)	Loss due to the BESS efficiency (CTUe)	BESS production (CTUe)	BESS repurposing (CTUe)	BESS recycling (CTUe)
C1	1.83E+05	2.26E+04	4.11E+04	8.27E+03	8.20E+04
C2	3.44E+05	4.82E+04	8.09E+04	8.27E+03	1.62E+05
C3	4.93E+05	7.64E+04	9.50E+04	7.44E+03	1.90E+05
C4	6.15E+05	1.08E+05	1.13E+05	8.27E+03	2.26E+05
C5	7.14E+05	1.26E+05	1.36E+05	1.03E+04	2.72E+05
C6	7.71E+05	1.37E+05	1.54E+05	1.24E+04	3.08E+05
C7	8.03E+05	1.42E+05	1.69E+05	1.45E+04	3.37E+05
C8	8.21E+05	1.46E+05	1.81E+05	1.65E+04	3.61E+05
C9	8.34E+05	1.48E+05	1.91E+05	1.86E+04	3.81E+05
C10	8.44E+05	1.50E+05	2.00E+05	2.07E+04	3.99E+05

Figure 79 shows on the left the percentage variation of the impacts due to the BESS and to the electrical grid between each configuration and the previous one, and on the right the absolute difference one, for the impact categories belonging to cluster 2.

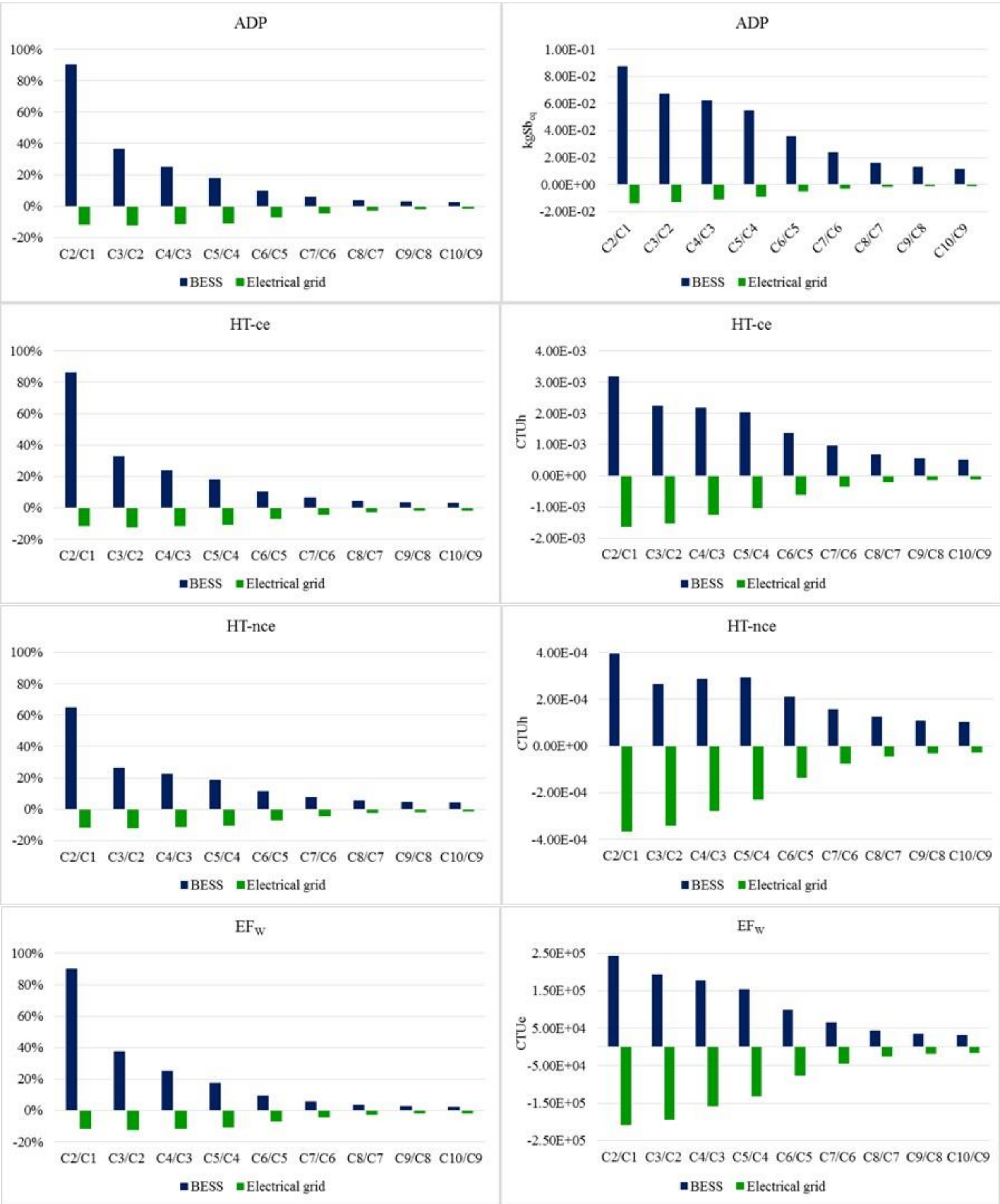

Figure 79. Cluster 2 - Left: Percentage variations of the impacts due to the BESS and to the electrical grid in each configuration (I_C) compared with the pervious one ((I_{Cn}-I_{Cn-1})/I_{Cn-1}); Right: Absolute differences of the impacts associated with the BESS and the electrical grid between each configuration and the previous one (I_{Cn}-I_{Cn-1}).

Concerning the third cluster, the contribution analysis highlights that in general, the reduction of the electricity imported from the grid, due to the increasing size of the energy storage capacity, is mainly responsible for the impacts reduction. However, in general the environmental benefits are partially offset by the higher impacts associated to the production of a larger energy storage system and by the increase of the consumption of the PV electricity.

Table 69. Life cycle impact assessment – process contribution analysis of BESS components on CED.

Configuration	PV electricity provided through the BESS ($MJ_{primary}$)	Loss due to the BESS efficiency ($MJ_{primary}$)	BESS production ($MJ_{primary}$)	BESS repurposing ($MJ_{primary}$)	BESS recycling ($MJ_{primary}$)
C1	1.15E+05	1.42E+04	2.98E+04	5.60E+03	2.50E+03
C2	2.16E+05	3.02E+04	5.86E+04	5.60E+03	4.66E+03
C3	3.09E+05	4.79E+04	6.87E+04	5.04E+03	5.39E+03
C4	3.86E+05	6.77E+04	8.18E+04	5.60E+03	6.40E+03
C5	4.48E+05	7.91E+04	9.84E+04	7.01E+03	7.71E+03
C6	4.84E+05	8.56E+04	1.12E+05	8.41E+03	8.77E+03
C7	5.04E+05	8.93E+04	1.22E+05	9.81E+03	9.63E+03
C8	5.15E+05	9.13E+04	1.31E+05	1.12E+04	1.03E+04
C9	5.23E+05	9.27E+04	1.38E+05	1.26E+04	1.10E+04
C10	5.29E+05	9.39E+04	1.45E+05	1.40E+04	1.15E+04

The impact categories of the cluster 3 present a mixed with the increasing BESS size. In fact, after a certain value of installed energy capacity, specific for each impact category, the environmental benefits related to the reduction of the electricity consumption from the grid are counterbalance by the increased impact due to the installation a larger BESS.

Table 70. Life cycle impact assessment – process contribution analysis of BESS components on PM.

Configuration	PV electricity provided through the BESS ($kgPM2.5_{eq}$)	Loss due to the BESS efficiency ($kgPM2.5_{eq}$)	BESS production ($kgPM2.5_{eq}$)	BESS repurposing ($kgPM2.5_{eq}$)	BESS recycling ($kgPM2.5_{eq}$)
C1	1.82E+00	2.26E-01	1.51E+00	3.25E-01	1.02E-01
C2	3.43E+00	4.81E-01	2.97E+00	3.25E-01	1.95E-01
C3	4.92E+00	7.62E-01	3.49E+00	2.92E-01	2.27E-01
C4	6.13E+00	1.08E+00	4.15E+00	3.25E-01	2.70E-01
C5	7.11E+00	1.26E+00	5.00E+00	4.06E-01	3.25E-01
C6	7.68E+00	1.36E+00	5.67E+00	4.87E-01	3.69E-01
C7	8.00E+00	1.42E+00	6.20E+00	5.69E-01	4.05E-01
C8	8.18E+00	1.45E+00	6.64E+00	6.50E-01	4.34E-01
C9	8.31E+00	1.47E+00	7.01E+00	7.31E-01	4.59E-01
C10	8.41E+00	1.49E+00	7.34E+00	8.12E-01	4.82E-01

Table 71. Life cycle impact assessment – process contribution analysis of BESS components on POFP.

Configuration	PV electricity provided through the BESS ($kgNMVOC_{eq}$)	Loss due to the BESS efficiency ($kgNMVOC_{eq}$)	BESS production ($kgNMVOC_{eq}$)	BESS repurposing ($kgNMVOC_{eq}$)	BESS recycling ($kgNMVOC_{eq}$)
C1	6.27E+00	7.76E-01	6.37E+00	1.15E+00	2.92E-01
C2	1.18E+01	1.65E+00	1.25E+01	1.15E+00	5.43E-01
C3	1.69E+01	2.62E+00	1.47E+01	1.04E+00	6.28E-01
C4	2.11E+01	3.70E+00	1.75E+01	1.15E+00	7.46E-01
C5	2.45E+01	4.32E+00	2.11E+01	1.44E+00	8.99E-01
C6	2.64E+01	4.68E+00	2.39E+01	1.73E+00	1.02E+00
C7	2.75E+01	4.88E+00	2.61E+01	2.02E+00	1.12E+00
C8	2.81E+01	4.99E+00	2.80E+01	2.30E+00	1.21E+00
C9	2.86E+01	5.07E+00	2.96E+01	2.59E+00	1.28E+00
C10	2.89E+01	5.13E+00	3.09E+01	2.88E+00	1.34E+00

In cumulative energy demand, while the contribution of the electricity from the grid decreases from 70% (in C1) to 40% (in C10), those related to the battery production and electricity from PV increase, respectively, from 1.3% and 27% (in C1) to 7% and 50% (in C10). In particulate matter, photochemical ozone formation, acidification potential and in terrestrial and freshwater eutrophication, the battery production contribution ranges from around 3% (in C1) to around 20% (in C10) of the total life cycle impacts, while in marine eutrophication from 5% (in C1) to around 27% (in C10).

The electricity loss due to the battery efficiency, the repurposing and the recycling process account for less than 5% in the impacts categories belonging to the cluster 3.

Table 72. Life cycle impact assessment – process contribution analysis of BESS components on AP.

Configuration	PV electricity provided through the BESS ($molH^{+}_{eq}$)	Loss due to the BESS efficiency ($molH^{+}_{eq}$)	BESS production ($molH^{+}_{eq}$)	BESS repurposing ($molH^{+}_{eq}$)	BESS recycling ($molH^{+}_{eq}$)
C1	1.32E+01	1.64E+00	1.87E+01	1.96E+00	7.75E-01
C2	2.49E+01	3.49E+00	3.67E+01	1.96E+00	1.46E+00
C3	3.57E+01	5.53E+00	4.31E+01	1.76E+00	1.69E+00
C4	4.45E+01	7.82E+00	5.13E+01	1.96E+00	2.00E+00
C5	5.16E+01	9.12E+00	6.18E+01	2.45E+00	2.41E+00
C6	5.58E+01	9.88E+00	7.01E+01	2.94E+00	2.75E+00
C7	5.81E+01	1.03E+01	7.67E+01	3.42E+00	3.01E+00
C8	5.94E+01	1.05E+01	8.20E+01	3.91E+00	3.23E+00
C9	6.03E+01	1.07E+01	8.67E+01	4.40E+00	3.43E+00
C10	6.11E+01	1.08E+01	9.08E+01	4.89E+00	3.60E+00

Table 73. Life cycle impact assessment – process contribution analysis of BESS components on EU_T.

Configuration	PV electricity provided through the BESS ($molN_{eq}$)	Loss due to the BESS efficiency ($molN_{eq}$)	BESS production ($molN_{eq}$)	BESS repurposing ($molN_{eq}$)	BESS recycling ($molN_{eq}$)
C1	1.79E+01	2.21E+00	2.04E+01	3.40E+00	1.02E+00
C2	3.36E+01	4.72E+00	4.01E+01	3.40E+00	1.90E+00
C3	4.82E+01	7.47E+00	4.71E+01	3.06E+00	2.20E+00
C4	6.01E+01	1.06E+01	5.60E+01	3.40E+00	2.61E+00
C5	6.98E+01	1.23E+01	6.74E+01	4.25E+00	3.15E+00
C6	7.54E+01	1.34E+01	7.65E+01	5.10E+00	3.58E+00
C7	7.85E+01	1.39E+01	8.37E+01	5.95E+00	3.93E+00
C8	8.03E+01	1.42E+01	8.96E+01	6.81E+00	4.22E+00
C9	8.15E+01	1.45E+01	9.46E+01	7.66E+00	4.47E+00
C10	8.26E+01	1.46E+01	9.91E+01	8.51E+00	4.70E+00

Table 74. Life cycle impact assessment – process contribution analysis of BESS components on EU_F.

Configuration	PV electricity provided through the BESS (kgP_{eq})	Loss due to the BESS efficiency (kgP_{eq})	BESS production (kgP_{eq})	BESS repurposing (kgP_{eq})	BESS recycling (kgP_{eq})
C1	1.51E+00	1.87E-01	1.21E+00	2.11E-01	9.59E-02
C2	2.84E+00	3.99E-01	2.38E+00	2.11E-01	1.79E-01
C3	4.08E+00	6.32E-01	2.79E+00	1.90E-01	2.07E-01
C4	5.08E+00	8.93E-01	3.32E+00	2.11E-01	2.45E-01
C5	5.90E+00	1.04E+00	4.00E+00	2.64E-01	2.95E-01
C6	6.37E+00	1.13E+00	4.54E+00	3.17E-01	3.36E-01
C7	6.64E+00	1.18E+00	4.97E+00	3.70E-01	3.69E-01
C8	6.79E+00	1.20E+00	5.31E+00	4.22E-01	3.96E-01
C9	6.89E+00	1.22E+00	5.61E+00	4.75E-01	4.20E-01
C10	6.98E+00	1.24E+00	5.88E+00	5.28E-01	4.41E-01

Table 75. Life cycle impact assessment – process contribution analysis of BESS components on EU_M.

Configuration	PV electricity provided through the BESS (kgN_{eq})	Loss due to the BESS efficiency (kgN_{eq})	BESS production (kgN_{eq})	BESS repurposing (kgN_{eq})	BESS recycling (kgN_{eq})
C1	2.01E+00	2.49E-01	3.95E+00	3.17E-01	1.14E-01
C2	3.79E+00	5.31E-01	7.77E+00	3.17E-01	2.10E-01
C3	5.43E+00	8.42E-01	9.12E+00	2.85E-01	2.43E-01
C4	6.77E+00	1.19E+00	1.08E+01	3.17E-01	2.88E-01
C5	7.86E+00	1.39E+00	1.31E+01	3.96E-01	3.47E-01
C6	8.49E+00	1.50E+00	1.48E+01	4.75E-01	3.95E-01
C7	8.84E+00	1.57E+00	1.62E+01	5.55E-01	4.34E-01
C8	9.04E+00	1.60E+00	1.73E+01	6.34E-01	4.66E-01
C9	9.18E+00	1.63E+00	1.83E+01	7.13E-01	4.94E-01
C10	9.30E+00	1.65E+00	1.92E+01	7.92E-01	5.20E-01

Figure 80 on the left the percentage variation of the impacts due to the BESS and to the electrical grid between each configuration and the previous one, and on the right the absolute difference one, for the impact categories belonging to cluster 3.

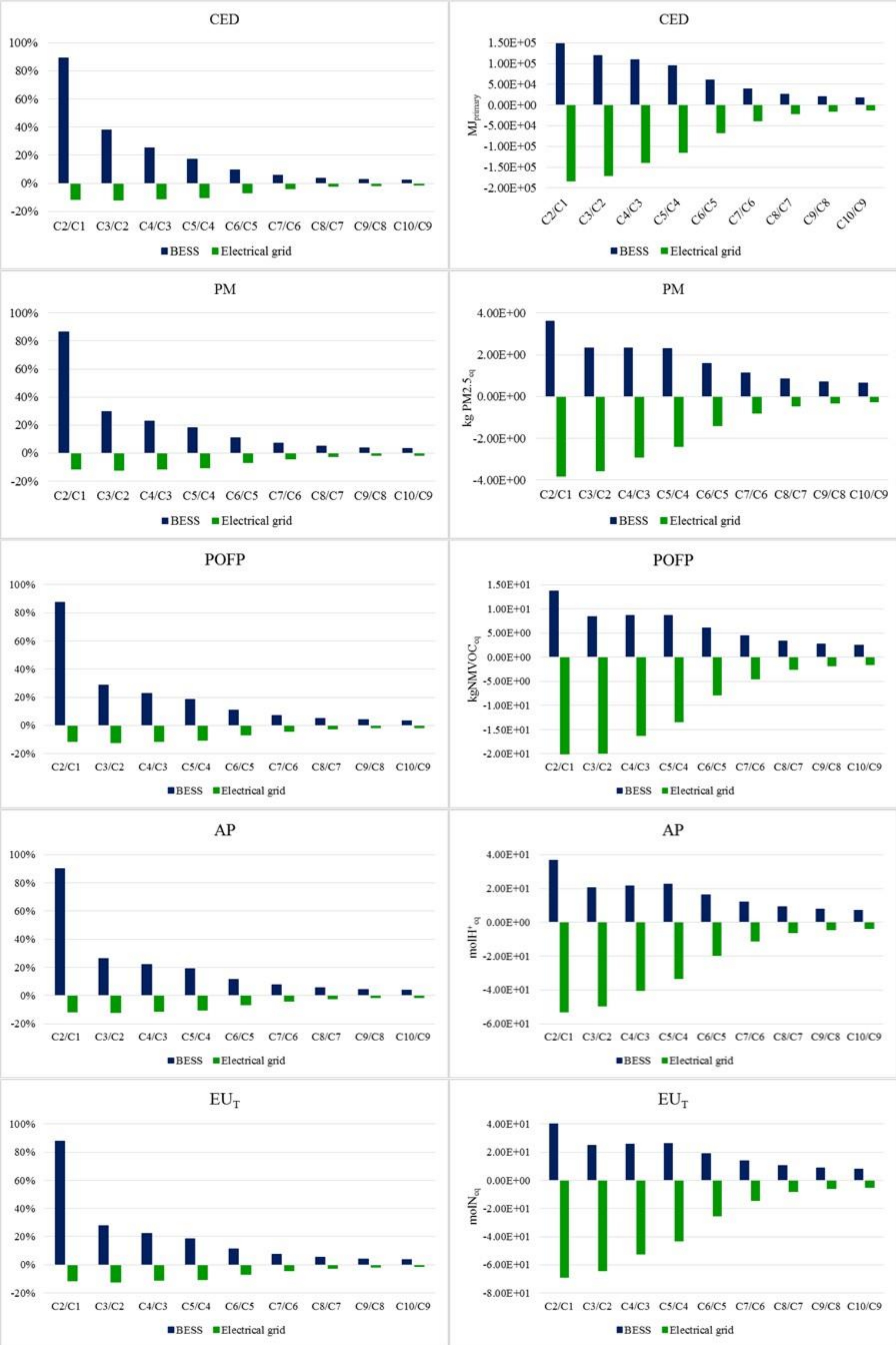
CED
100%
80%
60%
40%
20%
0%
-20%
C2/C1 C3/C2 C4/C3 C5/C4 C6/C5 C7/C6 C8/C7 C9/C8 C10/C9
BESS Electrical grid
CED
MJprimary
1.50E+05
1.00E+05
5.00E+04
0.00E+00
-5.00E+04
-1.00E+05
-1.50E+05
-2.00E+05
C2/C1 C3/C2 C4/C3 C5/C4 C6/C5 C7/C6 C8/C7 C9/C8 C10/C9
BESS Electrical grid
PM
100%
80%
60%
40%
20%
0%
-20%
C2/C1 C3/C2 C4/C3 C5/C4 C6/C5 C7/C6 C8/C7 C9/C8 C10/C9
BESS Electrical grid
PM
kg PM2.5eq
4.00E+00
2.00E+00
0.00E+00
-2.00E+00
-4.00E+00
C2/C1 C3/C2 C4/C3 C5/C4 C6/C5 C7/C6 C8/C7 C9/C8 C10/C9
BESS Electrical grid
POFP
100%
80%
60%
40%
20%
0%
-20%
C2/C1 C3/C2 C4/C3 C5/C4 C6/C5 C7/C6 C8/C7 C9/C8 C10/C9
BESS Electrical grid
POFP
kgNMVOCeq
1.50E+01
1.00E+01
5.00E+00
0.00E+00
-5.00E+00
-1.00E+01
-1.50E+01
-2.00E+01
C2/C1 C3/C2 C4/C3 C5/C4 C6/C5 C7/C6 C8/C7 C9/C8 C10/C9
BESS Electrical grid
AP
100%
80%
60%
40%
20%
0%
-20%
C2/C1 C3/C2 C4/C3 C5/C4 C6/C5 C7/C6 C8/C7 C9/C8 C10/C9
BESS Electrical grid
AP
molH+eq
4.00E+01
2.00E+01
0.00E+00
-2.00E+01
-4.00E+01
-6.00E+01
C2/C1 C3/C2 C4/C3 C5/C4 C6/C5 C7/C6 C8/C7 C9/C8 C10/C9
BESS Electrical grid
EUT
100%
80%
60%
40%
20%
0%
-20%
C2/C1 C3/C2 C4/C3 C5/C4 C6/C5 C7/C6 C8/C7 C9/C8 C10/C9
BESS Electrical grid
EUT
molNeq
4.00E+01
2.00E+01
0.00E+00
-2.00E+01
-4.00E+01
-6.00E+01
-8.00E+01
C2/C1 C3/C2 C4/C3 C5/C4 C6/C5 C7/C6 C8/C7 C9/C8 C10/C9
BESS Electrical grid

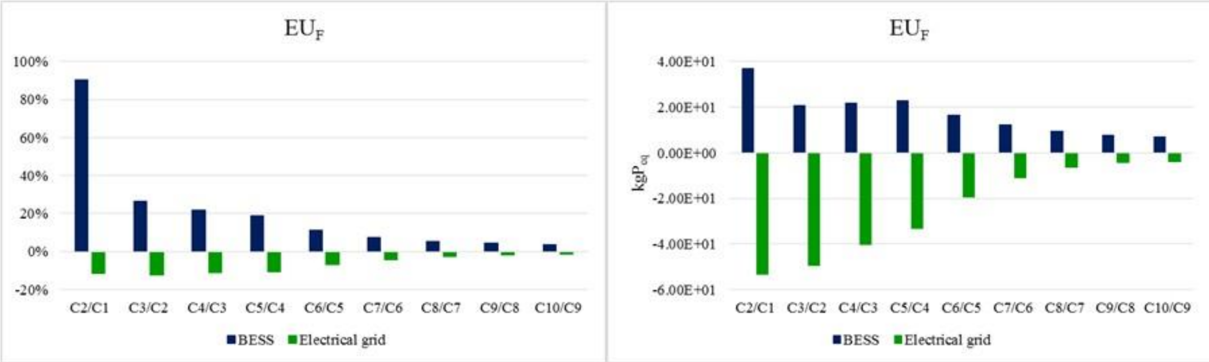

Figure 80. Cluster 3 - Left: Percentage variations of the impacts due to the BESS and to the electrical grid in each configuration compared with the pervious one ((I_{Cn}-I_{Cn-1})/I_{Cn-1}); Right: Differences of the impacts associated with the BESS and the electrical grid between each configuration and the previous one (I_{Cn}-I_{Cn-1}).

Table 76 illustrates the life cycle impact assessment results in the first and the last year of the BESS operation in each configuration examined in order to highlight the effect of both BESS energy capacity and efficiency degradation on them.

Table 76. Life cycle impact assessment results – effect of BESS energy capacity and efficiency degradation and of PV module degradation.

Impact category	C1		C2		C3		C4		C5	
	1st year	3rd year	1st year	6th year	1st year	10th year	1st year	12th year	1st year	12th year
CED (MJ)	1.42E+05	1.1%	1.36E+05	3.0%	1.30E+05	5.7%	1.25E+05	7.1%	1.23E+05	6.9%
ADP ($kgSb_{eq}$)	1.63E-02	-4.7%	2.08E-02	-6.9%	2.47E-02	-6.8%	2.78E-02	-2.8%	2.98E-02	1.7%
GWP ($kgCO_{2eq}$)	7.66E+03	2.2%	6.83E+03	5.7%	6.09E+03	10.3%	5.51E+03	11.7%	5.15E+03	9.7%
ODP ($kgCFC\text{-}11_{eq}$)	8.45E-04	2.0%	7.62E-04	5.2%	6.89E-04	9.4%	6.31E-04	10.8%	5.95E-04	9.1%
HT-nce (CTUh)	1.36E-03	-0.1%	1.39E-03	0.4%	1.41E-03	1.8%	1.43E-03	3.7%	1.45E-03	5.0%
HT-ce (CTUh)	2.85E-04	1.0%	2.73E-04	2.8%	2.62E-04	5.4%	2.54E-04	6.8%	2.49E-04	6.8%
PM (kg $PM2.5_{eq}$)	2.91E+00	1.5%	2.72E+00	3.8%	2.55E+00	7.0%	2.42E+00	8.3%	2.34E+00	7.6%
IR-hh ($kBqU^{235}{}_{eq}$)	1.07E+03	2.3%	9.50E+02	6.0%	8.42E+02	10.8%	7.57E+02	12.2%	7.03E+02	10.0%
POFP ($kgNMVOC_{eq}$)	1.59E+01	1.9%	1.45E+01	4.9%	1.32E+01	8.8%	1.22E+01	10.1%	1.16E+01	8.7%
AP ($molH^{+}{}_{eq}$)	3.92E+01	2.0%	3.54E+01	5.1%	3.21E+01	9.3%	2.95E+01	10.6%	2.78E+01	9.0%
EU_T ($molN_{eq}$)	5.10E+01	2.0%	4.61E+01	5.1%	4.19E+01	9.2%	3.86E+01	10.5%	3.64E+01	8.9%
EU_F (kgP_{eq})	2.24E+00	1.4%	2.10E+00	3.6%	1.98E+00	6.6%	1.89E+00	8.0%	1.83E+00	7.4%
EU_M (kgN_{eq})	5.05E+00	1.9%	4.60E+00	4.8%	4.20E+00	8.8%	3.89E+00	10.1%	3.69E+00	8.7%
E_{Fw} (CTUe)	1.67E+05	0.5%	1.64E+05	1.7%	1.62E+05	3.8%	1.60E+05	5.4%	1.59E+05	5.9%
Impact category	C6		C7		C8		C9		C10	
	1st year	12th year	1st year	12th year	1st year	12th year	1st year	12th year	1st year	12th year
CED (MJ)	1.21E+05	6.8%	1.20E+05	6.8%	1.19E+05	6.9%	1.19E+05	7.0%	1.18E+05	7.1%
ADP ($kgSb_{eq}$)	3.10E-02	4.2%	3.16E-02	5.3%	3.20E-02	5.6%	3.24E-02	5.7%	3.26E-02	5.7%
GWP ($kgCO_{2eq}$)	4.94E+03	8.3%	4.81E+03	7.6%	4.73E+03	7.6%	4.67E+03	7.7%	4.62E+03	8.0%
ODP ($kgCFC\text{-}11_{eq}$)	5.74E-04	7.9%	5.62E-04	7.4%	5.54E-04	7.4%	5.48E-04	7.6%	5.43E-04	7.8%
HT-nce (CTUh)	1.45E-03	5.8%	1.46E-03	6.2%	1.46E-03	6.4%	1.46E-03	6.5%	1.47E-03	6.5%
HT-ce (CTUh)	2.46E-04	6.7%	2.44E-04	6.7%	2.43E-04	6.8%	2.42E-04	6.9%	2.42E-04	7.1%
PM (kg $PM2.5_{eq}$)	2.29E+00	7.2%	2.26E+00	7.0%	2.24E+00	7.0%	2.23E+00	7.1%	2.22E+00	7.3%
IR-hh ($kBqU^{235}{}_{eq}$)	6.72E+02	8.4%	6.54E+02	7.7%	6.42E+02	7.7%	6.33E+02	7.8%	6.26E+02	8.2%
POFP ($kgNMVOC_{eq}$)	1.12E+01	7.7%	1.10E+01	7.3%	1.09E+01	7.3%	1.08E+01	7.4%	1.07E+01	7.7%
AP ($molH^{+}{}_{eq}$)	2.69E+01	7.9%	2.63E+01	7.4%	2.60E+01	7.4%	2.57E+01	7.5%	2.54E+01	7.8%
EU_T ($molN_{eq}$)	3.52E+01	7.9%	3.45E+01	7.4%	3.40E+01	7.4%	3.37E+01	7.5%	3.34E+01	7.8%
EU_F (kgP_{eq})	1.80E+00	7.0%	1.78E+00	6.9%	1.77E+00	7.0%	1.76E+00	7.1%	1.75E+00	7.3%
EU_M (kgN_{eq})	3.57E+00	7.7%	3.51E+00	7.3%	3.46E+00	7.3%	3.43E+00	7.4%	3.40E+00	7.7%
E_{Fw} (CTUe)	1.59E+05	6.3%	1.58E+05	6.5%	1.58E+05	6.6%	1.58E+05	6.7%	1.58E+05	6.8%

Data analysis highlights that in each configuration the impacts increase during the operation phase in almost all the examined impact categories due to the battery capacity fade that results in a lower electricity dischargeable and to the efficiency degradation that involve higher electricity losses per kWh of electricity discharged. Moreover, the amount of electricity available for charging the BESS decreases from one year to the next one due to the PV module efficiency degradation. The exceptions are represented by the abiotic depletion potential and human toxicity – cancer effect impact categories, where, from an environmental point of view, the electricity from the grid performs better than the electricity from PV. In fact, due to the capacity degradation, during the operation phase the electricity consumption from PV decreases while the import from the grid increases.

Concerning the abiotic depletion potential, the impact in the first four configurations (from C1 to C4) decreases during the operation phase since the consumption of electricity from PV (highly impacting in this environmental category) decreases due to the battery capacity degradation, however, from C5 the impact starts to increase. Although the amount of electricity consumption from PV decreases during the operation phase, as in the previous configurations, starting from C5 the impact associated to the electricity loss due to a battery efficiency, that is electricity produced by the PV power plant, offset the environmental benefits related to the reduced consumption of PV electricity provided through the BESS (Figure 81). The same considerations apply to the human toxicity – cancer effect impact category (Figure 82).

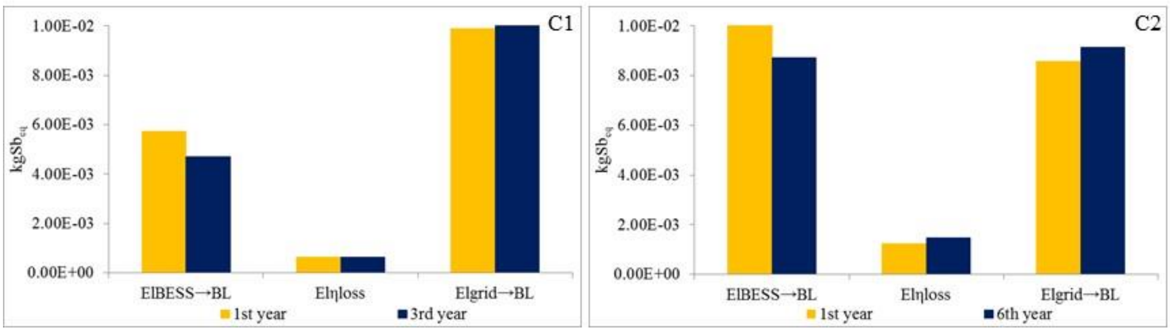

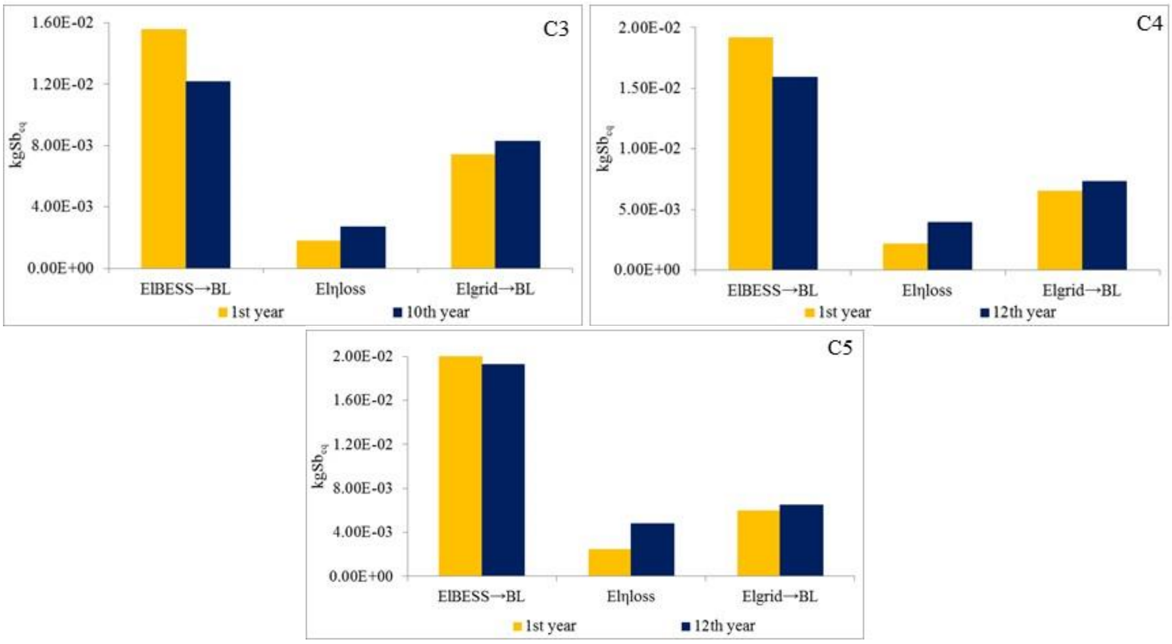

Figure 81. Abiotic depletion potential – effect of BESS energy capacity and efficiencydegradation.

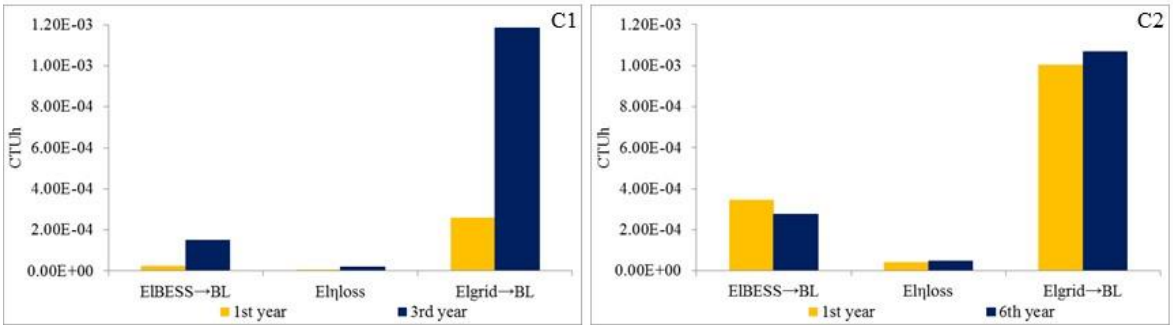

Figure 82. Human toxicity – cancer effect – effect of BESS energy capacity and efficiencydegradation.

Table 77 illustrates the environmental credits arising from the potential production of secondary raw materials expressed as a percentage of the total life cycle impacts.

From data analysis results that the environmental credits arising from the potential production of secondary raw materials from the recycling process are negligible representing in each configuration a percentage lower than 5% of the life cycle impact in almost all the environmental categories. The exceptions are human toxicity – cancer effect, human toxicity – non cancer effect and marine eutrophication impact categories. However, in order to obtain significant information on the contribution of the recycling phase, it is more appropriate to compare them only with the life cycle phases that involve a consumption of raw materials, i.e. production, repurposing and recycling phases of the batteries excluding the operation phase. The obtained results, illustrated in Table 77 and Table 78.

Table 77. Environmental credits from BESS recycling expressed as a percentage of the total life cycle impacts.

Impact category	**C1**	**C2**	**C3**	**C4**	**C5**
CED (MJ)	-0.23%	-0.40%	-0.46%	-0.55%	-0.67%
ADP ($kgSb_{eq}$)	-1.98%	-3.05%	-3.19%	-3.45%	-3.83%
GWP ($kgCO_{2eq}$)	-0.33%	-0.58%	-0.71%	-0.89%	-1.13%
ODP ($kgCFC\text{-}11_{eq}$)	-0.19%	-0.35%	-0.42%	-0.52%	-0.66%
HT-nce (CTUh)	-1.92%	-2.97%	-3.22%	-3.65%	-4.25%
HT-ce (CTUh)	-4.56%	-6.45%	-6.97%	-8.03%	-9.56%
PM (kg $PM2.5_{eq}$)	-0.88%	-1.49%	-1.71%	-2.05%	-2.49%
IR-hh ($kBqU^{235}{}_{eq}$)	-0.25%	-0.49%	-0.61%	-0.78%	-1.00%
POFP ($kgNMVOC_{eq}$)	-0.59%	-1.01%	-1.19%	-1.45%	-1.80%
AP ($molH^{+}{}_{eq}$)	-0.70%	-1.33%	-1.61%	-1.99%	-2.46%
EU_T ($molN_{eq}$)	-0.58%	-1.03%	-1.23%	-1.51%	-1.88%
EU_F (kgP_{eq})	-1.02%	-1.74%	-2.01%	-2.40%	-2.90%
EU_M (kgN_{eq})	-1.92%	-3.69%	-4.46%	-5.42%	-6.58%
EF_w (CTUe)	-0.49%	-0.81%	-0.90%	-1.05%	-1.24%
Impact category	**C6**	**C7**	**C8**	**C9**	**C10**
CED (MJ)	-0.76%	-0.84%	-0.91%	-0.97%	-1.02%
ADP ($kgSb_{eq}$)	-4.14%	-4.40%	-4.61%	-4.79%	-4.95%
GWP ($kgCO_{2eq}$)	-1.33%	-1.49%	-1.62%	-1.73%	-1.84%
ODP ($kgCFC\text{-}11_{eq}$)	-0.78%	-0.87%	-0.94%	-1.01%	-1.07%
HT-nce (CTUh)	-4.72%	-5.11%	-5.44%	-5.73%	-5.99%
HT-ce (CTUh)	-10.80%	-11.82%	-12.69%	-13.47%	-14.18%
PM (kg $PM2.5_{eq}$)	-2.84%	-3.12%	-3.34%	-3.55%	-3.73%
IR-hh ($kBqU^{235}{}_{eq}$)	-1.18%	-1.32%	-1.44%	-1.53%	-1.62%
POFP ($kgNMVOC_{eq}$)	-2.08%	-2.31%	-2.49%	-2.65%	-2.80%
AP ($molH^{+}{}_{eq}$)	-2.83%	-3.12%	-3.34%	-3.53%	-3.70%
EU_T ($molN_{eq}$)	-2.18%	-2.41%	-2.60%	-2.76%	-2.91%
EU_F (kgP_{eq})	-3.30%	-3.61%	-3.87%	-4.10%	-4.30%
EU_M (kgN_{eq})	-7.45%	-8.10%	-8.60%	-9.01%	-9.37%
EF_w (CTUe)	-1.40%	-1.52%	-1.63%	-1.72%	-1.80%

Table 78. Environmental credits from BESS recycling expressed as a percentage of the battery pack production, battery repurposing and battery pack EoL impacts.

Impact category	**C1**	**C2**	**C3**	**C4**	**C5**
CED (MJ)	-13.64%	-12.78%	-12.54%	-12.49%	-12.52%
ADP ($kgSb_{eq}$)	-17.78%	-17.10%	-16.92%	-16.88%	-16.90%
GWP ($kgCO_{2eq}$)	-14.36%	-13.07%	-12.72%	-12.64%	-12.69%
ODP ($kgCFC\text{-}11_{eq}$)	-11.55%	-10.51%	-10.23%	-10.17%	-10.20%
HT-nce (CTUh)	-27.33%	-24.92%	-24.27%	-24.13%	-24.21%
HT-ce (CTUh)	-52.42%	-49.23%	-48.16%	-47.90%	-48.04%
PM (kg $PM2.5_{eq}$)	-20.53%	-18.99%	-18.57%	-18.48%	-18.53%
IR-hh ($kBqU^{235}{}_{eq}$)	-15.13%	-14.95%	-14.89%	-14.88%	-14.88%
POFP ($kgNMVOC_{eq}$)	-17.10%	-15.51%	-15.09%	-14.99%	-15.04%
AP ($molH^{+}{}_{eq}$)	-18.23%	-17.64%	-17.47%	-17.44%	-17.46%
EU_T ($molN_{eq}$)	-16.90%	-15.66%	-15.33%	-15.25%	-15.29%
EU_F (kgP_{eq})	-23.53%	-22.01%	-21.59%	-21.50%	-21.55%
EU_M (kgN_{eq})	-32.68%	-32.73%	-32.72%	-32.72%	-32.72%
EF_w (CTUe)	-11.02%	-9.77%	-9.45%	-9.38%	-9.42%
Impact category	**C6**	**C7**	**C8**	**C9**	**C10**
CED (MJ)	-12.56%	-12.62%	-12.67%	-12.73%	-12.79%
ADP ($kgSb_{eq}$)	-16.93%	-16.97%	-17.02%	-17.06%	-17.11%
GWP ($kgCO_{2eq}$)	-12.75%	-12.83%	-12.92%	-13.00%	-13.09%
ODP ($kgCFC\text{-}11_{eq}$)	-10.25%	-10.32%	-10.38%	-10.45%	-10.52%
HT-nce (CTUh)	-24.33%	-24.48%	-24.64%	-24.80%	-24.96%
HT-ce (CTUh)	-48.25%	-48.50%	-48.77%	-49.03%	-49.28%
PM (kg $PM2.5_{eq}$)	-18.61%	-18.70%	-18.81%	-18.91%	-19.02%
IR-hh ($kBqU^{235}{}_{eq}$)	-14.89%	-14.91%	-14.92%	-14.94%	-14.95%
POFP ($kgNMVOC_{eq}$)	-15.12%	-15.22%	-15.32%	-15.43%	-15.54%
AP ($molH^{+}{}_{eq}$)	-17.49%	-17.52%	-17.56%	-17.60%	-17.64%
EU_T ($molN_{eq}$)	-15.36%	-15.43%	-15.51%	-15.60%	-15.68%
EU_F (kgP_{eq})	-21.63%	-21.72%	-21.82%	-21.93%	-22.03%
EU_M (kgN_{eq})	-32.72%	-32.72%	-32.72%	-32.73%	-32.73%
EF_w (CTUe)	-9.48%	-9.55%	-9.63%	-9.70%	-9.78%

The environmental credits related to the avoided electricity from the grid (Table 79) are particularly relevant in impact categories such as global warming potential, ozone depletion potential, acidification potential, ionizing radiation in which the electricity from the electrical grid performs worse compared to the electricity from PV.

These environmental credits are higher for the configurations with a lower BESS size since the electricity fed into the grid is higher. However, it is important to underling that higher penetration of

RESs in the electrical grid affects its stability and reliability. Then, although the environmental credits decrease in correspondence of larger energy capacity installed, the benefits for the grid operation increase.

Table 79. Environmental credits from the electricity fed into the grid expressed as a percentage of the total life cycle impacts.

Impact category	**C1**	**C2**	**C3**	**C4**	**C5**
CED (MJ)	-64.5%	-56.0%	-48.0%	-40.5%	-34.7%
ADP ($kgSb_{eq}$)	-21.4%	-15.2%	-11.6%	-8.8%	-6.9%
GWP ($kgCO_{2eq}$)	-81.1%	-74.2%	-67.5%	-60.0%	-53.6%
ODP ($kgCFC\text{-}11_{eq}$)	-78.2%	-71.1%	-64.0%	-56.4%	-50.1%
HT-nce (CTUh)	-48.4%	-38.6%	-31.4%	-25.2%	-20.6%
HT-ce (CTUh)	-58.9%	-49.2%	-41.6%	-34.3%	-28.5%
PM (kg $PM2.5_{eq}$)	-67.3%	-58.0%	-50.1%	-42.3%	-36.1%
IR-hh ($kBqU^{235}_{eq}$)	-83.4%	-77.4%	-71.1%	-64.0%	-57.8%
POFP ($kgNMVOC_{eq}$)	-74.5%	-66.1%	-58.5%	-50.7%	-44.2%
AP ($molH^{+}_{eq}$)	-75.9%	-67.4%	-59.8%	-52.0%	-45.3%
EU_T ($molN_{eq}$)	-75.8%	-67.6%	-60.1%	-52.3%	-45.7%
EU_F (kgP_{eq})	-66.0%	-56.6%	-48.6%	-40.9%	-34.8%
EU_M (kgN_{eq})	-72.5%	-62.6%	-54.7%	-46.7%	-40.0%
EF_w (CTUe)	-56.2%	-46.5%	-38.6%	-31.7%	-26.4%
Impact category	**C6**	**C7**	**C8**	**C9**	**C10**
CED (MJ)	-31.2%	-29.2%	-28.1%	-27.2%	-26.5%
ADP ($kgSb_{eq}$)	-5.9%	-5.3%	-5.0%	-4.7%	-4.6%
GWP ($kgCO_{2eq}$)	-49.4%	-46.8%	-45.2%	-44.0%	-42.9%
ODP ($kgCFC\text{-}11_{eq}$)	-46.0%	-43.6%	-42.1%	-41.0%	-40.1%
HT-nce (CTUh)	-17.9%	-16.4%	-15.5%	-14.9%	-14.3%
HT-ce (CTUh)	-25.0%	-22.9%	-21.7%	-20.7%	-19.8%
PM (kg $PM2.5_{eq}$)	-32.3%	-30.0%	-28.7%	-27.6%	-26.8%
IR-hh ($kBqU^{235}_{eq}$)	-53.7%	-51.2%	-49.6%	-48.4%	-47.4%
POFP ($kgNMVOC_{eq}$)	-40.0%	-37.5%	-36.0%	-34.8%	-33.8%
AP ($molH^{+}_{eq}$)	-41.0%	-38.4%	-36.8%	-35.6%	-34.6%
EU_T ($molN_{eq}$)	-41.5%	-38.9%	-37.4%	-36.1%	-35.2%
EU_F (kgP_{eq})	-31.0%	-28.8%	-27.5%	-26.5%	-25.7%
EU_M (kgN_{eq})	-35.7%	-33.1%	-31.5%	-30.3%	-29.3%
EF_w (CTUe)	-23.3%	-21.5%	-20.5%	-19.7%	-19.1%

5.4.2 Identification of the best configuration in terms of load match and life cycle environmental impacts

According to the LCIA results, the impact categories can be grouped into three different clusters depending on their trend in correspondence of the increasing capacity. For each cluster, the different impact categories follow comparable trends with the increasing installed capacity. Thus, it is possible to examine each cluster by analysing only one impact category, assumed as representative.

Since all impacts categories within each cluster have comparable trends, for the first cluster, global warming potential is selected because of its relevance to society and policy [198].

For the second cluster, abiotic depletion potential is selected because of the relevance of natural resource availability to economic development and also because of increasing political interest in resource consumption [199,200].

For the third cluster, particulate matter is selected since this impact category takes into account the air pollutants that adversely affect human health [201] and it is of particular concern in urban areas because of the highly dense populations exposed to air pollution and the high number of emission sources (e.g. road transportation).

Figure 83 shows the comparison of γ_{load}, global warming potential, abiotic depletion potential and particulate matter with the installed capacity. The analysis highlighted that C5 could represent the best BESS size in terms of load matching and environmental sustainability for 3 reasons:

- The employment of an additional repurposed EV battery (C6) causes a negligible improvement of γ_{load} (+3.3%) and of the impact categories represented by global warming potential (-2.7%) respect to the previous configurations;
- Particulate matter shows a decrease until C5 and an increase starting from C6.
- C5 performs better than the previous configurations in 10 out of 14 environmental impact categories investigated. While, for example, C6 performs better than C5 only in 7 out of 14.

Moreover, if a market for retired EV battery will develop in the future, also economic considerations will favour configurations with a lower number of batteries, less expensive.

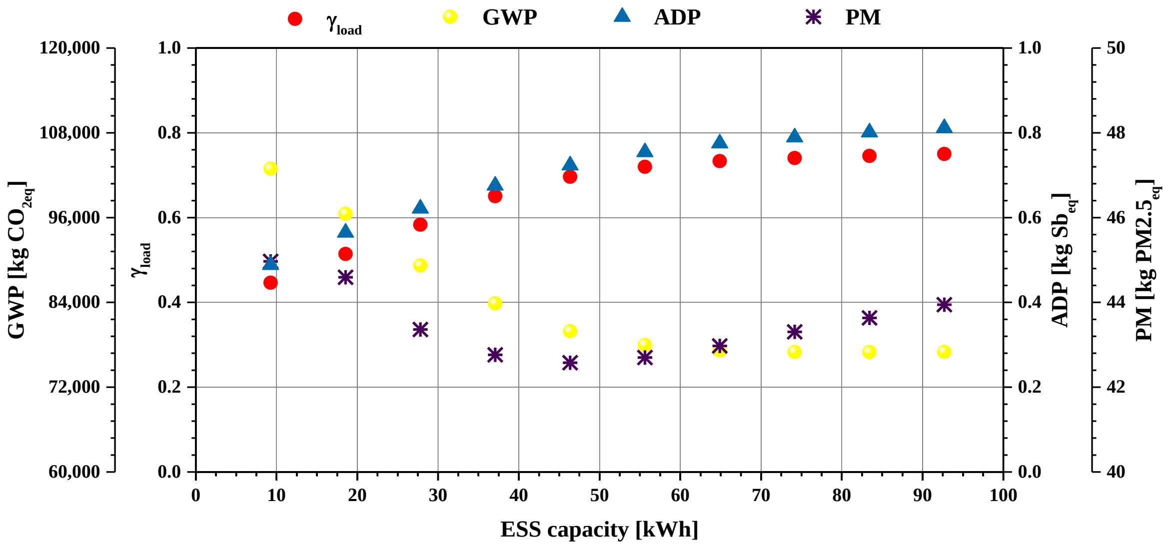

Figure 83. Comparison of γ_{load}, global warming potential, abiotic depletion potential and particulate matter with the installed capacity.

5.4.3 Life cycle environmental comparison of the life cycle environmental impacts associated to the best design solution with the "reference scenario" and with the "fresh battery scenario"

In this section, the results of the comparison of the life cycle impacts associated to the best configuration identified in Section 5.5 with the "reference scenario" and the "fresh battery scenario" (BESS realized with fresh EV batteries) are illustrated and discussed.

Concerning the comparison between the "reuse battery scenario" and the "fresh battery scenario", it is assumed that the compared alternatives are equivalent if they present the same average γ_{load} in the same application. Then, the energy system consisting of the PV power plant described in Section 3.2, the fresh BESS and the electrical grid is modelled for different value of BESS capacity in order to identify the configuration able to ensure the same average γ_{load} of the C5, i.e. $\gamma_{load} = 0.69$.

The battery parameters (SoC_{max}, SoC_{min}, etc.) used to model the "PV – fresh BESS – electricity grid" are the same of those illustrated in Table 11, with the exception of the battery energy capacity and the charge/discharge battery efficiency since in this case the values for a fresh EV battery are used (Table 5). From the simulation of the PV – fresh BESS – electrical grid results the value of installed energy capacity able to guarantee the same value of γ_{load} is 46.5 kWh corresponding to the employment of 4 fresh EV batteries.

Figure 84 Figure 85 and show, respectively, the coloured contour graph of the γ_{load} and ne in the Reuse and Fresh battery scenarios, in the first operation year of the investigated time frame. Since the compared systems are equivalent, they present the same the coloured contour graphs of the γ_{load} and ne indicators.

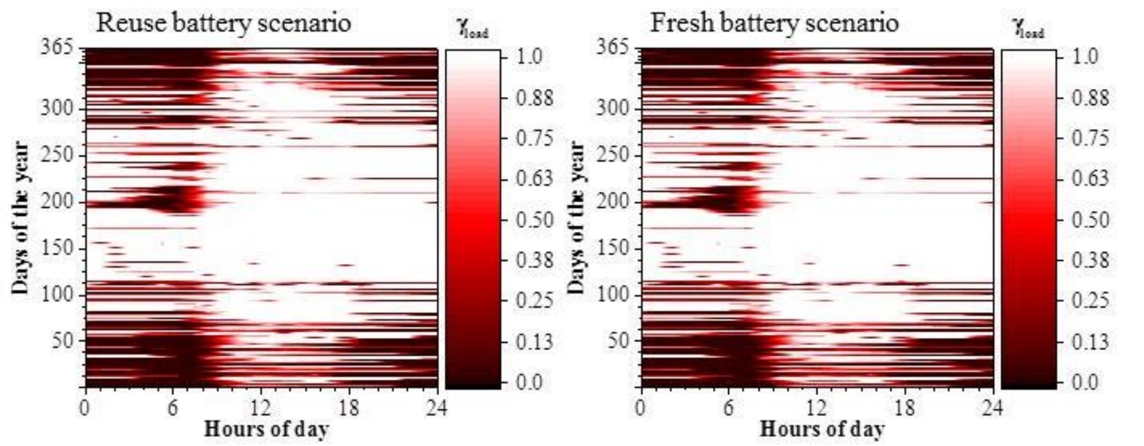

Figure 84. Coloured contour graph of the γ_{load} for the first year of operation in the Reuse battery scenario (left) and Fresh battery scenario (right).

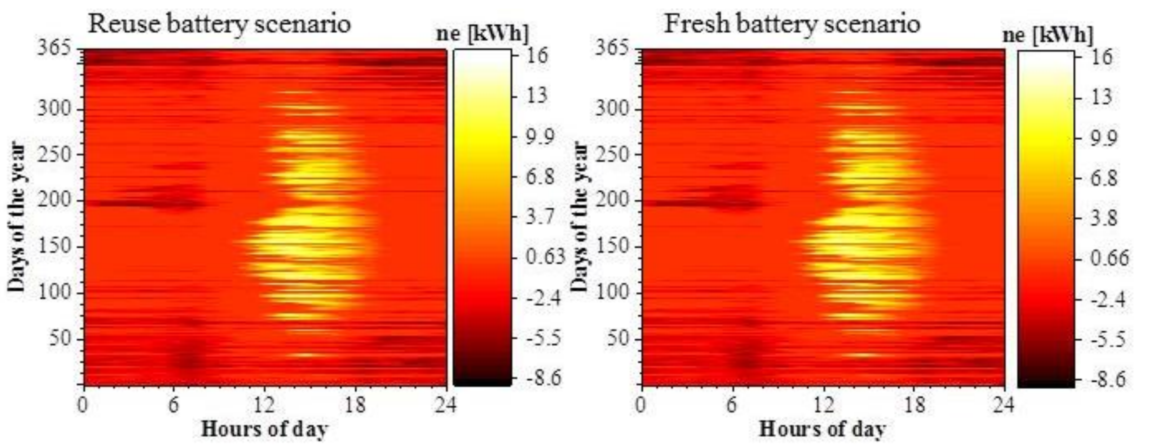

Figure 85. Coloured contour graph of the *ne* for the first year of operation in the Reuse battery scenario (left) and Fresh battery scenario (right).

The hourly γ_{load} averaged on annual basis for the examined timeframe of the energy model are illustrated in Table 80.

In Table 81 are illustrated the results of the energy modelling referred to the three scenarios investigated.

The electricity produced by the PV plant and directly consumed by the building assumes the same value in each scenario since it is unaffected by the BESS installation and size.

Table 80. Hourly γ_{load} values averaged on annual basis for each configuration in the whole modelled period.

Years	γ_{load}
1	0.71
2	0.71
3	0.70
4	0.70
5	0.69
6	0.69
7	0.69
8	0.68
9	0.68
10	0.67
11	0.67
12	0.66

Table 81. Energy model results – Reference, Reuse battery and Fresh battery scenarios.

Operational phase parameters	**Reference scenario**	**Reuse battery scenario**	**Fresh scenario**
$El_{PV \rightarrow BL}$ [kWh]	99,134.97	99,134.97	99,134.97
$El_{BESS \rightarrow BL}$ [kWh]	-	90,033.34	89,483.77
$El_{\eta loss}$ [kWh]	-	15,905.11	9,060.35
$El_{grid \rightarrow BL}$ [kWh]	201,587.27	111,553.93	112,103.50
$EL_{PV \rightarrow grid}$ [kWh]	188,723.32	82,818.53	90,211.40

In the Fresh battery scenario, the installation of fresh EV battery characterized by an higher charge/discharge battery efficiency (98%) allow to reduce the electricity loss by around 40% compared to the Reuse battery scenario. However, it is worth mentioning that the most common solution as stationary energy storage system is represented by the lead acid batteries. Lead acid battery technology is characterized by lower charge/discharge efficiency (70 – 85%) then, compared with this technology the retired EV battery characterized by higher performance, could involve lower electricity loss, despite the efficiency degradation due to its first use in EV.

In both Reuse and Fresh battery scenarios, the import from the electrical grid decreases while the export into the grid increases by around 50% compared to the reference scenario. Thus, both scenarios contribute to the mitigating of the negative effects on the grid related to the intermittency of the PV electricity.

Figure 86 shows the results of the life cycle impacts of the Reference, Reuse and Fresh battery scenarios in all the investigates environmental categories. From LCIA results that both the Reuse and the Fresh battery scenarios perform better than the Reference one in almost all the environmental impact categories. In detail, the impacts in both reuse and fresh battery scenarios decreases of a percentage ranging from around -5% (in marine eutrophication) to -33% (in ionizing radiation – human health) compared to the reference scenario.

The exceptions are the abiotic depletion potential, the human toxicity – cancer and – non cancer effect and the freshwater ecotoxicity due mainly to the higher consumption of electricity from PV that is highly impacting in terms of resources efficiency and chemical toxicity. Concerning the abiotic depletion potential, the impact increases of around 100% in both reuse and fresh battery scenarios compared to the reference one.

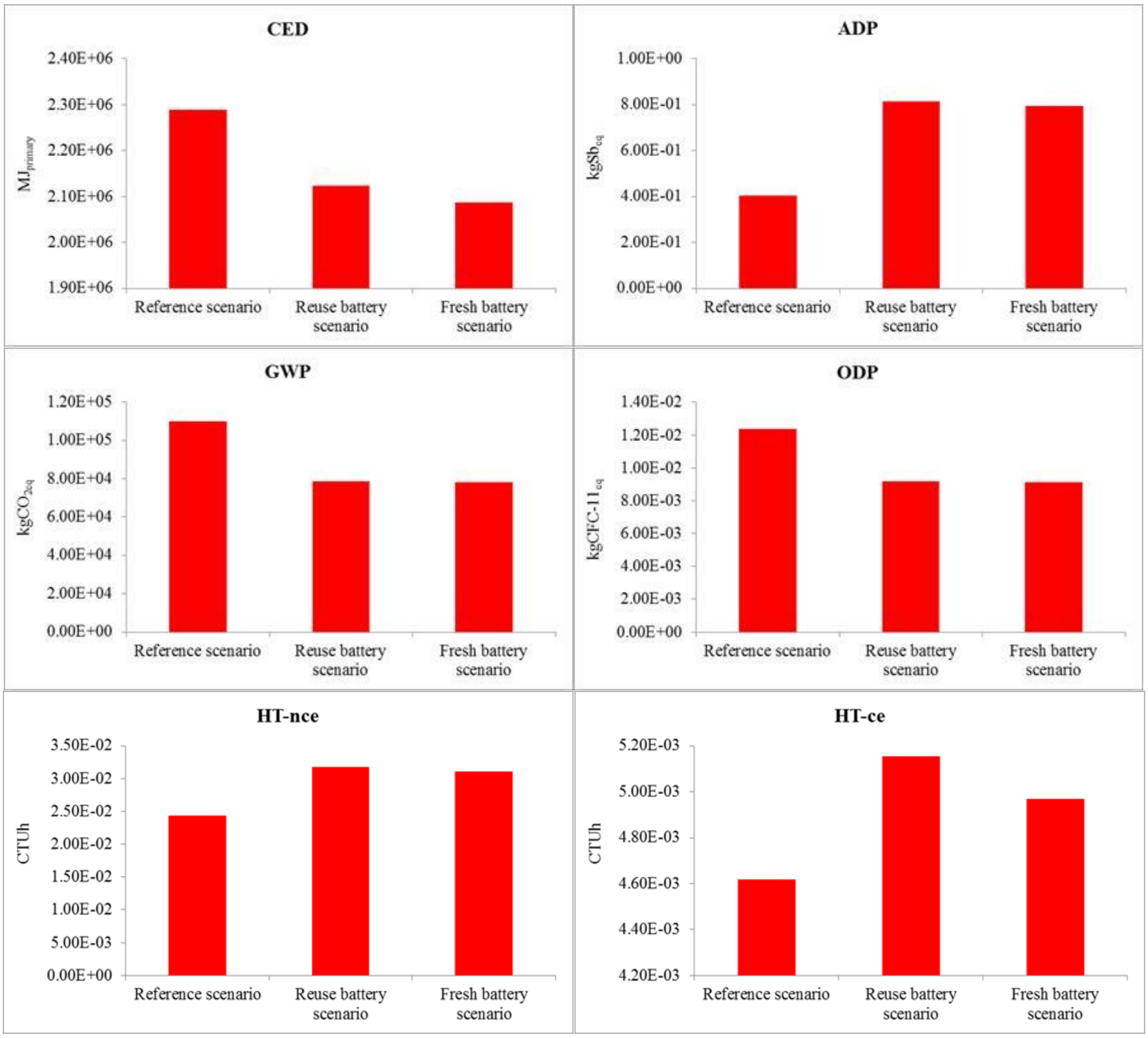

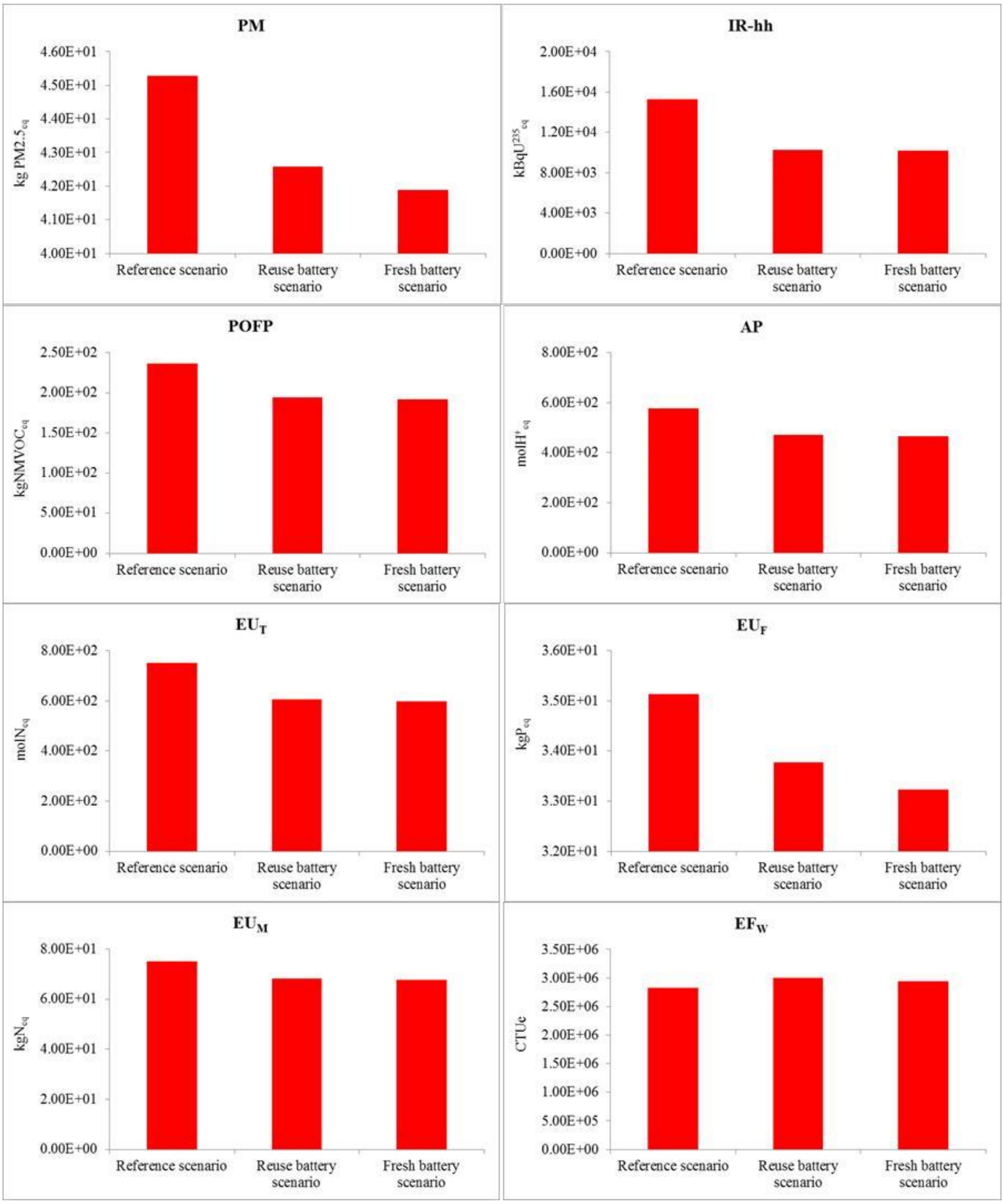

Figure 86. Life cycle impacts comparison - Reference, Reuse and Fresh battery scenarios.

Concerning the comparison between the Reuse battery scenario and the Fresh battery scenarios, from the analysis results that the systems, to provide the electricity required by the house in 12 years, cause energy and environmental impacts of the same order of magnitude. In the Reuse battery scenario, the impacts associated to the production and recycling process of five EV batteries are allocated between the first and the second application (Table 57). In the Fresh battery scenario, the impacts related to the production and recycling process of four EV batteries are fully allocated to the investigated system but proportionally to the effective operation years. In fact, the lifetime of a fresh battery is assumed equal to 20 years, but in the investigated system, it is used only for 12 years. Then, the impacts related to the battery production process results equivalent. Moreover, in the Reuse battery scenario higher impact associated to lower charge/discharge battery efficiency and the additional impacts of the repurposing phase offset the environmental benefits related to the extension of the EV battery lifetime.

In addition, also for the environmental impacts as for the operation phase, different results could be obtained if the performances of the retired EV batteries in a stationary application are compared with those resulting from the installation of a new less efficient lead acid battery that, as previously said, currently is the more widespread technology in stationary storage system. In fact, the lead acid technology has several negative aspects, such as a fairly low expected life and a not excessively high energy density and power. Consequently, it could require higher installed capacity to provide a certain service, compared to the lithium-ion technology or more battery replacement resulting in higher environmental impacts.

Table 82 illustrates the environmental credits related to the electricity fed into the grid. Although they are higher in the Reference scenario, it is important to underling that a higher penetration of RESs in the electrical grid affects its stability and reliability. Then reducing the amount of electricity fed into the grid through the adoption of energy storage system can help to solve these technical challenges.

Moreover, the environmental credits of the Reference scenario could be lower than those obtained in this study if it is considered that the high RESs penetration into the grid may cause fossil-fuelled generators to cycle on and off and ramp down to part load more frequently and potentially more rapidly and degraded performance over time. The emissions from fossil fuelled generators may be higher during cycling and ramping than during steady-state operation [202] resulting in higher environmental impact of 1 kWh from the electrical grid.

Table 82. Environmental credits related to the electricity fed into the grid – Reference, Reuse and fresh battery scenarios.

Impact categoty	Reference scenario	Reuse battery scenario	Fresh battery scenario
CED (MJ)	-1.68E+06	-7.38E+05	-8.04E+05
ADP ($kgSb_{eq}$)	-1.28E-01	-5.60E-02	-6.10E-02
GWP ($kgCO_{2eq}$)	-9.65E+04	-4.24E+04	-4.61E+04
ODP ($kgCFC\text{-}11_{eq}$)	-1.05E-02	-4.62E-03	-5.03E-03
HT-nce (CTUh)	-1.49E-02	-6.54E-03	-7.12E-03
HT-ce (CTUh)	-3.35E-03	-1.47E-03	-1.60E-03
PM (kg $PM2.5_{eq}$)	-3.51E+01	-1.54E+01	-1.68E+01
IR-hh ($kBqU^{235}{}_{eq}$)	-1.36E+04	-5.97E+03	-6.50E+03
POFP ($kgNMVOC_{eq}$)	-1.97E+02	-8.62E+01	-9.39E+01
AP ($molH^{+}{}_{eq}$)	-4.87E+02	-2.14E+02	-2.33E+02
EU_T ($molN_{eq}$)	-6.34E+02	-2.78E+02	-3.03E+02
EU_F (kgP_{eq})	-2.68E+01	-1.18E+01	-1.28E+01
EU_M (kgN_{eq})	-6.25E+01	-2.74E+01	-2.99E+01
E_{Fw} (CTUe)	-1.91E+06	-8.37E+05	-9.11E+05

As mentioned in Method chapter, in order to have a comprehensive evaluation of the potential environmental benefits of reusing retired EV batteries, the system boundaries are expanded in order to include also the first life in the EV (Figure 30). The overall impacts are compared with the expanded Fresh scenario (Figure 31) in which EV batteries are recycled after the first use in the EV and a new energy storage system in used in the examined building. The results of the comparison are illustrated in Figure 87.

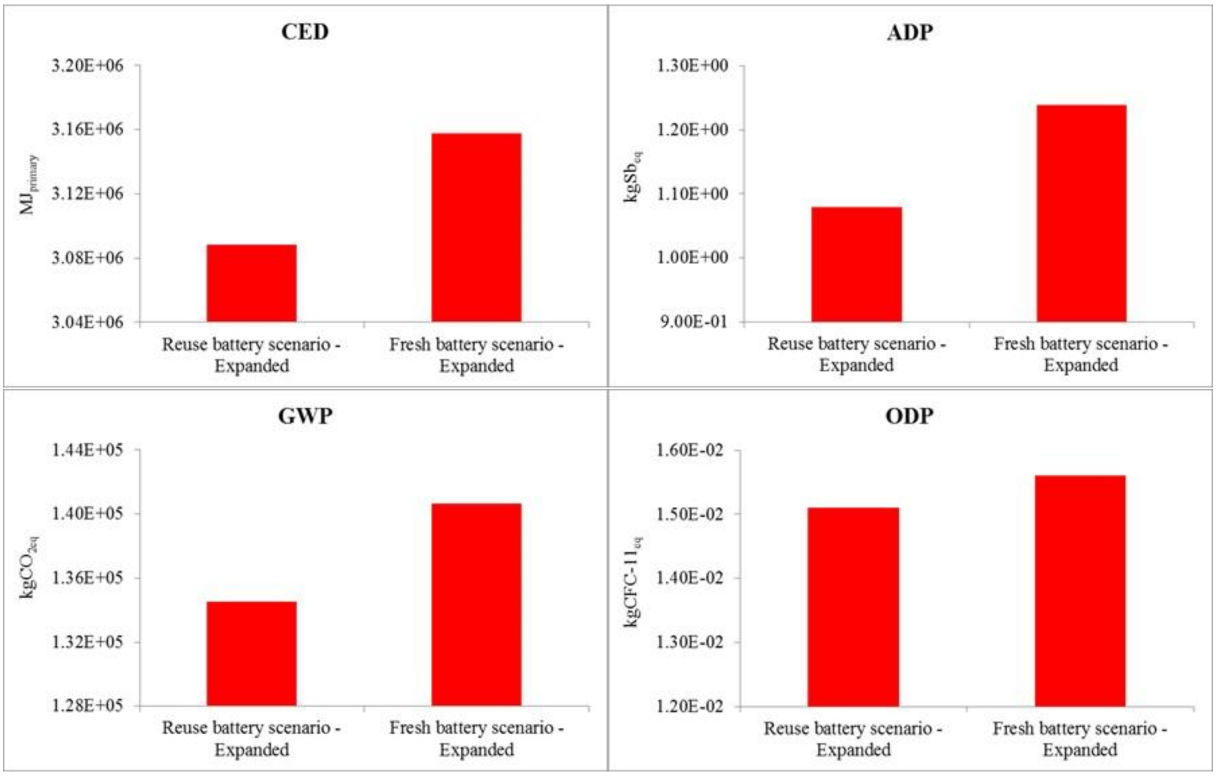

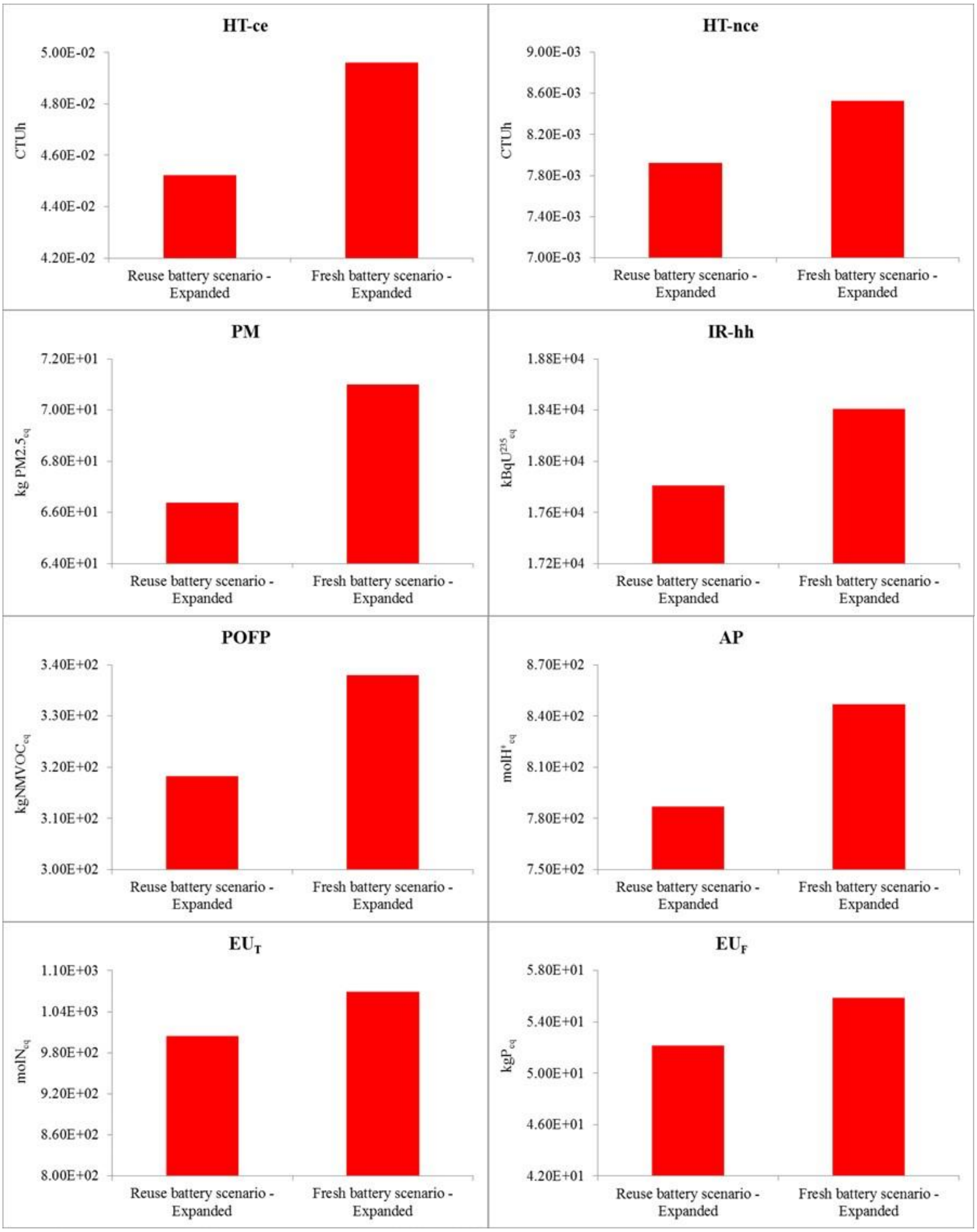
HT-ce
CTUh
5.00E-02
4.80E-02
4.60E-02
4.40E-02
4.20E-02
HT-nce
CTUh
9.00E-03
8.60E-03
8.20E-03
7.80E-03
7.40E-03
7.00E-03
PM
kg $PM2.5_{eq}$
7.20E+01
7.00E+01
6.80E+01
6.60E+01
6.40E+01
IR-hh
$kBqU^{235}_{eq}$
1.88E+04
1.84E+04
1.80E+04
1.76E+04
1.72E+04
POFP
$kgNMVOC_{eq}$
3.40E+02
3.30E+02
3.20E+02
3.10E+02
3.00E+02
AP
$molH^{+}_{eq}$
8.70E+02
8.40E+02
8.10E+02
7.80E+02
7.50E+02
EU_T
$molN_{eq}$
1.10E+03
1.04E+03
9.80E+02
9.20E+02
8.60E+02
8.00E+02
EU_F
kgP_{eq}
5.80E+01
5.40E+01
5.00E+01
4.60E+01
4.20E+01
Reuse battery scenario - Expanded
Fresh battery scenario - Expanded

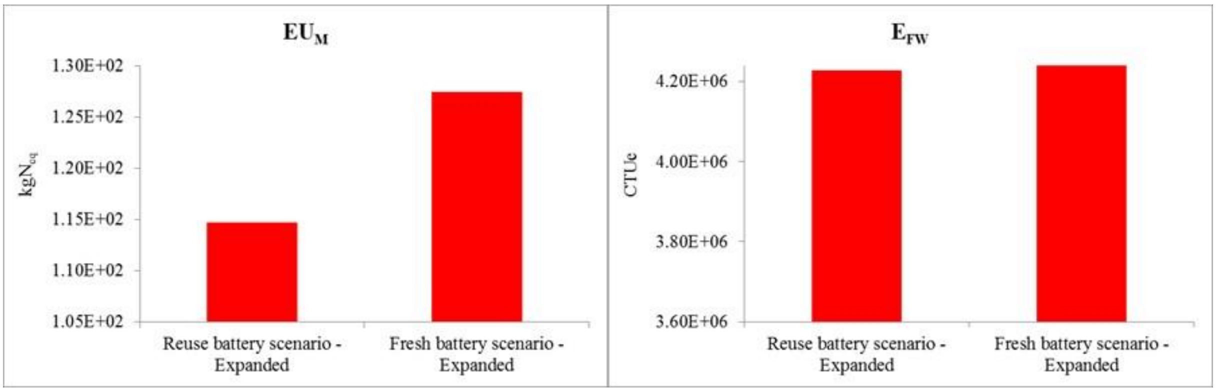

Figure 87. Life cycle impacts comparison - Expanded Reuse and Fresh battery scenarios.

The comparison highlights that the Extended Reuse battery scenario presents better environmental performance in all the examined impacts categories. Then, extending the EV batteries lifetime by reusing them in stationary storage application allows to reduce the overall impacts of the system including both the EV and the building, demonstrating the potential environmental benefits of the proposed circular economy application. In detail, reusing EV batteries in the examined system allow to reduce the impacts of a percentage ranging from -2% (for the cumulative energy demand) to -13% (for abiotic depletion potential). The environmental benefits are greater for the impact categories mainly affected by the battery production phase. Besides abiotic depletion potential, these are marine eutrophication (-10%), human toxicity – cancer effect (-9%), human toxicity – non cancer effect (-7%).

In Table 83 and Table 84 are illustrated, respectively, the life cycle impacts related to the battery use in the EV in the Fresh battery scenario – Expanded (recycling after the use in the EV) and in the Reuse battery scenario - Expanded (second use application after the first use in the EV).

From data analysis, it results that, from the perspective of the use in EV the potential environmental benefits associated to the addition of a secondary reuse application of the batteries are significant. The environmental impacts decease of a percentage ranging from -8% (for ionizing radiation – human health) to – 40% (for abiotic depletion potential). Then, reusing EV batteries in a secondary application in building promises to increase the environmental sustainability of the electric mobility do to the allocation of the impacts related to the EV battery production and recycling between the first application in the EV and the second application as stationary energy storage system.

Table 83. Life cycle impact assessment during the battery use in the EV. Fresh battery scenario – Expanded.

Impact category	EV battery production (%)	Use in the EV (%)	Recycle (%)	Total
CED (MJ)	19.8	78.7	1.5	1.07E+06
ADP ($kgSb_{eq}$)	84.6	14.3	1.1	4.45E-01
GWP ($kgCO_{2eq}$)	21.3	77.2	1.5	6.26E+04
ODP ($kgCFC\text{-}11_{eq}$)	15.6	81.2	3.2	6.49E-03
HT-nce (CTUh)	57.5	39.8	2.7	1.86E-02
HT-ce (CTUh)	51.3	47.0	1.6	3.57E-03
PM (kg $PM2.5_{eq}$)	37.3	60.4	2.3	2.91E+01
IR-hh ($kBqU^{235}{}_{eq}$)	14.1	83.0	2.9	8.20E+03
POFP ($kgNMVOC_{eq}$)	31.2	67.5	1.3	1.46E+02
AP ($molH^{+}{}_{eq}$)	34.6	64.1	1.3	3.81E+02
EU_T ($molN_{eq}$)	31.0	67.7	1.4	4.69E+02
EU_F (kgP_{eq})	38.0	59.3	2.7	2.26E+01
EU_M (kgN_{eq})	46.4	52.4	1.2	5.97E+01
E_{Fw} (CTUe)	16.2	52.6	31.2	1.47E+06

Table 84. Life cycle impact assessment during the first battery use in the EV. Reuse battery scenario - Expanded.

Impact category	EV battery production (%)	Use in the EV (%)	Recycle (%)	Total
CED (MJ)	11.5	87.6	0.9	9.63E+05
ADP ($kgSb_{eq}$)	74.8	24.3	0.9	2.64E-01
GWP ($kgCO_{2eq}$)	12.5	86.7	0.9	5.59E+04
ODP ($kgCFC\text{-}11_{eq}$)	9.0	89.2	1.8	5.92E-03
HT-nce (CTUh)	42.2	55.9	2.0	1.34E-02
HT-ce (CTUh)	35.9	63.0	1.1	2.67E-03
PM (kg $PM2.5_{eq}$)	24.0	74.5	1.5	2.36E+01
IR-hh ($kBqU^{235}{}_{eq}$)	8.0	90.3	1.6	7.55E+03
POFP ($kgNMVOC_{eq}$)	19.3	79.9	0.8	1.23E+02
AP ($molH^{+}{}_{eq}$)	21.8	77.4	0.8	3.16E+02
EU_T ($molN_{eq}$)	19.1	80.0	0.8	3.97E+02
EU_F (kgP_{eq})	24.7	73.6	1.7	1.83E+01
EU_M (kgN_{eq})	31.4	67.8	0.8	4.62E+01
E_{Fw} (CTUe)	10.9	67.9	21.1	1.41E+06

6 Conclusions

Coupling the electrification of end-use services in the transportation and building sectors with low - carbon electricity generation, through the exploitation of RESs, has been recognised as a key strategy in the transition towards a more competitive, secure, sustainable and decarbonized EU economy.

In the building sector, the increasing penetration of the distributed electricity generation from RESs will result in an increasing demand of BESS in the near future in order to reduce the mismatch between the highly variable RESs generation and the building load. At the same time, in the transportation sector, due to the diffusion of the electric mobility, an increase of flows of waste batteries that need to be collected and treated is expected. According to several studies retired EV batteries retain enough capacity to be used in secondary applications.

In this context, this dissertation explores the life cycle environmental sustainability of a circular economy and industrial symbiosis inspired pathway. In detail, the reuse of retired EV battery as a storage stationary system in a residential nZEB is examined by using an integrated approach based on load match considerations and life – cycle environmental impacts.

The observations, conclusions and recommendations of each part of the dissertation are summarized in the following.

Part I: Life cycle assessment of the traction lithium-ion battery pack

Concerning the LCA of the EV lithium-ion battery pack reused in the stationary application, the analysis is carried out with reference to one battery pack by using both primary and literature data.

The data and results of this dissertation allow the expansion of the state of the art in relation to Li-ion traction batteries, providing one of the first contribution analyses of the materials in a LMO–NMC cell technology for PHEVs and one of the first assessment of the energy and environmental data related to its production and recycling processes.

The study confirms that the electricity required for cell assembly is responsible for the highest contribution in almost all the investigated environmental impacts categories. The amount of electricity required for cell assembly varies widely in the literature examined. For this reason it is considered a hot spot to be further investigated. However, the sensitivity analysis carried out with reference to this parameter highlights that, even when considering the lowest value available in the literature, battery production remains the stage with the greatest life cycle impact, and cell assembly remains the phase responsible for the greatest contribution to the cumulative energy demand, global warming potential and ozone depletion potential impact categories. Although it would be preferable to increase the reliability of the assessment by using primary data from battery manufacturers, the results obtained, nevertheless, allow to identify some key issues for decreasing the impact of EVs. In particular, reducing the electricity consumed during the battery production and using a low carbon electricity mix could provide a significant contribution in improving the environmental sustainability of the EVs, especially considering the target of reducing overall global warming potential.

With regard to the use phase, this accounts, on average, for about 20% of the overall life cycle impact. Moreover, a deeper analysis highlights that the impact of electricity losses due to battery efficiency can be up to 30% greater for certain impact categories than that due to battery transport. This outcome confirms that battery efficiency is a very important parameter for the battery use phase.

Finally, the results of the analysis of EoL treatment show that recycling the battery is environmentally beneficial for almost all of the impact categories examined; however, to increase the sustainability of traction battery production it is important to recover not only the valuable materials contained in the cells but also the materials contained in other battery components. With this in mind, battery components could be designed to enable easy and secure separation of the various material fractions and increase the recycling rates of those that are recoverable.

Considering that the production stage accounts for the highest impact in almost all the categories examined, and in all the configurations considered in the sensitivity analysis, a LCA based on primary data provided by the battery industry is urgently required, in particular for the energy consumed in cell assembly. This would allow a more reliable set of environmental data to be provided to decision makers to improve the design of future batteries.

Moreover, the obtained results suggests that consideration should be given to extending traction batteries' lifetime as a further strategy to increase their sustainability beyond the environmental benefits provided by recycling at EoL.

Part II: PV – BESS – electrical grid system: load match and net exported analysis results

The energy analysis of the PV – BESS – electrical grid system highlights that the installation of an increasing BESS size allows to reduce the electricity imported from the electrical grid and then to increase the building self-consumption of the electricity locally produced by PV. However, the analysis demonstrates that the improvement became negligible to justify the installation of a larger BESS exceeded a certain size based on the specific application.

In detail, for the examined nZEB, characterized by a PV peak power of 20 kW_p and an average yearly electricity demand of about 25 MWh, after reaching the thresholds of 46.5 kWh (corresponding to the employment of five retired EV batteries), the effect of the storage on the load match is very limited. The percentage variation between the γ_{load} obtained in the configuration with six EV batteries increases of a percentage lower than 3% compared with the value obtained in the configuration employing five EV batteries. At the same time, the additional technical benefits on the grid, related to the reduced electricity exported into the grid become negligible. This outcome demonstrates that it is important to perform an ex-ante and detailed modelling of the operational phase in order to identify the maximum size of the storage beyond which the obtained benefits could become marginal, and then avoid an unusual additional investment in terms of cost and resource employment.

The operational phase is extremely important since a large amount of electricity consumption is involved. Then, it is relevant to estimate energy flows based on detailed energy model and real data on RESs generation and building load in order to obtain reliable results. Modelling retired EV batteries as stationary energy storage systems requires the analysis of different parameters: retained capacity and battery charge/discharge efficiency after the first use in the EV, capacity and efficiency fade due to the battery degradation. These parameters affect the battery lifetime in the second life application; the lack of data in this field is reflected by the fact that in several studies the battery lifetime is based on manufacturer's warranty or assumptions. The aging of the EV batteries results not only in capacity fade but also in charge/discharge efficiency fade that further reduces the amount of electricity dischargeable. Therefore, further efforts to gather data about the aging model of the battery in both the first use in the EV and in the second use as stationary applications are needed to establish the suitability for a given second use application.

Part III: Life cycle impact assessment and interpretation - PV + BESS + electrical grid system

The installation of an increasing energy storage capacity causes an improvement of the energy system environmental performance in almost all the examined impact categories with the exception of the abiotic depletion potential, human toxicity – cancer and non cancer effect and freshwater ecotoxicity mainly related to the increasing consumption of the PV electricity generated on-site.

In general, the reduction of the electricity imported from the grid, due to the increasing size of the BESS, is mainly responsible for the impacts reduction. However, in general the environmental benefits are partially offset by the increasing impacts associated to the production of larger BESS and to the increasing consumption of the PV electricity generated on-site. Moreover, the adoption of energy storage system, reducing the amount of electricity fed into the grid, can help to solve the technical challenges, in terms of electrical grid stability and reliability caused by a higher penetration of RESs.

The contribution of the impacts related to the battery recycling and repurposing and to the electricity loss due to the battery efficiency are negligible in almost all the examined impact categories. Since, due to the high amount of electricity involved in the investigated system and the high impacts related to the battery production, the contributions of the production and operational phases are relevant. The exception is represented by the human toxicity – non cancer effect impact category in which the battery repurposing presents a not negligible contribution. Due to a lack of data, in this dissertation the repurposing stage is modelled based on literature studies. However, more efforts are needed to gather more detailed information and primary data for future analysis.

The obtained results suggest that although the integration of storage systems allows the improvement of the environmental sustainability of the electricity supply in a residential building equipped with RESs in almost all the impact categories examined, it is necessary to improve the technologies currently available in order to obtain better performance in a wide range of environmental impact categories. In particular, it is relevant to improve the design of the PV system (in terms of resources efficiency and the chemical toxicity control) and the battery production process in order to increase the environmental performance both in the automotive (first life application) and in the building sector (second life application).

Part IV: Identification of the best configuration in terms of load match and life cycle environmental impacts

The integration of the results obtained in the load match analysis and the life cycle assessment allow to identify the configuration that could represent the best BESS size in terms of load matching and environmental sustainability. In detail, for the examined nZEB, the installation of a BESS capacity of 46.5 kWh (corresponding to the employment of five retired EV batteries) results the best solution. In fact, both the environmental and load match improvement achievable increasing the BESS are negligible. This consideration could be supported also by economic consideration, if a market for retired EV battery will develop in the future, since in this case configuration with a lower number, less expensive, will be more appreciate.

Considering that RESs can play a key role in the decarbonisation of the building sector and that storage systems are needed to increase the reliability of the electricity supply, the sizing approach proposed can be useful during the preliminary design of BESS made with retired EV batteries or with fresh batteries in buildings.

Part V: Comparison of the life cycle environmental impacts associated to "reuse battery scenario" with the "reference scenario" and with the configuration of the "fresh battery scenario".

The comparison between the reuse battery scenario and the reference battery scenario (scenario without energy storage system) highlights that the second life use of the retired EV batteries as stationary storage system in a residential application improves the environmental sustainability of providing the electricity required by the building. In detail, the reuse battery scenario allows significant improvement in almost all the examined impact categories compared with the reference scenario. The exceptions are the abiotic depletion potential, human toxicity cancer and non cancer effect and freshwater ecotoxicity, due to the increased electricity consumption from PV and to the BESS production process. Then, the same consideration of the Part III about the need to improve the technologies currently available can be done.

Concerning the comparison between the reuse and the fresh battery scenario, from the analysis results that, under the assumption made in this dissertation, they are equivalent in terms of energy and environmental impacts. Since, in order to compare the scenarios based on an equivalent function, four fresh EV batteries are needed to perform the same function of five retired EV batteries. However, considering the volume of EV batteries expected in the near future, key uncertainties surround the emergence and management of this increasing number of EV batteries in the waste stream and the ability of domestic recycling infrastructure to recover scarce and valuable materials from a highly variable mix of discarded batteries. In this context, potential benefits could arise by reusing retired EV batteries as stationary storage system in second life applications as this can delay the recycling process up to 10 years permitting the development of new recycling technologies and practices allowing a high rate of recovery.

The potential benefits related to the extension of the EV batteries lifetime and the partitioning of the environmental impacts between the EV and the stationary applications are offset by the lower number of fresh EV battery employed, by the higher lifetime and charge/discharge efficiency of the fresh batteries compared to the retired ones.

This is an important outcome of the dissertation, demonstrating the relevance of comparing the product system based on an equivalent function in order to avoid misleading results.

The expansion of the system boundaries in order to include also the first life in the EV and to assess the environmental sustainability of the proposed circular economy application in a wide perspective shows that reusing EV batteries as stationary storage system in residential building can enhance the environmental sustainability of each economic sector involved.

However, because the novelty of the topic and the limited available primary data about the key parameters of the energy model, that affect also the environmental impacts (e.g. charge/discharge efficiency and battery lifetime), more investigation are needed to confirm these results.

References

[1] H. Winkler, Closed-loop production systems-A sustainable supply chain approach, CIRP J. Manuf. Sci. Technol. (2011). doi:10.1016/j.cirpj.2011.05.001.

[2] European Commission, Communication from the Commission to the European Parliament, the Council, the European Economic and Social Committee and the Committee of the Regions Next steps for a sustainable European future European action for sustainability. COM(2016) 739 final. St, (2016).

[3] European Environmental Agency, Environmental indicator - Report 2014 Environmental impacts of Production - Consumption system in Europe., 2014. doi:10.2800/22394.

[4] K. Richa, C.W. Babbitt, G. Gaustad, Eco-Efficiency Analysis of a Lithium-Ion Battery Waste Hierarchy Inspired by Circular Economy, J. Ind. Ecol. 21 (2017) 715–730. doi:10.1111/jiec.12607.

[5] European Commission, Communication from the Commission to the European Parliament, the Council, the European Economic and Social Committee and the Committee of the Regions - Towards a circular economy: A zero waste programme for Europe. COM(2014) 398 final, Brussels, 2.7.2014, (2014) 14.

[6] European Commission, Communication from the Commission to the European Parliament, the Council, the European Economic and Social Committee and the Committee of the Regions. Closing the loop - An EU action plan for the Circular Economy. COM(2015) 614 final. Brussels, 2.12.2015, (2015).

[7] European Commission, Communication from the Commission to the European Parliament, the Council, the European Economic and Social Committee and the Committee of the Regions on a monitoring framework for the circular economy. COM(2018) 29 final. Strasbourg, 16.1.2018, (2018).

[8] Deloitte Sustainability, Circular economy potential for climate change mitigation, (2016) 0–43.

[9] European Commission, Green Paper - A 2030 framework for climate and energy policies, (2013) 16.

[10] European Commission, Communication from the Commission to the European Parliament, the Council, the Euro-pean Economic and Social Committee and the Committee of the Regions A policy frame-work for climate and energy in the period from 2020 to 2030, COM/2014/015 final., (2014).

[11] United Nations, Resolution adopted by the General Assembly on 25 September 2015. Transforming our world: the 2030 Agenda for Sustainable Development, 16301 (2015) 1–35.

[12] European Commission, Circular Economy - Implementation of the Circular Economy Action Plan. http://ec.europa.eu/environment/circular-economy/index_en.htm, (2018).

[13] European Parliament and Council, Directive 2008/98/EC of the European Parliament and of the Council of 19 November 2008 on waste and repealing certain directives, Off. J. Eur. Union. (2008) 3–30. doi:2008/98/EC.; 32008L0098.

[14] D. D'Agostino, P. Zangheri, Development of the NZEBs concept in Member States, EUR 28252 EN, 2016. doi:10.2788/278314.

[15] European Commission, Factsheet: The revised Energy Performance of Buildings Directive (EPBD), Energy Perform. Build. Dir. (2018) 1–6. doi:http://dx.doi.org/10.1080/19768354.2010.504347.

[16] Eurostat, Eurostat - Statistics explained. Energy consumption in households. https://ec.europa.eu/eurostat/statistics-explained/index.php/Energy_consumption_in_households., (2018).

[17] European Commission, Buildings. https://ec.europa.eu/energy/en/topics/energy-efficiency/buildings, (2018).

[18] European Environment Agency (EEA), Greenhouse gas emissions from transport. https://www.eea.europa.eu/data-and-maps/indicators/transport-emissions-of-greenhouse-gases/transport-emissions-of-greenhouse-gases-10, (2018).

[19] European Environment Agency, GHG emissions by aggregated sector. https://www.eea.europa.eu/data-and-maps/daviz/ghg-emissions-by-aggregated-sector-1#tab-used-in-indicators., (2017).

[20] P. Finocchiaro, M. Beccali, M. Cellura, F. Guarino, S. Longo, Life Cycle Assessment of a

compact Desiccant Evaporative Cooling system: The case study of the “Freescoo,” Sol. Energy Mater. Sol. Cells. 156 (2016) 83–91. doi:10.1016/j.solmat.2016.03.026.

[21] M. Cellura, F. Guarino, S. Longo, M. Mistretta, Modeling the energy and environmental life cycle of buildings: A co-simulation approach, Renew. Sustain. Energy Rev. 80 (2017) 733–742. doi:10.1016/j.rser.2017.05.273.

[22] T. Spencer, R. Pierfederici, O. Sartor, N. Berghmans, S. Samadi, M. Fischedick, K. Knoop, S. Pye, P. Criqui, S. Mathy, P. Capros, P. Fragkos, M. Bukowski, A. Śniegocki, M. Rosa Virdis, M. Gaeta, K. Pollier, C. Cassisa, Tracking sectoral progress in the deep decarbonisation of energy systems in Europe, Energy Policy. 110 (2017) 509–517. doi:10.1016/j.enpol.2017.08.053.

[23] European Commision, Roadmap 2050, Policy. (2012) 1–9. doi:10.2833/10759.

[24] European Commission, Communication from the Commission: A Roadmap for moving to a competitive low carbon economy in 2050, COM(2011) 112 Final. 34 (2011) 1–34. doi:10.1002/jsc.572.

[25] Eurelectric - Electricity for Europe, Electrification of European energy demand. https://www.eurelectric.org/the-european-power-sector-in-transition/electrification-of-european-energy-demand/., (2016).

[26] IPCC, Climate Change 2014: Mitigation of Climate Change. Contribu-tion of Working Group III to the Fifth Assessment Report of the Intergovernmen-tal Panel on Climate Change [Edenho-fer, O., R. Pichs-Madruga, Y. Sokona, E. Farahani, S. Kadner, K. Seyboth, A. Adl, (2014).

[27] T. Bruckner, I. Bashmakov, Y. Mulugetta, A. Chum, A. de la V. Navarro, J. Edmonds, A. Faaij, B. Fungtammasan, A. Garg, E. Hertwich, D. Honnery, D. Infield, M. Kainuma, S. Khennas, S. Kim, H. Nimir, K. Riahi, N. Strachan, R. Wiser, X. Zhang, Energy Systems. In: Climate Change 2014: Mitigation of Climate Change. Contribution of Working Group III to the Fifth Assessment Report of the Intergovernmental Panel on Climate Change [Edenhofer, O., R. Pichs-Madruga, Y. Sokona, E. Farahani, S. Kadner, K, (2014).

[28] Eurostat, Renewable energy statistics. https://ec.europa.eu/eurostat/statistics-

explained/index.php/Renewable_energy_statistics#Renewable_energy_produced_in_the_EU_increased_by_two_thirds_in_2006-2016, (2018).

[29] M. Beccali, M. Cellura, M. Mistretta, Environmental effects of energy policy in sicily: The role of renewable energy, Renew. Sustain. Energy Rev. (2007). doi:10.1016/j.rser.2005.02.001.

[30] M. Cellura, A. Di Gangi, S. Longo, A. Orioli, An Italian input-output model for the assessment of energy and environmental benefits arising from retrofit actions of buildings, Energy Build. 62 (2013) 97–106. doi:10.1016/j.enbuild.2013.02.056.

[31] European Commission, IRENA, Renewable Energy Prospects for the European Union, 2018.

[32] EU, Directive 2010/31/EU of the European Parliament and of the Council of 19 May 2010 on the energy performance of buildings (recast), Off. J. Eur. Union. (2010) 13–35. doi:doi:10.3000/17252555.L_2010.153.eng.

[33] European Union, Directive 2006/66/EC of the European Parliament and of the Council of 6 September 2006 on batteries and accumulators and waste batteries and accumulators and repealing Directive 91/157/EEC, Off. J. Eur. Union. L 266 (2006) 1–14. doi:12.12.2013.

[34] European Union, Directive (EU) 2018/844 of the European Parliament and of the Council of 30 May 2018 amending Directive 2010/31/EU on the energy performance of buildings and Directive 2012/27/EU on energy efficiency, Off. J. Eur. Union. 2018 (2018) 75–91.

[35] M. Sandhu, T. Thakur, Issues, Challenges, Causes, Impacts and Utilization of Renewable Energy Sources - Grid Integration, J. Eng. Res. Appl. (2014).

[36] F. Guarino, P. Cassarà, S. Longo, M. Cellura, E. Ferro, Load match optimisation of a residential building case study: A cross-entropy based electricity storage sizing algorithm, Appl. Energy. 154 (2015) 380–391. doi:10.1016/j.apenergy.2015.04.116.

[37] F. Guarino, S. Longo, G. Tumminia, M. Cellura, M. Ferraro, Ventilative cooling application in Mediterranean buildings: impacts on grid interaction and load match, Int. J. Vent. (2017). doi:10.1080/14733315.2016.1214389.

[38] M. Ferraro, F. Sergi, V. Antonucci, F. Guarino, G. Tumminia, M. Cellura, Load match and grid interaction optimization of a net zero energy building through electricity storage: An Italian case-study, in: EEEIC 2016 - Int. Conf. Environ. Electr. Eng., 2016.

doi:10.1109/EEEIC.2016.7555812.

[39] European Commission, COMMISSION STAFF WORKING DOCUMENT Energy storage – the role of electricity EN, (2017) 1–25. https://ec.europa.eu/energy/sites/ener/files/documents/swd2017_61_document_travail_service_part1_v6.pdf.

[40] A. Purvins, H. Wilkening, G. Fulli, E. Tzimas, G. Celli, S. Mocci, F. Pilo, S. Tedde, A European supergrid for renewable energy: Local impacts and far-reaching challenges, J. Clean. Prod. (2011). doi:10.1016/j.jclepro.2011.07.003.

[41] J.M. Santos, P.S. Moura, A.T. de Almeida, Technical and economic impact of residential electricity storage at local and grid level for Portugal, Appl. Energy. 128 (2014) 254–264. doi:10.1016/j.apenergy.2014.04.054.

[42] A. Hermelink, S. Schimschar, T. Boermans, L. Pagliano, P. Zangheri, R. Armani, K. Voss, E. Musall, Towards nearly zero- energy buildings: Definition of common principles under the EPBD, Ecofys Eur. Union. (2013) 467. doi:10.1016/j.annfar.2009.12.001.

[43] B. Gohla-Neudecker, M. Bowler, S. Mohr, Battery 2nd life: Leveraging the sustainability potential of EVs and renewable energy grid integration, in: 5th Int. Conf. Clean Electr. Power Renew. Energy Resour. Impact, ICCEP 2015, 2015: pp. 311–318. doi:10.1109/ICCEP.2015.7177641.

[44] European Commission, A European Strategy for Low-Emission Mobility, 2016.

[45] International Energy Agency (IEA), Global EV Outlook 2018. Towards cross-modal electrification, (2018). doi:EIA-0383(2016).

[46] European Environment Agency, Renewable Energy in Europe - 2017 Update, 2017. doi:10.2800/313983.

[47] European Energy Agency, Electric Vehicles in Europe., 2016. doi:10.2800/100230.

[48] U.S. EPA, Application of Life-Cycle Assessment to Nanoscale Technology: Lithium-ion Batteries for Electric Vehicles, United States Environ. Prot. Agency. (2013) 1–119. doi:10.1038/nchem.2085.

[49] International Energy Agency - IEA, Energy Technology Perspectives 2017 - Executive

Summary, Iea. (2017) 371. doi:10.1787/energy_tech-2014-en.

[50] International Energy Agency, Global EV Outlook 2017, IEA Publ. (2017) 1–71. doi:10.1787/9789264278882-en.

[51] S.M. Schexnayder, S. Das, R. Dhingra, J.G. Overly, B.E. Tonn, J.H. Peretz, G. Waidley, G.A. Davis, Environmental evaluation of new generation vehicles and vehicle components, 2001. http://www-cta.ornl.gov/cta/Publications/Reports/ORNL_TM_2001_266.pdf.

[52] P. Van den Bossche, F. Vergels, J. Van Mierlo, J. Matheys, W. Van Autenboer, SUBAT: An assessment of sustainable battery technology, J. Power Sources. 162 (2006) 913–919. doi:10.1016/j.jpowsour.2005.07.039.

[53] S. Vazquez, S.M. Lukic, E. Galvan, L.G. Franquelo, J.M. Carrasco, Energy Storage Systems for Transport and Grid Applications, IEEE Trans. Ind. Electron. 57 (2010) 3881–3895. doi:10.1109/TIE.2010.2076414.

[54] L.A.W. Ellingsen, G. Majeau-Bettez, B. Singh, A.K. Srivastava, L.O. Valøen, A.H. Strømman, Life Cycle Assessment of a Lithium-Ion Battery Vehicle Pack, J. Ind. Ecol. 18 (2014) 113–124. doi:10.1111/jiec.12072.

[55] A. Ciocia, J. Ahmad, G. Chicco, P. Di Leo, F. Spertino, Optimal size of photovoltaic systems with storage for office and residential loads in the Italian net-billing scheme, in: Proc. - 2016 51st Int. Univ. Power Eng. Conf. UPEC 2016, 2017: pp. 1–6. doi:10.1109/UPEC.2016.8114082.

[56] B. Simon, S. Ziemann, M. Weil, Potential metal requirement of active materials in lithium-ion battery cells of electric vehicles and its impact on reserves: Focus on Europe, Resour. Conserv. Recycl. (2015). doi:10.1016/j.resconrec.2015.07.011.

[57] C. Samaras, K. Meisterling, Life Cycle Assessment of Greenhouse Gas Emissions from Plug-in Hybrid Vehicles: Implications for Policy, Environ. Sci. Technol. 42 (2008) 3170–3176. doi:10.1021/es702178s.

[58] T.R. Hawkins, B. Singh, G. Majeau-Bettez, A.H. Strømman, Comparative Environmental Life Cycle Assessment of Conventional and Electric Vehicles, J. Ind. Ecol. 17 (2013) 53–64. doi:10.1111/j.1530-9290.2012.00532.x.

[59] S. Longo, V. Antonucci, M. Cellura, M. Ferraro, Life cycle assessment of storage systems: The case study of a sodium/nickel chloride battery, J. Clean. Prod. 85 (2014) 337–346. doi:10.1016/j.jclepro.2013.10.004.

[60] L. Ahmadi, A. Yip, M. Fowler, S.B. Young, R.A. Fraser, Environmental feasibility of re-use of electric vehicle batteries, Sustain. Energy Technol. Assessments. 6 (2014) 64–74. doi:10.1016/j.seta.2014.01.006.

[61] L. Oliveira, M. Messagie, S. Rangaraju, J. Sanfelix, M. Hernandez Rivas, J. Van Mierlo, Key issues of lithium-ion batteries - From resource depletion to environmental performance indicators, J. Clean. Prod. (2015). doi:10.1016/j.jclepro.2015.06.021.

[62] S.H. Mohr, G. Mudd, D. Giurco, Lithium Resources and Production: Critical Assessment and Global Projections, Minerals. (2012). doi:10.3390/min2010065.

[63] L. Gaines, P. Nelson, Lithium-ion batteries: examining material demand and recycling issues, Miner. Met. Mater. Soc. 420 Commonw. Dr., P. O. Box 430 Warrendale PA 15086 USA.[Np]. 14-18 Feb. (2010). doi:10.1111/j.1439-0426.2008.01098.x.

[64] M. Zackrisson, L. Avellán, J. Orlenius, Life cycle assessment of lithium-ion batteries for plug-in hybrid electric vehicles-Critical issues, J. Clean. Prod. 18 (2010) 1517–1527. doi:10.1016/j.jclepro.2010.06.004.

[65] G. Majeau-Bettez, T.R. Hawkins, A.H. StrØmman, Life cycle environmental assessment of lithium-ion and nickel metal hydride batteries for plug-in hybrid and battery electric vehicles, Environ. Sci. Technol. 45 (2011) 4548–4554. doi:10.1021/es103607c.

[66] T. Schmidt, M. Buchert, L. Schebek, Investigation of the primary production routes of nickel and cobalt products used for Li-ion batteries, Resour. Conserv. Recycl. (2016). doi:10.1016/j.resconrec.2016.04.017.

[67] N. Lebedeva, F. Di Persio, L. Boon-brett, Lithium ion battery value chain and related opportunities for Europe, EUR 28534 EN, Publications Office of the European Union, Luxembourg, 2016. doi:10.2760/6060, JRC105010.

[68] Science for Environment Policy, Towards the battery of the future. Future Brief 20. Brief produced for the European Commission DG Environment by the Science Communication Unit,

UWE, Bristol. Available at: http://ec.europa.eu/science-environment-policy, 2018. doi:10.2779/610526.

[69] D.A. Notter, M. Gauch, R. Widmer, W.A. Patrick, A. Stamp, R. Zah, R.G. Althaus, Contribution of Li-Ion Batteries to the Environmental Impact of Electric Vehicles, 44 (2010) 6550–6556.

[70] F. Mathieux, F. Ardente, S. Bobba, P. Nuss, G. Blengini, P. Alves Dias, D. Blagoeva, C. Torres De Matos, D. Wittmer, C. Pavel, T. Hamor, H. Saveyn, B. Gawlik, G. Orveillon, D. Huygens, E. Garbarino, E. Tzimas, F. Bouraoui, S. Solar, Critical raw materials and the circular economy - Background report, 2017. doi:10.2760/378123.

[71] European Commission, COMMUNICATION FROM THE COMMISSION TO THE EUROPEAN PARLIAMENT, THE COUNCIL, THE EUROPEAN ECONOMIC AND SOCIAL COMMITTEE AND THE COMMITTEE OF THE REGIONS on the 2017 list of Critical Raw Materials for the EU, (2017).

[72] G.A. Blengini, D. Blagoeva, J. Dewulf, C. Torres de Matos, V. Nita, B. Vidal-Legaz, C.E.L. Latunussa, Y. Kayam, L. Talens Peirò, C. Baranzelli, S. Manfredi, L. Mancini, P. Nuss, A. Marmier, P. Alves-Dias, C. Pavel, E. Tzimas, F. Mathieux, D. Pennington, C. Ciupagea, JRC Technical reports - Assessment of the Methodology for Establishing the EU List of Critical Raw Materials, 2017. doi:10.2760/73303.

[73] European Commission, Communication from the Commission to the European Parliament, the Council, the European Economic and Social Committee and the Committee of the Regions Roadmap to a Resource Efficient Europe. COM(2011) 571 final. Brussels, 20.9.2011, (2011).

[74] European Union, Directive 2000/53/EC of the European Parliament and of the Council of 18 September 2000 on end-of life vehicles, Off. J. Eur. Union. L (2000) 34–42. doi:10.1016/j.jclepro.2010.02.014.

[75] EU, Directive 2006/66/EC of the European Parliament and of the Council of 6 September 2006 on batteries and accumulators and waste batteries and accumulators and repealing Directive 91/157/EEC, OJ L 266, 2006.

[76] A. Chagnes, B. Pospiech, A brief review on hydrometallurgical technologies for recycling

spent lithium-ion batteries, J. Chem. Technol. Biotechnol. 88 (2013) 1191–1199. doi:10.1002/jctb.4053.

[77] European Commission, Study on the review of the list of Critical Raw Materials Criticality Assessments, 2017.

[78] J. Dewulf, G. Van der Vorst, K. Denturck, H. Van Langenhove, W. Ghyoot, J. Tytgat, K. Vandeputte, Recycling rechargeable lithium ion batteries: Critical analysis of natural resource savings, Resour. Conserv. Recycl. 54 (2010) 229–234. doi:10.1016/j.resconrec.2009.08.004.

[79] T.P. Hendrickson, O. Kavvada, N. Shah, R. Sathre, C. D Scown, Life-cycle implications and supply chain logistics of electric vehicle battery recycling in California, Environ. Res. Lett. 10 (2015). doi:10.1088/1748-9326/10/1/014011.

[80] J.B. Dunn, L. Gaines, M. Barnes, J. Sullivan, M.Q. Wang, Material and Energy Flows in the Materials Production, Assembly, and End-of-Life Stages of the Automotive Lithium-Ion Battery Life Cycle, J. Chem. Inf. Model. 53 (2012) 1689–1699. doi:10.1017/CBO9781107415324.004.

[81] K. Richa, C.W. Babbitt, G. Gaustad, X. Wang, A future perspective on lithium-ion battery waste flows from electric vehicles, Resour. Conserv. Recycl. 83 (2014) 63–76. doi:10.1016/j.resconrec.2013.11.008.

[82] K. Fisher, E. Wallén, Battery waste management life cycle assessment, Environ. Resour. Manag. (2006) 0–3. http://www.lcm2007.ethz.ch/paper/424.pdf.

[83] L. Gaines, The future of automotive lithium-ion battery recycling: Charting a sustainable course, Sustain. Mater. Technol. 1 (2014) 2–7. doi:10.1016/j.susmat.2014.10.001.

[84] J. Heelan, E. Gratz, Z. Zheng, Q. Wang, M. Chen, D. Apelian, Y. Wang, Current and Prospective Li-Ion Battery Recycling and Recovery Processes, JOM. (2016). doi:10.1007/s11837-016-1994-y.

[85] E. Cready, J. Lippert, J. Pihl, I. Weinstock, P. Symons, Technical and Economic Feasibility of Applying Used EV Batteries in Stationary Applications, Other Inf. PBD 1 Mar 2003. (2003) Medium: ED; Size: 130 pages. doi:SAND2002-4084.

[86] G. Lacey, G. Putrus, A. Salim, The use of second life electric vehicle batteries for grid support,

IEEE EuroCon 2013. (2013) 1255–1261. doi:10.1109/EUROCON.2013.6625141.

[87] R. Faria, P. Marques, R. Garcia, P. Moura, F. Freire, J. Delgado, A.T. De Almeida, Primary and secondary use of electric mobility batteries from a life cycle perspective, J. Power Sources. 262 (2014) 169–177. doi:10.1016/j.jpowsour.2014.03.092.

[88] L. Ahmadi, S.B. Young, M. Fowler, R.A. Fraser, M.A. Achachlouei, A cascaded life cycle: reuse of electric vehicle lithium-ion battery packs in energy storage systems, Int. J. Life Cycle Assess. 22 (2017) 111–124. doi:10.1007/s11367-015-0959-7.

[89] S. Bobba, F. Mathieux, F. Ardente, G.A. Blengini, M.A. Cusenza, A. Podias, A. Pfrang, Life Cycle Assessment of repurposed electric vehicles batteries : an adapted method based on modelling of energy flows, J. Energy Storage. 19 (2018) 213–225. doi:10.1016/j.est.2018.07.008.

[90] R. Hein, P.R. Kleindorfer, S. Spinler, Valuation of electric vehicle batteries in vehicle-to-grid and battery-to-grid systems, Technol. Forecast. Soc. Change. (2012). doi:10.1016/j.techfore.2012.06.002.

[91] A.F. Burke, Performance, Charging, and Second-use Considerations for Lithium Batteries for Plug-in Electric Vehicles, 2009. doi:10.1007/s11116-007-9132-x.

[92] L. Ahmadi, M. Fowler, S.B. Young, R.A. Fraser, B. Gaffney, S.B. Walker, Energy efficiency of Li-ion battery packs re-used in stationary power applications, Sustain. Energy Technol. Assessments. 8 (2014) 9–17. doi:10.1016/j.seta.2014.06.006.

[93] R.T. Long, M. Kahn, C. Mikolajczak, Lithium-ion battery hazards. Fire Protection Engineering. https://www.sfpe.org/page/2012_Q4_2/Lithium-Ion-Battery-Hazards.htm, (n.d.).

[94] C. Heymans, S.B. Walker, S.B. Young, M. Fowler, Economic analysis of second use electric vehicle batteries for residential energy storage and load-levelling, Energy Policy. 71 (2014) 22–30. doi:10.1016/j.enpol.2014.04.016.

[95] L.C. Casals, B.A. García, F. Aguesse, A. Iturrondobeitia, Second life of electric vehicle batteries: relation between materials degradation and environmental impact, Int. J. Life Cycle Assess. 22 (2017) 82–93. doi:10.1007/s11367-015-0918-3.

[96] C. Koch-Ciobotaru, A. Saez-De-Ibarra, E. Martinez-Laserna, D.I. Stroe, M. Swierczynski, P.

Rodriguez, Second life battery energy storage system for enhancing renewable energy grid integration, 2015 IEEE Energy Convers. Congr. Expo. ECCE 2015. (2015) 78–84. doi:10.1109/ECCE.2015.7309672.

[97] A. Tamiang, D. Angka, Electrode and Cells Manufacturing White Paper - Chapter 5: Batteries and End of Life Management, ELIBAMA (European Li-ion Battery Advanced Manufacturing for Electric Vehicles), (2014) Available at: https://elibama. wordpress.com/electrodes-and-cells-manuf, 2014.

[98] S.J. Tong, A. Same, M.A. Kootstra, J.W. Park, Off-grid photovoltaic vehicle charge using second life lithium batteries: An experimental and numerical investigation, Appl. Energy. (2013). doi:10.1016/j.apenergy.2012.11.046.

[99] R. Sathre, C.D. Scown, O. Kavvada, T.P. Hendrickson, Energy and climate effects of second-life use of electric vehicle batteries in California through 2050, J. Power Sources. (2015). doi:10.1016/j.jpowsour.2015.04.097.

[100] J. Neubauer, A. Pesaran, The ability of battery second use strategies to impact plug-in electric vehicle prices and serve utility energy storage applications, J. Power Sources. 196 (2011) 10351–10358. doi:10.1016/j.jpowsour.2011.06.053.

[101] C.K. Narula, R. Martinez, O. Onar, M.R. Starke, G. Andrews, ORNL, Final Report: Economic analysis of deploying used batteries in power systems, 2011.

[102] B. Williams, T. Lipman, Analysis of the Combined Vehicle - Use Value of Lithiumion Plug-In-Vehicle Propulsion Batteries - Task 3, Second Life Applications and Value of “Traction” Lithium batteries, (2011)., 2011.

[103] V. V. Viswanathan, M. Kintner-Meyer, Second use of transportation batteries: Maximizing the value of batteries for transportation and grid services, IEEE Trans. Veh. Technol. (2011). doi:10.1109/TVT.2011.2160378.

[104] K. Richa, C.W. Babbitt, N.G. Nenadic, G. Gaustad, Environmental trade-offs across cascading lithium-ion battery life cycles, Int. J. Life Cycle Assess. 22 (2015) 66–81. doi:10.1007/s11367-015-0942-3.

[105] A. Saez-De-Ibarra, E. Martinez-Laserna, C. Koch-Ciobotaru, P. Rodriguez, D.I. Stroe, M.

Swierczynski, Second life battery energy storage system for residential demand response service, in: Proc. IEEE Int. Conf. Ind. Technol., 2015. doi:10.1109/ICIT.2015.7125532.

[106] European Union, Directive 2012/19/EU of the European Parliament and of the Council of 4 July 2012 on waste electrical and electronic equipment (WEEE) (recast), Off. J. Eur. Union L197/38. (2012) 38–71. doi:10.3000/19770677.L_2012.197.eng.

[107] S. Bobba, A. Podias, F. Di Persio, M. Messagie, P. Tecchio, M.A. Cusenza, U. Eynard, F. Mathieux, A. Pfrang, Sustainability Assessment of Second Life Application of Automotive Batteries (SASLAB): JRC Exploratory Research (2016-2017): Final technical report: August 2018; EUR 29321 EN, Publications Office of the European Union, Luxembourg, 2018, JRC112543, 2018. doi:10.2760/53624.

[108] P. Bronski, J. Creyts, M.C. X, S. Doig, J. Glassmire, H. Energy, P. Lilienthal, H. Energy, B. Rader, D. Seif, T. Butler, The economics of load defection how grid-connected solar-plus battery systems will compete with traditional electric service, why it matters, and possible paths forward, (2015).

[109] A. Assunção, P.S. Moura, A.T. de Almeida, Technical and economic assessment of the secondary use of repurposed electric vehicle batteries in the residential sector to support solar energy, Appl. Energy. 181 (2016) 120–131. doi:10.1016/j.apenergy.2016.08.056.

[110] S. Shokrzadeh, E. Bibeau, Repurposing Batteries of Plug-In Electric Vehicles to Support Renewable Energy Penetration in the Electric Grid, (2012). doi:10.4271/2012-01-0348.

[111] L. Ahmadi, S.B. Young, M. Fowler, R.A. Fraser, M.A. Achachlouei, A cascaded life cycle: reuse of electric vehicle lithium-ion battery packs in energy storage systems, Int. J. Life Cycle Assess. 22 (2017) 111–124. doi:10.1007/s11367-015-0959-7.

[112] M. Beccali, M. Cellura, S. Longo, F. Guarino, Solar heating and cooling systems versus conventional systems assisted by photovoltaic: Application of a simplified LCA tool, Sol. Energy Mater. Sol. Cells. (2016). doi:10.1016/j.solmat.2016.03.025.

[113] ISO, ISO 14040: Environmental management — Life Cycle Assessment — Principles and Framework, 2006. doi:10.1002/jtr.

[114] ISO, ISO 14044: Environmental management — Life cycle assessment — Requirements and

guidelines, 2006. doi:10.1136/bmj.332.7555.1418.

[115] J. Weniger, T. Tjaden, J. Bergner, V. Quaschning, Sizing of Battery Converters for Residential PV Storage Systems, in: Energy Procedia, 2016. doi:10.1016/j.egypro.2016.10.092.

[116] J.F. Peters, M. Baumann, B. Zimmermann, J. Braun, M. Weil, The environmental impact of Li-Ion batteries and the role of key parameters – A review, Renew. Sustain. Energy Rev. 67 (2017) 491–506. doi:10.1016/j.rser.2016.08.039.

[117] L.A.W. Ellingsen, C.R. Hung, A.H. Strømman, Identifying key assumptions and differences in life cycle assessment studies of lithium-ion traction batteries with focus on greenhouse gas emissions, Transp. Res. Part D Transp. Environ. 55 (2017) 82–90. doi:10.1016/j.trd.2017.06.028.

[118] M.A. Cusenza, S. Bobba, F. Ardente, M. Cellura, F. Di Persio, Energy and environmental assessment of a traction lithium-ion battery pack for plug-in hybrid electric vehicles, Under Rev. J. Clean. Prod. (Ref. No. JCLEPRO-D-18-04856). (2018).

[119] IPCC, IPCC Climate Change Fourth Assessment Report: Climate Change 2007. http://www.ipcc.ch/ipccreports/assessments-reports.htm, 2007.

[120] H.C. Kim, T.J. Wallington, R. Arsenault, C. Bae, S. Ahn, J. Lee, Cradle-to-Gate Emissions from a Commercial Electric Vehicle Li-Ion Battery: A Comparative Analysis, Environ. Sci. Technol. 50 (2016) 7715–7722. doi:10.1021/acs.est.6b00830.

[121] Miljøbil Grenland, Bill of materials. Porsgrunn, Norway., (2012).

[122] R. Frischknecht, N. Jungbluth, H. Althaus, G. Doka, R. Dones, T. Heck, S. Hellweg, R. Hischier, T. Nemecek, G. Rebitzer, M. Spielmann, G. Wernet, Overview and Methodology, Ecoinvent Cent. (2007) 1–77. http://www.ecoinvent.org/fileadmin/documents/en/01_OverviewAndMethodology.pdf.

[123] R. Hischier, M. Classen, M. Lehmann, Life Cycle Inventories of Electric and Electronic Equipment : Production , Use and Disposal, Cycle. 0 (2007) 116. doi:10.1038/nnano.2007.139.

[124] B. Li, X. Gao, J. Li, C. Yuan, Life cycle environmental impact of high-capacity lithium ion battery with silicon nanowires anode for electric vehicles, Environ. Sci. Technol. 48 (2014) 3047–3055. doi:10.1021/es4037786.

[125] U.S. EPA, Application of Life-Cycle Assessment to Nanoscale Technology: Lithium-ion Batteries for Electric Vehicles, 2013. doi:10.1038/nchem.2085.

[126] R. Frischknecht, N. Jungbluth, H.-J. Althaus, G. Doka, R. Dones, T. Heck, S. Hellweg, R. Hischier, T. Nemecek, G. Rebitzer, M. Spielmann, The ecoinvent Database: Overview and Methodological Framework (7 pp), Int. J. Life Cycle Assess. 10 (2005) 3–9. doi:10.1065/lca2004.10.181.1.

[127] L. Gaines, R. Cuenca, Costs of Lithium-Ion Batteries for Vehicles, Energy. 48 (2000) 73. doi:10.1002/art.10781.

[128] C.J. Rydh, B.A. Sandén, Energy analysis of batteries in photovoltaic systems. Part I: Performance and energy requirements, Energy Convers. Manag. 46 (2005) 1957–1979. doi:10.1016/j.enconman.2004.10.003.

[129] Saft, Batteries Annual Report. Saft Batteries, Bagnolet,France., 2008.

[130] C.J. Rydh, B.A. Sandén, Energy analysis of batteries in photovoltaic systems. Part II: Energy return factors and overall battery efficiencies, Energy Convers. Manag. (2005). doi:10.1016/j.enconman.2004.10.004.

[131] J. Matheys, W. Van Autenboer, SUBAT: Sustainable Batteries. Work package 5: Overall Assessment Final Public Report, Assessment. (2005) 58.

[132] J. Matheys, J. Timmermans, Comparison of the environmental impact of 5 electric vehicle battery technologies using LCA, … Conf. Life- …. (2006) 97–102. doi:10.1504/IJSM.2009.023977.

[133] K. Ishihara, N. Kihira, Environmental burdens of large lithium-ion batteries developed in a Japanese national project, … Power Ind. Japan. (2002) 11. https://www.electrochem.org/dl/ma/202/pdfs/0068.PDF.

[134] Kokam, Cell specification data. http://www.superlatticeinc. com/downloads/SLPB100216216H.pdf, (2009).

[135] R. Frischknecht, R. Heijungs, P. Hofstetter, Einstein’ssons for energy accounting in LCA, Int. J. Life Cycle Assess. 3 (1998) 266–272. doi:10.1007/BF02979833.

[136] M. Zackrisson, L. Avellán, J. Orlenius, Life cycle assessment of lithium-ion batteries for plug-

in hybrid electric vehicles-Critical issues, J. Clean. Prod. 18 (2010) 1517–1527. doi:10.1016/j.jclepro.2010.06.004.

[137] Argonne National Laboratory, BatPac (Battery Performance and Cost Model) Version 2.0., 2011.

[138] G. Zubi, R. Dufo-López, M. Carvalho, G. Pasaoglu, The lithium-ion battery: State of the art and future perspectives, Renew. Sustain. Energy Rev. (2018). doi:10.1016/j.rser.2018.03.002.

[139] J.W. Fergus, Recent developments in cathode materials for lithium ion batteries, J. Power Sources. 195 (2010) 939–954. doi:10.1016/j.jpowsour.2009.08.089.

[140] M. Dubarry, C. Truchot, M. Cugnet, B.Y. Liaw, K. Gering, S. Sazhin, D. Jamison, C. Michelbacher, Evaluation of commercial lithium-ion cells based on composite positive electrode for plug-in hybrid electric vehicle applications. Part I: Initial characterizations, J. Power Sources. 196 (2011) 10328–10335. doi:10.1016/j.jpowsour.2011.08.077.

[141] A. Manthiram, An Outlook on Lithium Ion Battery Technology, ACS Cent. Sci. 3 (2017) 1063–1069. doi:10.1021/acscentsci.7b00288.

[142] Battery University., Types of Lithium-ion., (2018). www.batteryuniversity.com (accessed July 23, 2018).

[143] Cobalt Institute, Lithium - ion. www.cobaltinstitute.org (https://www.cobaltinstitute.org/lithium-ion-batteries.html), (2018).

[144] European Commission, COMMUNICATION FROM THE COMMISSION TO THE EUROPEAN PARLIAMENT, THE COUNCIL, THE EUROPEAN ECONOMIC AND SOCIAL COMMITTEE AND THE COMMITTEE OF THE REGIONS on the 2017 list of Critical Raw Materials for the EU, (2017). http://eur-lex.europa.eu/legal-content/EN/TXT/PDF/?uri=CELEX:52017DC0490&from=EN.

[145] S. Bobba, A. Podias, F. Di Persio, M. Messagie, P. Tecchio, M.A. Cusenza, U. Eynard, F. Mathieux, A. Pfrang, Sustainability Assessment of Second Life Application of Automotive Batteries (SASLAB): JRC Exploratory Research (2016-2017): Final technical report: August 2018; EUR 29321 EN, Publications Office of the European Union, Luxembourg, 2018, ISBN 978-92-79-928, 2018. doi:10.2760/53624.

[146] M.M. Kabir, D.E. Demirocak, Degradation mechanisms in Li-ion batteries : a state-of- the-art review, (2017) 1963–1986. doi:10.1002/er.

[147] P. Keil, S.F. Schuster, J. Wilhelm, J. Travi, A. Hauser, R.C. Karl, A. Jossen, Calendar Aging of Lithium-Ion Batteries, J. Electrochem. Soc. (2016). doi:10.1149/2.0411609jes.

[148] International Electrotechnical Commission (IEC)., IEC 62660-1:2010. International Standard IEC 62660-1:2010, Secondary lithium-ion cells for the propulsion of electric road vehicles – Part 1: Performance testing, (2011).

[149] International Standard Organization, ISO 12405-1, Electrically propelled road vehicles – test specification for lithium-ion battery packs and systems - Part1: High-power applications, 2010; International Standard ISO 12405-2, Electrically propelled road vehicles – test, (2010).

[150] International Electrotechnical Commission (IEC)., International Standard IEC 61427-1, Secondary cells and batteries for renewable energy storage – General requirements and methods of test - Part 1: Photovoltaic off-grid application, Edition 1.0., (2013).

[151] International Electrotechnical Commission (IEC)., International Standard IEC 61427-2, Secondary cells and batteries for renewable energy storage – General requirements and methods of test - Part 2: On-grid applications, Edition 1.0., (2015).

[152] D.R. Conoer, A.J. Crawford, J. Fuller, S.N. Gourisetti, V. Viswanathan, S.R. Ferreira, D.A. Schoenwald, D.M. Rosewater, Protocol for Uniformly Measuring and Expressing the Performance of Energy Storage Systems. PNNL─22010 Rev. 2 / SAND2016-3078 R, Pacific Northwest National Laboratory, and Sandia National Laboratories, Richland, Washington, and Albuquerque. New Mexico (USA, (2016).

[153] M. Cellura, F. Guarino, S. Longo, M. Mistretta, Energy life-cycle approach in Net zero energy buildings balance: Operation and embodied energy of an Italian case study, Energy Build. 72 (2014) 371–381. doi:10.1016/j.enbuild.2013.12.046.

[154] M. Cellura, F. Guarino, S. Longo, M. Mistretta, Different energy balances for the redesign of nearly net zero energy buildings: An Italian case study, Renew. Sustain. Energy Rev. 45 (2015) 100–112. doi:10.1016/j.rser.2015.01.048.

[155] M. Cellura, F. Guarino, S. Longo, M. Mistretta, Different energy balances for the redesign of

nearly net zero energy buildings: An Italian case study, Renew. Sustain. Energy Rev. (2015). doi:10.1016/j.rser.2015.01.048.

[156] J. Salom, A.J. Marszal, J. Widén, J. Candanedo, K.B. Lindberg, Analysis of load match and grid interaction indicators in net zero energy buildings with simulated and monitored data, Appl. Energy. 136 (2014) 119–131. doi:10.1016/j.apenergy.2014.09.018.

[157] J. Salom, A.J. Marszal, J. Candanedo, J. Widén, K. Byskov Lindberg, I. Sartori, Analysis of Load Match and Grid Integration Indicators in Net Zero Energy Buildings with High-Resolution Data. A report of Subtask A IEA Task 40/Annex 52 Towards Net Zero Energy Solar Buildings., (2014) 102.

[158] European Commission, COMMUNICATION FROM THE COMMISSION TO THE EUROPEAN PARLIAMENT, THE COUNCIL, THE EUROPEAN ECONOMIC AND SOCIAL COMMITTEE AND THE COMMITTEE OF THE REGIONS on a monitoring framework for the circular economy. COM(2018) 29 final. Strasbourg, 16.1.2018, (2018).

[159] European Commission, COMMUNICATION FROM THE COMMISSION TO THE EUROPEAN PARLIAMENT, THE COUNCIL, THE EUROPEAN ECONOMIC AND SOCIAL COMMITTEE AND THE COMMITTEE OF THE REGIONS Closing the loop - An EU action plan for the Circular Economy. COM(2015) 614 final. Brussels, 2.12.2015, (2015).

[160] M.A. Curran, Life Cycle Assessment Handbook, 2012. doi:10.1002/9781118528372.

[161] EC - JRC, European Commission - Joint Research Centre - Institute for Environment and Sustainability. International Reference Life Cycle Data System (ILCD) Handbook - General guide for Life Cycle Assessment - Detailed guidance. First edition March 2010. EUR 24708 E, 2010.

[162] D.C. Jordan, S.R. Kurtz, Photovoltaic Degradation Rates — An Analytical Review. Progress in Photovoltaics: Research and Applications. National Renewable Energy Laboratory - NRESL. NREL/JA-5200-51664, 2012.

[163] J. Neubauer, A. Pesaran, The ability of battery second use strategies to impact plug-in electric vehicle prices and serve utility energy storage applications, J. Power Sources. 196 (2011) 10351–10358. doi:10.1016/j.jpowsour.2011.06.053.

[164] European Commission, Recommendation 2013/179/EU on the use of common methods to measure and communicate the life cycle environmental performance of products and organisations, Off. J. Eur. Union. (2013) 210. doi:doi:10.3000/19770677.L_2013.124.eng.

[165] M. Hauschild, R.K. Rosenbaum, S.I. Olsen, E. Al., Life Cycle Assessment - Theory and Practice, 2017. doi:10.1007/978-3-319-56475-3.

[166] R. Frischknecht, N. Jungbluth, H. Althaus, C. Bauer, G. Doka, R. Dones, R. Hischier, S. Hellweg, T. Köllner, Y. Loerincik, M. Margni, Implementation of Life Cycle Impact Assessment Methods, Am. Midl. Nat. 150 (2007) 1–151. http://www.ecoinvent.org/fileadmin/documents/en/03_LCIA-Implementation.pdf.

[167] S. Bobba, F. Ardente, F. Mathieux, Environmental and economic assessment of durability of energy-using products: Method and application to a case-study vacuum cleaner, J. Clean. Prod. 137 (2016) 762–776. doi:10.1016/j.jclepro.2016.07.093.

[168] C.E.L. Latunussa, F. Ardente, G.A. Blengini, L. Mancini, Life Cycle Assessment of an innovative recycling process for crystalline silicon photovoltaic panels, Sol. Energy Mater. Sol. Cells. 156 (2016) 101–111. doi:10.1016/j.solmat.2016.03.020.

[169] G. Wernet, C. Bauer, B. Steubing, J. Reinhard, E. Moreno-Ruiz, B. Weidema, The ecoinvent database version 3 (part I): overview and methodology, Int. J. Life Cycle Assess. 21 (2016) 1218–1230. doi:10.1007/s11367-016-1087-8.

[170] N. Lebedeva, V. Ruiz, F. Di Persio, A. Kriston, A. Pfrang, T. Kosmidou, J. Ungeheuer, D. Dams, L. Brett, Evaluation of volume of free electrolyte in various cell types - Method and preliminary result. 7th GTR EVS meeting, 18-20 March 2015, Paris; https://www2.unece.org/wiki/download/attachments/25265483/EVS-07-24e.pdf?api=v2, (2015).

[171] J. Li, C. Daniel, D. Wood, Materials processing for lithium-ion batteries, J. Power Sources. 196 (2011) 2452–2460. doi:10.1016/j.jpowsour.2010.11.001.

[172] D. Liu, L.-C. Chen, T.-J. Liu, T. Fan, E.-Y. Tsou, C. Tiu, An Effective Mixing for Lithium Ion Battery Slurries, Adv. Chem. Eng. Sci. 04 (2014) 515–528. doi:10.4236/aces.2014.44053.

[173] P.A. Nelson, K.G. Gallagher, I. Bloom, D.W. Dees, Modeling the Performance and Cost of

Lithium-Ion Batteries for Electric-Drive Vehicles, (2011) 1–102. doi:10.2172/1027714.

[174] Mitsubishi Motors, PHEV - Outlander, Catalogue. www.mitsubishi-motors.com, (2018).

[175] Recharge, The Advanced Rechargeable & Lithium Batteries Association PEFCR - Product Environmental Footprint Category Rules for High Specific Energy Rechargeable Batteries for Mobile Applications Version : H Time of validity : 31 December 2020. (http://ec.europa.eu/, (2018) 1–98.

[176] B. Swain, Recovery and recycling of lithium: A review, Sep. Purif. Technol. 172 (2017) 388–403. doi:10.1016/j.seppur.2016.08.031.

[177] A. Tamiang, D. Angka, Electrode and cells manufacturing white paper - chapter 5: Batteries and end of life management, ELIBAMA (European Li-ion battery advanced manufacturing for electric vehicles). Available at: https://elibama.wordpress.com/electrodes-and-cells-manufacturing-white-paper/, 2014.

[178] UMICORE, Battery recycling - Our recycling process. http://csm.umicore.com/en/recycling/battery-recycling/our-recycling-process/, (2018).

[179] D. Kushnir, Lithium Ion Battery Recycling Technology 2015: Current State and Future Prospects, (2015) 1–56. http://publications.lib.chalmers.se/records/fulltext/230991/local_230991.pdf.

[180] M.R. Mancini, S. Frangini, C. Alvani, Recupero eco-sostenibile di materiali da batterie litio-ione esauste : studi preliminari. Report ENEA - Ricerca di Sistema Elettrico. Report RdS/2013/256, (2013).

[181] Elibama, Electrodes and Cells Manufacturing White Paper, (2014) 280.

[182] P. Meshram, B.D. Pandey, T.R. Mankhand, Extraction of lithium from primary and secondary sources by pre-treatment, leaching and separation: A comprehensive review, Hydrometallurgy. 150 (2014) 192–208. doi:10.1016/j.hydromet.2014.10.012 Review.

[183] Batteries 2020 Project., WP8: ECONOMIC ASSESSMENT D.8.8: Safety and environmental analysis. Seventh Framework Programme, 2016.

[184] P. Chancerel, M. Marwede, Feasibility study for setting-up reference values to support the calculation of recyclability / recoverability rates of electr(on)ic products, 2016.

doi:10.2788/901715.

[185] J. Matheys, J.-M. Timmermans, J. Van Mierlo, S. Meyer, P. Van den Bossche, Comparison of the environmental impact of five electric vehicle battery technologies using LCA, Int. J. Sustain. Manuf. 1 (2009) 318–329. doi:10.1504/IJSM.2009.023977.

[186] J.B. Dunn, L. Gaines, J. Sullivan, M.Q. Wang, Impact of recycling on cradle-to-gate energy consumption and greenhouse gas emissions of automotive lithium-ion batteries, Environ. Sci. Technol. 46 (2012) 12704–12710. doi:10.1021/es302420z.

[187] F. Ardente, P. Tecchio, S. Bobba, F. Mathieux, Assessment of resource efficiency in a life cycle perspective: the case of reuse, in: Atti Del XI Convegno Della Rete Ital. LCA - Resour. Effic. e Sustain. Dev. Goals Ruolo Del Life Cycle Thinking. Siena, 22-23 Giugno 2017, ENEA. ISBN: 978-88-8286-352-4, 2017. http://www.enea.it/it/seguici/pubblicazioni/pdf-volumi/v2017-atti-lca.pdf.

[188] M. Hiete, Waste management plants and technology for recycling construction and demolition (C&D) waste: state-of-the-art and future challenges, in: Handb. Recycl. Concr. Demolition Waste, 2013. doi:10.1533/9780857096906.1.53.

[189] M. Cellura, V. La Rocca, S. Longo, M. Mistretta, Energy and environmental impacts of energy related products (ErP): A case study of biomass-fuelled systems, J. Clean. Prod. 85 (2014) 359–370. doi:10.1016/j.jclepro.2013.12.059.

[190] F. Ardente, G. Beccali, M. Cellura, V. Lo Brano, Life cycle assessment of a solar thermal collector: Sensitivity analysis, energy and environmental balances, Renew. Energy. 30 (2005) 109–130. doi:10.1016/j.renene.2004.05.006.

[191] M. Cellura, S. Longo, M. Mistretta, Sensitivity analysis to quantify uncertainty in Life Cycle Assessment: The case study of an Italian tile, Renew. Sustain. Energy Rev. 15 (2011) 4697–4705. doi:10.1016/j.rser.2011.07.082.

[192] E. Igos, E. Benetto, R. Meyer, P. Baustert, B. Othoniel, How to treat uncertainties in life cycle assessment studies?, Int. J. Life Cycle Assess. (2018) 1–14. doi:10.1007/s11367-018-1477-1.

[193] F. Cerdas, P. Titscher, N. Bognar, R. Schmuch, M. Winter, A. Kwade, C. Herrmann, Exploring the effect of increased energy density on the environmental impacts of traction batteries: A

comparison of energy optimized lithium-ion and lithium-sulfur batteries for mobility applications, Energies. 11 (2018). doi:10.3390/en11010150.

[194] R. Hein, P.R. Kleindorfer, S. Spinler, Valuation of electric vehicle batteries in vehicle-to-grid and battery-to-grid systems, Technol. Forecast. Soc. Change. 79 (2012) 1654–1671. doi:10.1016/j.techfore.2012.06.002.

[195] European Commission - Joint Research Centre - Institute for Environment and Sustainability, General guide for Life Cycle Assessment - Detailed guidance, 2010. doi:10.2788/38479.

[196] G. Reid, J. Julve, Second Life-Batteries As Flexible Storage For Renewables Energies, Bundesverbandes Erneuerbare Energ. E.V. (2016).

[197] International Organization for Standardization, UNI EN 15978:2011 - Sustainability of construction works - Assessment of environmental performance of buildings - Calculation method, Sustain. Constr. Work. - Assess. Environ. Perform. Build. - Calc. Method. (2011).

[198] UNFCCC, Paris Agreement, Conf. Parties Its Twenty-First Sess. 21932 (2015) 32. doi:FCCC/CP/2015/L.9/Rev.1.

[199] E. Crenna, S. Sozzo, S. Sala, Natural biotic resources in LCA: Towards an impact assessment model for sustainable supply chain management, J. Clean. Prod. (2017). doi:10.1016/j.jclepro.2017.07.208.

[200] J. Dewulf, L. Benini, L. Mancini, S. Sala, G.A. Blengini, F. Ardente, M. Recchioni, J. Maes, R. Pant, D. Pennington, Rethinking the area of protection “natural resources” in life cycle assessment, Environ. Sci. Technol. 49 (2015) 5310–5317. doi:10.1021/acs.est.5b00734.

[201] European Environment Agency, Particulate matter (PM10) - Daily limit value for the protection of human health. https://www.eea.europa.eu/data-and-maps/figures/particulate-matter-pm10-daily-limit-value-for-the-protection-of-human-health-6, (2014).

[202] D. Lew, G. Brinkman, N. Kumar, P. Besuner, D. Agan, S. Lefton, Impacts of wind and solar on emissions and wear and tear of fossil-fueled generators, in: IEEE Power Energy Soc. Gen. Meet., 2012. doi:10.1109/PESGM.2012.6343967.